Dissertation zur Erlangung des Doktorgrades
der Fakultät für Chemie und Pharmazie
der Ludwig-Maximilians-Universität München

Relationship between the Reactivities of Different Classes of Nucleophiles towards C_{sp2} and C_{sp3} Electrophilic Centers

Anna Antipova
aus
Bryansk, Russland

2015

Erklärung

Diese Dissertation wurde im Sinne von § 7 der Promotionsordnung vom 28. November 2011 von Herrn Prof. Dr. Mayr betreut.

Eidesstattliche Versicherung

Diese Dissertation wurde eigenständig und ohne unerlaubte Hilfe erarbeitet.

München, 14.05.2015

....

Anna Antipova

Dissertation eingereicht am 21.05.2015

1. Gutachter: Prof. Dr. Herbert Mayr
2. Gutachter: Prof. Dr. Manfred Heuschmann

Mündliche Prüfung am 14.07.2015

ACKNOWLEDGMENTS

First of all, I would like to thank Professor Mayr for giving me the possibility of making this thesis in his group. I am most grateful to him for his help, endless patience and for motivating me to finish this thesis.

I wish to express my sincere thanks to Professor Heuschmann for being the second evaluator of this thesis, as well as to other members of the examination committee for their time and interest in this work.

I would like to thank Nathalie Hampel for synthesis of the reference electrophiles extensively used in this work and for her most helpful assistance in some experiments.

My very special thanks goes out to Mrs. Lipfert for organisational assistance and readiness to help me in any situation.

For contribution to this work, I would like to thank my trainees Vera Hartdegen, Irina Becker and Renata Maraschin Amaro.

For help in carrying out laser flash experiments, I am grateful to Johannes Ammer and to Jörg Bartl.

I must also thank the members of the analytical division of the faculty, and especially Dr. Stephenson, for carrying out NMR experiments.

I am grateful to Armin R. Ofial for advice and help in passing through technical difficulties while carrying out my experiments, as well as for taking care of my safety in the laboratory.

For detailed and most useful discussions, and for careful reading of parts of this thesis, I would like to thank Konstantin Troshin and Johannes Ammer. Special thanks to Konstantin for his competence in mathematics!

For asking interesting questions and suggesting new ideas at the group seminars, for collaboration and for interesting conversations I would like to thank my colleagues (and ex-colleagues): Johannes Ammer, Dominic Allgäuer, Haruyasu Asahara, Roland Appel, Mahiuddin Baidya, Guillaume Berionni, Martin Breugst, Katharina Böck, Saloua Chelli, Xi Chen, Francisco Corral, Julia E. Fleckenstein, Elsa Follet, Xingwei Guo, Nathalie Hampel, Markus Horn, Tanja Kanzian, Konrad Koszinowski, Sami Lakhdar, Hans Laub, Biplab Maji, Tobias Nigst, Christoph Nolte, Armin R. Ofial, Angel R. Puente, Dorothea Richter, Nicolas Streidl, Alexander Wagner, Elija Wiedemann and Ivo Zenz. I must also thank Brigitte Janker for her enormous contribution to the collaboration of the group members.

For being an important part of my life in Munich, for exciting trips and wonderful and warm “well-sittings” I would like to thank Konstantin Troshin, Boris Maryasin, Veronika Geller, Evgeny Larionov, Varvara Morozova and Johannes Ammer.

I am most grateful to my friend Barbara Thalhammer for being my guide in the musical life of Munich, for inspiration, encouragement at difficult times and for sharing a lot of nice moments with me.

Last but not least, I express the profound gratitude to my family: to my parents for raising me and for giving me the possibility to study, to my son Peter for being so nice and sweet and for sleeping well while I was writing, and most of all to my husband Sergey, who always encouraged and motivated me, helped me with many experiments and readily took care of Peter to ensure some time for writing of this thesis.

Thank you! Danke!

TABLE OF CONTENTS

SUMMARY

CHAPTER 1. *Nucleophilic reactivities of neutral N- and P-nucleophiles towards C_{sp2} electrophilic centers.* The rate constants for the reactions of reference benzhydrylium ions and quinone methides with several neutral nitrogen and phosphorus nucleophiles were determined spectrophotometrically in DMSO and acetonitrile, respectively, and were found to follow the linear free energy relationship 1 (Figure A.1, the structures of the reference electrophiles and their E parameters are listed in Table 1.1 on page 15). This allowed the determination of the s_N and N parameters for these nucleophiles.

$$\log k_2 = s_N (E + N) \qquad (1)$$

a)

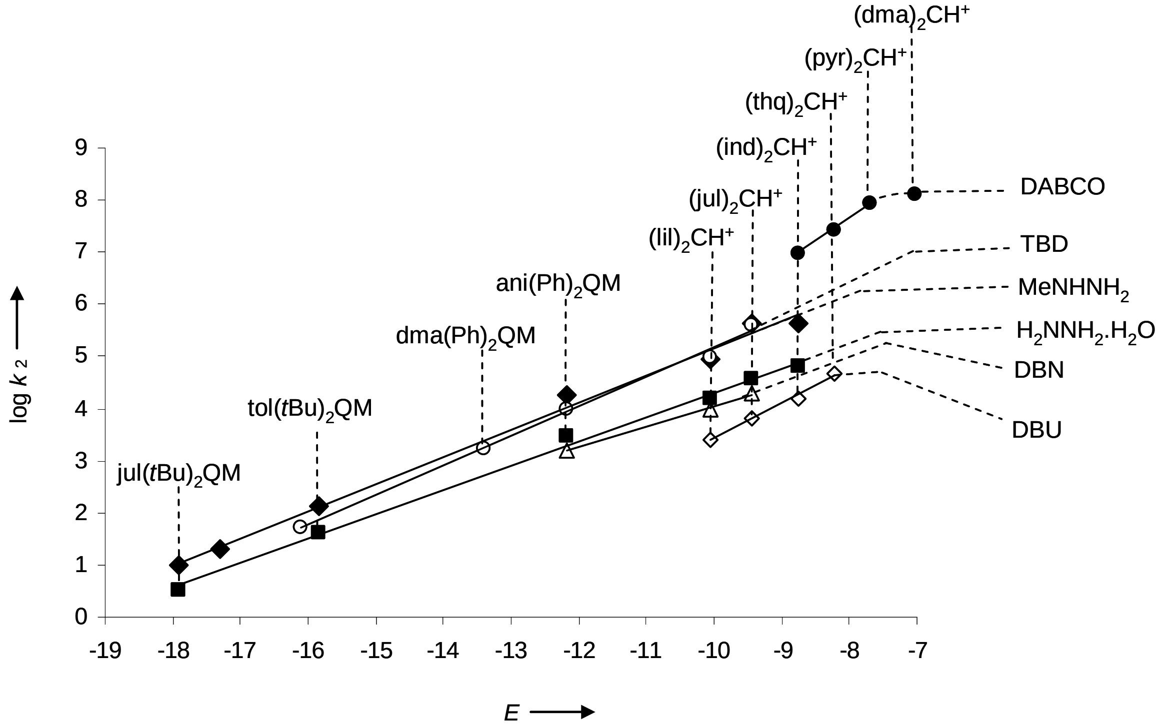

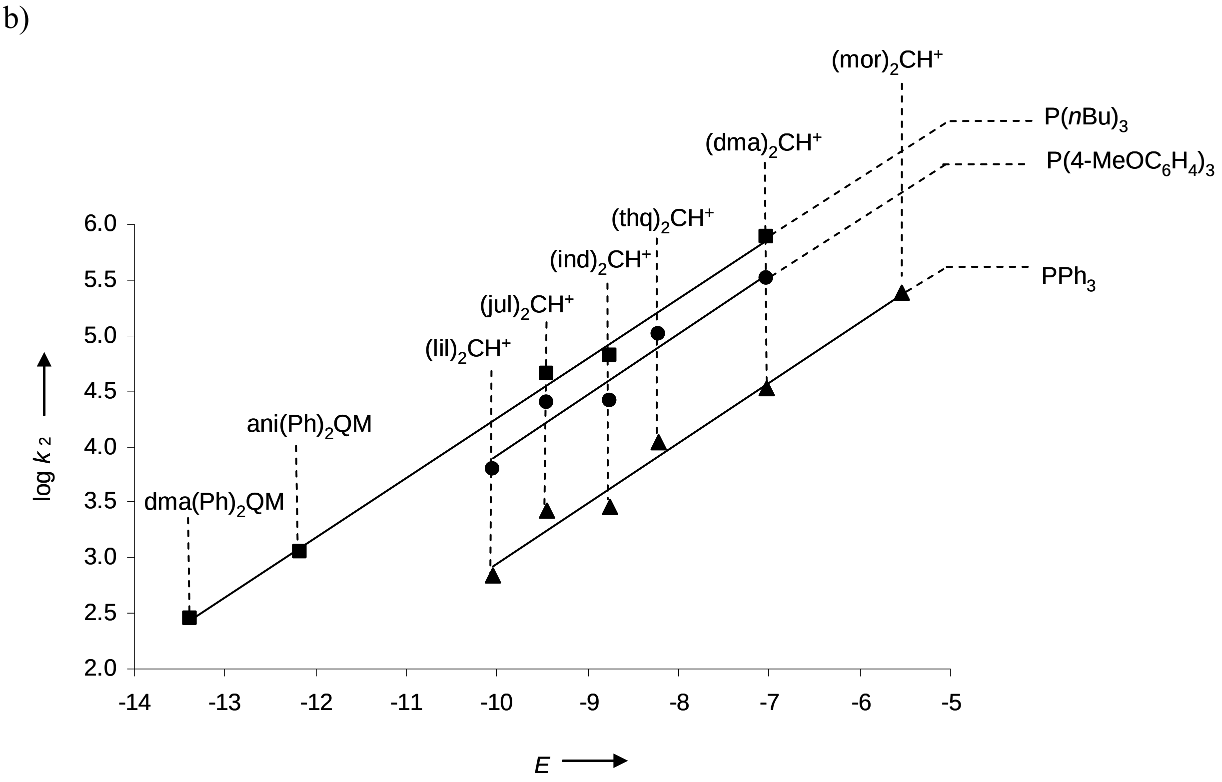

Figure A.1. Correlation of the logarithms of the second-order rate constants with previously reported E parameters for the reactions of reference benzhydrylium tetrafluoroborates and quinone methides with a) N-nucleophiles (DMSO, 20°C) and b) P-nucleophiles (acetonitrile, 20°C).

It was shown that the ratio $k_{CH_2Cl_2}/k_{MeCN}$ for the reactions of phosphanes with benzhydrylium ions increases with increasing the electrophilicity parameter of the cation, which is reflected by higher s_N parameters in dichloromethane than in acetonitrile. This reactivity phenomenon was analyzed using the Marcus Equation on the example of triphenylphosphane, for which several rate and equilibrium constants in both solvents are available. It was shown that this change in the sensitivity parameters is caused by the interplay of intrinsic and thermodynamic factors. It was also suggested that this reactivity crossover in different solvents may be a general phenomenon for the reactions of neutral N- and P-nucleophiles with benzhydrylium ions, which is reflected in the following order of s_N values: $s_{CH_2Cl_2} > s_{MeCN} > s_{DMSO} > s_{H_2O}$.

CHAPTER 2. *Reactivities of neutral N- and P-nucleophiles towards typical neutral S_N2 substrates. Comparison with the reactivities towards benzhydrylium ions and analysis of trends.* Second-order rate constants for the reactions of several benzyl and phenacyl halides, methyl iodide and methyl tosylate with neutral N- and P-nucleophiles were determined conductimetrically in DMSO and acetonitrile at 20°C. The rate constants for the reactions of nitrogen nucleophiles with S_N2 substrates were shown to correlate linearly with the calculated rate constants for their reactions with the benzhydrylium ion lil_2CH^+ in the same solvents (Figure A2). Tertiary amines and triarylphosphanes (not shown in Figure A.2) deviate downwards from these correlations, probably for steric reasons.

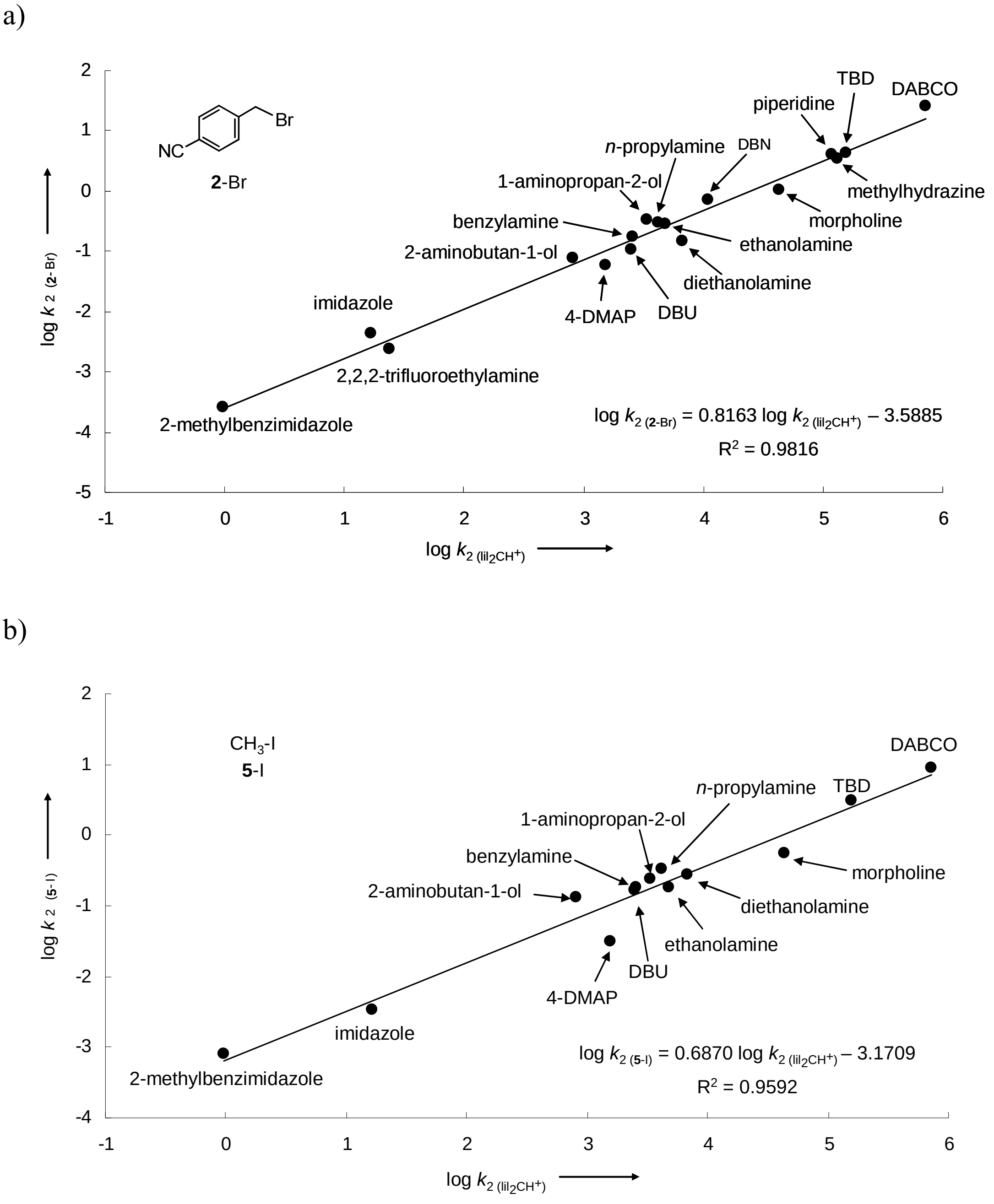

Figure A.2. Correlation of log k_2 for the reactions of various N-nucleophiles with (a) 4-cyanobenzyl bromide **2**-Br and (b) methyl iodide **5**-I versus log k_2 for their reactions with the lil_2CH^+ cation in DMSO.

The applicability of the extended version of the Mayr equation log $k_2 = s_E s_N (N + E)$ for predicting the rate constants for the S_N2 type reactions was investigated. We have shown that the accuracy of estimation of the rate constants for the substitution reactions with this equation depends on the set of the nucleophiles used in the study: when the nucleophiles are chosen in such a way that s_N depends on N linearly, a good linear plot of log k_{S_N2} / s_N versus N is a consequence of the linearity of the plot of log k_{S_N2} versus log $k_{\mathrm{lil_2CH^+}}$.

The correlations of log k_{S_N2} for the reactions of uncharged electrophiles with neutral nitrogen nucleophiles versus log $k_{\mathrm{lil_2CH^+}}$ make separate lines in different solvents, which implies that the solvent effects on the electrophilic reactivities of neutral S_N2 substrates and benzhydrylium ions are different (Figure A.3).

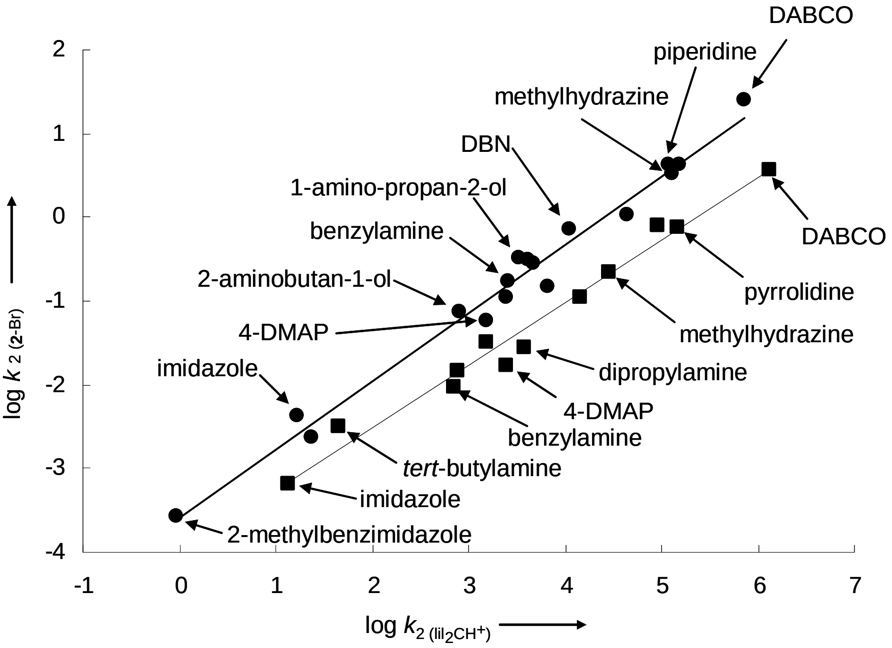

● In DMSO and ■ in acetonitrile

Figure A.3. Correlation of log k_2 for the reactions of various N-nucleophiles with 4-cyanobenzyl bromide (**2**-Br) versus log k_2 of their reactions with the $\mathrm{lil_2CH^+}$ cation.

In the series of aminolysis reactions of benzyl halides, the CN and OMe groups in the para position of the phenyl ring have a very small (2-3-fold) rate enhancing effect. Phenacyl halides react about 10 times faster with amines than the corresponding unsubstituted benzyl halides.

The ratio k_{RBr}/k_{RCl} is ca. 150 for all benzyl and phenacyl halides studied in this work, and it does not systematically depend on the nucleophilicity of the reaction partner, as illustrated by the parallel lines of the correlations of log k_{RX} versus log $k_{lil_2CH^+}$ for X = Cl and Br. The line for the bromide is slightly more than two logarithmic units higher than that for the corresponding chloride (Figure A.4).

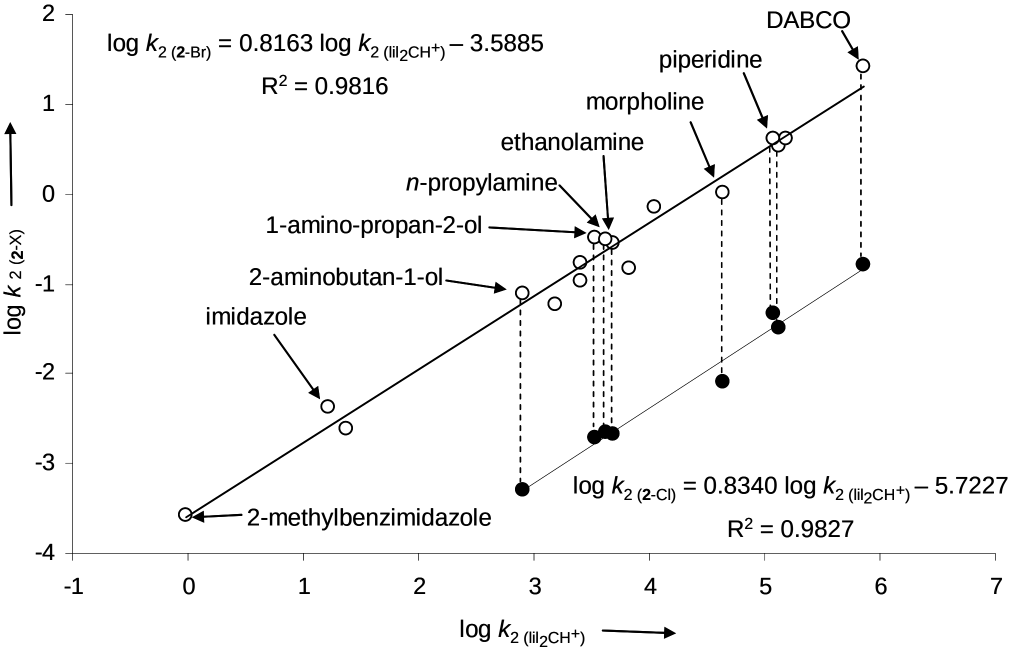

Figure A.4. Influence of the leaving group on the S_N2 reactivity of benzyl and phenacyl halides: correlations of log k_2 for the reactions of various N-nucleophiles with 4-cyanobenzyl bromide **2**-Br (○) and 4-cyanobenzyl chloride **2**-Cl (●) versus log k_2 for their reactions with the lil_2CH^+ cation in DMSO.

Despite the fact that tosylate was reported to be a better nucleofuge than iodide in S_N1 processes, S_N2 reactions of methyl iodide with amines in DMSO are 3 to 15 times faster than those of methyl tosylate. The ratio k^I/k^{OTs} increases with increasing reactivity of the reaction partner.

CHAPTER 3. *Reactivities of Stabilized 9-Substituted Fluorenyl Anions Towards Quinone Methides and Benzhydrylium Ions in Dimethyl Sulfoxide.* The rate constants for the reactions of anions **1-3** with reference quinone methides were determined spectrophotometrically at 20°C in DMSO.

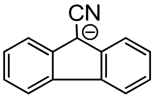

1

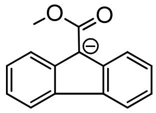

2

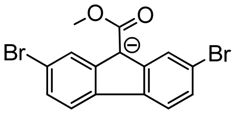

3

The kinetics of the reactions of carbanions **1-3** with quinone methides, which were studied in presence of the conjugated C-H acid, showed three different reactivity patterns: A, B and C. In case A, the observed rate constants were linearly dependent on the concentration of the nucleophile and independent of the concentration of the corresponding C-H acid. In case B, k_{obs} increased with the concentration of the C-H acid when the latter was small, but reached a plateau at some point; further increase of the C-H acid concentration did not influence the rate constant anymore. In case C, the reaction got faster as more C-H acid was present in the solution.

The change from reactivity pattern A to the reactivity pattern B is due to the change in the rate-determining step of the reaction (Scheme A.1). In case A the attack of the nucleophile at the quinone methide is fast and irreversible, while in case B the equilibrium constant k_1/k_{-1} is small, and the attack of the nucleophile at the quinone methide is followed by a relatively slow proton transfer step.

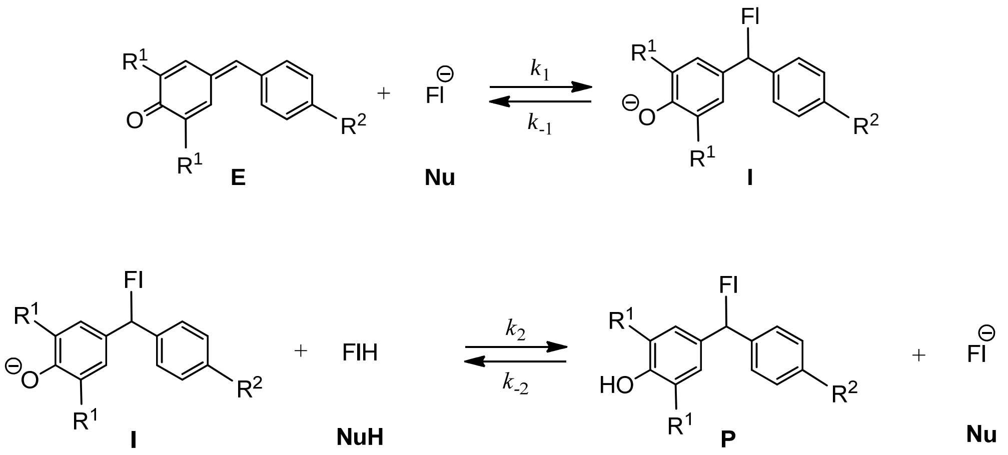

Scheme A.1. Suggested mechanism of the reactions of quinone methides with fluorenyl anions (**Nu**) in presence of the conjugated C-H acid (**NuH**).

We assume that in case C the quinone methide is partially protonated by a strong C-H acid (Scheme A.2), and this causes the acceleration of the reaction as its concentration increases.

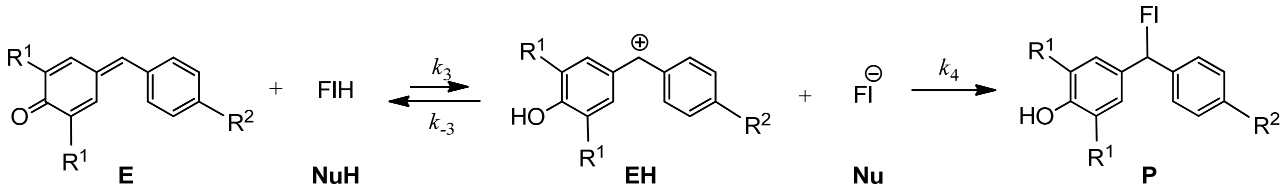

Scheme A.2. Protonation of a quinone methide by a fluorene with subsequent recombination of the charged species.

In cases A and B, it was possible to evaluate the kinetic data to obtain the second-order rate constants for the attack of the fluorene at the quinone methide. In case C, there are too many processes which have to be taken into account. Experimentally obtained time-dependent absorbances of **E** do not provide enough information for unambiguous determination of the second-order rate constants.

The sensitivity parameters *N* and s_N for these carbanions were derived from the rate constants of the reactions with quinone methides, according to equation 1.

The rate constants for the reactions of **1** with benzhydrylium ions in DMSO were determined using the laser-flash photolysis technique. They did not follow the same correlation with the rate constants for the reactions with quinone methides, and were therefore not used for determination of *N* and s_N for **1** (Figure A.5).

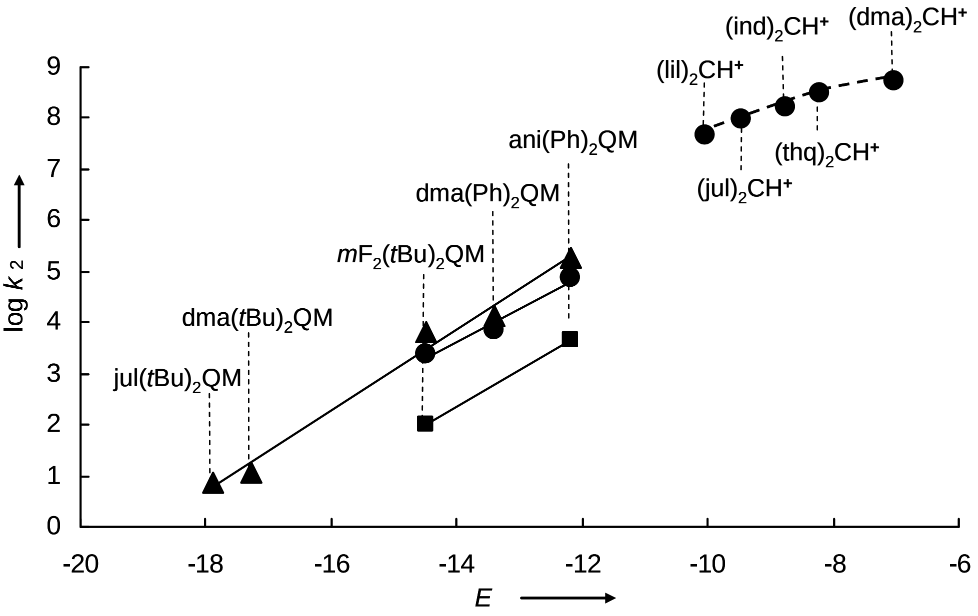

Figure A.5. Plot of the logarithms of the second-order rate constants for the reactions of **1-3** with quinone methides and benzhydrylium ions versus previously reported *E* parameters for the electrophiles (DMSO, 20°C). Data points: ● for **1,** ▲ for **2** and ■ for **3**.

The logarithms of rate constants for the reactions of several amines and anions **1-3** with benzyl chloride were plotted versus their reactivities towards ani(Ph)$_2$QM (**4e**) in DMSO, calculated from the s_N and N parameters (Figure A.6).

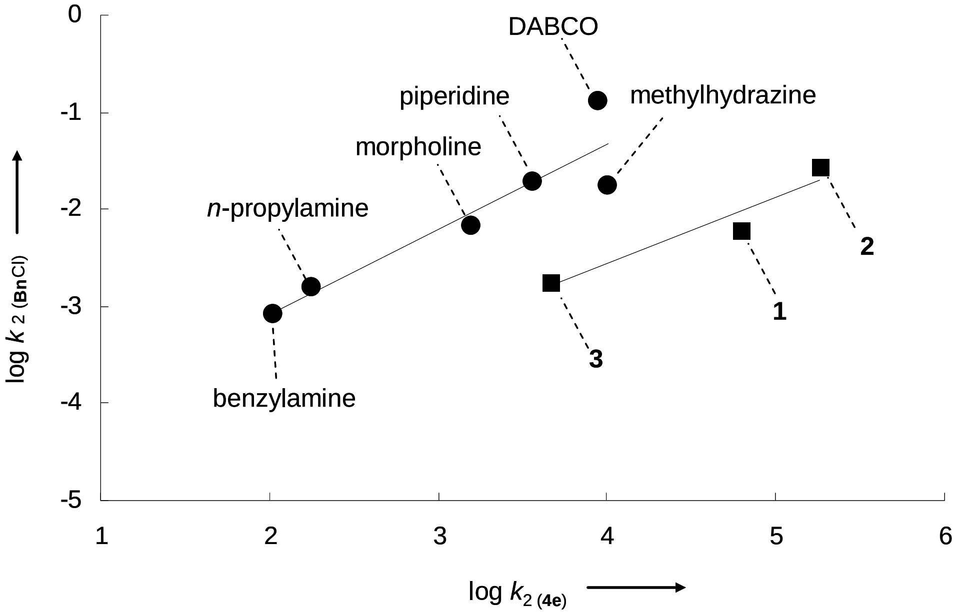

Figure A.6. Correlation of log k_2 for the reactions of various amines (at 20° in DMSO) and anions **1-3** (at 25°C in DMSO) with benzyl chloride versus calculated log k_2 for their reactions with ani(Ph)$_2$QM (**4e**) in DMSO.

The points for carbanions **1-3** deviate downwards from the line for amines, probably due to steric reasons.

INTRODUCTION

Nucleophilicity is a fundamental concept of organic chemistry with a long history. Quantification of nucleophilicity is essential for understanding the factors which influence organic reactivity. Several approaches have been developed which allow predicting the reactivity of a nucleophile in a specific type of reaction. Thus, in 1953, Swain and Scott suggested that the nucleophilic reactivity n in S_N2 type reaction can be defined by Equation 1, where s is the sensitivity of the rate constant to variations of the nucleophile and k_0 is the rate constant of the reaction of the studied electrophile with water. [1]

$$\log (k/k_0) = sn \qquad (1)$$

Soon afterwards, Edwards proposed an equation which defined nucleophilic reactivity in terms of two parameters, H (basicity) and E_{ox} (oxidation potential);[2] the latter was later substituted by a polarizability parameter, P.[3]

After a short period of disillusionment with the idea of quantification of nucleophilic reactivity,[4] Ritchie[5] reported a simple correlation (Eq. 2) which described the nucleophilic reactivity of a variety of nucleophiles towards a wide range of carbocations by an electrophile-independent nucleophilicity parameter, N_+.

$$\log (k/k_0) = N_+ \qquad (2)$$

The most extensive nucleophilicity scale has been created on the basis of Equation 3. It has been employed to describe the reactivities of numerous nucleophiles by N and s_N parameters, which are derived from the rate constants of their reactions with reference benzhydrylium ions and quinone methides.[6] This equation proved to be applicable for predicting the rates of the reactions of various nucleophiles with carbocations, electron-deficient arenes, Michael acceptors, and cationic metal π-complexes.

$$\log k_2 = s_N (E + N) \qquad (3)$$

Applicability of all these reactivity scales was initially restricted to a single reaction type: either S_N2 (Swain-Scott or Edwards equation) or addition to unsaturated carbon atom (Ritchie and Mayr approach).

Later, the nucleophilicity parameters N for different solvent mixtures, derived from their reactivities towards benzhydrylium ions,[7] were found to correlate linearly with Kevill's N_T parameters,[8] reflecting the rate constants for solvolysis of S-methyldibenzothiophenium ion in these mixtures. This indicated that nucleophilicity parameters N and s_N might also be applicable for predicting the rate constants of the S_N2 reactions. Indeed, an excellent linear correlation (R^2=0.987) of (log k)/s_N for the reactions of the S-methyldibenzothiophenium ion with various solvents and nucleophiles in methanol versus the nucleophilicity parameters N was published in 2006 (Figure B.1).[9]

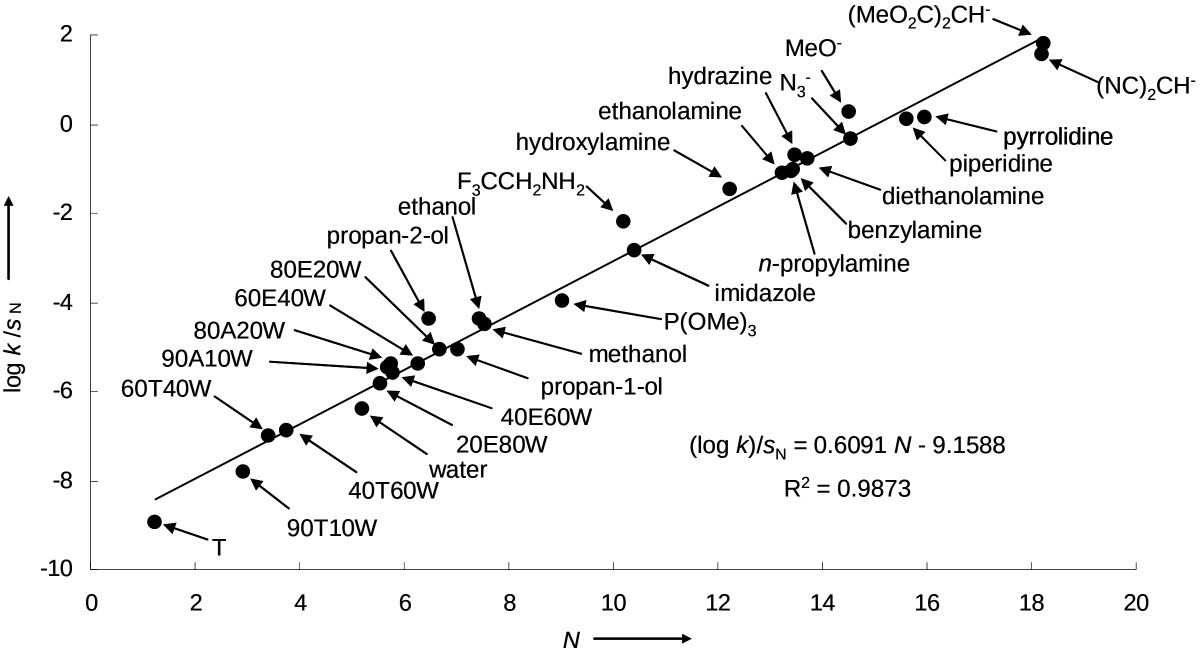

Figure B.1. Correlation of (log k)/s_N of the reactions of S-methyldibenzothiophenium ion with different solvents and with solutions of nucleophiles in methanol versus the nucleophilicty parameters N.

The authors suggested extending Equation 3 to Equation 4 by introducing an electrophile-specific parameter s_E:

$$\log k = s_E s_N (E + N) \qquad (4)$$

This was the first equation which related the reactivities towards Csp^2 and Csp^3 electrophilic centers, although the observation that the reactivities towards sp^2-and sp^3-hybridized carbon atoms are not fundamentally different had also been made by other authors.[10, 11]

The main objective of this work is to explore the scope and limitations of Equation 4 and to find out whether s_N and N parameters, derived from the reactivities towards benzhydrylium ions, are generally applicable for predicting the reactivities of various types of nucleophiles (with nitrogen, phosphorus and carbon nucleophilic centers) in bimolecular nucleophilic substitution at saturated carbon atom.

CHAPTER 1 of this thesis provides information about the reactivities of several neutral nitrogen and phosphorus nucleophiles towards reference benzhydrylium ions and quinone methides in DMSO and acetonitrile, from which the N and s_N parameters were derived according to Equation 3. In CHAPTER 2, the reactivities of amines and phosphanes towards typical neutral S_N2 substrates are described and compared with those towards sp^2-hybridized carbon. Applicability of Equation 4 and s_N and N parameters for bimolecular substitution reactions is discussed. CHAPTER 3 describes the reactivities of 9-substituted fluorenyl anions towards quinone methides and benzhydrylium ions in DMSO and provides comparison with the reactivities towards benzyl halides, published earlier.

References

(1) C. G. Swain, C. B. Scott, *J. Am. Chem.* Soc. 1953, 75, 141 –147.

(2) J. O. Edwards, *J. Am. Chem. Soc.* 1954, 76, 1540 –1547

(3) J. O.Edwards, *J. Am. Chem. Soc.* 1956, 78, 1819 –1820.

(4) J. F. Bunnett, *Annu. Rev. Phys. Chem.* 1963, 14, 271 –290,

(5) a) C. D. Ritchie, *Acc. Chem. Res*. **1972**, *5*, 348 –354 ; b) C. D. Ritchie, P. O. I. Virtanen, *J. Am. Chem. Soc*. **1972**, *94*, 4966 –4971.

(6) a) H. Mayr, M. Patz, *Angew. Chem.* **1994**, *106*, 990; *Angew. Chem. Int. Ed. Engl.* **1994**, *33*, 938–957; b) H. Mayr, T. Bug, M. F. Gotta, N. Hering, B. Irrgang, B. Janker, B. Kempf, R. Loos, A. R. Ofial, G. Remennikov, H. Schimmel, *J. Am. Chem. Soc.* **2001**, *123*, 9500–9512; c) R. Lucius, R. Loos, H. Mayr, *Angew. Chem.* **2002**, *114*, 97-102; *Angew. Chem. Int. Ed.* **2002**, *41*, 91–95; d) H. Mayr, B. Kempf, A. R. Ofial, *Acc. Chem. Res.* **2003**, *36*, 66–77; e) H. Mayr, A. R. Ofial, *Pure Appl. Chem.* **2005**, *77*, 1807–1821; f) H. Mayr, *Angew. Chem.*

2011, *123*, 3692; *Angew. Chem. Int. Ed.* **2011**, *50*, 3612–3618; g) J. Ammer, C. Nolte, H. Mayr, *J. Am. Chem. Soc.* **2012**, *134*, 13902–13911; h) for a comprehensive listing of nucleophilicity parameters *N* and electrophilicity parameters *E*, see http://www.cup.uni-muenchen.de/oc/mayr/DBintro.html.

(7) S. Minegishi, S. Kobayashi, H. Mayr, *J. Am. Chem. Soc*. **2004**, *126*, 5174 –5181.

(8) D. N. Kevill, S. W. Anderson, *J. Org. Chem*. **1991**, *56*, 1845 –1850.

(9) T. B. Phan, M. Breugst, H. Mayr, *Angew. Chem. Int. Ed*. **2006**, *45*, 3869 –3874

(10) J. W. Bunting, J. M. Mason, C. K. M. Heo**,** *J. Chem. Soc. Perkin Trans.* 2 **1994**, 2291-2300.

(11) J. P. Richard, M. M. Toteva, J. Crugeiras, *J. Am. Chem. Soc.* **2000**, *122*, 1664 –1674.

CHAPTER 1

Nucleophilic reactivities of neutral N- and P-nucleophiles towards C_{sp2} electrophilic centers

1.1. Introduction

Neutral nitrogen nucleophiles represent an interesting class of nucleophiles in which a wide variation of properties through structural change is possible, while the nucleophilic center is kept constant. This makes them versatile organocatalysts and important reagents in many transformations as well as attractive model objects for studying the physical basis of nucleophilic reactivity. Numerous kinetic studies on the reactivities of amines,[1] hydrazines,[2] pyridines,[3, 4] azoles,[5] guanidines[6] etc. in various types of reactions under different conditions have been performed in order to understand the factors which control nucleophilic reactivity. A lot of N-nucleophiles have been characterized by Swain-Scott's *n* parameter[7] and included into Ritchie's N_+ scale[1d, 8] of nucleophilicity.

In our group, Equation 1 has extensively been employed to describe the reactivities of numerous nucleophiles by N and s_N parameters, which are derived from the rate constants of their reactions with reference benzhydrylium ions and quinone methides[9]. A large number of neutral nitrogen nucleophiles have already been included into our reactivity data base.[10-16]

$$\log k_2 = s_N (E + N) \qquad (1)$$

As the reactivities of N-nucleophiles are strongly solvent-dependent,[17] direct comparisons of the reactivities of nucleophiles in different types of reactions, such as nucleophilic additions to C_{sp2} centers or nucleophilic substitutions, are only justified if both reactions are performed in the same solvent.

The next chapter will be concerned with the S_N2-type reactions of N-nucleophiles with benzyl, phenacyl and alkyl halides and tosylates. Such reactions are typically carried out in dipolar aprotic solvents, and we studied them in DMSO and acetonitrile. In order to compare the reactivities of nitrogen nucleophiles towards C_{sp2} and C_{sp3} centers, we required additional reactivity data for different types of nitrogen nucleophiles in these solvents, which supplement the existing data obtained previously for these nucleophiles in other media. In this chapter, we have thus measured the rate constants for reactions of DBU, DBN, TBD, methylhydrazine, hydrazine and DABCO in DMSO and will use them to derive the nucleophilicity parameters of these nucleophiles according to eq. 1.

In order to make the comparison between N- and P-nucleophilic centers possible, we also wanted to include data for some phosphanes, which have previously been characterized in dichloromethane.[18] Due to their high susceptibility to oxidation, we were not able to determine the nucleophilicities of phosphanes in DMSO and employed acetonitrile to study their reactions with reference electrophiles, as there are plenty of rate constants already available for N-nucleophiles in this solvent.[10c,d,f-h,12b-d,13a,14,15]

1.2. Results and Discussion

1.2.1. Kinetics of the Reactions of Neutral Nucleophiles with Benzhydrylium Ions and Quinone Methides

Methods employed for kinetic measurements

The rates of the reactions of DBN (**1**), DBU (**2**), TBD (**3**), hydrazines (**4**, **5**) and phosphanes (**6**, **7**, **8**) with reference electrophiles **10a-m** (Table 1.1), were studied spectrophotometrically by following the decays of the absorbances of the coloured electrophiles. Conventional and stopped-flow methods employed for these studies have been described earlier.[9] The experiments were performed under pseudo-first-order conditions by combining benzhydrylium tetrafluoroborates or quinone methides with more than 8 equivalents of the nucleophiles in DMSO or acetonitrile.

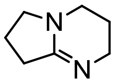

1

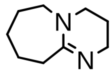

2

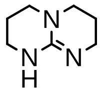

3

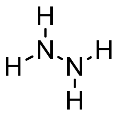

4

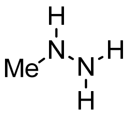

5

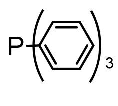

6

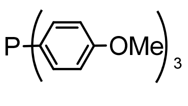

7

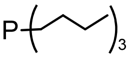

8

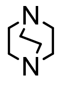

9

The reactions of DABCO (**9**) even with moderately reactive benzhydrylium ions (E > -9) were too fast to be followed by a stopped-flow method, while very small conversions were observed in the reactions with more stabilized reference electrophiles because of the small equilibrium constants. The laser-flash photolysis technique was therefore employed to study the reactivity of DABCO towards reference electrophiles **10i-l** in DMSO.

Table 1.1. List of the reference electrophiles used in this study.

Reference electrophile			E^a
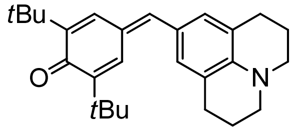		jul(tBu)$_2$QM (**10a**)	-17.90
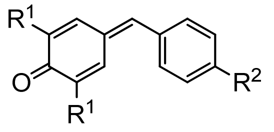	R^1 = tBu, R^2 = NMe_2	dma(tBu)$_2$QM (**10b**)	-17.29
	R^1 = tBu, R^2 = OMe	ani(tBu)$_2$QM (**10c**)	-16.11
	R^1 = tBu, R^2 = Me	tol(tBu)$_2$QM (**10d**)	-15.83
	R^1 = Ph, R^2 = NMe_2	dma(Ph)$_2$QM (**10e**)	-13.39
	R^1 = Ph, R^2 = OMe	ani(Ph)$_2$QM (**10f**)	-12.18
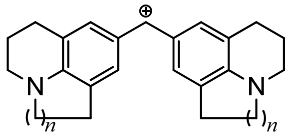	$n = 1$	(lil)$_2$CH$^+$ (**10g**)	-10.04
	$n = 2$	(jul)$_2$CH$^+$ (**10h**)	-9.45
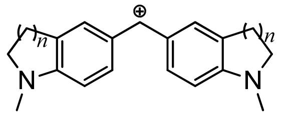	$n = 1$	(ind)$_2$CH$^+$ (**10i**)	-8.76
	$n = 2$	(thq)$_2$CH$^+$ (**10j**)	-8.22
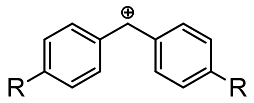	R = N-pyrrolidino	(pyr)$_2$CH$^+$ (**10k**)	-7.69
	R = NMe_2	(dma)$_2$CH$^+$ (**10l**)	-7.02
	R = N-morpholino	(mor)$_2$CH$^+$ (**10m**)	-5.53

(a) Electrophilicity parameters are taken from ref. 9

In previous investigations, benzhydryl cations **10** and other carbocations have usually been generated in dichloromethane or acetonitrile solutions with a 266 nm laser pulse from the precursors (usually corresponding halides,[19] phosphonium,[20] or ammonium[10d] ions) which had significant UV absorbances at this wavelength. In our case it was problematic to use the standard procedure, as DMSO also has a significant absorption coefficient at this wavelength, which would prevent a sufficient excitation of the precursor molecules in the usual experimental setup[21] featuring a 90° angle between pump and probe pulses. An alternative method of generation of cations with a 355 nm pulse is known, which employs 3,4,5-triamino-substituted pyridines as photoleaving groups which absorb in the near-UV range.[12d] However, these compounds give stable adducts only with benzhydrylium ions which are more reactive than **10l** and can be expected to react with **9** with rate constants close to the diffusion limit. The rate constants for these reactions thus would not provide much quantitative information about the nucleophilic reactivity of **9** in DMSO.

For measuring rate constants for activation-controlled reactions of **9** with less reactive reference electrophiles in DMSO, we therefore used nucleophile **9** as the photoleaving group and employed a laser flash photolysis setup with a near-parallel geometry (~ 15°) between pump and probe pulses (266nm), which allows the detection of the photo-products at precisely the same spot where the excitation pulse hits the sample solution.

The solutions of the precursors were freshly prepared prior to use by combining solutions of **9** and benzhydrylium tetrafluoroborates **10i-l** in DMSO. Benzhydrylium ions were generated by laser-flash photolysis (7 ns pulse, 266 nm) of thus prepared solutions. Subsequently, the UV-vis absorbance decays of the cations were monitored in the presence of an excess of **9**.

Evaluation of kinetic data

All reactions of benzhydrylium ions with **1-5** and **8** as well as the reactions of **9** with **10j-l** proceeded with quantitative formation of adducts, and complete consumption of the electrophiles was observed in the UV-vis spectra. A typical absorbance decay of the electrophile is shown in Figure 1.1.

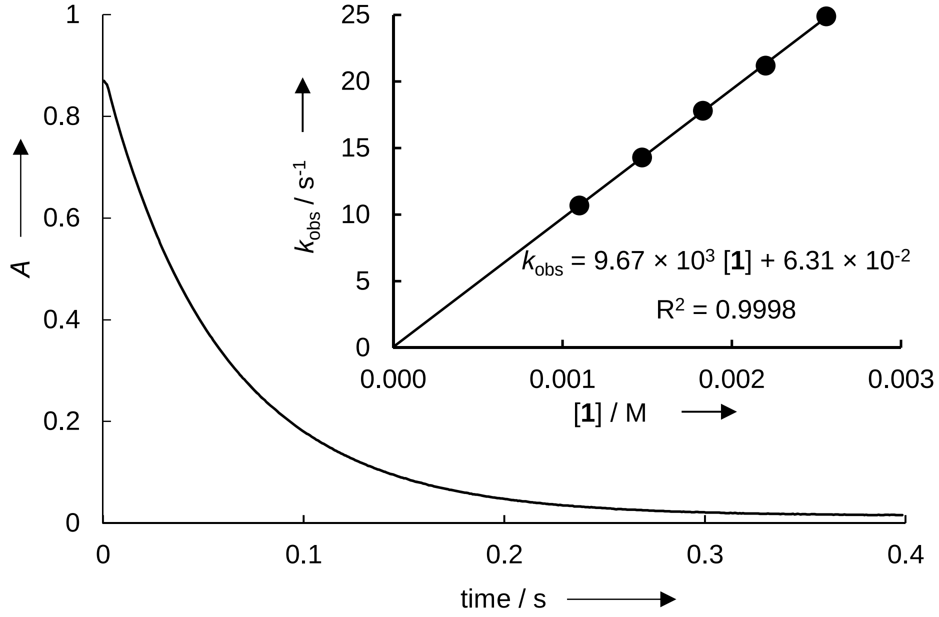

Figure 1.1. Plot of the absorbance (λ = 630 nm) versus *t* for the reaction of **1** with **10g** in DMSO at 20°C. Inset: Plot of the observed pseudo-first-order rate constants versus the concentrations of **1**.

In some combinations of triarylphosphanes with benzhydrylium ions, as well as in the reaction of **9** with **10i** and some reactions of other nitrogen nucleophiles with quinone methides, the electrophiles were consumed incompletely (an example is given in Figure 1.2). An analogous behaviour of triarylphosphanes in the reactions with benzhydrylium ions had previously been observed in dichloromethane.[18] As stated before, very low conversions were observed in the reactions of **9** with **10g,h** and therefore no kinetic data could be obtained for these reactions.

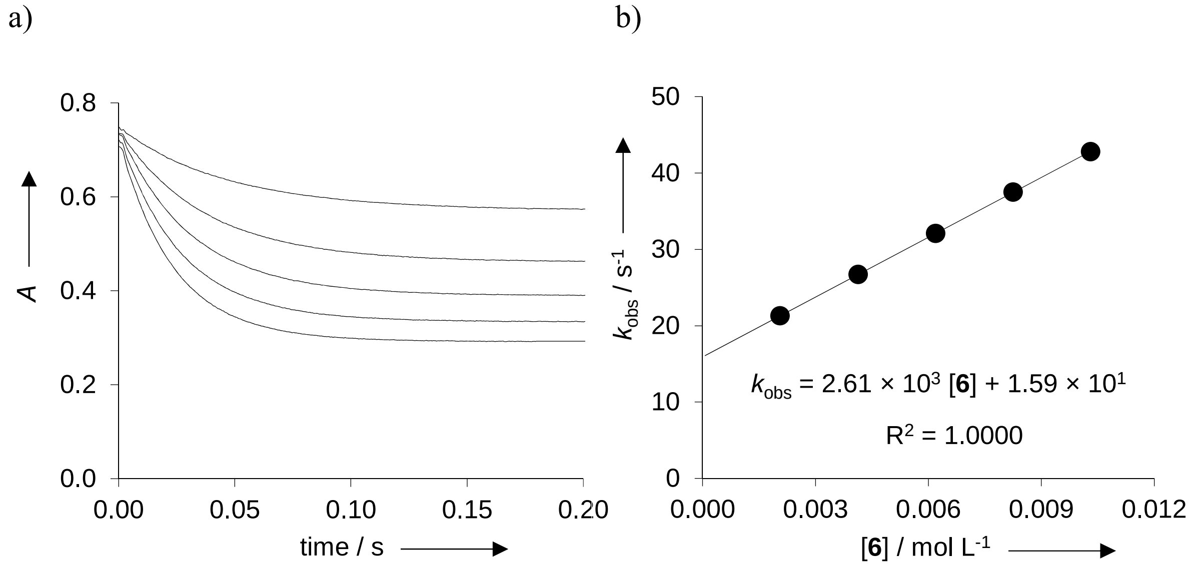

Figure 1.2. a) Plots of the absorbance (λ = 635 nm) versus t for the reactions of **6** with **10h** (c_0 = 7.88 × 10^{-6} M) at different concentrations of **6** (2.06 × 10^{-3} – 1.03 × 10^{-2} M) in acetonitrile at 20°C. b) Plot of the observed pseudo-first-order rate constants versus the concentrations of **6**.

For all studied combinations, except the reaction of **3** with **10d** (it will be discussed later), the pseudo-first-order rate constants k_{obs} (s^{-1}) were obtained by least-squares fitting of the monoexponential function $A = A_0\, e^{-k_{obs}t} + C$ to the time-dependent absorbances decays of the electrophiles. Plots of k_{obs} versus the nucleophile concentrations were linear for all reactions of **1, 2, 4** and **6-9** with the reference electrophiles **10**. The second-order rate constants k_2 (M^{-1} s^{-1}) were obtained from the slopes of these plots, according to Equation 2.

$$k_{obs} = k_2\,[\mathrm{Nu}] + k_0 \qquad (2)$$

The correlations between k_{obs} and nucleophile concentrations for the reactions of **3** with **10d** and of **5** with **10a,b,d** showed upward curvatures (Figure 1.3). This feature indicates that the attack of the nucleophile on the quinone methide is followed by a rate-determining proton transfer step, in which a second nucleophile molecule acts as general base catalyst (Scheme 1.1). Similar behavior was previously observed for the reactions of secondary amines and hydrazines with quinone methides,[10f,h] as well as with thiocarbonates,[22] thionobenzoates,[23] and activated esters of indole-3-acetic acid.[24] As the direct determination of k_2 from the slopes of the plots of k_{obs} versus [Nu] was not possible in these cases, the following method of evaluation was used for these kinetic data.

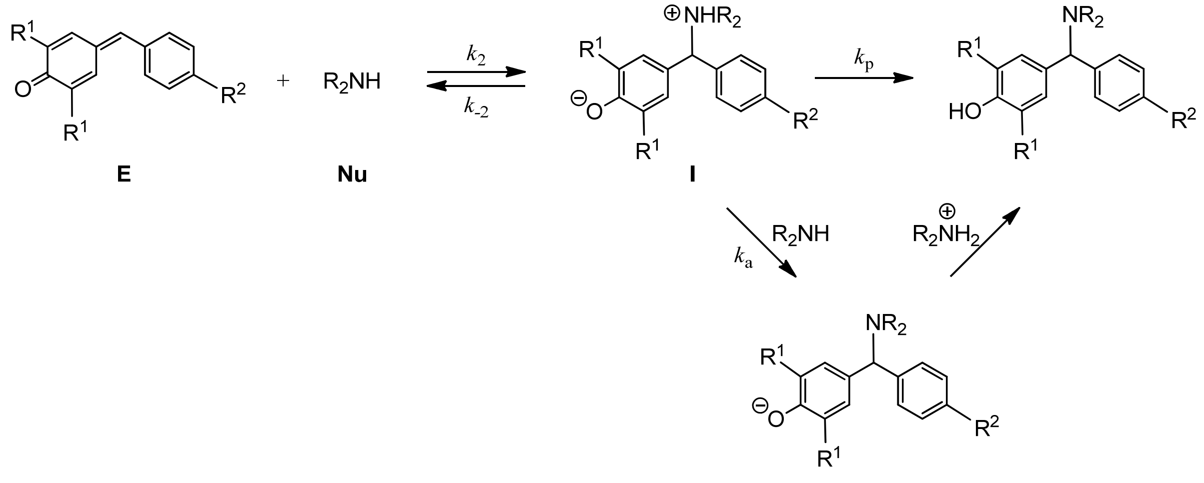

Scheme 1.1. Reactions of secondary amines with quinone methides.

The change in the concentrations of the electrophile **E** and zwitterionic intermediate **I** can be described by Equations 3 and 4.

$$-\frac{\mathrm{d[E]}}{\mathrm{dt}} = k_2[\mathrm{E}]\cdot[\mathrm{Nu}] - k_{-2}[\mathrm{I}] \qquad (3)$$

$$\frac{\mathrm{d[I]}}{\mathrm{dt}} = k_2[\mathrm{E}]\cdot[\mathrm{Nu}] - k_{-2}[\mathrm{I}] - k_{\mathrm{a}}[\mathrm{I}]\cdot[\mathrm{Nu}] - k_p[\mathrm{I}] \qquad (4)$$

When a steady-state assumption is made for the concentration of the intermediate **I** (Equation 5), the rate law for the concentration of the electrophile will be transformed to Equation 6:

$$\frac{\mathrm{d[I]}}{\mathrm{dt}} = 0 \Rightarrow [I] = \frac{k_2[\mathrm{E}]\cdot[\mathrm{Nu}]}{k_{-2} + k_{\mathrm{a}}[\mathrm{Nu}] + k_{\mathrm{p}}} \qquad (5)$$

$$-\frac{\mathrm{d[E]}}{\mathrm{dt}} = k_2[\mathrm{E}]\cdot[\mathrm{Nu}] - k_{-2}\frac{k_2[\mathrm{E}]\cdot[\mathrm{Nu}]}{k_{-2} + k_{\mathrm{a}}[\mathrm{Nu}] + k_{\mathrm{p}}} = k_2[\mathrm{E}]\cdot[\mathrm{Nu}]\cdot\left(\frac{k_{\mathrm{a}}[\mathrm{Nu}] + k_{\mathrm{p}}}{k_{-2} + k_{\mathrm{a}}[\mathrm{Nu}] + k_{\mathrm{p}}}\right) \qquad (6)$$

Thus, the expression for k_{obs} is formulated in Equation 7:

$$k_{\text{obs}} = k_2[\text{Nu}] \cdot \left(\frac{k_{\text{a}}[\text{Nu}] + k_{\text{p}}}{k_{-2} + k_{\text{a}}[\text{Nu}] + k_{\text{p}}} \right) \tag{7}$$

Finally, if the direct proton transfer is neglected (k_{p} is assumed to be much smaller than $k_{-2} + k_{\text{a}}[\mathbf{Nu}]$), Equation 7 is reduced to Equation 8. The transformation of the latter will finally give Equation 9, which suggests the linearity of the plot of $[\mathbf{Nu}]/k_{\text{obs}}$ versus $1/[\mathbf{Nu}]$.

$$k_{\text{obs}} = \frac{k_{\text{a}} k_2 [\text{Nu}]^2}{k_{-2} + k_{\text{a}}[\text{Nu}]} \tag{8}$$

$$\frac{[\text{Nu}]}{k_{\text{obs}}} = \frac{1}{k_2} + \frac{k_{-2}}{k_2 k_{\text{a}} [\text{Nu}]} \tag{9}$$

Indeed, the plots of $[\mathbf{Nu}]/k_{\text{obs}}$ versus $1/[\mathbf{Nu}]$ were found to be linear for the reactions of **5** with **10a,b,d** (Figure 1.3), which shows that the formalism holds for these cases in a wide range of concentrations.

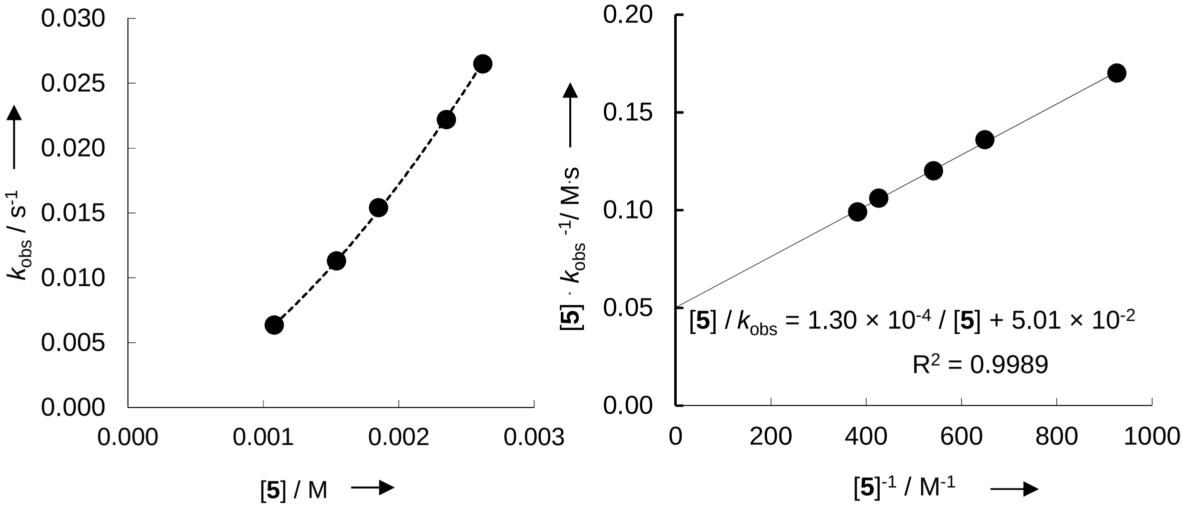

Figure 1.3. The plot of k_{obs} versus [**5**] (on the left) and [**5**] / k_{obs} versus 1 / [**5**] (on the right) for the reaction of **5** with quinone methide **10b** in DMSO at 20°C.

However, this way of evaluation was found to be inapplicable for the reaction of **3** with **10d**. In this case, the assumption d[**I**]/d*t* = 0 appeared to be incorrect: the concentration of the intermediate **I** changes during the reaction. The experimental data were fitted to the exact solution of the system of linear ordinary differential equations 3 and 4 using MATLAB program (for details, see the experimental part). The plot of thus obtained $k_{1\text{calc}}$ values versus [**3**] was linear and went down through the origin, as expected from the model, and the rate constant k_2 was derived from the slope of this plot.

Second-order rate constants for the reactions of **1-5** and **9** with reference electrophiles **10** in DMSO are listed in Table 1.2.

Table 1.2. Second-order rate constants (k_2, DMSO 20°C) for the reactions of benzhydrylium tetrafluoroborates and quinone methides with N-nucleophiles and resulting N and s_N parameters.

Nucleophile	N	s_N	Reference electrophile	k_2 / $M^{-1}s^{-1}$
DBN (**1**)	20.40	0.39	ani(Ph)$_2$QM (**10f**)	1.63×10^3
			(lil)$_2$CH$^+$BF$_4^-$ (**10g**)	9.67×10^3
			(jul)$_2$CH$^+$BF$_4^-$ (**10h**)	1.91×10^4
DBU (**2**)	15.11	0.67	(lil)$_2$CH$^+$BF$_4^-$ (**10g**)	2.56×10^3
			(jul)$_2$CH$^+$BF$_4^-$ (**10h**)	6.78×10^3
			(ind)$_2$CH$^+$BF$_4^-$ (**10i**)	1.60×10^4
			(thq)$_2$CH$^+$BF$_4^-$ (**10j**)	4.68×10^4
TBD (**3**)	19.15	0.57	ani(*t*Bu)$_2$QM (**10c**)	5.20×10^1
			dma(Ph)$_2$QM (**10e**)	1.75×10^3
			ani(Ph)$_2$QM (**10f**)	1.00×10^4
			(lil)$_2$CH$^+$BF$_4^-$ (**10g**)	9.75×10^4
			(jul)$_2$CH$^+$BF$_4^-$ (**10h**)	4.05×10^5
Hydrazine monohydrate (**4**)	19.21	0.47	jul(*t*Bu)$_2$QM (**10a**)	3.37
			tol(*t*Bu)$_2$QM (**10d**)	4.06×10^1
			ani(Ph)$_2$QM (**10f**)	2.94×10^3
			(lil)$_2$CH$^+$BF$_4^-$ (**10g**)	1.56×10^4
			(jul)$_2$CH$^+$BF$_4^-$ (**10h**)	3.59×10^4
			(ind)$_2$CH$^+$BF$_4^-$ (**10i**)	6.60×10^4
Methylhydrazine (**5**)	19.89	0.52	jul(*t*Bu)$_2$QM (**10a**)	1.01×10^1
			dma(*t*Bu)$_2$QM (**10b**)	2.00×10^1
			tol(*t*Bu)$_2$QM (**10d**)	1.36×10^2
			ani(Ph)$_2$QM (**10f**)	1.84×10^4
			(lil)$_2$CH$^+$BF$_4^-$ (**10g**)	9.18×10^4
			(jul)$_2$CH$^+$BF$_4^-$ (**10h**)	4.27×10^5
			(ind)$_2$CH$^+$BF$_4^-$ (**10i**)	4.32×10^5

Nucleophile	N	s_N	Reference electrophile	k_2 / M^{-1}s^{-1}
DABCO (**9**)	16.62	0.89	(lil)$_2$CH$^+$BF$_4^-$ (**10g**)	-
			(jul)$_2$CH$^+$BF$_4^-$ (**10h**)	-
			(ind)$_2$CH$^+$BF$_4^-$ (**10i**)	9.79×10^6
			(thq)$_2$CH$^+$BF$_4^-$ (**10j**)	2.65×10^7
			(pyr)$_2$CH$^+$BF$_4^-$ (**10k**)	8.77×10^7
			(dma)$_2$CH$^+$BF$_4^-$ (**10l**)	1.31×10^8

As mentioned above, some reactions of triarylphosphanes with highly stabilized benzhydrylium ions were reversible and did not proceed with quantitative consumption of the electrophile. In such cases positive intercepts were observed in the plots of k_{obs} versus [**Nu**] (Figure 1.2, graph on the right), which have been shown[18] to correspond to the first-order rate constants for the decomposition of the resulting phosphonium ions back to the reactants (Equation 10). Thus, we were able to determine k_{-1} for the reactions of **6** with benzhydrylium tetrafluoroborates **10g-j** and derive the corresponding equilibrium constants as $K = k_2/k_{-1}$. These were found to be in a very good agreement with those previously determined by another method[25] (for comparison of the equilibrium constants, see the experimental part).

$$\mathrm{Ar_2CH^+\,BF_4^-} + \mathrm{PR_3} \xrightleftharpoons[k_{-1}]{k_2} \mathrm{Ar_2CH\text{-}PR_3^+\,BF_4^-} \qquad (10)$$

The reactivities of phosphanes **6-8** towards reference benzhydrylium ions and quinone methides **10** and the rate constants for the backward reactions, obtained from the intercepts of the plots of k_{obs} vs [**6**] in acetonitrile are listed in Table 1.3.

Table 1.3. Second-order rate constants (k_2, acetonitrile 20°C) for the reactions of benzhydrylium tetrafluoroborates and quinone methides with phosphanes and resulting N and s_N parameters. The rate constants for the backward reaction (k_{-1}) are given where available.

Nucleophile	N	s_N	Reference electrophile	k_2 / M^{-1}s^{-1}	k_{-1} / s^{-1}
Ph$_3$P (**6**)	15.43	0.54	(lil)$_2$CH$^+$BF$_4^-$ (**10g**)	6.96×10^2	8.23
			(jul)$_2$CH$^+$BF$_4^-$ (**10h**)	2.61×10^3	1.59×10^1
			(ind)$_2$CH$^+$BF$_4^-$ (**10i**)	2.84×10^3	1.85
			(thq)$_2$CH$^+$BF$_4^-$ (**10j**)	1.10×10^4	2.50
			(dma)$_2$CH BF$_4^-$ (**10l**)	3.33×10^{4} [a]	-
			(mor)$_2$CH$^+$BF$_4^-$ (**10m**)	2.41×10^5	-
P(4-MeOC$_6$H$_4$)$_3$ (**7**)	17.14	0.55	(lil)$_2$CH$^+$BF$_4^-$ (**10g**)	6.25×10^3	-
			(jul)$_2$CH$^+$BF$_4^-$ (**10h**)	2.43×10^4	-

Nucleophile	N	s_N	Reference electrophile	k_2 / M^{-1}s^{-1}	k_{-1} / s^{-1}
			(ind)$_2$CH$^+$BF$_4^-$ (**10i**)	2.61×10^4	-
			(thq)$_2$CH$^+$BF$_4^-$ (**10j**)	1.03×10^5	-
			(dma)$_2$CH BF$_4^-$ (**10l**)	3.25×10^5	-
*n*Bu$_3$P (**8**)	17.94	0.54	dma(Ph)$_2$QM (**10e**)	2.88×10^2	-
			ani(Ph)$_2$QM (**10f**)	1.12×10^3	-
			(jul)$_2$CH$^+$BF$_4^-$ (**10h**)	4.53×10^4	-
			(ind)$_2$CH$^+$BF$_4^-$ (**10i**)	6.49×10^4	-
			(dma)$_2$CH$^+$BF$_4^-$ (**10l**)	7.58×10^5	-

(a) From ref. 18

1.2.2. Determination of the Nucleophilicity and Sensitivity Parameters

When the logarithms of the second-order rate constants of the reactions of **1-8** with benzhydrylium ions and quinone methides **10** were plotted versus the previously described electrophilicity parameters of the reference systems,[9b,c] straight lines were obtained (Figure 1.4). The nucleophilicity and sensitivity parameters N and s_N for **1-8** were derived from these correlations and are listed in Tables 1.2 and 1.3. In the case of DABCO (**9**) the correlation line bends downwards close to the diffusion limit; for this reason only three rate constants could be used for the determination of its N and s_N parameters. They are not very accurate therefore, but still give a good idea of the reactivity of **9** in DMSO.

a)

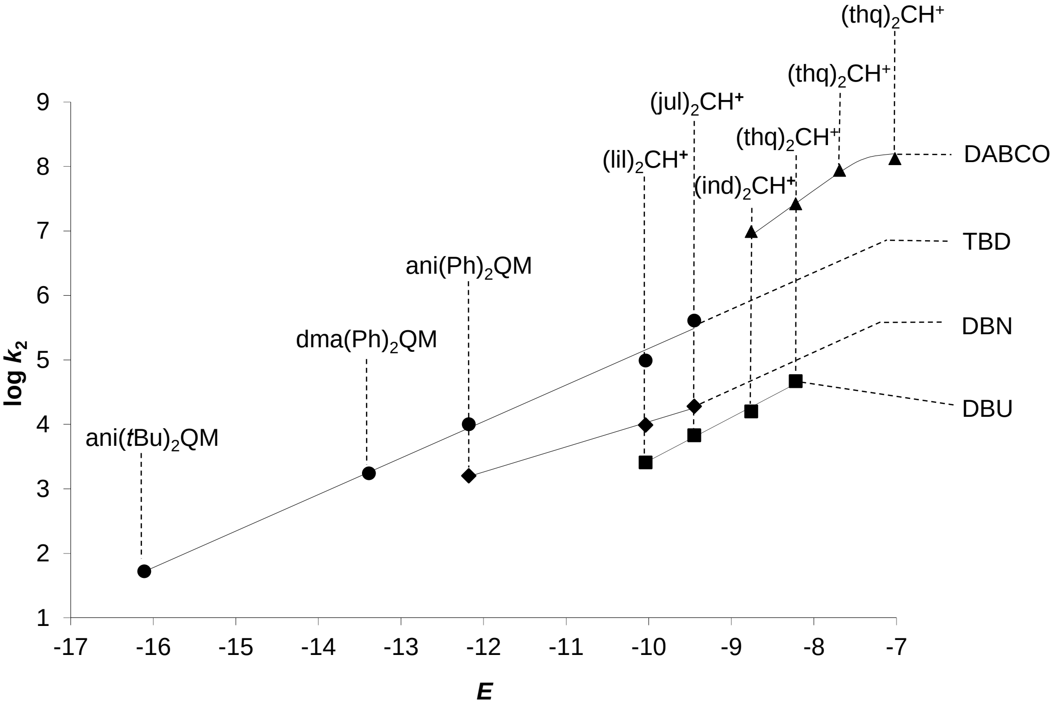

b)

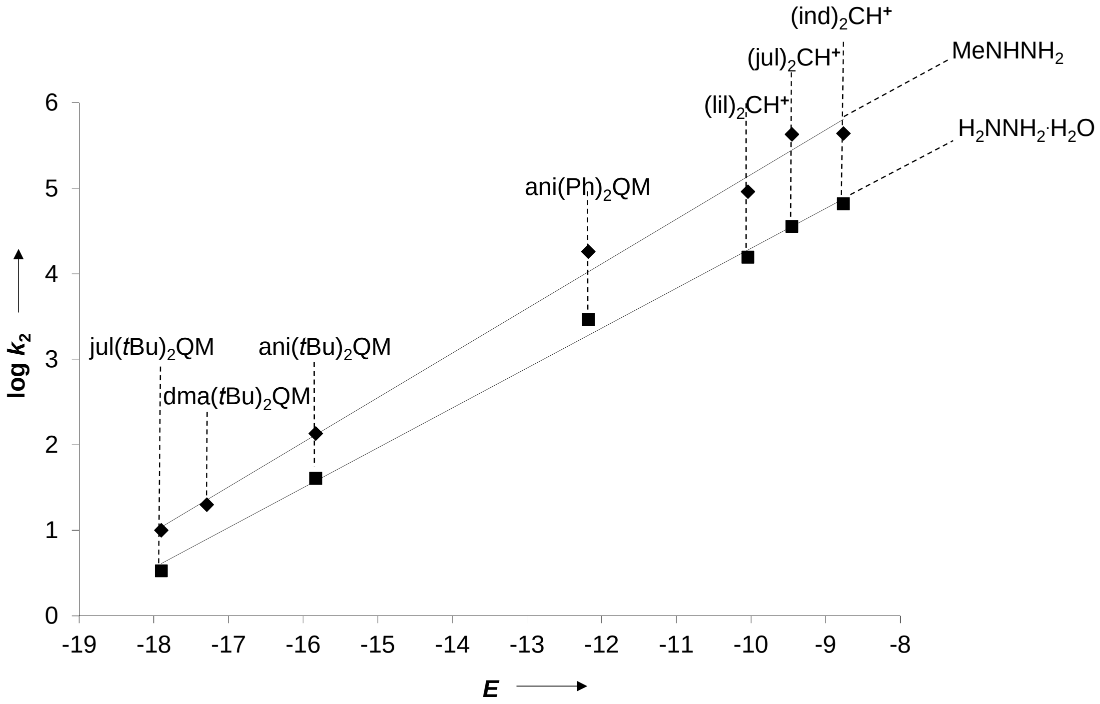

c)

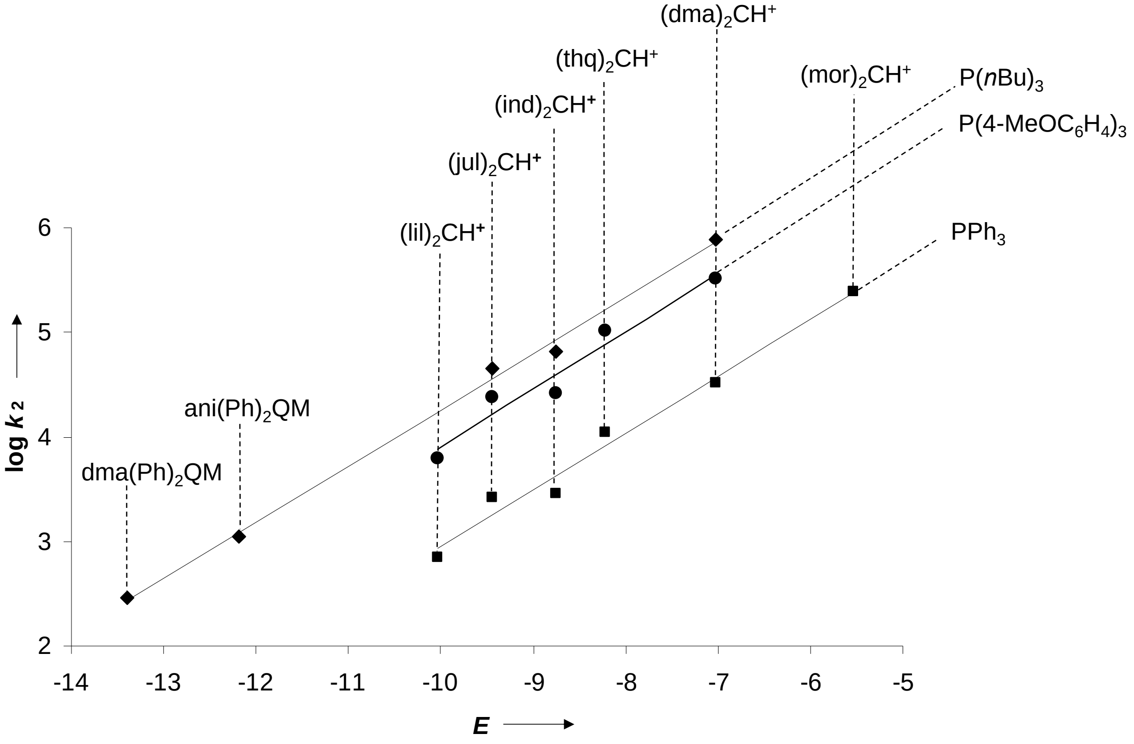

Figure 1.4. Correlation of the logarithms of the second-order rate constants with previously reported *E* parameters for the reactions of a) **1-3** and **9** (DMSO, 20°C), b) **4** and **5** **(**DMSO, 20°C) and c) **6-8** (acetonitrile, 20°C) with reference electrophiles.

1.2.3. Influence of the Solvent on the Reactivities of Neutral Nucleophiles towards Benzhydrylium Ions

Comparison of the obtained reactivity parameters for several neutral nitrogen and phosphorus nucleophiles with those determined previously in other solvents clearly indicates that the nucleophilicity parameters *N* alone cannot be used as a guideline for predicting relative reactivities of a given nucleophile in different media. For example, the rate constants for the reactions of **7** with benzhydrylium ions **10** in dichloromethane and acetonitrile differ only slightly (Table 1.4), while the *N* parameters for **7** in these media are 16.17 and 17.94, respectively. This phenomenon is reflected in the sensitivity parameters s_N for these nucleophiles, which change significantly with variation of the solvent.

Let us try to analyze these changes, using the data on the reactions of triarylphosphanes with benzhydrylium ions in both dichloromethane and acetonitrile. This system is very suitable for this purpose, as the rate constants for these reactions are in many cases supplemented with the experimentally obtained thermodynamic data.

Table 1.4. Comparison of the second-order rate constants for the reactions of nucleophiles **1-9** with reference electrophiles **10** in different solvents at 20°C.

		k_2 / $M^{-1}s^{-1}$		
Nucleophile	Ar_2CH^+	in CH_2Cl_2	in MeCN	in DMSO
1	(lil)$_2CH^+BF_4^-$ (**10g**)	1.51×10^{4a}	1.38×10^{4b}	9.67×10^3
	(jul)$_2CH^+BF_4^-$ (**10h**)	3.20×10^{4a}	3.98×10^{4b}	1.91×10^4
	(ind)$_2CH^+BF_4^-$ (**10i**)	1.50×10^{5a}	9.44×10^{4b}	-
	(thq)$_2CH^+BF_4^-$ (**10j**)	3.20×10^{5a}	2.43×10^{5b}	-
2	(lil)$_2CH^+BF_4^-$ (**10g**)	-	4.46×10^{3b}	2.56×10^3
	(jul)$_2CH^+BF_4^-$ (**10h**)	-	1.36×10^{4b}	6.78×10^3
	(ind)$_2CH^+BF_4^-$ (**10i**)	-	3.17×10^{4b}	1.60×10^4
	(thq)$_2CH^+BF_4^-$ (**10j**)	-	8.43×10^{4b}	4.68×10^4
3	(lil)$_2CH^+BF_4^-$ (**10g**)	4.24×10^{4a}	-	9.75×10^4
	(jul)$_2CH^+BF_4^-$ (**10h**)	9.72×10^{4a}	-	4.05×10^5
4	(lil)$_2CH^+BF_4^-$ (**10g**)	-	3.41×10^{3c}	1.56×10^4
	(jul)$_2CH^+BF_4^-$ (**10h**)	-	8.74×10^{3c}	3.59×10^4
	(ind)$_2CH^+BF_4^-$ (**10i**)	-	2.09×10^{4c}	6.60×10^4
5	(lil)$_2CH^+BF_4^-$ (**10g**)	-	3.32×10^{4c}	9.18×10^4
	(ind)$_2CH^+BF_4^-$ (**10i**)	-	2.15×10^{5c}	4.32×10^5
6	(lil)$_2CH^+BF_4^-$ (**10g**)	4.85×10^{2d}	6.96×10^2	-

		k_2 / $M^{-1}s^{-1}$		
Nucleophile	Ar_2CH^+	in CH_2Cl_2	Nucleophile	Ar_2CH^+
	$(jul)_2CH^+BF_4^-$ (**10h**)	2.56×10^{3d}	2.61×10^{3}	-
	$(dma)_2CH^+BF_4^-$ (**10l**)	5.73×10^{4d}	3.33×10^{4d}	1.51×10^{4d}
	$(mor)_2CH^+BF_4^-$ (**10m**)	4.27×10^{5d}	2.41×10^{5}	-
7	$(lil)_2CH^+BF_4^-$ (**10g**)	5.07×10^{3d}	6.25×10^{3}	-
	$(jul)_2CH^+BF_4^-$ (**10h**)	1.93×10^{4d}	2.43×10^{4}	-
	$(thq)_2CH^+BF_4^-$ (**10j**)	1.03×10^{5d}	1.03×10^{5}	-
	$(dma)_2CH^+BF_4^-$ (**10l**)	4.87×10^{5d}	3.25×10^{5}	-
8	$(jul)_2CH^+BF_4^-$ (**10h**)	1.61×10^{4d}	4.53×10^{4}	-
	$(dma)_2CH^+BF_4^-$ (**10l**)	7.68×10^{5d}	7.58×10^{5}	-
9	$(ind)_2CH^+BF_4^-$ (**10i**)	-	1.10×10^{7e}	9.79×10^{6}
	$(thq)_2CH^+BF_4^-$ (**10j**)	-	2.79×10^{7e}	2.65×10^{7}
	$(pyr)_2CH^+BF_4^-$ (**10k**)	-	6.95×10^{7e}	8.77×10^{7}

(a) k_2 are from ref. 13c. (b) k_2 are from ref. 13a. (c) k_2 are from ref. 10h. (d) k_2 are from ref. 18. (e) k_2 are from ref. 10d.

It was previously shown[18] that the rate constants for the reaction of **6** with **10l** decrease slightly with increasing Gutmann's donor number DN[26] of the solvent. This holds for all three phosphanes **6-8** studied in this work: the reactions with **10l** in dichloromethane are 1.5 to 2 times as fast as in acetonitrile. However, for the combinations of phosphanes with the better stabilized electrophiles **10g** or **10h** the situation is inverted: the rate constants for these reactions in dichloromethane are lower than those in acetonitrile.

We will now try to explain this reactivity crossover using the Marcus equation (11), where $\Delta_r G_0$ is the standard reaction free energy (thermodynamic term), and $\Delta G_0^{\ddagger}$ is the intrinsic barrier (kinetic term, which corresponds to the activation free energy of the reaction at $\Delta_r G_0 = 0$). The advantage of this approach is that it gives the possibility to analyze the contribution of the thermodynamic and intrinsic factors into the activation free energy of the reaction ($\Delta G^{\ddagger}$) separately.

$$\Delta G^{\ddagger} = \Delta G_0^{\ddagger} + 0.5\Delta_r G_0 + (\Delta_r G_0)^2/16\Delta G_0^{\ddagger} \qquad (11)$$

If the quadratic term $(\Delta_r G_0)^2/16\Delta G_0^{\ddagger}$ is neglected,[27] the difference of the activation free energies of the reaction in two solvents ($\delta\Delta G^{\ddagger}$) can be expressed by equation 12.

$$\Delta G^{\ddagger}(_{\mathrm{MeCN}}) - \Delta G^{\ddagger}(_{\mathrm{CH_2Cl_2}}) = \delta\Delta G^{\ddagger} = \delta\Delta G_0^{\ddagger} + 0.5\delta\Delta_r G_0 \qquad (12)$$

Let us see how $\delta\Delta G^{\ddagger}$ changes as we go from the highly stabilized carbocations to the more reactive ones.)

Initially, the positive charge of the stabilized benzhydrylium ion is highly delocalized. In the product, on the contrary, it is localized on the phosphorus atom of the resulting phosphonium ion. Consequently, the loss of charge delocalization during the reaction will generally be facilitated more efficiently by the more polar solvent (acetonitrile in this case). As the stability and the extent of the delocalization of the charge in the starting carbocation increases, this effect should get more pronounced. It will influence the thermodynamic term $\delta\Delta_rG_0$, which will systematically decrease (become more negative) with the decrease in the reactivity of the benzhydrylium ion. This hypothesis is confirmed by the equilibrium constants for the reactions of the phosphanes with benzhydrylium ions in both solvents (Table 1.5) and the graph in Figure 1.5. The equilibrium constants for the reactions of **6** with benzhydrylium ions, which were used for calculating the data points in Figure 1.5a are listed in Table 1.5.

Table 1.5. Thermodynamic data for the reactions of **6** with benzhydrylium ions **10g-j** and **10l** in dichloromethane and acetonitrile at 20°C.

Electrophile	In acetonitrile		In dichloromethane		
	K / M^{-1}	Δ_rG^0/ kJ·mol^{-1}	K / M^{-1}	Δ_rG^0, kJ·mol^{-1}	$\delta\Delta_rG^0$, kJ·mol^{-1}
$(lil)_2CH^+BF_4^-$ (**10g**)	7.77×10^{1a}	-10.6	1.91×10^{1d}	-7.2	-3.4
$(jul)_2CH^+BF_4^-$ (**10h**)	1.66×10^{2a}	-12.5	5.57×10^{1d}	-9.8	-2.7
$(ind)_2CH^+BF_4^-$ (**10i**)	1.60×10^{3a}	-18.0	1.21×10^{3d}	-17.3	-0.7
$(thq)_2CH^+BF_4^-$ (**10j**)	4.40×10^{3b}	-20.4	2.27×10^{3d}	-18.8	-1.6
$(dma)_2CH^+BF_4^-$ (**10l**)	8.32×10^{4c}	-27.6	1.26×10^{5d}	-28.6	1.0

(a) K are from ref. 25. (b) K is calculated using k_2 and k_{-1} (Eq. 10) from Table 1.3. (c) K is calculated from equation $\log K = LA + LB$, the values of LA for benzhydrylium ions and LB for **6** in acetonitrile are taken from ref. 25. (d) K are from ref. 18.

On the other hand, redistribution of the charge and rehybridization of the carbocationic center in the course of the reaction, accompanied by the solvent rearrangement, will be reflected in the intrinsic term of Equation 12. In acetonitrile one can expect a higher extent of carbocation solvation and consequently a higher energy of the solvent rearrangement along the reaction coordinate than in dichloromethane, which will result in $\delta\Delta G_0^{\ddagger} > 0$. The values of $\delta\Delta G_0^{\ddagger}$ for the reactions of **6** with **10g-j** and **10l** calculated from the Marcus equation (11) are given in Table 1.6 and the trend for $\delta\Delta G_0^{\ddagger}$ is shown in Figure 1.5b.

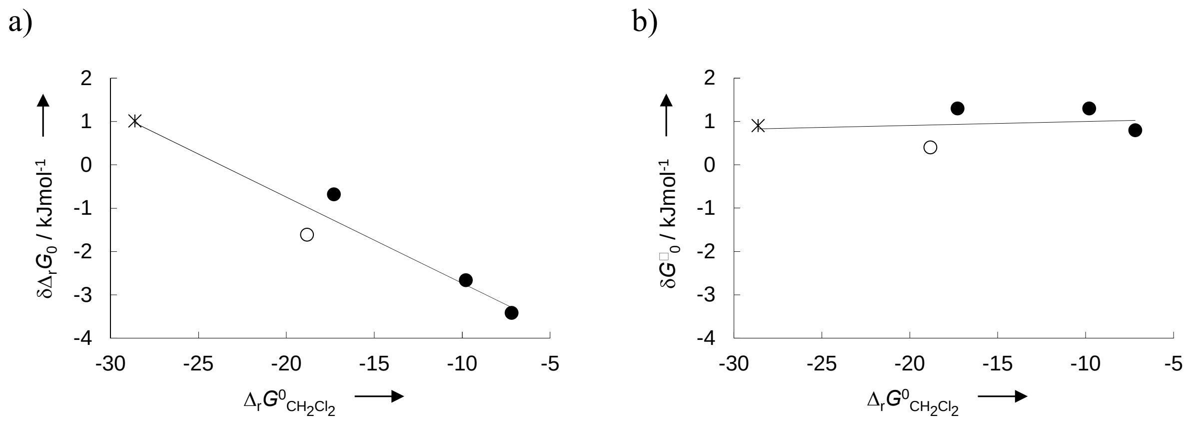

Figure 1.5. The dependence of a) the thermodynamic term $\delta\Delta_r G_0$ and b) the intrinsic term $\delta\Delta G_0^{\ddagger}$ in Equation 12 for the combination of triphenylphosphane **6** with benzhydrylium ions **10g-j** and **10l** on the exergonity of the reaction in dichloromethane.

● The equilibrium constants were directly measured. ○ The equilibrium constant was determined indirectly. ✳ The equilibrium constant was calculated.

Table 1.6. Activation free energies and intrinsic barriers for the reactions of **6** with benzhydrylium ions **10g-j** and **10l** in dichloromethane and acetonitrile at 20°C.

Electrophile	In acetonitrile		In dichloromethane		
	$\Delta G^{\ddagger}$, kJ·mol$^{-1a,c}$	$\Delta G_0^{\ddagger}$, kJ·mol^{-1b}	$\Delta G^{\ddagger}$, kJ·mol^{-1a}	$\Delta G_0^{\ddagger}$, kJ·mol^{-1b}	$\delta\Delta G_0^{\ddagger}$, kJ·mol^{-1}
$(lil)_2CH^+BF_4^-$ (**10g**)	55.8	61.0	56.7^d	60.2	0.8
$(jul)_2CH^+BF_4^-$ (**10h**)	52.6	58.7	52.6^d	57.4	1.3
$(ind)_2CH^+BF_4^-$ (**10i**)	52.3	61.0	51.4^e	59.7	1.3
$(thq)_2CH^+BF_4^-$ (**10j**)	49.0	58.8	49.4^e	58.4	0.4
$(dma)_2CH^+BF_4^-$ (**10l**)	46.3	59.3	45.0^d	58.4	0.9

(a) $\Delta G^{\ddagger}$ are calculated from the rate constants using the Eyring equation. (b) The values of $\Delta G_0^{\ddagger}$ are calculated using the Marcus equation (11). (c) The rate constants are taken from Table 1.3. (d) The rate constants are taken from ref. 18. (e) The rate constants are calculated using Equation 1 using N and s_N parameters for **6** from ref. 18.

When the $\delta\Delta_r G_0$ is negative enough to compensate the positive $\delta\Delta G_0^{\ddagger}$, so that $\delta\Delta G^{\ddagger}$ is negative, the reaction in acetonitrile is faster, which is observed for highly stabilized carbocations. It is not the case for more reactive cations, and, consequently, their combinations with phosphanes become faster in dichloromethane.

If this approach based on the Marcus equation and the data for the reactions of benzhydrylium ions with triarylphosphanes is generally applicable for the reactions of reference electrophiles with neutral nucleophiles, this interplay of thermodynamic and intrinsic factors should lead to the systematic increase of the sensitivities of the nucleophiles towards the changes in the reactivities of the cations with decreasing Gutmann's donor number (DN) of the solvent. This hypothesis is confirmed by the fact that for most neutral nucleophiles characterized in our group (enamines, enol ethers, aliphatic amines, amidines, azoles, guanidine TBD, hydrazines), the values of s_N change in the following order: $s_{\mathrm{CH_2Cl_2}} > s_\mathrm{MeCN} > s_\mathrm{DMSO} > s_\mathrm{H_2O}$.[9h] Of course, cases where only a single rate constant for the reaction with one reference electrophile was used for the determination of the N value and the s_N parameter was estimated, can't be taken into consideration.

1.3. Conclusion

The nucleophilicity and sensitivity parameters N and s_N for nitrogen nucleophiles **1-5** and **9** in DMSO and for phosphanes **6-8** in acetonitrile have been derived from the rates of their reactions with reference benzhydrylium ions and quinone methides **10a-m**. Comparison of these data with kinetic data obtained previously in other solvents shows that the sensitivities of neutral nucleophiles towards the changes in the reactivities of the reference electrophiles systematically decrease with increasing the polarity (Gutmann's donor number) of the solvent. The thermodynamic data on the reactions of triarylphosphanes with benzhydrylium ions in dichloromethane and acetonitrile confirm the hypothesis that this change in the sensitivities is caused by interplay of the thermodynamic and the intrinsic factors.

1.S. Experimental Section

1.S.1. General

Materials. The benzhydrylium tetrafluoroborates[9c] **10g-m** and quinone methides[9b,28] **10a-f** were synthesized as described in the literature. Hydrazine monohydrate (**4**·H_2O), triphenylphosphane (**6**), tris-(4-methoxyphenyl)phosphane (**7**) and tributylphosphane (**8**) were purchased and used without further purification. Methylhydrazine (**5**), DBN (**1**), DBU (**2**), TBD (**3**) and DABCO (**9**) were purchased and purified by distillation or sublimation prior to use.

Acetonitrile (>99.9%, extra dry) and DMSO (99.7%, etra dry) were purchased and used without further purification.

Kinetic measurements. The kinetics of the reactions of **1-5** and **9** with the benzhydrylium ions and quinone methides **10** were followed by UV−vis spectroscopy in DMSO or acetonitrile at 20 °C.

J&M technique was used for slow reactions ($\tau 1/2 > 10$ s). The spectra were collected at different times by using a diode array spectrophotometer that was connected to a quartz immersion probe (5 mm light path) by fiber optic cables with standard SMA connectors. All kinetic were carried out in Schlenk glassware under exclusion of moisture. The temperature of the solutions during the kinetic studies was maintained at 20 ± 0.1 °C and monitored with a thermocouple probe that was inserted into the reaction mixture.

Stopped-flow spectrophotometer systems were used for the investigation of faster reactions (10 ms $< \tau 1/2 <$ 10 s). The kinetic runs were initiated by mixing equal volumes of the solutions of the reactants.

Reactions of **9** with **10i-l** (with $\tau 1/2 < 10$ ms) were analyzed by laser-flash photolytic generation of the cations from the corresponding ammonium ions in the presence of excess nucleophile. Solutions of the carbocation precursors were irradiated with a 7 ns pulse from a quadrupled Nd:YAG laser (266 nm, 40−60 mJ/pulse), and a xenon lamp was used as probe light for UV−vis detection. The system was equipped with a fluorescence flow cell and a synchronized pump system, which allows complete exchange of the sample volume between subsequent laser pulses. For each concentration, ≥ 50 individual measurements were averaged.

The nucleophiles **1−9** were used in large excess (>8 equiv) relative to the electrophiles **10** to ensure first-order conditions with $k_{obs} = k_2[\mathrm{Nu}]_0 + k_0$. From the time-dependent decays of the absorbances at λ_{max} of **10**, the first-order rate constants k_{obs} (s^{-1}) were obtained by least-squares fitting to the monoexponential curve $A = A_0\, e^{-k_{\text{obs}}t} + C$. The slopes of plots of k_{obs} versus the concentrations of the nucleophiles yielded the second-order rate constants k_2 (M^{-1} s^{-1}).

1.S.2. Rate constants for DBN (1) in DMSO

Rate constants for the reaction of DBN (**1**) with ani(Ph)$_2$QM (**10f**) at 20°C in DMSO (stopped-flow technique).

No	$[E]_0$/M	$[Nu]_0$/M	$[Nu]_0$/ $[E]_0$	k_{obs}/s^{-1}
1	2.88×10^{-5}	1.10×10^{-3}	38	1.95
2	2.88×10^{-5}	1.47×10^{-3}	51	2.55
3	2.88×10^{-5}	1.83×10^{-3}	64	3.16
4	2.88×10^{-5}	2.20×10^{-3}	76	3.73
5	2.88×10^{-5}	2.56×10^{-3}	89	4.33
$k_2 = 1.63 \times 10^3\ M^{-1}s^{-1}$				

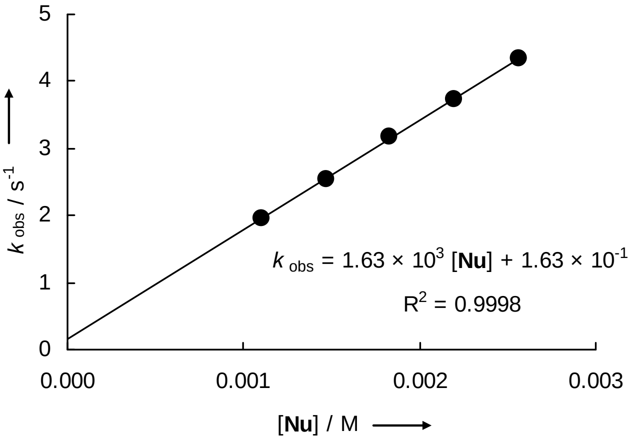

Rate constants for the reaction of DBN (**1**) with (lil)$_2$CH$^+$BF$_4^-$ (**10g**) at 20°C in DMSO (stopped-flow technique).

No	$[E]_0$/M	$[Nu]_0$/M	$[Nu]_0$/ $[E]_0$	k_{obs}/s^{-1}
1	8.17×10^{-6}	1.10×10^{-3}	135	1.07×10^1
2	8.17×10^{-6}	1.47×10^{-3}	180	1.43×10^1
3	8.17×10^{-6}	1.83×10^{-3}	224	1.78×10^1
4	8.17×10^{-6}	2.20×10^{-3}	269	2.12×10^1
5	8.17×10^{-6}	2.56×10^{-3}	313	2.49×10^1
$k_2 = 9.67 \times 10^3\ M^{-1}s^{-1}$				

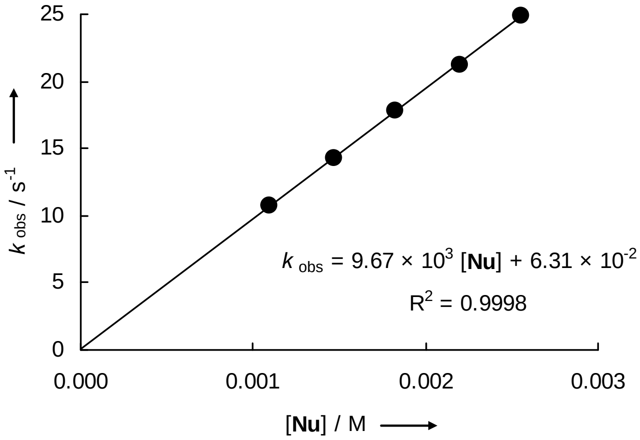

Rate constants for the reaction of DBN (**1**) with $(jul)_2CH^+BF_4^-$ (**10h**) at 20°C in DMSO (stopped-flow technique).

No	$[E]_0$/M	$[Nu]_0$/M	$[Nu]_0$/ $[E]_0$	k_{obs}/s^{-1}
1	9.72×10^{-6}	1.10×10^{-3}	113	2.52×10^{1}
2	9.72×10^{-6}	1.47×10^{-3}	151	3.21×10^{1}
3	9.72×10^{-6}	1.83×10^{-3}	188	3.90×10^{1}
4	9.72×10^{-6}	2.20×10^{-3}	226	4.56×10^{1}
5	9.72×10^{-6}	2.56×10^{-3}	263	5.33×10^{1}

$k_2 = 1.91 \times 10^4$ M^{-1}s^{-1}

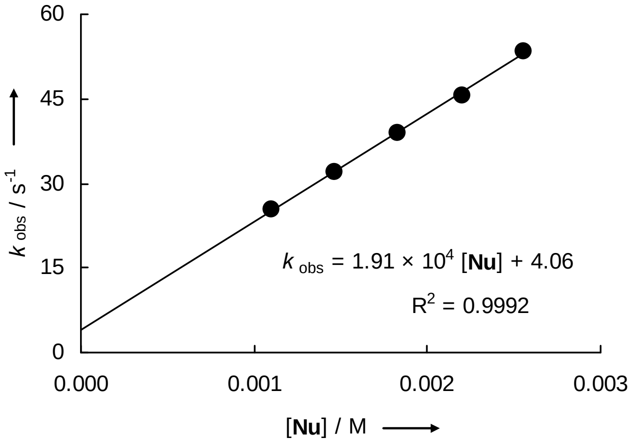

Determination of the nucleophilicity parameters *N* and s_N for DBN (**1**) in DMSO

Rate constants for the reaction of DBN (**1**) with reference electrophiles **10**.

Electrophile	*E*	k_2/M^{-1}s^{-1}	log k_2
ani(Ph)$_2$QM	-12.18	1.63×10^3	3.20
(lil)$_2$CH$^+$	-10.04	9.67×10^3	3.99
(jul)$_2$CH$^+$	-9.45	1.91×10^4	4.28
$N = 20.40$, $s = 0.39$			

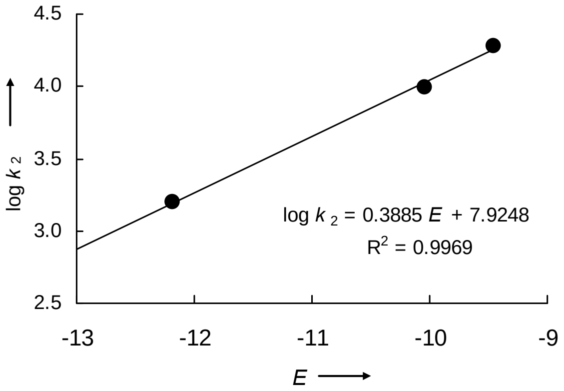

1.S.3. Rate constants for DBU (2) in DMSO.

Rate constants for the reaction of DBU (**2**) with (lil)$_2$CH$^+$BF$_4^-$ (**10g**) at 20°C in DMSO (stopped-flow technique).

No	[E]$_0$ / M	[Nu]$_0$ / M	[Nu]$_0$ / [E]$_0$	k_{obs} / s^{-1}
1	1.97×10^{-5}	5.71×10^{-4}	29	1.65
2	1.97×10^{-5}	1.14×10^{-3}	58	3.13
3	1.97×10^{-5}	1.71×10^{-3}	87	4.54
4	1.97×10^{-5}	2.29×10^{-3}	116	6.02
5	1.97×10^{-5}	2.86×10^{-3}	145	7.53
$k_2 = 2.56 \times 10^3$ M^{-1}s^{-1}				

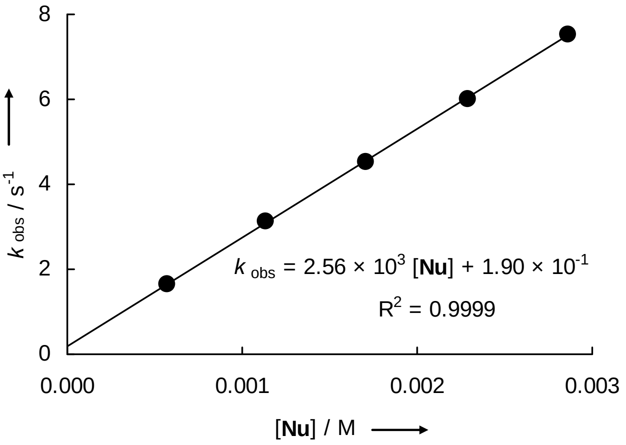

Rate constants for the reaction of DBU (**2**) with $(jul)_2CH^+BF_4^-$ (**10h**) at 20°C in DMSO (stopped-flow technique).

No	$[E]_0$ / M	$[Nu]_0$ / M	$[Nu]_0$ / $[E]_0$	k_{obs} / s^{-1}
1	1.96×10^{-5}	5.71×10^{-4}	29	4.14
2	1.96×10^{-5}	1.14×10^{-3}	58	7.77
3	1.96×10^{-5}	1.71×10^{-3}	87	1.15×10^{1}
4	1.96×10^{-5}	2.29×10^{-3}	117	1.57×10^{1}
5	1.96×10^{-5}	2.86×10^{-3}	146	1.96×10^{1}
$k_2 = 6.78 \times 10^3$ $M^{-1}s^{-1}$				

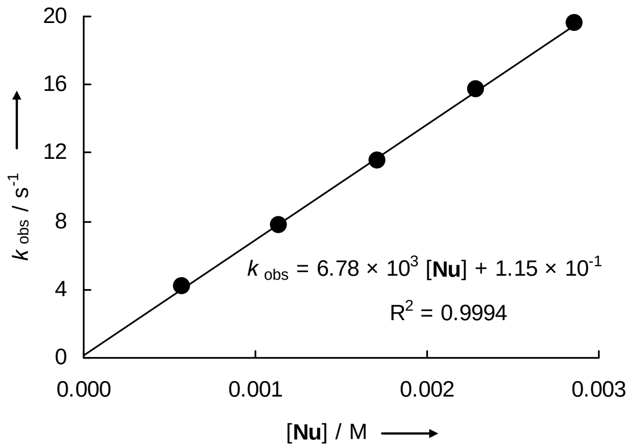

Rate constants for the reaction of DBU (**2**) with $(ind)_2CH^+BF_4^-$ (**10i**) at 20°C in DMSO (stopped-flow technique).

No	$[E]_0$ / M	$[Nu]_0$ / M	$[Nu]_0$ / $[E]_0$	k_{obs} / s^{-1}
1	1.07×10^{-5}	4.47×10^{-4}	42	7.09
2	1.07×10^{-5}	8.93×10^{-4}	83	1.54×10^{1}
3	1.07×10^{-5}	1.34×10^{-3}	125	2.22×10^{1}
4	1.07×10^{-5}	1.79×10^{-3}	167	2.92×10^{1}
5	1.07×10^{-5}	2.23×10^{-3}	208	3.59×10^{1}
$k_2 = 1.60 \times 10^4$ $M^{-1}s^{-1}$				

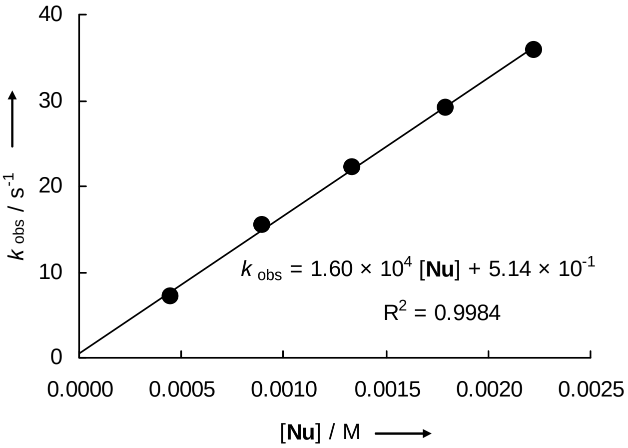

Rate constants for the reaction of DBU (**2**) with $(thq)_2CH^+BF_4^-$ (**10j**) at 20˚C in DMSO (stopped-flow technique).

No	$[E]_0$ / M	$[Nu]_0$ / M	$[Nu]_0$ / $[E]_0$	k_{obs} / s^{-1}
1	4.74×10^{-6}	2.50×10^{-4}	53	1.39×10^{1}
2	4.74×10^{-6}	4.99×10^{-4}	105	2.67×10^{1}
3	4.74×10^{-6}	7.49×10^{-4}	158	3.87×10^{1}
4	4.74×10^{-6}	9.98×10^{-4}	211	4.96×10^{1}
5	4.74×10^{-6}	1.25×10^{-3}	264	6.09×10^{1}

$k_2 = 4.68 \times 10^4$ M^{-1}s^{-1}

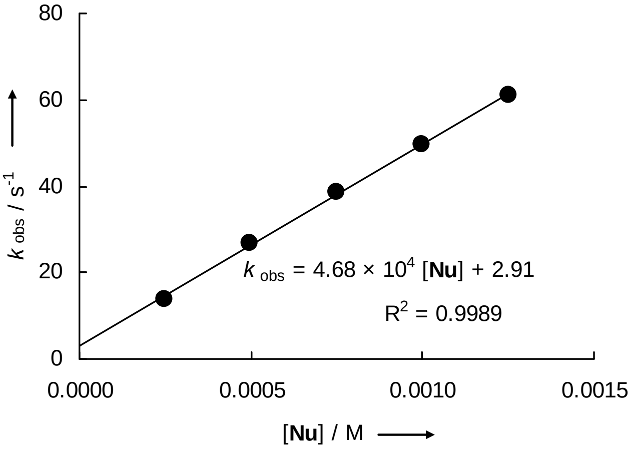

Determination of the nucleophilicity parameters *N* and s_N for DBU (**2**) in DMSO.

Rate constants for the reaction of DBU (**2**) with reference electrophiles **10**.

Electrophile	*E*	k_2 / $M^{-1}s^{-1}$	log k_2
$(lil)_2CH^+$	-10.04	2.56×10^3	3.41
$(jul)_2CH^+$	-9.45	6.78×10^3	3.83
$(ind)_2CH^+$	-8.76	1.60×10^4	4.20
$(thq)_2CH^+$	-8.22	4.68×10^4	4.67
$N = 15.11$, $s = 0.67$			

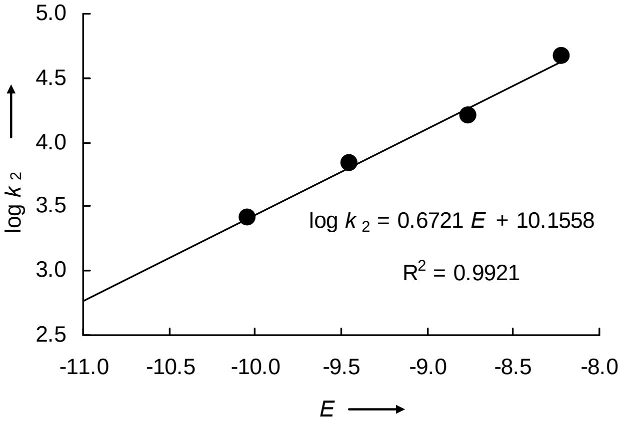

1.S.4. Rate constants in for TBD (3) in DMSO.

Rate constants for the reaction of TBD (**3**) with ani(tBu)$_2$QM (**10c**) at 20°C in DMSO (stopped-flow technique).

No	$[E]_0$ / M	$[Nu]_0$ / M	$[Nu]_0$ / $[E]_0$	$k_{1\psi\ calc}$ / s^{-1} [a]
1	3.07×10^{-5}	1.20×10^{-3}	39	5.55×10^{-2}
2	3.07×10^{-5}	2.00×10^{-3}	65	9.77×10^{-2}
3	3.07×10^{-5}	3.00×10^{-3}	98	1.48×10^{-1}
4	3.07×10^{-5}	3.99×10^{-3}	130	1.98×10^{-1}
5	3.07×10^{-5}	4.99×10^{-3}	163	2.54×10^{-1}
$k_2 = 5.20 \times 10^1\ M^{-1}s^{-1}$				

(a) The values of $k_{1\psi\ calc}$ were obtained by fitting the experimental curves to the theoretical function based on the model described in Scheme 1.1 derived in the way similar to that reported in ref. 29.

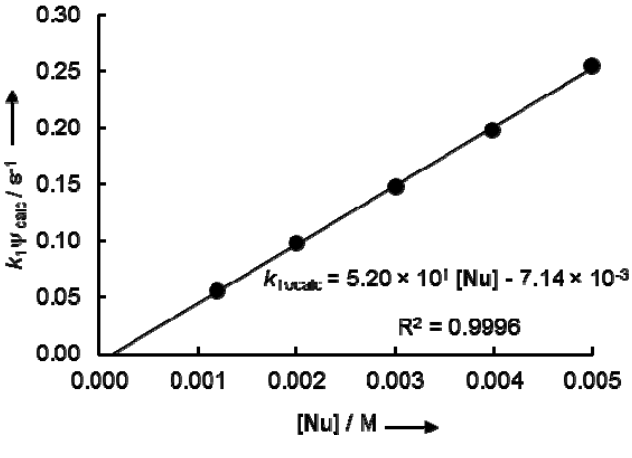

Rate constants for the reaction of TBD (**3**) with dma(Ph)$_2$QM (**10e**) at 20°C in DMSO (stopped-flow technique).

No	$[E]_0$ / M	$[Nu]_0$ / M	$[Nu]_0$ / $[E]_0$	k_{obs} / s^{-1}
1	1.86×10^{-5}	7.37×10^{-4}	40	1.29
2	1.86×10^{-5}	1.47×10^{-3}	79	2.56
3	1.86×10^{-5}	2.21×10^{-3}	119	3.79
4	1.86×10^{-5}	2.95×10^{-3}	159	5.05
5	1.86×10^{-5}	3.69×10^{-3}	198	6.35
6	1.86×10^{-5}	4.42×10^{-3}	238	7.78
$k_2 = 1.75 \times 10^3$ $M^{-1}s^{-1}$				

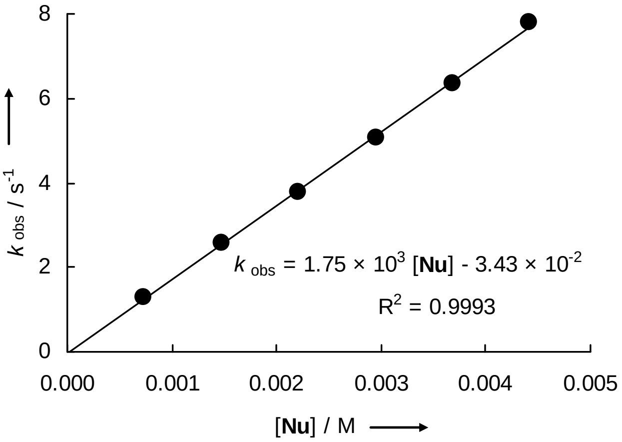

Rate constants for the reaction of TBD (**3**) with ani(Ph)$_2$QM (**10f**) at 20°C in DMSO (stopped-flow technique).

No	$[E]_0$ / M	$[Nu]_0$ / M	$[Nu]_0$ / $[E]_0$	k_{obs} / s^{-1}
1	2.11×10^{-5}	1.20×10^{-3}	57	1.07×10^1
2	2.11×10^{-5}	2.00×10^{-3}	95	1.85×10^1
3	2.11×10^{-5}	3.00×10^{-3}	142	2.80×10^1
4	2.11×10^{-5}	3.99×10^{-3}	189	3.88×10^1
5	2.11×10^{-5}	4.99×10^{-3}	236	4.86×10^1
$k_2 = 1.00 \times 10^4$ $M^{-1}s^{-1}$				

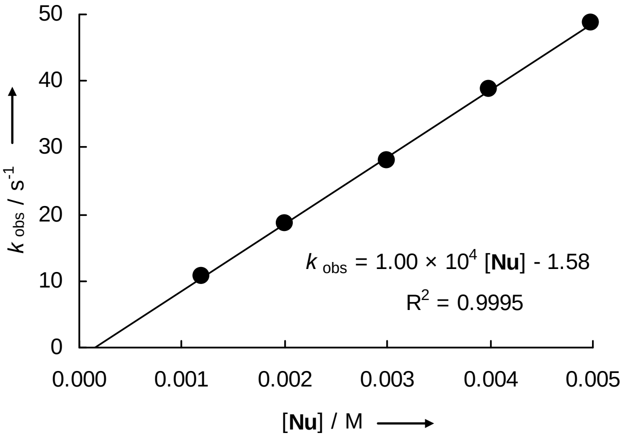

Rate constants for the reaction of TBD (**3**) with $(lil)_2CH^+$ (**10g**) at 20°C in DMSO (stopped-flow technique).

No	$[E]_0$ / M	$[Nu]_0$ / M	$[Nu]_0$ / $[E]_0$	k_{obs} / s^{-1}
1	7.21×10^{-6}	2.56×10^{-4}	36	2.54×10^{1}
2	7.21×10^{-6}	3.84×10^{-4}	53	3.80×10^{1}
3	7.21×10^{-6}	5.11×10^{-4}	71	5.00×10^{1}
4	7.21×10^{-6}	6.39×10^{-4}	89	6.25×10^{1}
5	7.21×10^{-6}	7.67×10^{-4}	106	7.54×10^{1}
$k_2 = 9.75 \times 10^4$ M^{-1}s^{-1}				

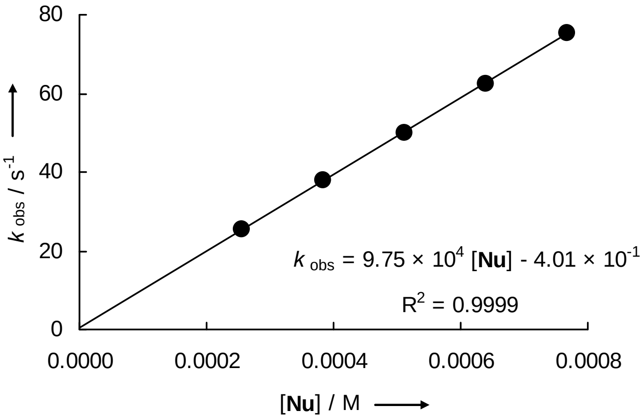

Rate constants for the reaction of TBD (**3**) with $(jul)_2CH^+BF_4^-$ (**10h**) at 20°C in DMSO (stopped-flow technique).

No	$[E]_0$ / M	$[Nu]_0$ / M	$[Nu]_0$ / $[E]_0$	k_{obs} / s^{-1}
1	7.20×10^{-6}	1.08×10^{-4}	15	4.15×10^{1}
2	7.20×10^{-6}	1.44×10^{-4}	20	5.76×10^{1}
3	7.20×10^{-6}	1.80×10^{-4}	25	7.18×10^{1}
4	7.20×10^{-6}	2.16×10^{-4}	30	8.64×10^{1}
5	7.20×10^{-6}	2.51×10^{-4}	35	9.96×10^{1}
$k_2 = 4.05 \times 10^5$ $M^{-1}s^{-1}$				

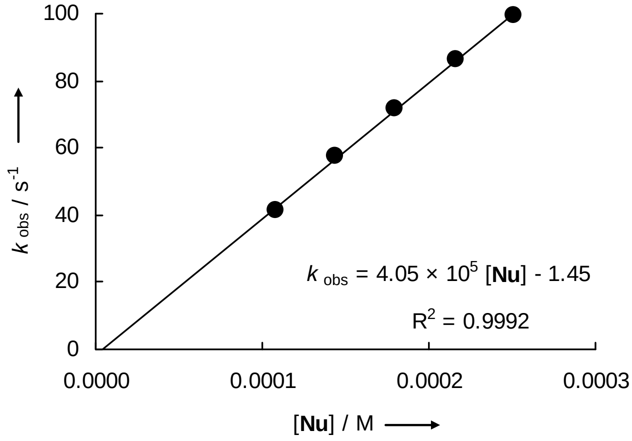

Determination of the nucleophilicity parameters N and s_N for TBD (**3**) in DMSO

Rate constants for the reaction of TBD (**3**) with reference electrophiles **10**.

Electrophile	E	k_2 / $M^{-1}s^{-1}$	log k_2
ani(tBu)$_2$QM	-16.11	5.20×10^{1}	1.72
dma(Ph)$_2$QM	-13.39	1.75×10^{3}	3.24
ani(Ph)$_2$QM	-12.18	1.00×10^{4}	4.00
$(lil)_2CH^+BF_4^-$	-10.04	9.75×10^{4}	4.99
$(jul)_2CH^+BF_4^-$	-9.45	4.05×10^{5}	5.61
$N = 19.15$, $s = 0.57$			

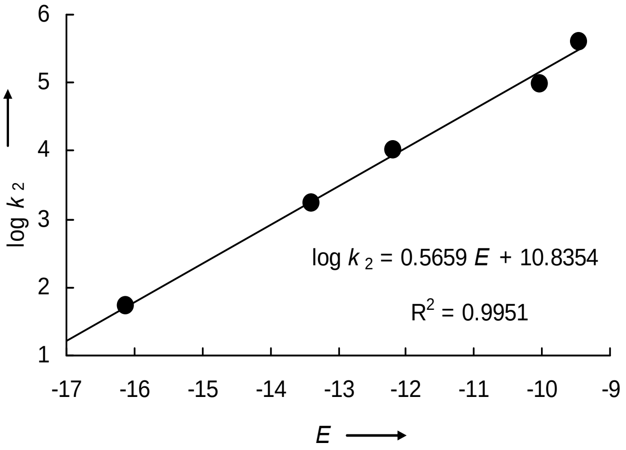

1.S.5. Rate constants for hydrazine (4) in DMSO.

Rate constants for the reaction of hydrazine (**4**) with jul(*t*Bu)$_2$QM (**10a**) at 20°C in DMSO (J&M).

No	$[E]_0$ / M	$[Nu]_0$ / M	$[Nu]_0$ / $[E]_0$	k_{obs} / s^{-1}
1	4.33×10^{-5}	6.75×10^{-4}	16	2.23×10^{-3}
2	4.35×10^{-5}	8.29×10^{-4}	19	2.76×10^{-3}
3	4.40×10^{-5}	1.40×10^{-3}	32	4.68×10^{-3}
		$k_2 = 3.37\ M^{-1}s^{-1}$		

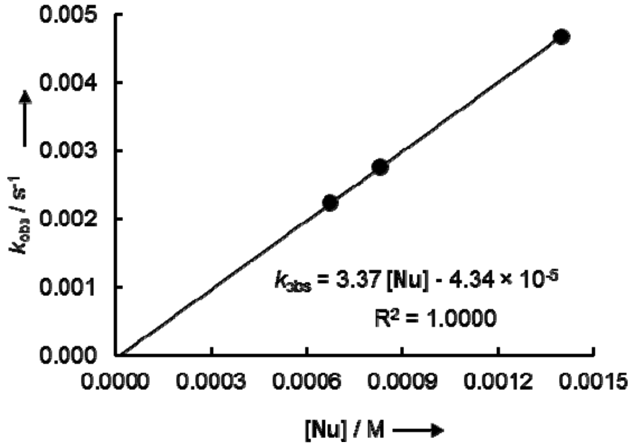

Rate constants for the reaction of hydrazine (**4**) with tol(*t*Bu)$_2$QM (**10d**) at 20°C in DMSO (J&M).

No	$[E]_0$ / M	$[Nu]_0$ / M	$[Nu]_0$ / $[E]_0$	k_{obs} / s^{-1}
1	4.38×10^{-5}	4.63×10^{-4}	11	1.52×10^{-2}
2	4.36×10^{-5}	6.15×10^{-4}	14	2.18×10^{-2}
3	4.21×10^{-5}	7.43×10^{-4}	18	2.76×10^{-2}
4	4.23×10^{-5}	8.96×10^{-4}	21	3.23×10^{-2}
5	4.19×10^{-5}	1.04×10^{-3}	25	3.91×10^{-2}
		$k_2 = 4.06 \times 10^{1}\ M^{-1}s^{-1}$		

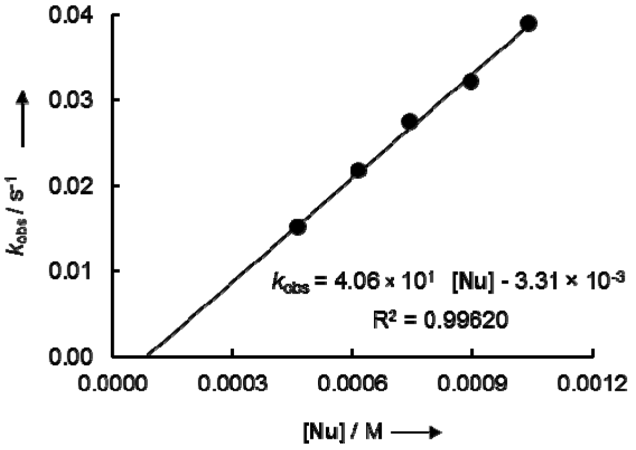

Rate constants for the reaction of hydrazine (**4**) with ani(Ph)$_2$QM (**10f**) at 20°C in DMSO (stopped-flow technique).

No	$[E]_0$ / M	$[Nu]_0$ / M	$[Nu]_0$ / $[E]_0$	k_{obs} / s^{-1}
1	2.20×10^{-5}	3.82×10^{-4}	17	1.04
2	1.98×10^{-5}	7.63×10^{-4}	39	2.28
3	1.98×10^{-5}	1.14×10^{-3}	58	3.34
4	1.98×10^{-5}	1.53×10^{-3}	77	4.56
5	1.98×10^{-5}	1.91×10^{-3}	96	5.72
6	1.98×10^{-5}	3.82×10^{-3}	193	1.12×10^{1}
		$k_2 = 2.94 \times 10^{3}$ M^{-1}s^{-1}		

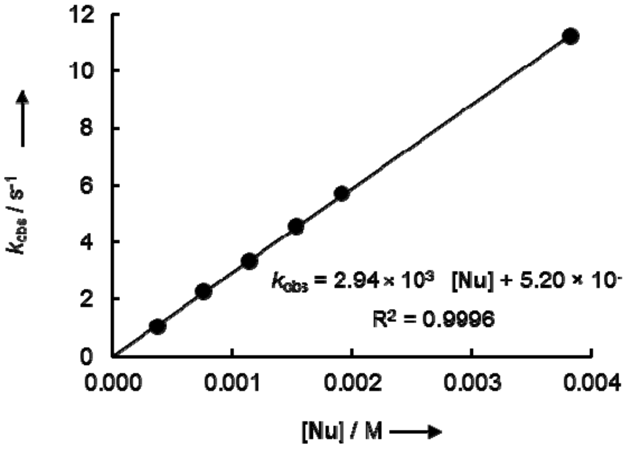

Rate constants for the reaction of hydrazine (**4**) with $(lil)_2CH^+$ (**10g**) at 20°C in DMSO (stopped-flow technique).

No	$[E]_0$ / M	$[Nu]_0$ / M	$[Nu]_0$ / $[E]_0$	k_{obs} / s^{-1}
1	1.06×10^{-5}	3.17×10^{-4}	30	4.62
2	1.06×10^{-5}	4.76×10^{-4}	45	7.68
3	1.06×10^{-5}	6.34×10^{-4}	60	1.02×10^{1}
4	1.06×10^{-5}	7.93×10^{-4}	75	1.19×10^{1}
5	1.06×10^{-5}	9.52×10^{-4}	90	1.49×10^{1}
		$k_2 = 1.56 \times 10^{4}\ M^{-1}s^{-1}$		

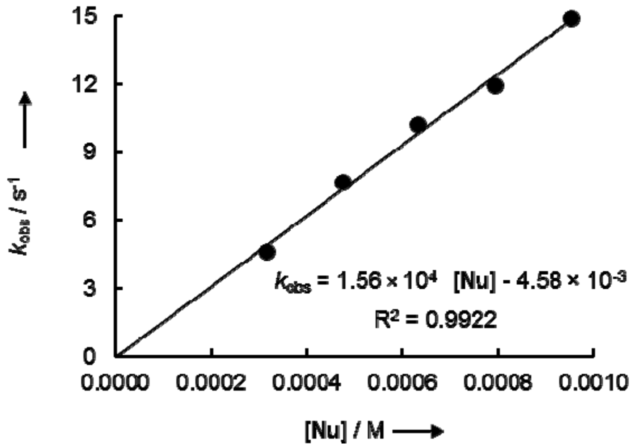

Rate constants for the reaction of hydrazine (**4**) with $(jul)_2CH^+$ (**10h**) at 20°C in DMSO (stopped-flow technique).

No	$[E]_0$ / M	$[Nu]_0$ / M	$[Nu]_0$ / $[E]_0$	k_{obs} / s^{-1}
1	1.17×10^{-5}	2.01×10^{-4}	17	7.65
2	1.17×10^{-5}	3.36×10^{-4}	29	1.26×10^{1}
3	1.17×10^{-5}	4.47×10^{-4}	38	1.63×10^{1}
4	1.17×10^{-5}	5.59×10^{-4}	48	2.12×10^{1}
5	1.17×10^{-5}	6.71×10^{-4}	57	2.42×10^{1}
		$k_2 = 3.59 \times 10^{4}\ M^{-1}s^{-1}$		

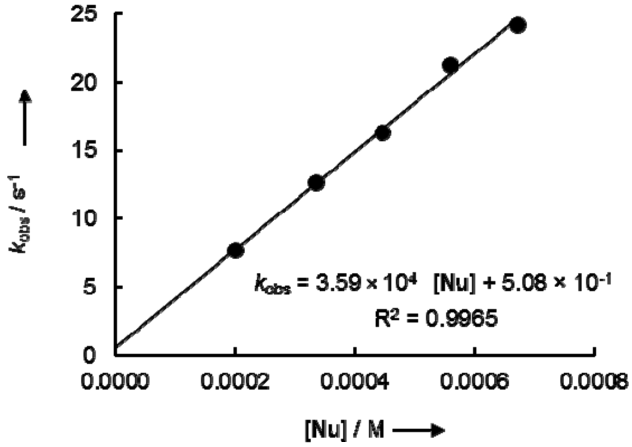

Rate constants for the reaction of hydrazine (**4**) with $(ind)_2CH^+$ (**10i**) at 20°C in DMSO (stopped-flow technique).

No	$[E]_0$ / M	$[Nu]_0$ / M	$[Nu]_0$ / $[E]_0$	k_{obs} / s^{-1}
1	9.88×10^{-6}	8.55×10^{-5}	9	5.65
2	9.88×10^{-6}	1.14×10^{-4}	12	7.74
3	9.88×10^{-6}	1.43×10^{-4}	14	9.53
4	9.88×10^{-6}	1.71×10^{-4}	17	1.13×10^{1}
5	9.88×10^{-6}	2.85×10^{-4}	29	1.89×10^{1}
		$k_2 = 6.60 \times 10^4$ $M^{-1}s^{-1}$		

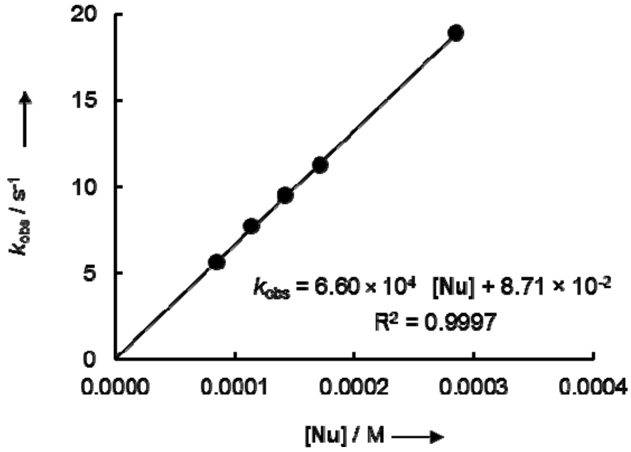

Determination of the nucleophilicity parameters *N* and s_N for hydrazine (**4**) in DMSO

Rate constants for the reaction of hydrazine (**4**) with reference electrophiles **10**.

Electrophile	*E*	k_2 / $M^{-1}s^{-1}$	log k_2
jul(*t*Bu)$_2$QM	-17.90	3.37	0.53
tol(*t*Bu)$_2$QM	-15.83	4.06×10^1	1.61
ani(Ph)$_2$QM	-12.18	2.94×10^3	3.47
(lil)$_2$CH$^+$BF$_4^-$	-10.04	1.56×10^4	4.19
(jul)$_2$CH$^+$BF$_4^-$	-9.45	3.59×10^4	4.56
(ind)$_2$CH$^+$BF$_4^-$	-8.76	6.60×10^4	4.82
N = 19.21, *s* = 0.47			

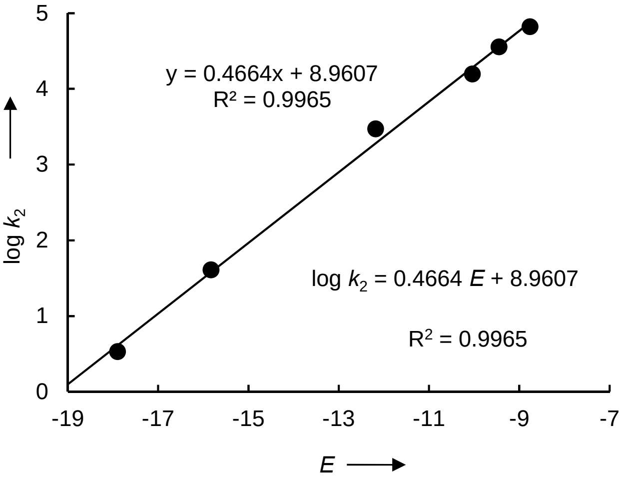

1.S.6. Rate constants for methylhydrazine (5) in DMSO.

Rate constants for the reaction of methylhydrazine (**5**) with jul(*t*Bu)$_2$QM (**10a**) at 20°C in DMSO (diode array spectrophotometer).

No	[E]$_0$ / M	[Nu]$_0$ / M	[Nu]$_0$ / [E]$_0$	k_{obs} / s^{-1}	[Nu]$^{-1}$ / M^{-1}	[Nu] k_{obs}^{-1}
1	3.48×10^{-5}	7.80×10^{-4}	22	2.06×10^{-3}	7.80×10^{-4}	2.06×10^{-3}
2	3.47×10^{-5}	1.09×10^{-3}	31	3.80×10^{-3}	1.09×10^{-3}	3.80×10^{-3}
3	3.49×10^{-5}	1.57×10^{-3}	45	6.52×10^{-3}	1.57×10^{-3}	6.52×10^{-3}
4	3.42×10^{-5}	1.85×10^{-3}	54	8.55×10^{-3}	1.85×10^{-3}	8.55×10^{-3}
5	3.43×10^{-5}	2.31×10^{-3}	67	1.16×10^{-2}	2.31×10^{-3}	1.16×10^{-2}
6	3.47×10^{-5}	2.65×10^{-3}	76	1.51×10^{-2}	2.65×10^{-3}	1.51×10^{-2}
$k_2 = 1.01 \times 10^1$ $M^{-1}s^{-1}$						

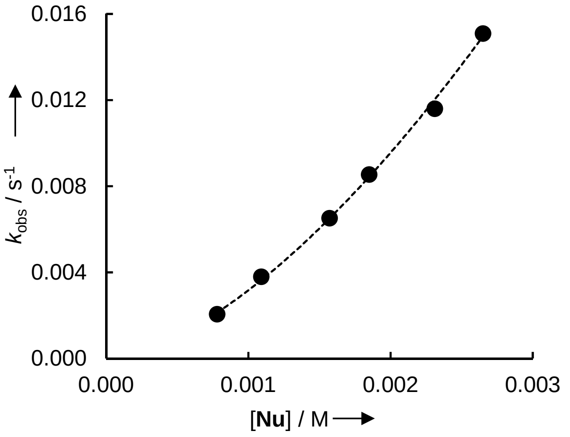

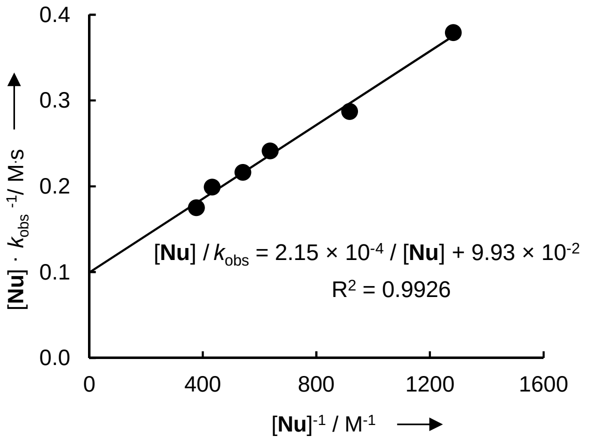

Rate constants for the reaction of methylhydrazine (**5**) with dma(tBu)$_2$QM (**10b**) at 20°C in DMSO (diode array spectrophotometer).

No	$[E]_0$ / M	$[Nu]_0$ / M	$[Nu]_0$ / $[E]_0$	k_{obs} / s^{-1}	$[Nu]^{-1}$ / M^{-1}	[Nu] k_{obs}^{-1}
1	4.45×10^{-5}	1.08×10^{-3}	24	6.35×10^{-3}	9.26×10^{2}	1.70×10^{-1}
2	4.43×10^{-5}	1.54×10^{-3}	35	1.13×10^{-2}	6.49×10^{2}	1.36×10^{-1}
3	4.44×10^{-5}	1.85×10^{-3}	42	1.54×10^{-2}	5.41×10^{2}	1.20×10^{-1}
4	4.50×10^{-5}	2.35×10^{-3}	52	2.22×10^{-2}	4.26×10^{2}	1.06×10^{-1}
5	4.44×10^{-5}	2.62×10^{-3}	59	2.65×10^{-2}	3.82×10^{2}	9.90×10^{-2}
$k_2 = 2.00 \times 10^{1}$ $M^{-1}s^{-1}$						

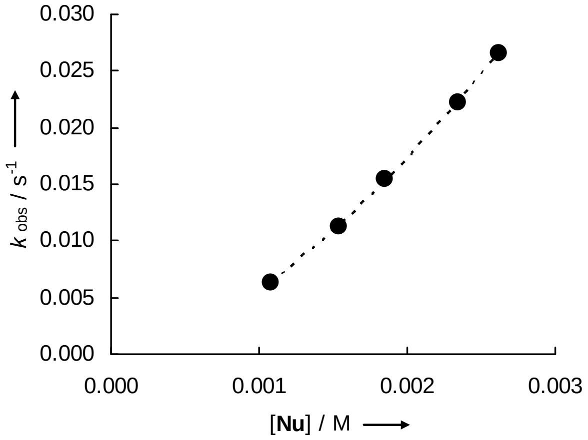

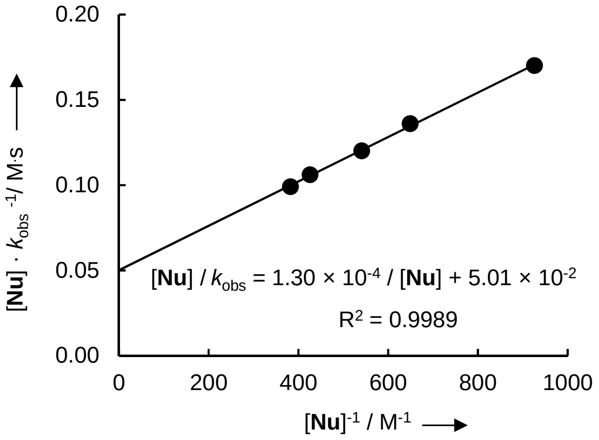

Rate constants for the reaction of methylhydrazine (**5**) with tol(*t*Bu)$_2$QM (**10d**) at 20°C in DMSO (diode array spectrophotometer).

No	$[E]_0$ / M	$[Nu]_0$ / M	$[Nu]_0$ / $[E]_0$	k_{obs} / s^{-1}	$[Nu]^{-1}$ / M^{-1}	$[Nu]\ k_{obs}^{-1}$
1	4.67×10^{-5}	2.84×10^{-3}	61	2.38×10^{-1}	3.52×10^{2}	1.19×10^{-2}
2	4.67×10^{-5}	5.69×10^{-3}	122	5.84×10^{-1}	1.76×10^{2}	9.74×10^{-3}
3	2.92×10^{-5}	7.11×10^{-3}	243	7.64×10^{-1}	1.41×10^{2}	9.31×10^{-3}
4	2.92×10^{-5}	8.53×10^{-3}	292	9.70×10^{-1}	1.17×10^{2}	8.79×10^{-3}
5	2.92×10^{-5}	9.95×10^{-3}	341	1.15	1.01×10^{2}	8.65×10^{-3}
6	2.92×10^{-5}	1.14×10^{-2}	390	1.35	8.80×10^{1}	8.44×10^{-3}

$k_2 = 1.36 \times 10^{2}\ M^{-1}s^{-1}$

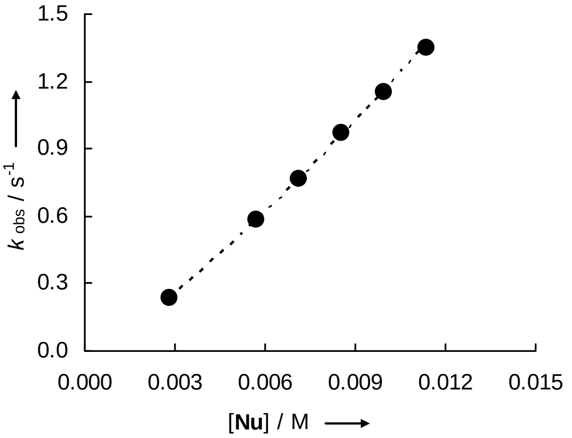

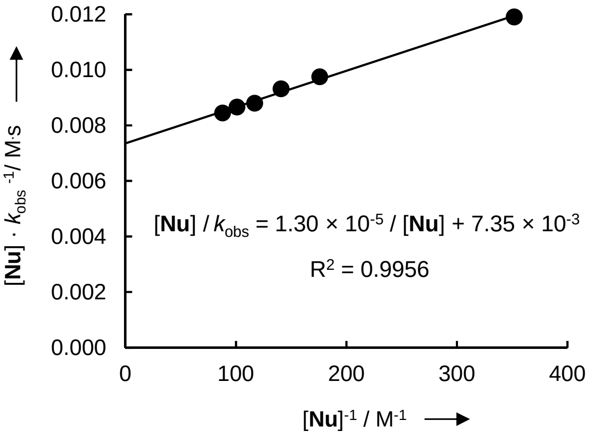

Rate constants for the reaction of methylhydrazine (**5**) with ani(Ph)$_2$QM (**10f**) at 20°C in DMSO (stopped-flow technique).

No	$[E]_0$ / M	$[Nu]_0$ / M	$[Nu]_0$ / $[E]_0$	k_{obs} / s^{-1}
1	4.17×10^{-5}	2.54×10^{-3}	61	2.58×10^{1}
2	4.17×10^{-5}	3.39×10^{-3}	81	4.33×10^{1}
3	4.17×10^{-5}	3.72×10^{-3}	89	5.04×10^{1}
4	4.17×10^{-5}	4.23×10^{-3}	101	5.75×10^{1}
5	4.17×10^{-5}	5.08×10^{-3}	122	7.32×10^{1}

$k_2 = 1.84 \times 10^{4}\ M^{-1}s^{-1}$

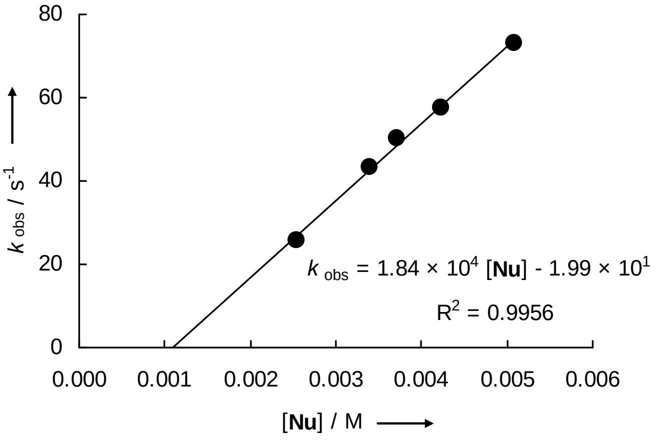

Rate constants for the reaction of methylhydrazine (**5**) with $(lil)_2CH^+$ (**10g**) at 20°C in DMSO (stopped-flow technique).

No	$[E]_0$ / M	$[Nu]_0$ / M	$[Nu]_0$ / $[E]_0$	k_{obs} / s^{-1}
1	3.12×10^{-6}	3.44×10^{-5}	11	3.20
2	3.12×10^{-6}	6.88×10^{-5}	22	6.36
3	3.12×10^{-6}	1.03×10^{-4}	33	9.18
4	3.12×10^{-6}	1.37×10^{-4}	44	1.26×10^{1}
5	3.12×10^{-6}	1.72×10^{-4}	55	1.61×10^{1}
6	3.12×10^{-6}	2.41×10^{-4}	77	2.20×10^{1}
$k_2 = 9.18 \times 10^4\ M^{-1}s^{-1}$				

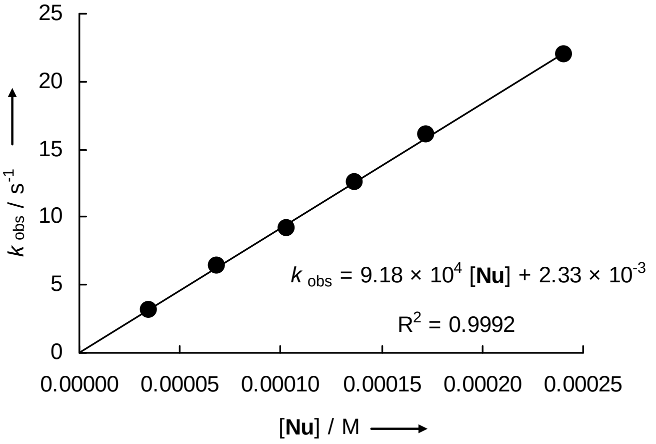

Rate constants for the reaction of methylhydrazine (**5**) with (jul)$_2$CH$^+$ (**10h**) at 20°C in DMSO (stopped-flow technique).

No	[E]$_0$ / M	[Nu]$_0$ / M	[Nu]$_0$ / [E]$_0$	k_{obs} / s^{-1}
1	2.16×10^{-6}	1.96×10^{-5}	9	9.30
2	2.16×10^{-6}	2.61×10^{-5}	12	1.19×10^{1}
3	2.16×10^{-6}	3.27×10^{-5}	15	1.43×10^{1}
4	2.16×10^{-6}	3.92×10^{-5}	18	1.72×10^{1}
5	2.16×10^{-6}	6.53×10^{-5}	30	2.87×10^{1}
		$k_2 = 4.27 \times 10^5$ M^{-1}s^{-1}		

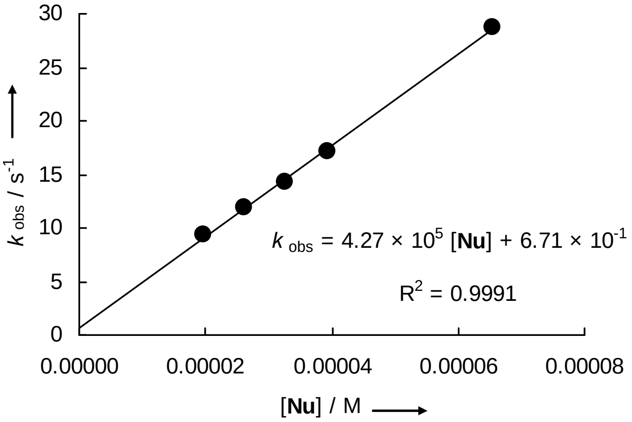

Rate constants for the reaction of methylhydrazine (**5**) with (ind)$_2$CH$^+$ (**10i**) at 20°C in DMSO (stopped-flow technique).

No	[E]$_0$ / M	[Nu]$_0$ / M	[Nu]$_0$ / [E]$_0$	k_{obs} / s^{-1}
1	3.02×10^{-6}	2.77×10^{-5}	9	1.19×10^{1}
2	3.02×10^{-6}	4.15×10^{-5}	14	1.80×10^{1}
3	3.02×10^{-6}	4.85×10^{-5}	16	2.19×10^{1}
4	3.02×10^{-6}	5.54×10^{-5}	18	2.41×10^{1}
5	3.02×10^{-6}	6.92×10^{-5}	23	2.98×10^{1}
		$k_2 = 4.32 \times 10^5$ M^{-1}s^{-1}		

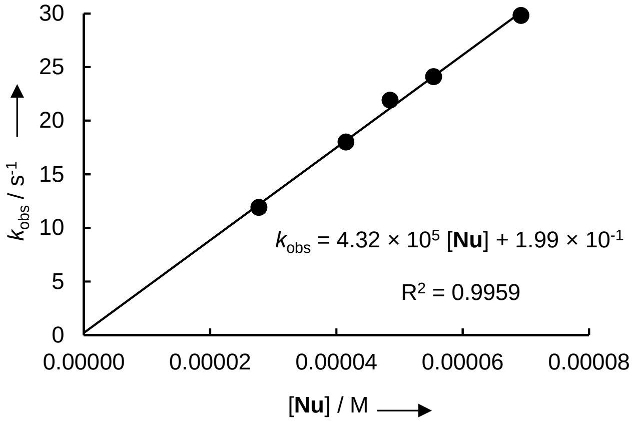

Determination of the nucleophilicity parameters *N* and s_N for methylhydrazine (**5**) in DMSO

Rate constants for the reaction of methylhydrazine (**5**) with reference electrophiles **10**.

Electrophile	*E*	k_2 / M^{-1}s^{-1}	log k_2
jul(*t*Bu)$_2$QM	-17.90	1.01×10^1	1.00
dma(*t*Bu)$_2$QM	-17.29	2.00×10^1	1.30
tol(*t*Bu)$_2$QM	-15.83	1.36×10^2	2.13
ani(Ph)$_2$QM	-12.18	1.84×10^4	4.26
(lil)$_2$CH$^+$BF$_4^-$	-10.04	9.18×10^4	4.96
(jul)$_2$CH$^+$BF$_4^-$	-9.45	4.27×10^5	5.63
(ind)$_2$CH$^+$BF$_4^-$	-8.76	4.32×10^5	5.64
N = 19.89, *s* = 0.52			

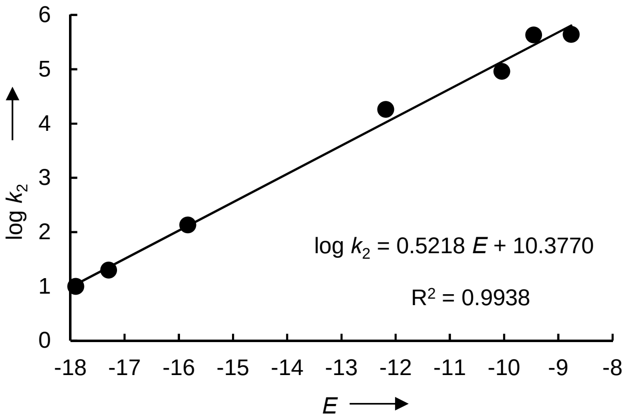

1.S.7. Rate constants in acetonitrile for triphenylphosphane (6).

Rate constants for the reaction of triphenylphosphane **6** with $(lil)_2CH^+BF_4^-$ **(10g)** at 20˚C in acetonitrile (stopped-flow technique).

No	$[E]_0$ / M	$[Nu]_0$ / M	$[Nu]_0$ / $[E]_0$	k_{obs} / s^{-1}
1	1.44×10^{-5}	1.17×10^{-3}	81	9.09
2	1.44×10^{-5}	2.33×10^{-3}	162	9.81
3	1.44×10^{-5}	3.50×10^{-3}	243	1.06×10^{1}
4	1.44×10^{-5}	4.67×10^{-3}	324	1.15×10^{1}
5	1.44×10^{-5}	5.83×10^{-3}	405	1.23×10^{1}
		$k_2 = 6.96 \times 10^2\ M^{-1}s^{-1}$		

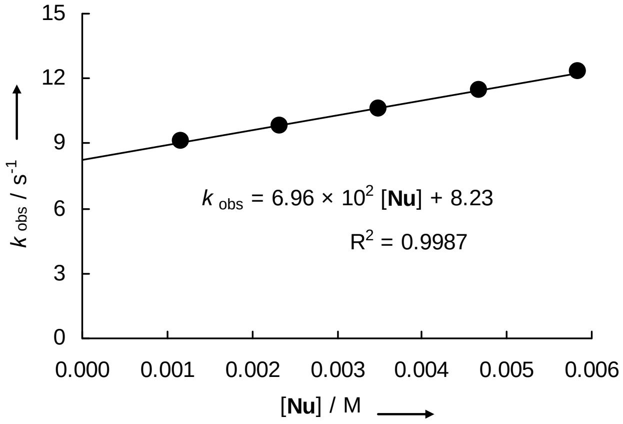

Rate constants for the reaction of triphenylphosphane **6** with $(jul)_2CH^+BF_4^-$ **(10h)** at 20˚C in acetonitrile (stopped-flow technique).

No	$[E]_0$ / M	$[Nu]_0$ / M	$[Nu]_0$ / $[E]_0$	k_{obs} / s^{-1}
1	7.88×10^{-6}	2.06×10^{-3}	261	2.13×10^{1}
2	7.88×10^{-6}	4.13×10^{-3}	524	2.67×10^{1}
3	7.88×10^{-6}	6.19×10^{-3}	786	3.21×10^{1}
4	7.88×10^{-6}	8.25×10^{-3}	1047	3.75×10^{1}
5	7.88×10^{-6}	1.03×10^{-2}	1308	4.28×10^{1}
		$k_2 = 2.61 \times 10^3\ M^{-1}s^{-1}$		

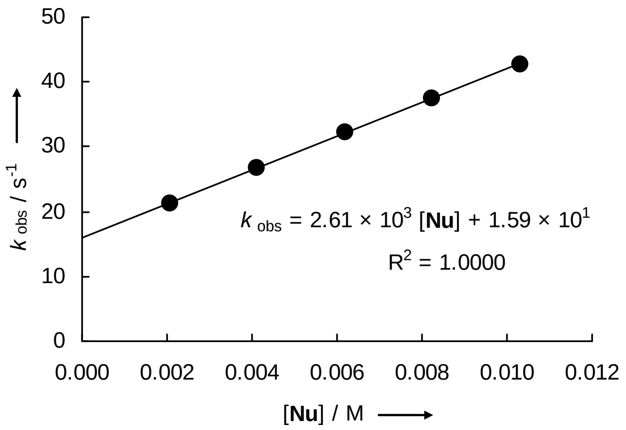

Rate constants for the reaction of triphenylphosphane **6** with $(ind)_2CH^+BF_4^-$ **(10i)** at 20°C in acetonitrile (stopped-flow technique).

No	$[E]_0$ / M	$[Nu]_0$ / M	$[Nu]_0$ / $[E]_0$	k_{obs} / s^{-1}
1	1.21×10^{-5}	8.62×10^{-4}	71	4.29
2	1.21×10^{-5}	1.29×10^{-3}	107	5.51
3	1.21×10^{-5}	1.72×10^{-3}	142	6.77
4	1.21×10^{-5}	2.15×10^{-3}	178	7.98
5	1.21×10^{-5}	2.58×10^{-3}	213	9.16
		$k_2 = 2.84 \times 10^3$ M^{-1}s^{-1}		

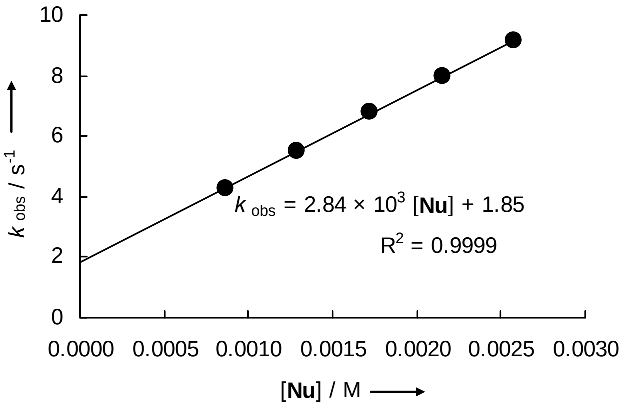

Rate constants for the reaction of triphenylphosphane **6** with $(thq)_2CH^+BF_4^-$ **(10j)** at 20°C in acetonitrile (stopped-flow technique).

No	$[E]_0$ / M	$[Nu]_0$ / M	$[Nu]_0$ / $[E]_0$	k_{obs} / s^{-1}
1	1.02×10^{-5}	8.62×10^{-4}	85	1.20×10^{1}
2	1.02×10^{-5}	1.29×10^{-3}	126	1.67×10^{1}
3	1.02×10^{-5}	1.72×10^{-3}	169	2.16×10^{1}
4	1.02×10^{-5}	2.15×10^{-3}	211	2.61×10^{1}
5	1.02×10^{-5}	2.58×10^{-3}	253	3.10×10^{1}
		$k_2 = 1.10 \times 10^{4}$ $M^{-1}s^{-1}$		

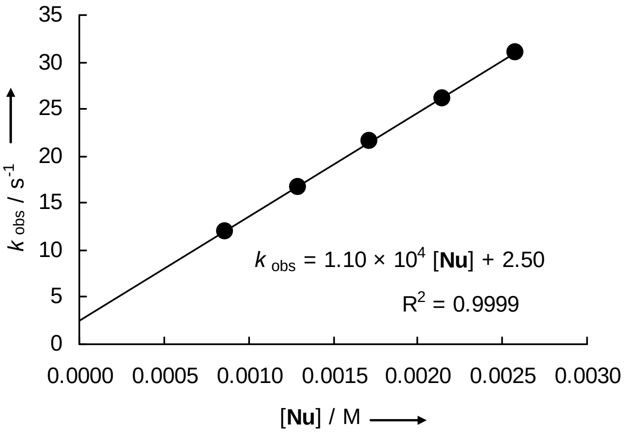

Rate constants for the reaction of triphenylphosphane **6** with $(mor)_2CH^+BF_4^-$ **(10m)** at 20°C in acetonitrile (stopped-flow technique).

No	$[E]_0$ / M	$[Nu]_0$ / M	$[Nu]_0$ / $[E]_0$	k_{obs} / s^{-1}
1	1.53×10^{-5}	3.20×10^{-4}	21	8.09×10^{1}
2	1.53×10^{-5}	4.80×10^{-4}	31	1.21×10^{2}
3	1.53×10^{-5}	6.41×10^{-4}	42	1.60×10^{2}
4	1.53×10^{-5}	8.01×10^{-4}	52	1.97×10^{2}
		$k_2 = 2.41 \times 10^{5}$ $M^{-1}s^{-1}$		

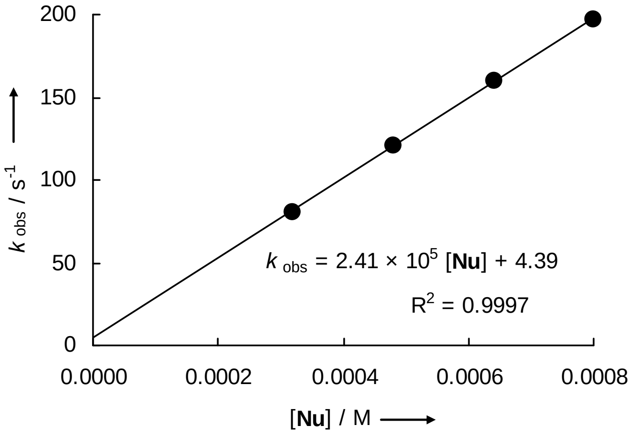

<u>Determination of the nucleophilicity parameters *N* and s_N for triphenylphosphane (**6**) in acetonitrile</u>

Rate constants for the reaction of triphenylphosphane (**6**) with reference electrophiles **10**.

Electrophile	*E*	k_2 / $M^{-1}s^{-1}$	log k_2
$(lil)_2CH^+$	-10.04	6.96×10^2	2.84
$(jul)_2CH^+$	-9.45	2.61×10^3	3.42
$(ind)_2CH^+$	-8.76	2.84×10^3	3.45
$(thq)_2CH^+$	-8.22	1.10×10^4	4.04
$(dma)_2CH^+$	-7.02	3.33×10^{4a}	4.52
$(mor)_2CH^+$	-5.53	2.41×10^5	5.38
N = 15.43, *s* = 0.54			

(a) k_2 from ref. 18.

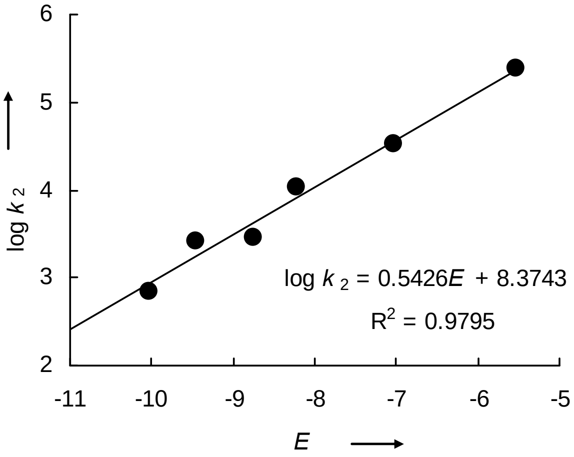

Comparison of the equilibrium constants for the reactions of **6** with **10g-j** in acetonitrile (K_{indirect}) calculated from k_2 and k_{-1} with those determined in ref. 18 (K_{direct}).

Rate constants for the reaction of triphenylphosphane (**6**) with reference electrophles **10g-j**, rate constants for the backward reaction and the resulting equilibrium constants.

Electrophile	k_2 / $M^{-1}s^{-1}$	k_{-1} / s^{-1}	K_{indirect}/ M^{-1}	K_{direct}/ M^{-1}
$(lil)_2CH^+BF_4^-$	6.96×10^2	8.23	8.46×10^1	7.77×10^{1a}
$(jul)_2CH^+BF_4^-$	2.61×10^3	1.59×10^1	1.64×10^2	1.66×10^{2a}
$(ind)_2CH^+BF_4^-$	2.84×10^3	1.85	1.54×10^3	1.60×10^{3a}
$(thq)_2CH^+BF_4^-$	1.10×10^4	2.50	4.49×10^3	-

(a) k_2 from ref. 25.

1.S.8. Rate constants in acetonitrile for tris-(4-methoxyphenyl)phosphane (7).

Rate constants for the reaction of tris-(4-methoxyphenyl)phosphane (**7**) with $(lil)_2CH^+BF_4^-$ (**10g**) at 20°C in acetonitrile (stopped-flow technique).

No	$[E]_0$ / M	$[Nu]_0$ / M	$[Nu]_0$ / $[E]_0$	k_{obs} / s^{-1}
1	6.73×10^{-6}	1.62×10^{-3}	241	1.13×10^1
2	6.73×10^{-6}	2.65×10^{-3}	394	1.79×10^1
3	6.73×10^{-6}	4.34×10^{-3}	645	2.79×10^1
4	6.73×10^{-6}	5.48×10^{-3}	814	3.42×10^1
5	6.73×10^{-6}	7.05×10^{-3}	1048	4.59×10^1
		$k_2 = 6.25 \times 10^3$ $M^{-1}s^{-1}$		

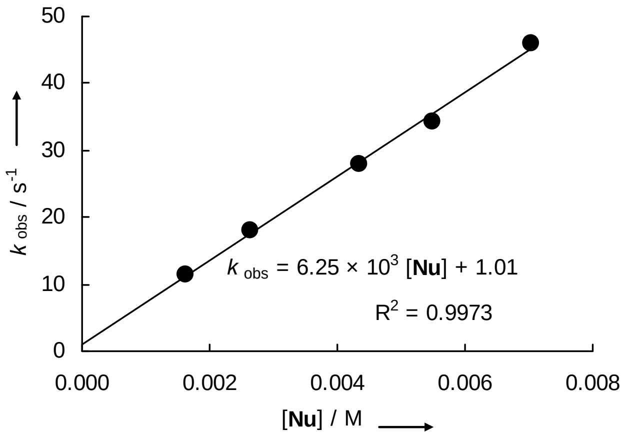

Rate constants for the reaction of tris-(4-methoxyphenyl)phosphane (**7**) with $(jul)_2CH^+BF_4^-$ (**10h**) at 20°C in acetonitrile (stopped-flow technique).

No	$[E]_0$ / M	$[Nu]_0$ / M	$[Nu]_0$ / $[E]_0$	k_{obs} / s^{-1}
1	6.75×10^{-6}	2.53×10^{-4}	37	6.35
2	6.75×10^{-6}	1.26×10^{-4}	19	3.37
3	6.75×10^{-6}	3.79×10^{-4}	56	9.49
4	6.75×10^{-6}	5.05×10^{-4}	75	1.25×10^{1}
5	6.75×10^{-6}	6.31×10^{-4}	93	1.56×10^{1}
		$k_2 = 2.43 \times 10^{4}$ $M^{-1}s^{-1}$		

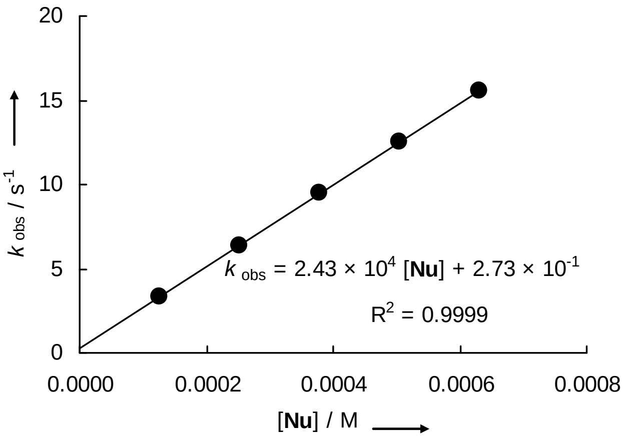

Rate constants for the reaction of tris-(4-methoxyphenyl)phosphane (**7**) with $(ind)_2CH^+BF_4^-$ (**10i**) at 20°C in acetonitrile (stopped-flow technique).

No	$[E]_0$ / M	$[Nu]_0$ / M	$[Nu]_0$ / $[E]_0$	k_{obs} / s^{-1}
1	7.69×10^{-6}	1.48×10^{-4}	19	3.63
2	7.69×10^{-6}	2.21×10^{-4}	29	5.56
3	7.69×10^{-6}	2.95×10^{-4}	38	7.51
4	7.69×10^{-6}	3.69×10^{-4}	48	9.51
5	7.69×10^{-6}	4.43×10^{-4}	58	1.13×10^{1}
		$k_2 = 2.61 \times 10^{4}$ $M^{-1}s^{-1}$		

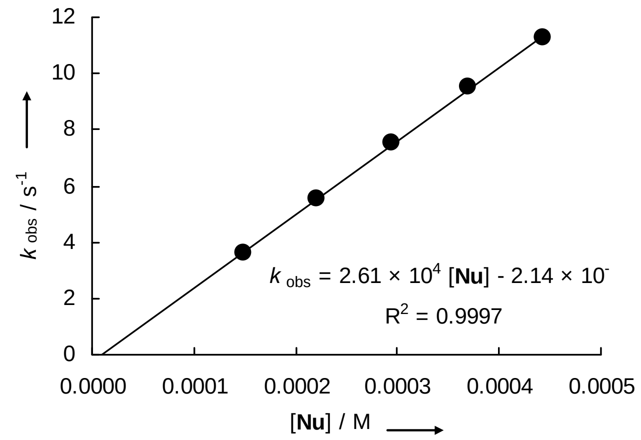

Rate constants for the reaction of tris-(4-methoxyphenyl)phosphane **(7)** with $(thq)_2CH^+BF_4^-$ **(10j)** at 20°C in acetonitrile (stopped-flow technique).

No	$[E]_0$ / M	$[Nu]_0$ / M	$[Nu]_0$ / $[E]_0$	k_{obs} / s^{-1}
1	8.16×10^{-6}	1.48×10^{-4}	18	1.33×10^{1}
2	8.16×10^{-6}	2.21×10^{-4}	27	2.06×10^{1}
3	8.16×10^{-6}	2.95×10^{-4}	36	2.82×10^{1}
4	8.16×10^{-6}	3.69×10^{-4}	45	3.64×10^{1}
5	8.16×10^{-6}	4.43×10^{-4}	54	4.33×10^{1}
$k_2 = 1.03 \times 10^{5}$ $M^{-1}s^{-1}$				

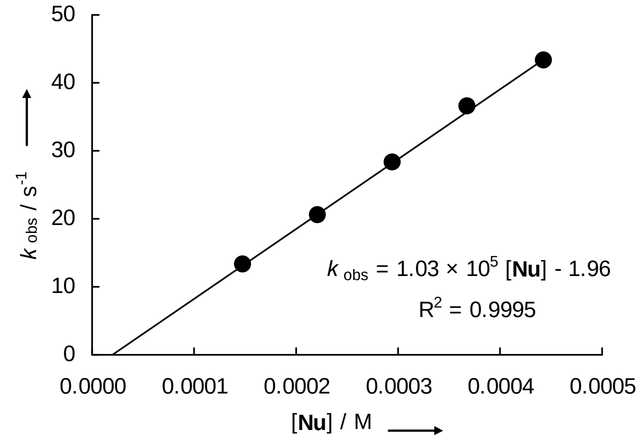

Rate constants for the reaction of tris-(4-methoxyphenyl)phosphane **(7)** with $(dma)_2CH^+BF_4^-$ **(10l)** at 20°C in acetonitrile (stopped-flow technique).

No	$[E]_0$ / M	$[Nu]_0$ / M	$[Nu]_0$ / $[E]_0$	k_{obs} / s^{-1}
1	1.13×10^{-5}	1.24×10^{-4}	11	3.94×10^{1}
2	1.13×10^{-5}	1.55×10^{-4}	14	4.94×10^{1}
3	1.13×10^{-5}	1.86×10^{-4}	16	5.94×10^{1}
4	1.13×10^{-5}	2.17×10^{-4}	19	7.02×10^{1}
5	1.13×10^{-5}	2.48×10^{-4}	22	7.93×10^{1}
$k_2 = 3.25 \times 10^5$ $M^{-1}s^{-1}$				

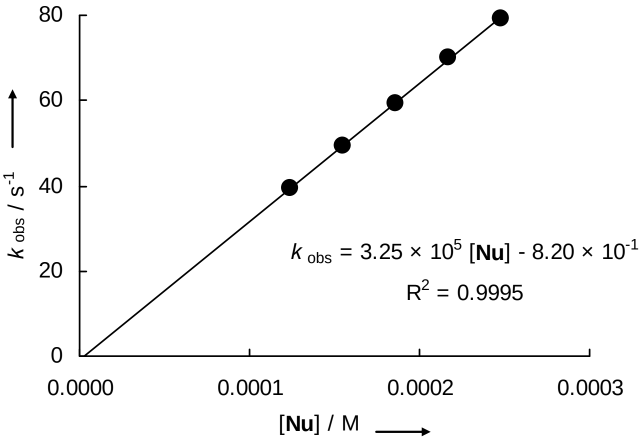

Determination of the nucleophilicity parameters *N* and s_N for tris-(4-methoxyphenyl)phosphane (**7**) in acetonitrile

Rate constants for the reaction of for tris-(4methoxyphenyl)phosphane (**7**) with reference electrophiles **10**.

Electrophile	*E*	k_2 / $M^{-1}s^{-1}$	log k_2
$(lil)_2CH^+$	-10.04	6.25×10^3	3.80
$(jul)_2CH^+$	-9.45	2.43×10^4	4.39
$(ind)_2CH^+$	-8.76	2.61×10^4	4.42
$(thq)_2CH^+$	-8.22	1.03×10^5	5.01
$(dma)_2CH^+$	-7.02	3.25×10^5	5.51
$N = 17.14$, $s = 0.55$			

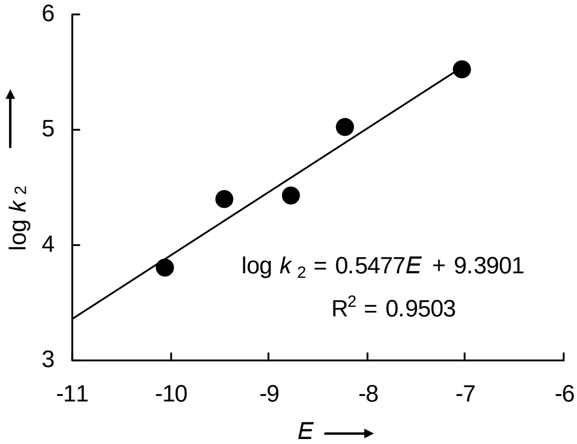

1.S.9. Rate constants in acetonitrile for tributylphosphane (8).

Rate constants for the reaction of tributylphosphane (**8**) with $dma(Ph)_2QM$ (**10e**) at 20˚C in acetonitrile (stopped-flow technique).

No	$[E]_0$/M	$[Nu]_0$/M	$[Nu]_0$/ $[E]_0$	k_{obs}/s^{-1}
1	2.78×10^{-5}	5.59×10^{-2}	201	1.53
2	2.78×10^{-5}	1.66×10^{-2}	597	4.68
3	2.78×10^{-5}	2.10×10^{-2}	755	5.87
4	2.78×10^{-5}	2.92×10^{-2}	1050	8.34
$k_2 = 2.88\times 10^2$ $M^{-1}s^{-1}$				

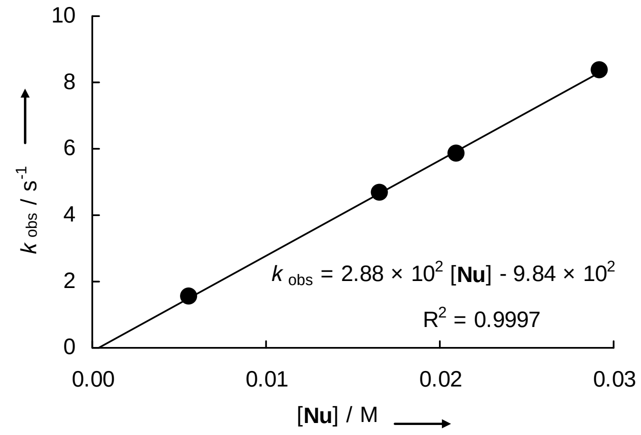

Rate constants for the reaction of tributylphosphane (**8**) with ani(Ph)$_2$QM **(10f)** at 20°C in acetonitrile (stopped-flow technique).

No	$[E]_0$ / M	$[Nu]_0$ / M	$[Nu]_0$ / $[E]_0$	k_{obs} / s^{-1}
1	4.39×10^{-5}	5.59×10^{-3}	127	6.00
2	4.39×10^{-5}	1.10×10^{-2}	251	1.22×10^{1}
3	4.39×10^{-5}	1.66×10^{-2}	378	1.86×10^{1}
4	4.39×10^{-5}	2.10×10^{-2}	478	2.33×10^{1}
5	4.39×10^{-5}	2.92×10^{-2}	665	3.24×10^{1}
$k_2 = 1.12 \times 10^{3}$ $M^{-1}s^{-1}$				

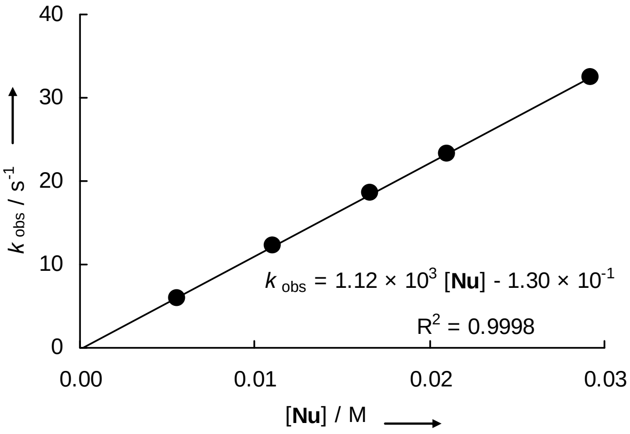

Rate constants for the reaction of tributylphosphane (**8**) with (jul)$_2CH^+BF_4^-$ **(10h)** at 20°C in acetonitrile (stopped-flow technique).

No	$[E]_0$ / M	$[Nu]_0$ / M	$[Nu]_0$ / $[E]_0$	k_{obs} / s^{-1}
1	4.50×10^{-6}	1.07×10^{-4}	24	4.69
2	4.50×10^{-6}	2.14×10^{-4}	48	9.72
3	4.50×10^{-6}	3.21×10^{-4}	71	1.47×10^{1}
4	4.50×10^{-6}	4.28×10^{-4}	95	1.92×10^{1}
$k_2 = 4.53 \times 10^{4}$ $M^{-1}s^{-1}$				

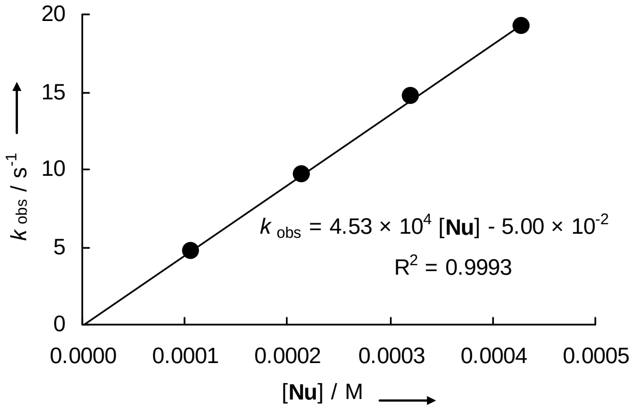

Rate constants for the reaction of tributylphosphane (**8**) with $(ind)_2CH^+BF_4^-$ (**10i**) at 20°C in acetonitrile (stopped-flow technique).

No	$[E]_0$ / M	$[Nu]_0$ / M	$[Nu]_0$ / $[E]_0$	k_{obs} / s^{-1}
1	7.14×10^{-6}	1.07×10^{-4}	15	6.01
2	7.14×10^{-6}	2.14×10^{-4}	30	1.31×10^{1}
3	7.14×10^{-6}	3.21×10^{-4}	45	1.99×10^{1}
		$k_2 = 6.49 \times 10^4\ M^{-1}s^{-1}$		

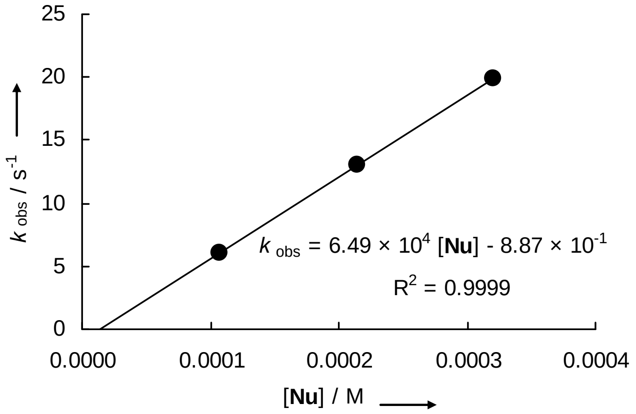

Rate constants for the reaction of tributylphosphane (**8**) with $(dma)_2CH^+BF_4^-$ (**10l**) at 20°C in acetonitrile (stopped-flow technique).

No	$[E]_0$ / M	$[Nu]_0$ / M	$[Nu]_0$ / $[E]_0$	k_{obs} / s^{-1}
1	1.35×10^{-5}	1.35×10^{-4}	10	1.07×10^{2}
2	1.35×10^{-5}	1.80×10^{-4}	13	1.40×10^{2}
3	1.35×10^{-5}	2.26×10^{-4}	17	1.75×10^{2}
4	1.35×10^{-5}	2.71×10^{-4}	20	2.10×10^{2}
		$k_2 = 7.58 \times 10^5$ $M^{-1}s^{-1}$		

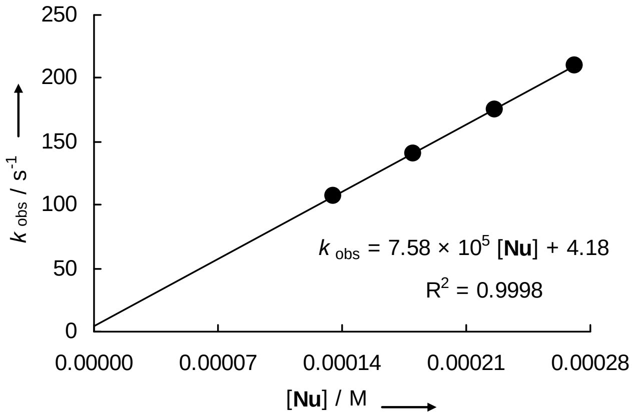

Determination of the nucleophilicity parameters *N* and s_N for tributylphosphane (**8**) in acetonitrile

Rate constants for the reaction of tributylphosphane (**8**) with reference electrophiles **10**.

Electrophile	*E*	k_2 / $M^{-1}s^{-1}$	log k_2
$dma(Ph)_2QM$	-13.39	2.88×10^{2}	2.46
ani(Ph)2QM	-12.18	1.12×10^{3}	3.05
$(jul)_2CH^+BF_4^-$	-9.45	4.53×10^{4}	4.66
$(ind)_2CH^+BF_4^-$	-8.76	6.49×10^{4}	4.81
$(dma)_2CH^+BF_4^-$	-7.02	7.58×10^{5}	5.88
$N = 17.94$, $s = 0.54$			

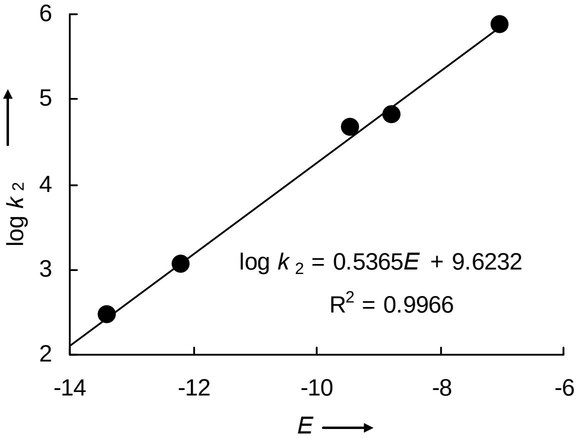

1.S.10. Rate constants for DABCO (9) in DMSO.

Rate constants for the reaction of DABCO (**9**) with $(ind)_2CH^+$ (**10i**) at 20°C in DMSO (laser-flash technique)

No	[E]$_0$ / M	[Nu]$_0$ / M	[Nu]$_0$ / [E]$_0$	k_{obs} / s^{-1}
1	7.41×10^{-5}	2.12×10^{-3}	29	2.87×10^{4}
2	7.41×10^{-5}	3.18×10^{-3}	43	3.89×10^{4}
3	7.41×10^{-5}	4.24×10^{-3}	57	4.93×10^{4}
4	7.41×10^{-5}	5.31×10^{-3}	72	6.00×10^{4}
5	7.41×10^{-5}	6.37×10^{-3}	86	7.02×10^{4}
$k_2 = 9.79 \times 10^{6}$ M^{-1}s^{-1}				

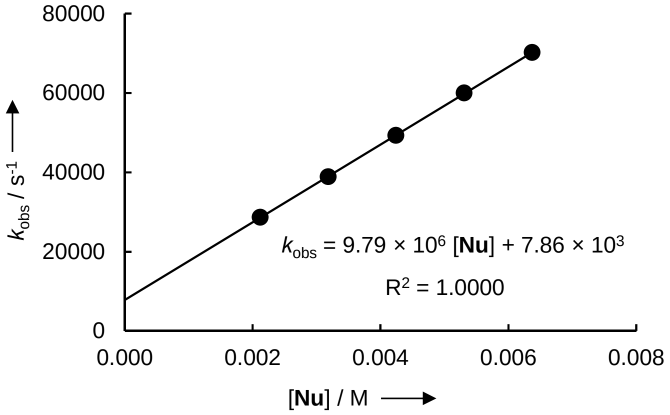

Rate constants for the reaction of DABCO (**9**) with (thq)$_2$CH$^+$ (**10j**) at 20°C in DMSO (laser-flash technique)

No	[E]$_0$ / M	[Nu]$_0$ / M	[Nu]$_0$ / [E]$_0$	k_{obs} / s^{-1}
1	1.20×10^{-4}	3.79×10^{-3}	32	8.90×10^{4}
2	1.20×10^{-4}	5.68×10^{-3}	47	1.36×10^{5}
3	1.20×10^{-4}	7.57×10^{-3}	63	1.85×10^{5}
4	1.20×10^{-4}	9.46×10^{-3}	79	2.36×10^{5}
5	1.20×10^{-4}	1.14×10^{-2}	95	2.91×10^{5}
$k_2 = 2.65 \times 10^{7}$ M^{-1}s^{-1}				

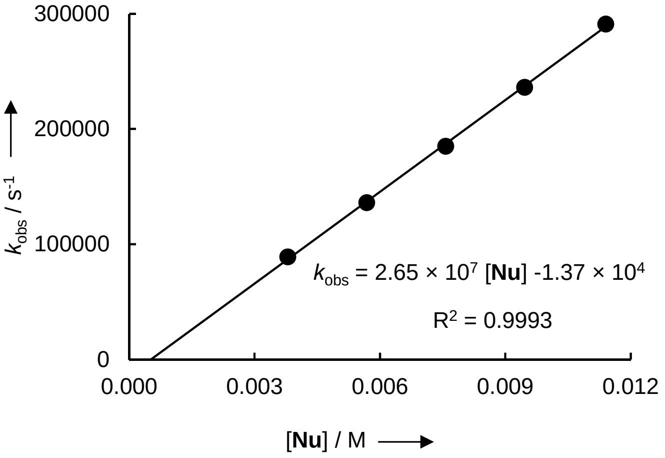

Rate constants for the reaction of DABCO (**9**) with $(pyr)_2CH^+$ (**10k**) at 20°C in DMSO (laser-flash technique)

No	$[E]_0$ / M	$[Nu]_0$ / M	$[Nu]_0$ / $[E]_0$	k_{obs} / s^{-1}
1	6.61×10^{-5}	9.46×10^{-4}	14	8.31×10^{4}
2	6.61×10^{-5}	1.18×10^{-3}	18	1.01×10^{5}
3	6.61×10^{-5}	1.42×10^{-3}	21	1.23×10^{5}
4	6.61×10^{-5}	1.66×10^{-3}	25	1.43×10^{5}
5	6.61×10^{-5}	1.89×10^{-3}	29	1.66×10^{5}
$k_2 = 8.77\times 10^7$ $M^{-1}s^{-1}$				

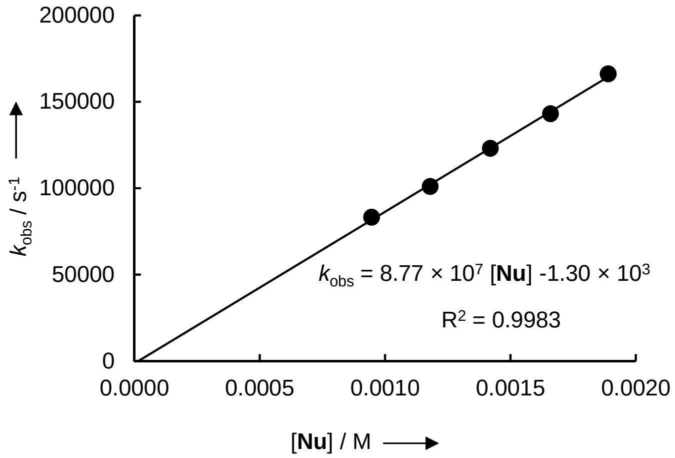

Rate constants for the reaction of DABCO (**9**) with $(dma)_2CH^+$ (**10l**) at 20°C in DMSO (laser-flash technique)

No	$[E]_0$ / M	$[Nu]_0$ / M	$[Nu]_0$ / $[E]_0$	k_{obs} / s^{-1}
1	3.65×10^{-5}	7.20×10^{-4}	20	8.23×10^{4}
2	3.65×10^{-5}	1.08×10^{-3}	30	1.27×10^{5}
3	3.65×10^{-5}	1.44×10^{-3}	39	1.74×10^{5}
4	3.65×10^{-5}	1.80×10^{-3}	49	2.22×10^{5}
5	3.65×10^{-5}	2.16×10^{-3}	59	2.70×10^{5}
$k_2 = 1.31 \times 10^8$ $M^{-1}s^{-1}$				

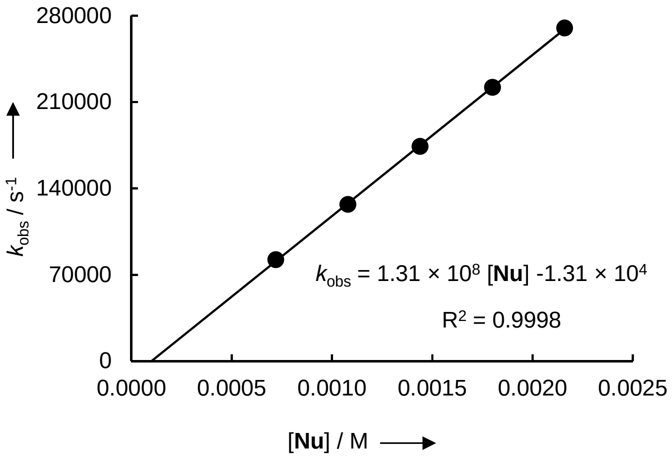

Determination of the nucleophilicity parameters *N* and s_N for DABCO (**9**) in DMSO

Rate constants for the reaction of DABCO (**9**) with reference electrophiles **10**.

Electrophile	*E*	k_2/M^{-1}s^{-1}	log k_2
$(ind)_2CH^+BF_4^-$	-8.76	9.79 × 10^6	6.99
$(thq)_2CH^+BF_4^-$	-8.22	2.65 × 10^7	7.42
$(pyr)_2CH^+BF_4^-$	-7.69	8.77 × 10^7	7.94
$(dma)_2CH^+BF_4^-$	-7.02	1.31 × 10^8	8.12
N = 16.62, *s* = 0.89			

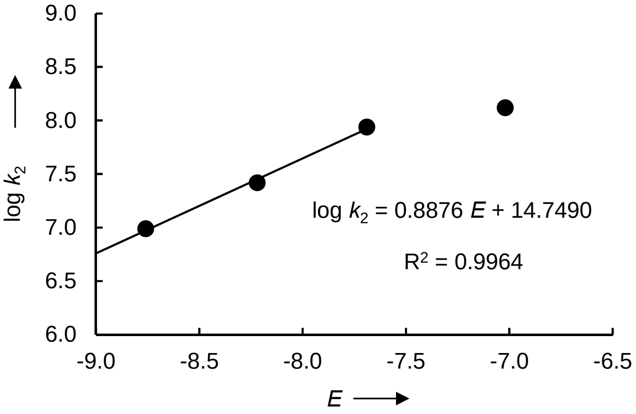

1.4. References

(1) a) W. P. Jencks, M. Gilchrist, *J. Am. Chem. Soc.* **1968**, *90*, 2622–2637; b) B. Schreiber, H. Martinek, P. Wolschann, P. Schuster, *J. Am. Chem. Soc.* **1979**, *101*, 4708-4713; c) L. A. P. Kane-Maguire, E. D. Honig, D. A. Sweigart, *Chem. Rev.* **1984**, *84*, 525-543; d) C. D. Ritchie, *Can. J. Chem.* **1986**, *64*, 2239–2250; e) C. F. Bernasconi, M. Panda, *J. Org. Chem.* **1987**, *52*, 3042–3050; f) Z. Rappoport, A. Topol, *J. Org. Chem.* **1989**, *54*, 5967–5977; g) N. S. Nudelman, *J. Phys. Org. Chem.* **1989**, *2*, 1–14; h) C. F. Bernasconi, M. W. Stronach, *J. Am. Chem. Soc.* **1991**, *113*, 2222–2227; i) J. P. Richard, T. L. Amyes, T. Vontor, *J. Am. Chem. Soc.* **1992**, *114*, 5626–5634; j) C. F. Bernasconi, A. E. Leyes, *J. Am. Chem. Soc.* **1993**, *115*, 7513–7514; k) L. García-Río, E. Iglesias, J. R. Leis, M. E. Peña, A. Ríos, *J. Chem. Soc. Perkin Trans. 2* **1993**, 29–37; l) C. K. M. Heo, J. W. Bunting, *J. Chem. Soc. Perkin Trans. 2* **1994**, 2279–2290; m) B. Varghese, S. Kothari, K. K. Banerji, *Int. J. Chem. Kinet.* **1999**, *31*, 245–252; n) A. D. Allen, T. T. Tidwell, *J. Org. Chem.* **1999**, *64*, 266–271; o) M. R. Crampton, J. Delaney, L. C. Rabbitt, *J. Chem. Soc. Perkin Trans. 2* **1999**, 2473–2480; p) J. P. Richard, M. M. Toteva, J. Crugeiras, *J. Am. Chem. Soc.* **2000**, *122*, 1664–1674; q) H. K. Oh, J. H. Yang, H. W. Lee, *J. Org. Chem.* **2000**, *65*,5391–5395; r) I.-H. Um, J.-S. Min, J.-A. Ahn, H.-J. Hahn, *J. Org. Chem.* **2000**, *65*, 5659–5663; s) C. F. Bernasconi, C. Whitesell, R. A. Johnson, *Tetrahedron* **2000**, *56*, 4917–4924; t) E. A. Castro, M. G. Ruiz, J. G. Santos, *Int. J. Chem. Kinet.* **2001**, *33*, 281–287; u) N. C. de Lucas, J. C. Netto-Ferreira, J. Andraos, J. C. Scaiano, *J. Org. Chem.* **2001**, *66*, 5016–5021; v) D. Rajarathnam, T. Jeyakumar, P. A. Nadar, *Int. J. Chem. Kinet.* **2002**, *34*, 366–373; w) H. K. Oh, T. S. Kim, H. W. Lee, I. Lee, *Bull. Korean Chem. Soc.* **2003**, *24*, 193–196; x) P. M. Mancini, G. G. Fortunato, L. R. Vottero, *J. Phys. Org. Chem.* **2004**, *17*, 138–147; y) H. K. Oh, I. K. Kim, H. W. Lee, I. Lee, *J. Org. Chem.* **2004**, *69*, 3806–3810; z) M. R. Crampton, T. A. Emokpae, C. Isanbor, *J. Phys. Org. Chem.* **2006**, *19*, 75–80.

(2) a) R. N. Washburne, J. G. Miller, A. R. Day, *J. Am. Chem. Soc.* **1958**, *80*, 5963 – 5965; b) J. F. Bunnett, G. T. Davis, *J. Am. Chem. Soc.* **1958**, *80*, 4337 – 4339; c) W. P. Jencks, J. Carriuolo, *J. Am. Chem. Soc.* **1960**, *82*, 1778 – 1786. d) T. C. Bruice, A. Donzel, R.W. Huffman, A. R. Butler, *J. Am. Chem. Soc.* **1967**, *89*, 2106 – 2121; e) J. E. Dixon, T. C. Bruice, *J. Am. Chem. Soc.* **1971**, *93*, 6592 – 6597; f) C. D. Ritchie, *J. Am. Chem. Soc.* **1975**, *97*, 1170 – 1179; g) J. W. Bunting, J. M. Mason, C. K. M. Heo, *J. Chem. Soc. Perkin Trans. 2* **1994**, 2291 – 2300; h) J. R. Leis, M. E. PeÇa, A. M. Rios, *J. Chem. Soc. Perkin Trans. 2* **1995**, 587 – 593.

(3) For investigations of pyridine nucleophilicities in S_N2 reactions see:

a) H. C. Brown, A. Cahn, *J. Am. Chem. Soc.* **1955**, *77*, 1715 –1723; b) K. Clark, K. Rothwell, *J. Chem. Soc.* **1960**, 1885 –1895; c) G. Coppens, F. Declerck, C. Gillet, J. Nasielski, *Bull. Soc. Chim. Belg.* **1963**, *72*, 25– 37; d) O. Rogne, *J. Chem. Soc. B* **1970**, 727 –730; e) K. J. Schaper, *Arch. Pharm.* **1978**, *311*, 641 –649; f) K. J. Schaper, *Arch. Pharm.* **1978**, *311*, 650 – 663; g) E. M. Arnett, R. Reich, *J. Am. Chem. Soc.* **1980**, *102*, 5892 – 5902; h) C. D. Johnson, I. Roberts, P. G. Taylor, *J. Chem. Soc. Perkin Trans. 2* **1981**, 409 – 413; i) Y. Kondo, M.Ogasa, S. Kusabayashi, *J. Chem. Soc. Perkin Trans. 2* **1984**, 2093 – 2097; j) C. Lim, S.-H. Kim, S.-D. Yoh, M. Fujio, Y. Tsuno, Tetrahedron Lett. **1997**, *38*, 3243 – 3246; k) Y. Kondo, R. Uematsu, Y. Nakamura, S. Kusabayashi, *J. Chem. Soc. Perkin Trans. 2* **1998**, 1219 – 1224; l) S.-D. Yoh, D.-Y. Cheong, C.-H. Lee, S.-H. Kim, J.-H. Park, M. Fujio, Y. Tsuno, *J. Phys. Org. Chem.* **2001**, *14*, 123 –130; m) S.-D. Yoh, D.-Y. Cheong, O.-S. Lee, *J. Phys. Org. Chem.* **2003**, *16*, 63– 68.

(4) For investigations of pyridine nucleophilicities towards cationic metal π complexes see:
a) L. A. P. Kane-Maguire, E. D. Honig, D. A. Sweigart, *Chem. Rev.* **1984**, *84*, 525 –543; b) T. I. Odiaka, L. A. P. Kane-Maguire, *J. Chem. Soc. Dalton Trans.* **1981**, 1162 – 1168.

(5) a) C. K. M. Heo and J. W. Bunting, *J. Chem. Soc., Perkin Trans. 2*, **1994**, 2279–2290; (b) A. A. Matveev, A. N. Vdovichenko, A. F. Popov, L. M. Kapkan, A. Y. Chervinskii and V. N. Matvienko, *Russ. J. Org. Chem.*, **1995**, *31*, 1646–1649.

(6) M. K. Kiesewetter, M. D. Scholten, N. Kirn, R. L. Weber, J. L. Hendrick, R. M. Waymouth, *J. Org. Chem.* **2009**, *74*, 9490-9496

(7) C. G. Swain, C. B. Scott, *J. Am. Chem. Soc.* **1953**, *75*, 141–147.

(8) a) C. D. Ritchie, *Acc. Chem. Res.* **1972**, *5*, 348–354; b) C. D. Ritchie, R. J. Minasz, A. A. Kamego, M. Sawada, *J. Am. Chem. Soc.* **1977**, *99*, 3747–3753; c) C. D. Ritchie, C. Kubisty, G. Y. Ting, *J. Am. Chem. Soc.* **1983**, *105*, 279–284.

(9) a) H. Mayr, M. Patz, *Angew. Chem.* **1994**, *106*, 990; *Angew. Chem. Int. Ed. Engl.* **1994**, *33*, 938–957; b) H. Mayr, T. Bug, M. F. Gotta, N. Hering, B. Irrgang, B. Janker, B. Kempf, R. Loos, A. R. Ofial, G. Remennikov, H. Schimmel, *J. Am. Chem. Soc.* **2001**, *123*, 9500–9512; c) R. Lucius, R. Loos, H. Mayr, *Angew. Chem.* **2002**, *114*, 97-102; *Angew. Chem. Int. Ed.* **2002**, *41*, 91–95; d) H. Mayr, B. Kempf, A. R. Ofial, *Acc. Chem. Res.* **2003**, *36*, 66–77; e) H. Mayr, A. R. Ofial, *Pure Appl. Chem.* **2005**, *77*, 1807–1821; f) H. Mayr, *Angew. Chem.* **2011**, *123*, 3692; *Angew. Chem. Int. Ed.* **2011**, *50*, 3612–3618; g) J. Ammer, C. Nolte, H. Mayr, *J. Am. Chem. Soc.* **2012**, *134*, 13902–13911; h) for a comprehensive listing of nucleophilicity parameters *N* and electrophilicity parameters *E*, see http://www.cup.uni-muenchen.de/oc/mayr/DBintro.html.

(10) For publications on the reactivities of aliphatic amines see:

a) S. Minegishi, H. Mayr, *J. Am. Chem. Soc.* **2003**, *125*, 286-295, b) T. B. Phan, M. Breugst, H. Mayr, *Angew. Chem. Int. Ed.* **2006**, *45*, 3869-3874, c) F. Brotzel, Y. C. Chu, H. Mayr, *J. Org. Chem.* **2007**, *72*, 3679-3688, d) M. Baidya, S. Kobayashi, F. Brotzel, U. Schmidhammer, E. Riedle, H. Mayr *Angew. Chem. Int. Ed.* **2007**, *46*, 6176-6179, e) T. B. Phan, C. Nolte, S. Kobayashi, A. R. Ofial, H. Mayr, *J. Am. Chem. Soc.* **2009**, *131*, 11392-11401, f) T. Kanzian, T. A. Nigst, A. Maier, S. Pichl, H. Mayr, *Eur. J. Org. Chem.* **2009**, 6379-6385, g) J. Ammer, M. Baidya, S. Kobayashi, H. Mayr, *J. Phys. Org. Chem.* **2010**, *23*, 1029-1035, h) T. A. Nigst, A. Antipova, H. Mayr, *J. Org. Chem.* **2012**, *77*, 8142-8155.

(11) For reactivities of anilines see ref. 10c

(12) For reactivities of pyridines and quinolines see:

a) F. Brotzel, B. Kempf, T. Singer, H. Zipse, H. Mayr, *Chem. Eur. J.* **2007**, *13*, 336-345, b) M. Baidya, M. Horn, H. Zipse, H. Mayr, *J. Org. Chem.* **2009**, *74*, 7157-7164, c) N. De Rycke, G. Berionni, F. Couty, H. Mayr, R. Goumont, O. R. P. David, *Org. Lett.* **2011**, *13*, 530-533, d) T. A. Nigst, J. Ammer, H. Mayr, *J. Phys. Chem. A* **2012**, *116*, 8494-8499.

(13) For reactivities of amidines, guanidines, isothioureas and imines see:

a) M. Baidya, H. Mayr, *Chem. Commun.* **2008**, 1792-1794, b) B. Maji, C. Joannesse, T. A. Nigst, A. D. Smith, H. Mayr, *J. Org. Chem.* **2011**, *76*, 5104-5112, c) B. Maji, D. S. Stephenson, H. Mayr, *ChemCatChem* **2012**, *4*, 993-999, d) B. Maji, H. Mayr, *Z. Naturforsch. B* **2013,** *68b*, 693-699.

(14) For reactivities of azoles see M. Baidya, F. Brotzel, H. Mayr, *Org. Biomol. Chem.* **2010**, *8*, 1929-1935.

(15) For reactivities of a-effect nucleophiles see:

a) T. A. Nigst, J. Ammer, H. Mayr, *Angew. Chem. Int. Ed.* **2012**, *51*, 1353-1356, b) see also ref. 10a and10h

(16) For reactivities of imidazolines and relative compounds see B. Maji, M. Baidya, J. Ammer, S. Kobayashi, P. Mayer, A. R. Ofial, H. Mayr, *Eur. J. Org. Chem.* **2013**, 3369-3377.

(17) For example, for comparison of the reactivities of amines in different solvent media see 10a, 10b, 10e and 10f.

(18) B. Kempf, H. Mayr, *Chem. Eur. J.* **2005**, *11*, 917 – 927.

(19) J. Bartl, S. Steenken, H. Mayr, R. A. McClelland, *J. Am. Chem. Soc.* **1990**, *112*, 6918−6928.

(20) J. Ammer, C. F. Sailer, E. Riedle, H. Mayr, *J. Am. Chem. Soc.* **2012**, *134*, 11481−11494.

(21) (a) J. C. Scaiano, In *Reactive Intermediate Chemistry*; R. A. Moss, M. S. Platz, M. J. Jones, Eds.,Wiley: Hoboken, NJ, 2004; pp 847−871. (b) N. P. Schepp, F. L. Cozens, In

Lasers in Chemistry; M. Lackner, Ed., Wiley-VCH: Weinheim, Germany, 2008; Vol. 2, pp 1073−1091.

(22) a) I.-H. Um, S. Yoon, H.-R. Park, H.-J. Han, *Org. Biomol. Chem.* **2008**, *6*, 1618–1624; b) E. A. Castro, *Pure Appl. Chem.* **2009**, *81*, 685–696.

(23) I.-H. Um, J.-A. Seok, H.-T. Kim, S.-K. Bae, *J. Org. Chem.* **2003**, *68*, 7742–7746.

(24) M. J. Pfeiffer, S. B. Hanna, *J. Org. Chem.* **1993**, *58*, 735–740.

(25) H. Mayr, J. Ammer, M. Baidya, B. Maji, T. A. Nigst, A. R. Ofial, T. Singer, *J. Am. Chem. Soc.* **2015**, *137*, 2580-2599.

(26) C. Reichardt, *Solvents and Solvent Effects in Organic Chemistry*, 3rd ed., Wiley-VCH, Weinheim, 2003.

(27) This can not be applied generally for all reactions, but appears to be justified for the reactions of phosphanes with reference benzhydrylium ions, for which both kinetic and thermodynamic data are available.

(28) (a) R Lucius,.H. Mayr, *Angew. Chem.* **2000**, *112*, 2086−2089; *Angew. Chem., Int. Ed.* **2000**, *39*, 1995−1997. (b) S. Evans, P. Nesvadba,. S. Allenbach,.(Ciba-Geigy AG) Patent EP-B744392, 1996; *Chem. Abstr.* **1997**, *126*, 46968v.

(29) K. Troshin, H. Mayr, *J. Am. Chem. Soc.* **2013**, *135*, 252-265.

CHAPTER 2

Reactivities of neutral N- and P-nucleophiles towards neutral S_N2 substrates. Comparison with the reactivities towards benzhydrylium ions and analysis of trends.

2.1. Introduction

In the introduction to this thesis, several linear free energy relationships have been mentioned which describe nucleophilic reactivity as a relative rate constant for the nucleophilic attack of an electron donor upon an electrophilic substrate. Among them are Swain-Scott's[1] and Ritchie's[2] equations, which are commonly used for defining the nucleophilic reactivities towards sp^3- and sp^2-hybridized electrophilic carbon, respectively.

The first study of the relationship between the reactivities of nucleophiles towards unsaturated and saturated carbon electrophiles in a systematic quantitative manner was performed by Bunting et al. on the example of the reactions of methyl 4-nitrobenzenesulfonate and 1-methyl-4-vinylpyridinium ion with amines.[3] A good agreement between the reactivities of primary and secondary amines towards structurally different electrophilic substrates was demonstrated in that work. Comparison of Ritchie N_+ nucleophilicity parameters for the addition reactions to sp^2-hybridized carbon with Swain-Scott n parameters for the S_N2 reactions, made by Richard and coworkers,[4] showed analogous orders of reactivities towards carbocations and alkyl halides for several nucleophiles, with the exception of N_3^- and α-effect nucleophiles.

The next important step to the understanding of the relationship between the nucleophilic reactivities towards structurally different electrophilic substrates was the observation that the N and s_N parameters, which have been derived from the rate constants for the reactions with benzhydryl cations and quinone methides on the basis of Equation 1,[5] were also relevant for the S_N2 reactions of S-methyldibenzothiophenium ion with different nucleophilic solvents and solvent mixtures, as well as N-, O-, P- and C-nucleophiles, both neutral and negatively charged, in methanol (Figure 2.1).[6]

$$\log k_2 = s_N (E + N) \qquad (1)$$

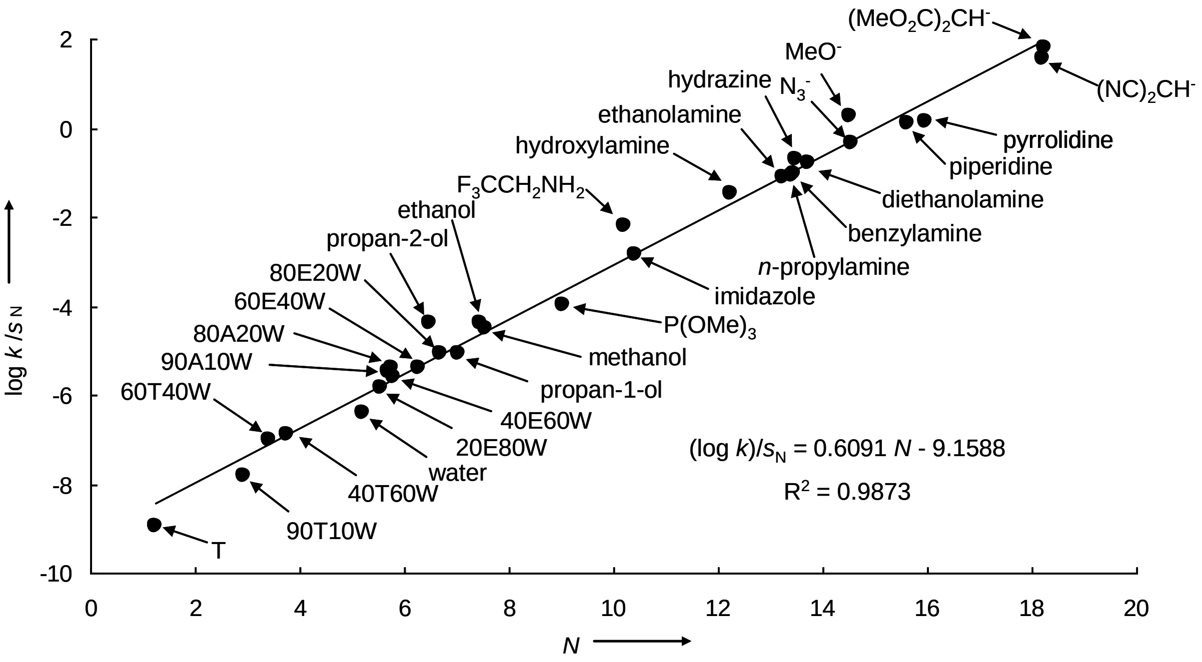

Figure 2.1. Correlation of (log k)/s_N of the reactions of S-methyldibenzothiophenium ion with different solvents and with solutions of nucleophiles in methanol versus the nucleophilicty parameters N.

The non-unity slope of the correlation of (log k)/s_N versus N in Figure 2.1 indicated, however, that Equation 1 is not applicable for predicting the reactivities towards S-methyldibenzothiophenium ion, which suggested extension of Equation 1 to Equation 2 by an electrophile-specific parameter s_E:

$$\log k = s_E s_N (E + N) \qquad (2)$$

Equation 2 includes the Swain-Scott, the Ritchie equations and Equation 1 as special cases.

To define the scope and limitations of Equation 2 is the main objective of this chapter. It is concerned with the S_N2 reactions of neutral nitrogen and phosphorus nucleophiles with benzyl, phenacyl and alkyl halides and tosylates. As most of these nucleophiles were characterized by N and s_N parameters on the basis of Equation 1 (some of the nucleophilicity parameters were determined in the previous chapter), we will be able to compare their reactivities towards Csp^2 and Csp^3 electrophilic centers directly.

2.2. Results and Discussion

2.2.1. Kinetics of the Reactions of Neutral Nucleophiles with Typical S_N2 Substrates

Methods employed for kinetic measurements

All reactions of benzyl and phenacyl halides **1**-**4**-Cl,Br as well as methyl iodide (**5**-I) and methyl tosylate (**5**-OTs) with neutral N- and P-nucleophiles were studied conductimetrically by following the increase of conductivity due to formation of ammonium or phosphonium salt from the uncharged species. Conventional and stopped-flow methods used for these experiments have already been described earlier.[7]

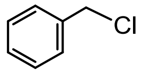

1-Cl

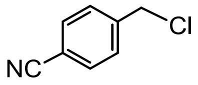

2-Cl

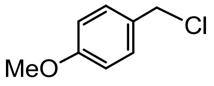

3-Cl

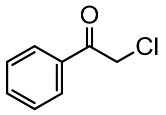

4-Cl

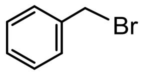

1-Br

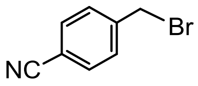

2-Br

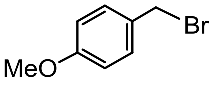

3-Br

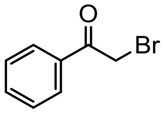

4-Br

MeI

5-I

MeOTs

5-OTs

Kinetic experiments were performed in dimethyl sulfoxide or in acetonitrile at 20 ºC.

All experiments were carried out under pseudo-first order conditions (≥10 equivalents of the nucleophiles over the electrophiles).

Evaluation of kinetic data

For all S_N2 reactions studied in this work, first-order rate constants were obtained by fitting the time-dependent conductivities to the monoexponential function (Eq. 3).

$$G = G_\infty(1 - e^{-k_1 t}) + C \qquad (3)$$

The plots of the observed pseudo-first order rate constants versus the nucleophile concentrations were linear for all studied combinations. The second-order rate constants for the substitution reactions were obtained from the slopes of these plots, according to Eq. 4.

$$k_{\mathrm{obs}} = k_2\,[\mathrm{Nu}] + k_1 \qquad (4)$$

A typical monoexponential time-dependent conductivity curve and a plot of k_{obs} (s^{-1}) versus the nucleophile concentration are shown in Figure 2.2.

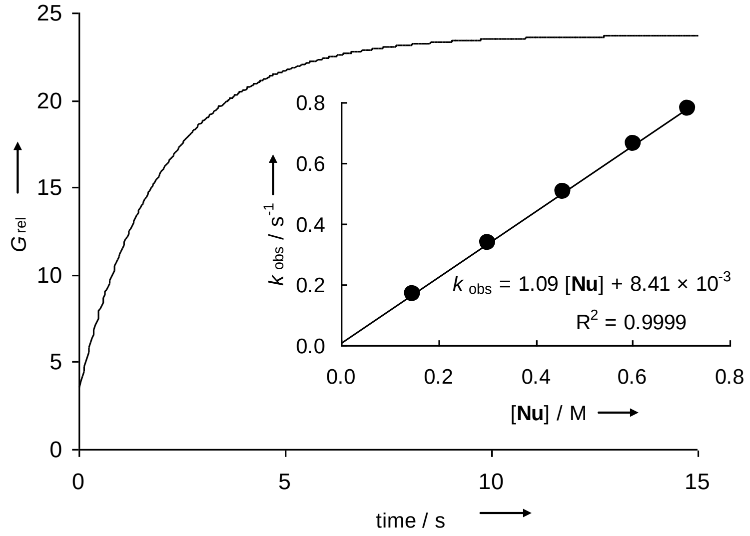

Figure 2.2. A monoexponential increase of conductivity during the reaction of phenacyl bromide **4**-Br with a 0.46 M solution of benzylamine in DMSO at 20ºC. Inset: Plot of k_{obs} versus different concentrations of benzylamine .

The obtained second-order rate constants for the reactions of electrophiles **1**-**4**-Cl,Br and **5**-I, OTs with neutral nucleophiles in DMSO and acetonitrile are listed in Tables 2.1 and 2.2, respectively.

Table 2.1. Rate constants k_2 ($M^{-1}s^{-1}$) for the reactions of electrophiles **1-4**-Cl,Br and **5**-I,OTs with nitrogen nucleophiles in DMSO at 20°C.

Nucleophiles	**1**-Cl	**2**-Cl	**3**-Cl	**4**-Cl	**1**-Br	**2**-Br	**3**-Br	**4**-Br	**5**-I	**5**-OTs
DABCO	1.31×10^{-1}	1.64×10^{-1}	2.96×10^{-1}	-	-	2.55×10^{1}	-	5.78×10^{1}	8.79	-
TBD	-	-	-	-	1.71	4.19	-	1.59×10^{2}	3.07	-
1,1-dimethylhydrazine[a]	2.29×10^{-2}	3.43×10^{-2}	6.51×10^{-2}	-	3.73	4.66	9.19	-	-	-
methylhydrazine[a]	1.77×10^{-2}	3.18×10^{-2}	3.62×10^{-2}	-	1.92	3.38	5.02	-	-	-
DBN	-	-	-	-	4.52×10^{-1}	7.15×10^{-1}	-	-	-	-
DBU	-	-	-	-		1.10×10^{-1}	-	-	1.63×10^{-1}	-
TMG	-	-	-	-	1.21×10^{-2}	1.81×10^{-2}	-	-	-	-
piperidine	1.94×10^{-2}	4.54×10^{-2}	4.82×10^{-2}	1.54×10^{-1}	-	4.15	6.13	3.07×10^{1}	-	1.80×10^{-1}
morpholine	6.66×10^{-3}	8.04×10^{-3}	-	3.31×10^{-2}	-	1.05	2.04	5.43	5.63×10^{-1}	4.08×10^{-2}
2-aminoethanol	-	2.15×10^{-3}	-	1.71×10^{-2}	-	2.85×10^{-1}	-	2.73	1.83×10^{-1}	2.76×10^{-2}
1-aminopropan-2-ol	-	1.90×10^{-3}	-	1.51×10^{-2}	-	3.29×10^{-1}	-	2.48	2.44×10^{-1}	2.84×10^{-2}
n-propylamine	1.59×10^{-3}	2.26×10^{-3}	3.25×10^{-3}	2.72×10^{-2}	-	3.07×10^{-1}	-	4.13	3.31×10^{-1}	4.27×10^{-2}
benzylamine	8.29×10^{-4}	-	1.72×10^{-3}	7.48×10^{-3}	-	1.71×10^{-1}	-	1.09	1.83×10^{-1}	2.38×10^{-2}
4-DMAP	-	-	-	5.88×10^{-3}	-	5.81×10^{-2}	-	9.28×10^{-1}	3.08×10^{-2}	3.98×10^{-3}
2-aminobutan-1-ol	-	5.06×10^{-4}	-	2.78×10^{-3}	-	7.62×10^{-2}	-	5.09×10^{-1}	1.32×10^{-1}	1.38×10^{-2}
diethanolamine	-	-	-	1.89×10^{-3}	-	1.50×10^{-1}	-	3.75×10^{-1}	2.75×10^{-1}	1.87×10^{-2}
imidazole	-	-	(4.75×10^{-5})[a]	3.98×10^{-4}	-	4.25×10^{-3}	-	6.61×10^{-2}	3.43×10^{-3}	7.99×10^{-4}
2-methylbenzimidazole			-			2.66×10^{-4}	-	2.83×10^{-3}	8.14×10^{-4}	2.47×10^{-4}
2,2,2-trifluoroethylamine	-	-	-	5.30×10^{-5}	-	2.40×10^{-3}	9.56×10^{-3}	7.91×10^{-3}	-	-

a) Rate constants are given for alkylation of the methylated nitrogen atom. b) Positive intercept in k_{obs}/[amine] plot, comparable with k_{obs} values

Table 2.2. Second-order rate constants ($M^{-1}s^{-1}$) for the reactions of **1-3**-Br and **5**-I with nitrogen and phosphorous nucleophiles in acetonitrile at 20°C.

Nucleophiles	**1**-Br	**2**-Br	**3**-Br	**5**-I
DABCO	4.45	3.69	1.47×10^{1}	1.73
methylhydrazine	1.74×10^{-1}	2.20×10^{-1}	4.53×10^{-1}	-
N-methylpyrrolidine	-	2.55×10^{-1}	-	3.23×10^{-1}
N-methylpiperidine	-	-	-	7.31×10^{-2}
triethylamine	-	2.27×10^{-3}	-	3.06×10^{-2}
tributylamine	-	1.61×10^{-3}	-	-
pyrrolidine	-	7.55×10^{-1}	-	3.22×10^{-1}
piperidine	7.20×10^{-1}	7.70×10^{-1}	1.76	2.86×10^{-1}
morpholine	1.33×10^{-1}	1.09×10^{-1}	3.95×10^{-1}	4.12×10^{-2}
2-aminoethanol	1.98×10^{-2}	1.48×10^{-2}	4.88×10^{-2}	1.03×10^{-2}
dipropylamine	-	2.82×10^{-2}	1.96×10^{-1}	3.91×10^{-2}
n-butylamine	3.67×10^{-2}	-	1.04×10^{-1}	2.19×10^{-2}
n-propylamine	2.86×10^{-2}	3.20×10^{-2}	7.83×10^{-2}	1.93×10^{-2}
benzylamine	-	9.54×10^{-3}	3.23×10^{-2}	7.87×10^{-3}
4-DMAP	-	1.67×10^{-2}	-	7.24×10^{-3}
tert-butylamine	-	3.09×10^{-3}	-	6.40×10^{-3}
imidazole	-	6.46×10^{-4}	-	-
2,2,2-trifluoroethylamine	-	-	$(9.10 \times 10^{-4})^{a}$	-
tributylphosphane	-	2.73×10^{-1}	-	4.36×10^{-1}
tris(4-methoxyphenyl)phosphane	-	1.33×10^{-2}	-	2.18×10^{-2}
triphenylphosphane	-	1.68×10^{-3}	-	5.24×10^{-3}

a) Negative intercept in k_{obs}/[amine] correlation

2.2.2. Applicability of s_N and N Parameters for Predicting the Rate Constants for the S_N2 Type Reactions

In order to check the applicability of Eq. 2 for predicting the rate constants of the substitution reactions at saturated carbon, the correlations of log k_2/s_N versus N were created for the reactions of all substrates studied in this work with N- and P-nucleophiles (the rate constants are listed in Tables 2.1 and 2.2).

Figure 2.3 shows the correlations of log k_2/s_N versus N for the S_N2 reactions of **2**-Br and **5**-I with various neutral nucleophiles in DMSO versus the nucleophilicity parameters N. Similar correlations for the reactions of other substrates in DMSO and acetonitrile are given in the Experimental section. The quality of the correlations of log k_2/s_N versus N for the substrates from this work (Figure 2.3 and Figures 2.S5.1-2.S5.10(A) in section 2.S.5) is significantly lower than that of the correlation published in 2006 (Figure 2.1),[6] although many amines follow the linear correlation.

Before we discuss the reasons why Eq. 2 has a poorer predicting power for the S_N2 reactions studied in this work, than for the reactions of the S-methyldibenzothiophenium ion with various solvents and nucleophiles in methanol, let us have a look at the plots of log k_2 for the S_N2 reactions versus log k_2 for the addition reactions to the C_{sp2} electrophilic center. For this purpose we have chosen the $(lil)_2CH^+$ cation, the least reactive of all reference benzhydryl cations[5h] used for quantification of the nucleophilic reactivities on the basis of Eq. 1.

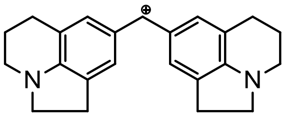

$(lil)_2CH^+$

The advantage of this choice is the fact that the reactions of this cation with most amines and phosphanes are not yet diffusion-controlled on the one hand, but are thermodynamically favoured on the other (for this reason, quinone methides, which are even less reactive, would not be suitable); this makes the rate constants of the reactions of $(lil)_2CH^+$ with amines and phosphanes not only predictable with Eq. 1, but also experimentally accessible in most cases.

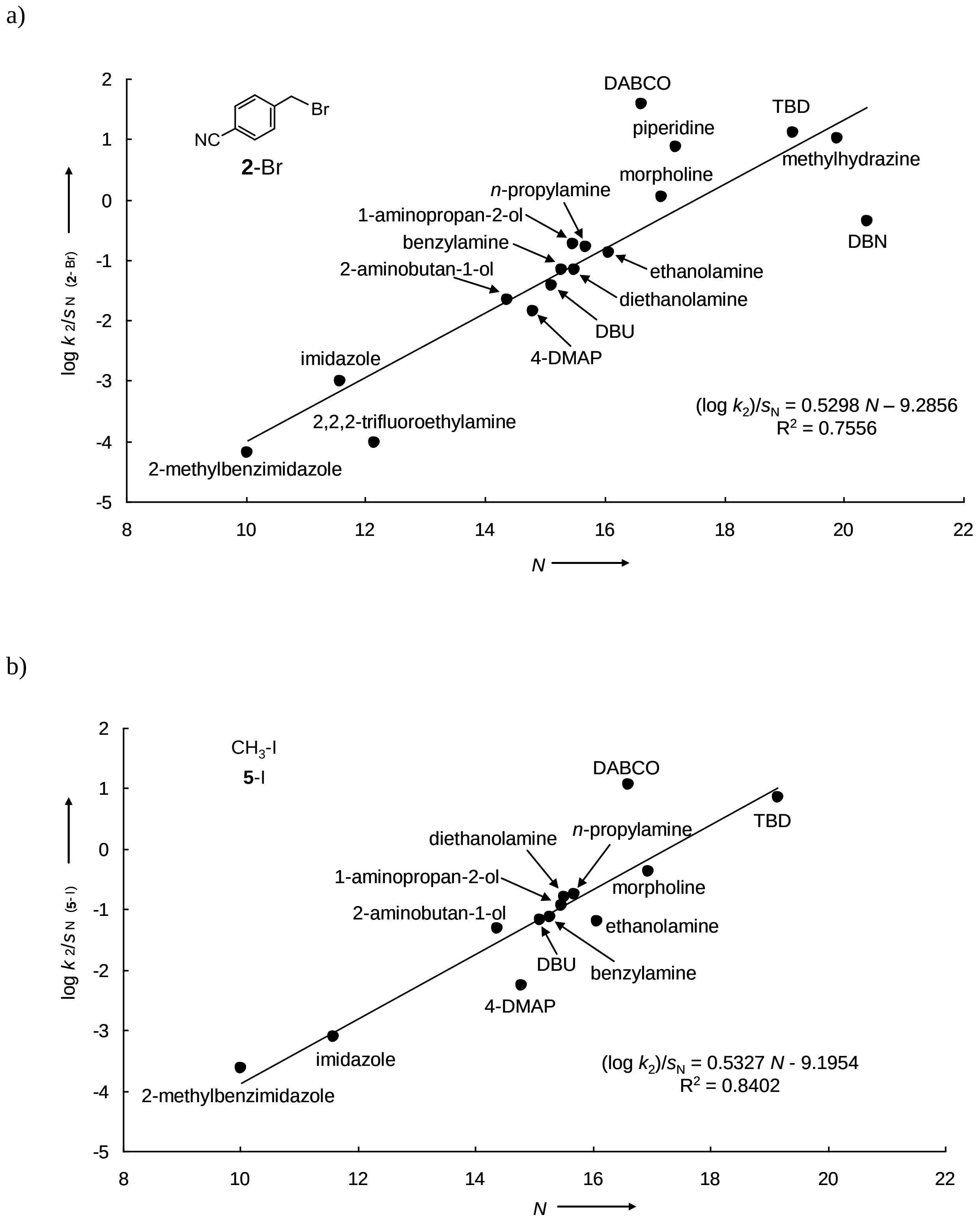

Figure 2.3. Correlation of log k_2/s_N of the reactions of the **2**-Br (a) and **5**-I (b) with various N-nucleophiles in DMSO versus the nucleophilicity parameters *N*.

.

Figure 2.4 shows the plots of log k_2 for the S_N2 reactions of amines with **2**-Br and **5**-I versus the calculated log k_2 values for the addition reactions of these amines to the $(\mathrm{lil})_2\mathrm{CH}^+$ cation in DMSO (analogous correlations for other substrates in DMSO and acetonitrile are shown in Figures 2.S5.1-2.S5.10(B) in section 2.S.5). The values of log $k_{(\mathrm{lil})_2\mathrm{CH}^+}$ in both solvents were calculated using Equation 1 with $E = -10.04^{5h}$ and are listed in Tables 2.S4.1 and 2.S4.2 in section 2.S.4. For both **2**-Br and **5**-I, the quality of the correlations of log k_2 of the S_N2 reaction versus log k_2 of the addition reaction to $(\mathrm{lil})_2\mathrm{CH}^+$ is much higher than that of the correlations of log k_2/s_N versus N.

We also created a plot of log k_{S_N2} for the reactions of S-methyldibenzothiophenium ion with different solvents and solutions of nucleophiles in methanol versus log $k_{(\mathrm{lil})_2\mathrm{CH}^+}$, which were calculated from s_N and N values of these nucleophiles and solvent mixtures (Figure 2.5, the values are listed in Table 2.S4.3)

Figures 2.4 and 2.5 show that the logarithmic rate constants of S_N2 reactions correlate linearly with the logarithms of the rate constants for addition reactions to the $(\mathrm{lil})_2\mathrm{CH}^+$. This fact supports the idea about a close relationship between the reactivities towads Csp^2 and Csp^3 electrophilic centers and shows that the deviations from the plots of log k_2/s_N versus N in Figure 2.3 are not due to the difference of the factors controlling the reactivity in the S_N2 type transformations and in the addition reactions to carbocations.

a)

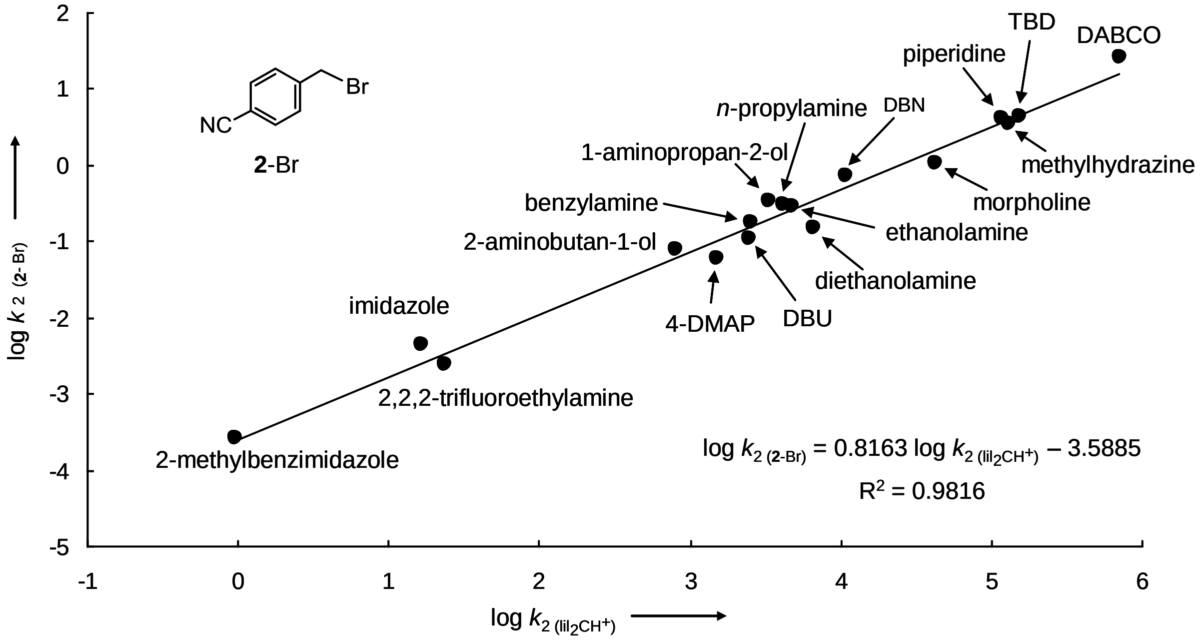

b)

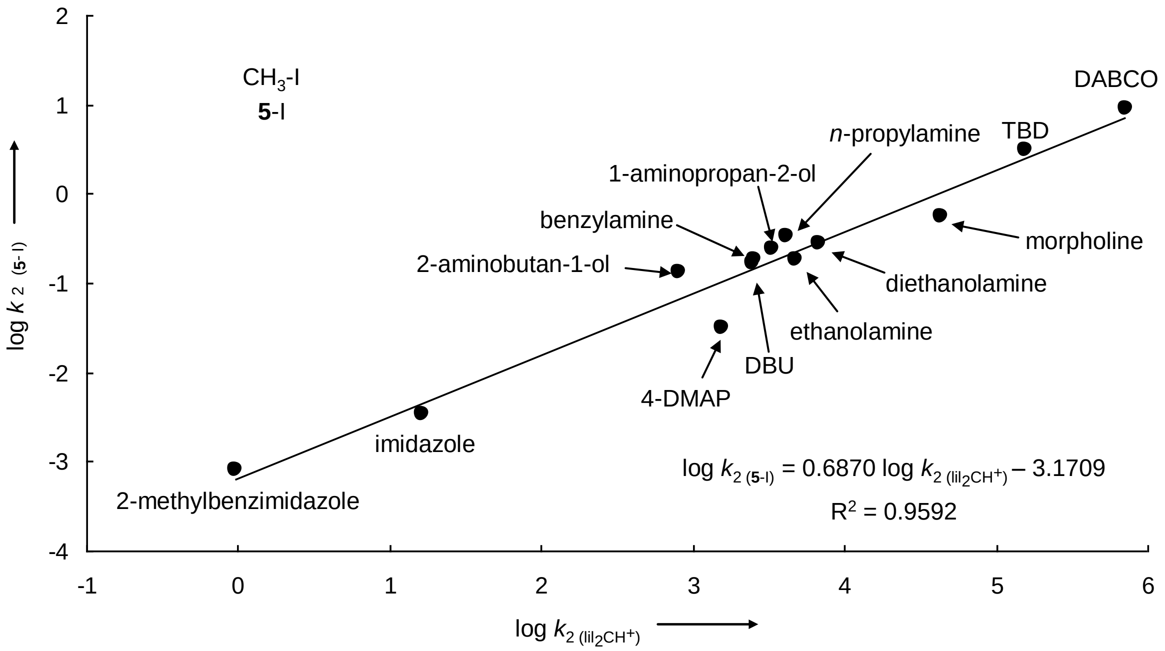

Figure 2.4. Correlation of log k_2 for the reactions of various N-nucleophiles with **2**-Br (a) and **5**-I (b) versus log k_2 for their reactions with the $\mathrm{lil_2CH^+}$ cation in DMSO.

Both ways of relating the S_N2 reactivity with the reactivity towards carbocationic center are based on s_N and N parameters of the nucleophiles. Why do they give different results? Is there any logical connection between the linearity of the plots of log $k_{\mathrm{S_N2}}$ versus log $k_{\mathrm{lil_2CH^+}}$ and Eq. 2?

According to Eq. 2, the rate constants for the reactions of a hypothetical S_N2 substrate with the electrophilicity parameter E_1 could be described with the following expression:

$$\log k_{\mathrm{S_N2}} = s_{\mathrm{E1}} s_{\mathrm{N}} (N + E_1) \qquad (5)$$

Let us now take another hypothetical electrophile, a benzhydrylium ion R^+ having the electrophilicity parameter E_2. Using Eq. 1, we can calculate the rate constants for the reactions of this electrophile with the same set of nucleophiles:

$$\log k_{\mathrm{R^+}} = s_{\mathrm{N}} (N + E_2) \qquad (6)$$

It is possible to express log $k_{\mathrm{S_N2}}$ through log $k_{\mathrm{R^+}}$:

$$\log k_{\mathrm{S_N2}} = s_{\mathrm{E1}} s_{\mathrm{N}} (N + E_2 - E_2 + E_1) = s_{\mathrm{E1}} s_{\mathrm{N}} (N + E_2 - \Delta E) = s_{\mathrm{E1}} \log k_{\mathrm{R^+}} - s_{\mathrm{E1}} s_{\mathrm{N}} \Delta E \qquad (7)$$

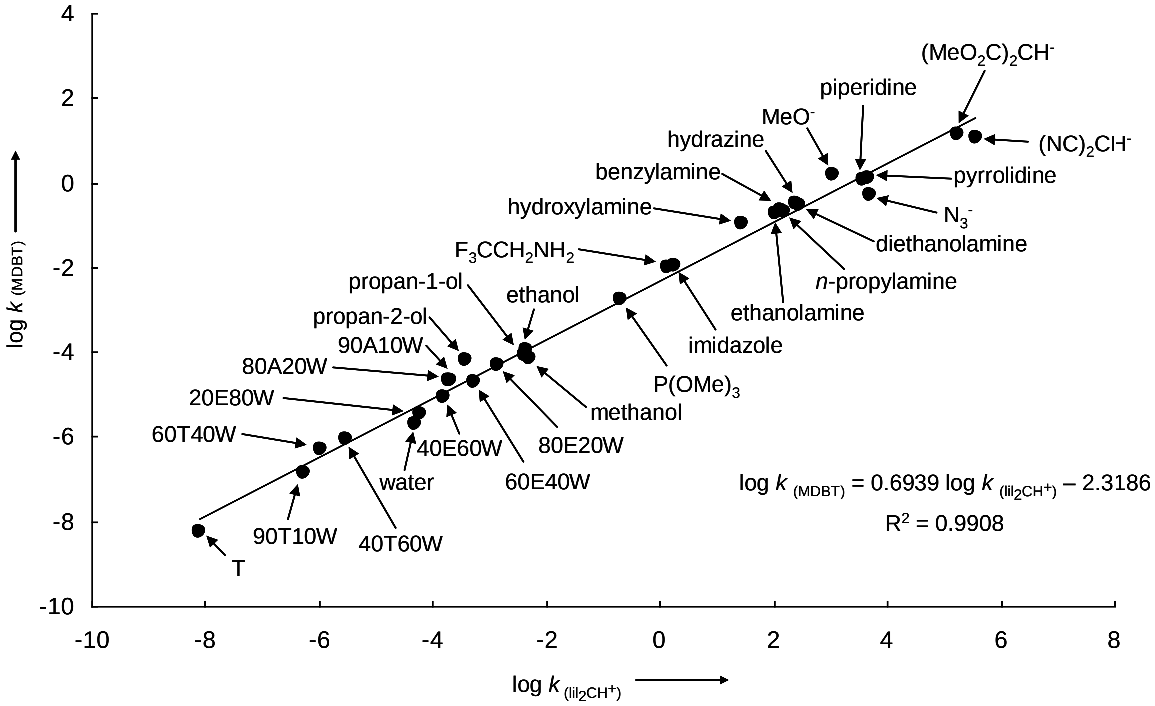

Figure 2.5. Correlation of log *k* for the S_N2 reactions of different solvents and solutions of nucleophiles with S-methyldibenzothiophenium ion in methanol versus log *k* of their reactions with lil_2CH^+.

Thus, according to Eq. 7, log k_{S_N2} is not a linear function of log k_{R^+}, because the term $s_{E1}s_N\ \Delta E$ depends on the nucleophile (s_N is neither a constant nor a linear function of log k_{R^+}).

Now another question arises: why did Eq. 2 hold for the reactions of S-methyldibenzothiophenium with different types of nucleophiles in methanol (Figure 2.1)? We are inclined to think that the choice of the nucleophiles played an important role in that case.

Figure 2.6a shows a plot of s_N versus N for the nucleophiles used by the authors in Ref. 6.

Although there is no perfect correlation between s_N and N parameters, one can definitely see a trend in the dependence of s_N on N. Whether it is a coincidence or a general property of the nucleophilicity scale, is a question worth a separate discussion (which is beyond the scope of this thesis). Anyway, with this observation it is possible to explain why both correlations of log k/s_N versus N and of log k_{S_N2} versus log $k_{lil_2CH^+}$ are linear in that specific case. Let us formulate the empirical equation describing the linear correlations in Figures 2.4 and 2.5:

$$\log k_{S_N2} = s's_N\,(N\text{-}10.04) + C \qquad (8)$$

where parameters s' and C are constant, while s_N and N are both variables. When s_N is a linear function of N, the correlation of $\log k_{S_N2}$ versus N should look parabolic, and it does indeed (Figure 2.6b), which reminds of Marcus curvature.

It is interesting to note that Eq. 8 is equivalent to the Swain-Scott equation,[1] the basis being the only difference (in the Swain-Scott equation, k_0 is the rate of the reaction of the substrate with water and the sensitivity parameter of the electrophile is calibrated to $s_{CH_3Br} = 1$, while in our case s of the $(lil)_2CH^+$ is unity by definition and k_0 is the rate of the reaction of the substrate with a hypothetical nucleophile reacting with $(lil)_2CH^+$ at the rate of 1 $M^{-1}s^{-1}$, that is, having an N parameter of 10.04).

Now let us devide both parts of Equation 8 by s_N:

$$\log k_{S_N2}/s_N = s'(N\text{-}10.04) + C/s_N \qquad (8a)$$

a)

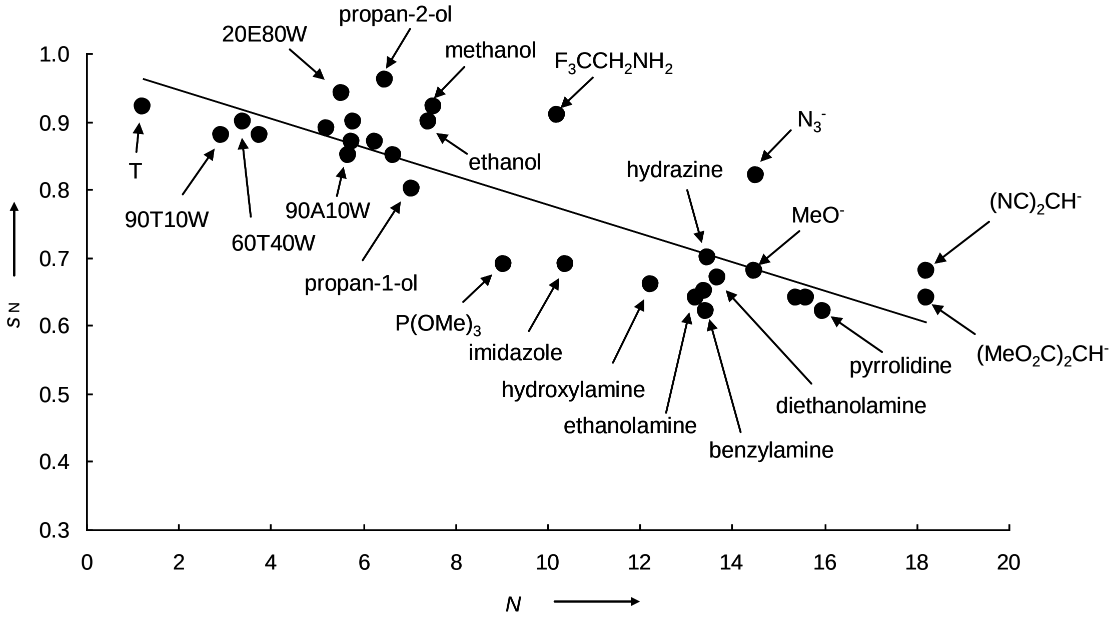

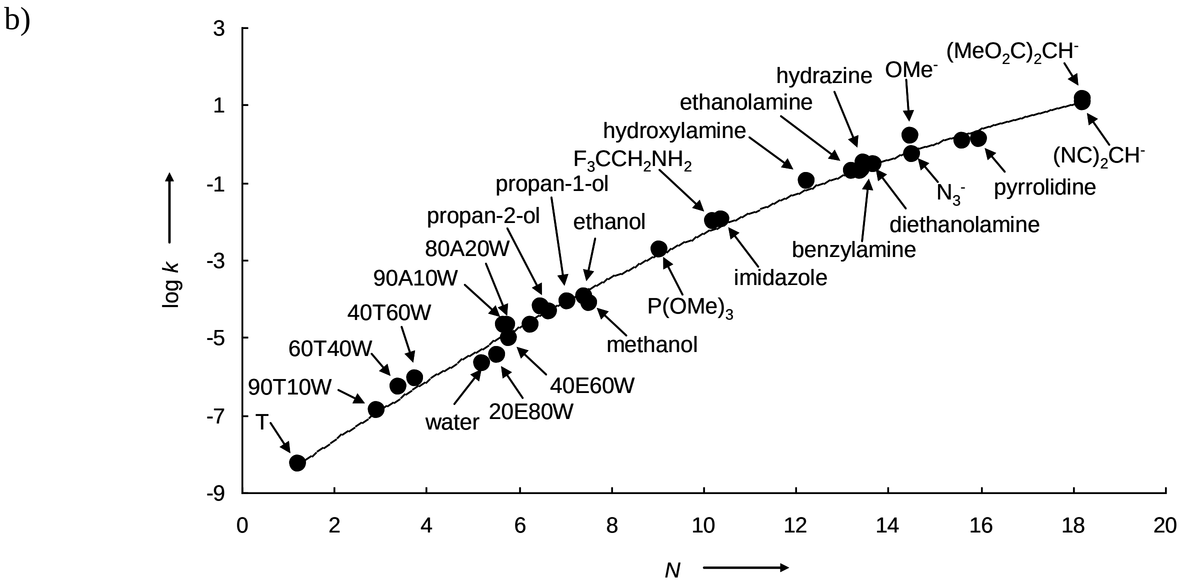

Figure 2.6. a) Plot of s_N versus N for the nucleophiles and solvent mixtures from Ref. 6. b) Plot of log k for the reactions of S-methyldibenzothiophenium ion with different solvents and solutions of nucleophiles in methanol versus their N parameters.

As s_N depends on N linearly and the coefficient of the variable N is rather small, the correlation of log k_{S_N2}/s_N versus N should be very close to linear (this statement is not mathematically rigorous, but is justified for the experimentally accessible k_{S_N2} values and real N and s_N parameters). This is the reason why we can see a linear plot of high quality in Figure 2.1. It is shown in more detail in a numerical experiment in section 2.S6.

The nucleophiles used in this study show rather a poor correlation of s_N versus N, there are several significant deviations from the linear trend (Figure 2.7a). The points for the corresponding nucleophiles deviate also most strongly from the plots of log k_{S_N2}/s_N versus N in Figure 2.3. On the contrary, the linearity of the plots of log k_{S_N2} versus log $k_{\mathrm{lil_2CH^+}}$ in Figure 2.4 and similar graphs for other electrophiles is not influenced by the scatter in the plot of s_N versus N.

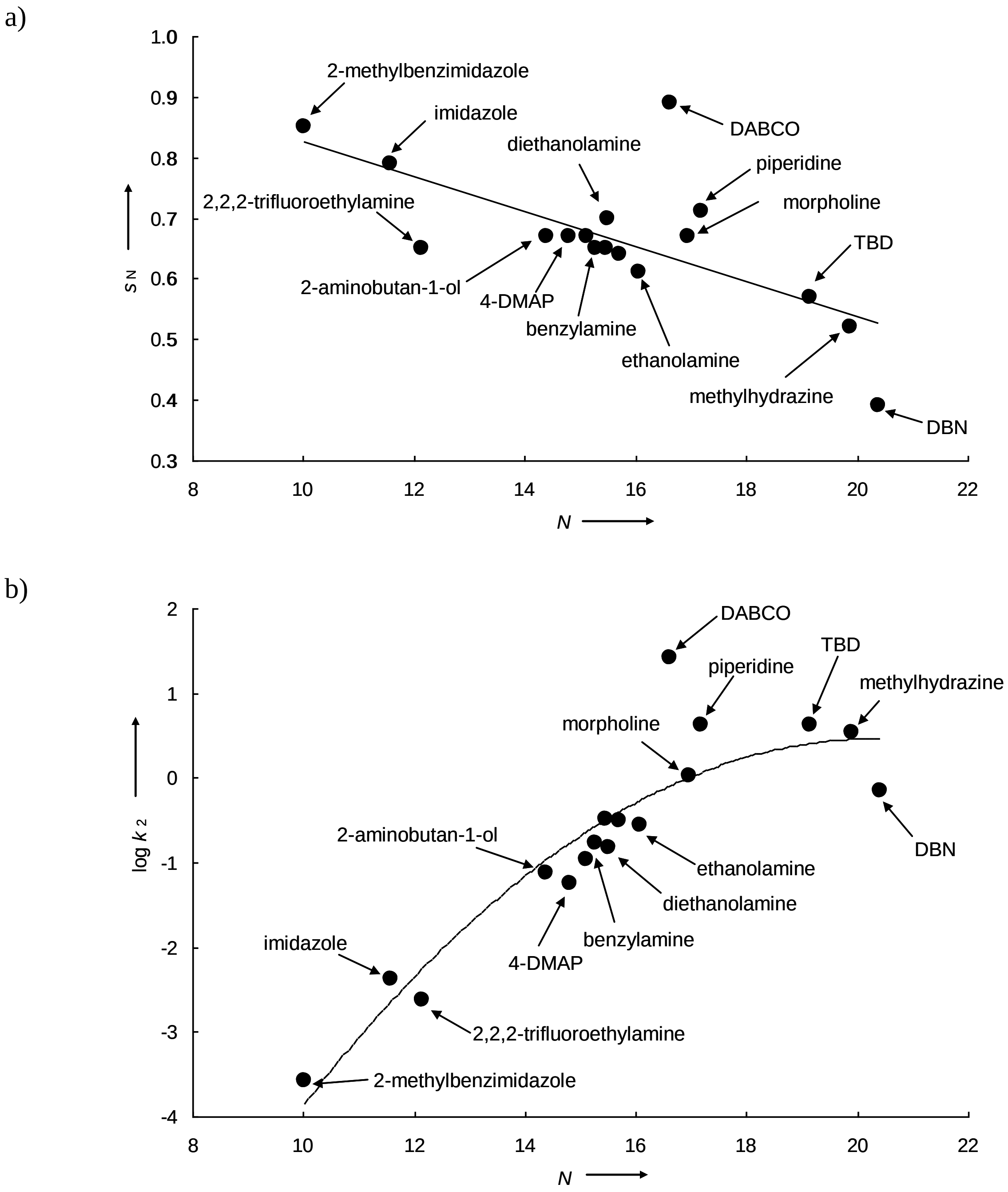

Figure 2.7. a) Plot of s_N versus N for the amines used in this study for the reactions in DMSO. b) Plot of log k_2 for the reactions of **2**-Br with solutions of amines in DMSO versus their N parameters.

The difficulties in applying s_N and N parameters for predicting the rate constants of the reactions with electrophiles other than benzhydrylium ions (and structurally related Michael acceptors) independent of the E values may be due to the fact that in derivation of the reactivity parameters on the basis of Eq. 1 the effect of solvation of the electrophile is shifted into the s_N and N parameters, as the E parameters are defined as solvent-independent. The nucleophile-specific parameters may still be closely associated with the benzhydrylium scale.

Marcus theory expresses the activation energy of a reaction ($\Delta G^{\ddagger}$) as a combination of the thermodynamic ($0.5\Delta_rG_0$) and intrinsic ($\Delta G_0{}^{\ddagger}$) factors (Eq. 9).

$$\Delta G^{\ddagger} = \Delta G_0{}^{\ddagger} + 0.5\Delta_rG^0 + (\Delta_rG^0)^2/16\Delta G_0{}^{\ddagger} \quad (9)$$

The thermodynamic driving force of the reaction Δ_rG_0 can be split into the contributions of the nucleophile and of the electrophile, as it has recently been shown.[8] However, it is highly questionable whether the same can be done with the intrinsic barrier as well. Even if the contributions of the reactants to $\Delta G_0{}^{\ddagger}$ of the reaction are additive, the quadratic term of Eq. 9 will complicate a simple and at the same time clear-cut separation of the activation free energy $\Delta G^{\ddagger}$ into the contributions of the reactants. The nucleophile-specific N and s_N parameters thus reflect the varying relative importance of the benzhydrylium ion substituent effects on $\Delta G^{\ddagger}$ of the reaction.

2.2.3. Relationship between the Reactivities of Neutral Nucleophiles towards Csp^3 and Csp^2 Electrophilic Centers

The fact that log k_{S_N2} correlate well with log $k_{\mathrm{lil_2CH^+}}$ indicates the similarity of the trends in intrinsic barriers controlling the reactivities towards Csp^3 and Csp^2 electrophilic centers. Particularly good correlations of log k_{S_N2} with log $k_{\mathrm{lil_2CH^+}}$ are observed for the reactions of amines with benzyl halides (Figures (2.S5.1-2.S5.3)B, 2.S5.6.1B and 2.S5.7.1B and Figures 2.S5.5.2B, 2.S5.7.2B in section 2.S.5). Similar plots for the reaction of phenacyl halides (Figures 2.S5.4B and 2.S5.8B in section 2.S.5) show some scatter (less than one order of magnitude), which may indicate the overlap of the p-orbital of the carbon atom of the carbonyl group with the orbitals on the entering and leaving groups in the transition state.[9]

The correlation in Figure 2.5 includes carbon, oxygen, nitrogen and phosphoros nucleophiles, and all of them belong to the same correlation line. This suggests that the linear relationship between log k_{S_N2} versus log $k_{C_{sp2}}$ may generally hold when the nucleophiles with the nucleophilic centres other than nitrogen are considered. Neither does the correlation between Ritchie N_+ and Swain-Scott n parameters in Ref. 6 show any significant difference in the order of reactivity towards saturated and unsaturated electrophilic centers for halide ions, acetate anion, amines and *n*-propylsulfide ion. As most of the reaction series in this work are restricted to N-nucleophiles, we cannot say whether the reactivities of the nucleophiles with different nucleophilic centers towards the S_N2 substrates studied in this work will follow the same correlation. When we complemented the set of nitrogen nucleophiles with a few phosphanes (Figures 2.S5.6.2B and 2.S5.9.2B in section 2.S.5), triarylphosphanes showed a slight downward deviation from the correlation line comparable to that observed for cyclic tertiary amines and smaller than that for triethylamine; tributylphosphane was found to react slightly faster than one would expect from the correlation line for most amines. In our view, the downward deviation of triarylphosphanes and bulky tertiary amines from the correlation lines indicates a higher steric demand of the S_N2 reaction compared to the addition reaction to benzhydryl cations.

The slopes of the correlations of log $k_{C_{sp3}}$ versus log $k_{C_{sp2}}$ for all substrates studied in this work are less than 1. This is in line with the observation that the mentioned above plot of the Ritchie N_+ and Swain-Scott n parameters in Ref. 6 has a slope more than unity. Bordwell et al. also reported a larger spread in the reactivities of different nucleophiles, and particularly 9-substituted fluorenyl anions, towards p-nitrohaloalkenes (S_NAr reactions) compared to that observed for the S_N2 reactions with benzyl halides.[10]

2.2.4. Solvent Effect on S_N2 Reactivity and on the Correlations of log k_{S_N2} with log $k_{lil_2CH^+}$

For the discussion of the solvent effect on the S_N2-reactivity, we will only use the correlations which do not show strong deviations from the trend lines, that is, include only N-nucleophiles with the exception of bulky tertiary amines.

It was found that log k_{S_N2} for the reactions of N-nucleophiles with neutral substrates studied in this work in different solvents plotted versus log $k_{lil_2CH^+}$ (these are calculated for the addition reactions in the same solvent as for the S_N2 transformation) belong to separate correlation lines. Thus, Figure 2.8, demonstrates that the correlation of the logarithmic rate constants for the reactions of N-nucleophiles with **2**-Br versus log $k_{lil_2CH^+}$, the line for DMSO is ca. 0.5-1 order of magnitude higher than that for MeCN. This implies that the S_N2 reactions and the additions to lil_2CH^+ are affected by the solvent not in the same way.

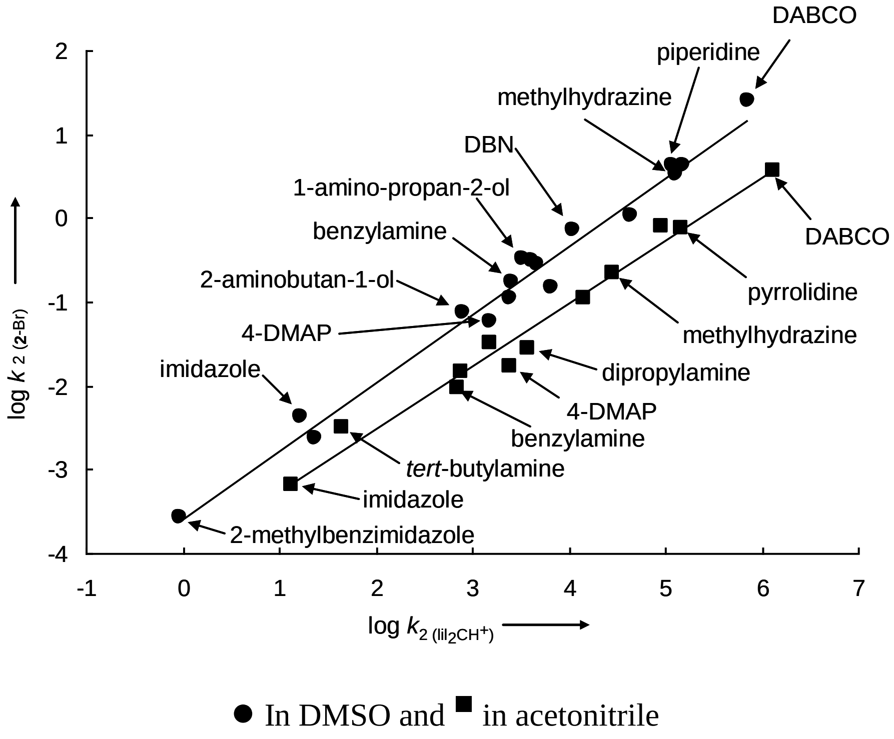

Figure 2.8. Correlation of log k_2 for the reactions of various N-nucleophiles with **2**-Br versus log k_2 of their reactions with the lil$_2$CH$^+$ cation. The rate constants are listed in Tables 2.S5.6.1 (in DMSO) and 2.S5.6.2 (in acetonitrile) in section 2.S.5. The equations describing the correlation lines are given in the separate graphs in section 2.S.5.6.

Although the applicability of the Hughes-Ingold rules[11] for predicting the solvent effects on polar organic reactions was reported to have some limitations,[12] they can be applied to explain the order of reactivity in different solvents in our case. The S_N2 reactions discussed in this work represent just one charge type depicted in Equation 10: ions are formed from the uncharged species in the course of the reaction.

$$X\text{-}R + :Nu \rightarrow X^- + R\text{-}Nu^+ \qquad (10)$$

As both the nucleophile and the substrate are uncharged, and the positive charge is developing along the reaction coordinate, the solvent with a higher donor number (DN)[11] is expected to stabilize the transition state and the ionic products relative to the reactants more effectively. It is therefore not surprising that DMSO (DN = 29.8 kcal/mol) facilitates this type of S_N2 reactions more efficiently than acetonitrile (DN = 14.1 kcal/mol).

The addition to lil$_2$CH$^+$ represents another charge type: both the starting cation and the product are positively charged. However, in the product the charge is more localized than in the starting benzhydrylium ion, and the loss of charge delocalization during the reaction should also be generally facilitated more efficiently by the solvent with a higher DN by decreasing the $\Delta_r G^0$ of the reaction. On the other hand, due to redistribution of the charge and rehybridization of the carbocationic center in the course of the reaction, accompanied by the solvent rearrangement, the intrinsic barrier of the reaction will grow with increasing polarity (DN) of the solvent, as the extent of solvation is also expected to increase. Thus, the intrinsic and thermodynamic factors "work" in different directions for the reaction of neutral N-nucleophiles with lil_2CH^+, and the role of the solvent is not as unambiguous as for the $\text{S}_\text{N}2$ reaction of charge type described by Eq. 10. Consequently, the addition reaction to lil_2CH^+ is less affected by the solvent than the substitution reactions studied in this work. This results in separate correlation lines of log $k_{\text{S}_\text{N}2}$ versus log $k_{\text{lil}_2\text{CH}^+}$ in different solvents.

For the substitution reactions of iodide from **5**-I, in addition to the kinetic data measured in this work (in DMSO and acetonitrile), several data points for the reactions with N-nucleophiles in methanol are available,[13] the data are compiled in Table 2.S5.9.3. The correlations of log $k_{\text{S}_\text{N}2}$ versus log $k_{\text{lil}_2\text{CH}^+}$ for the reactions in these solvents are represented in Figure 2.9. The rate constants for the reactions in methanol also belong to a separate correlation line, which lies above those for acetonitrile and DMSO.

The $\text{S}_\text{N}2$ reactions of **5**-I with different N-nucleophiles are faster in methanol than in DMSO and acetonitrile, due to a better stabilization of the incipient iodide ion by hydrogen-bonding. On the contrary, the reactions of benzhydrylium ions with N-nucleophiles are generally slower in MeOH than in the aprotic solvents DMSO and acetonitrile.[5h]

Obviously, the solvent effects on the reactivities of N-nucleophiles towards neutral $\text{S}_\text{N}2$ substrates and benzhydrylium ions are different. However, for positively charged $\text{S}_\text{N}2$ substrates this will not be the case, as suggested by the plot in Figure 2.5: the correlation of the reactivities of different nucleophiles and solvent mixtures towards N-methyldibenzothiophenium ion versus their reactivities towards lil_2CH^+ does not break when the solvent is varied.

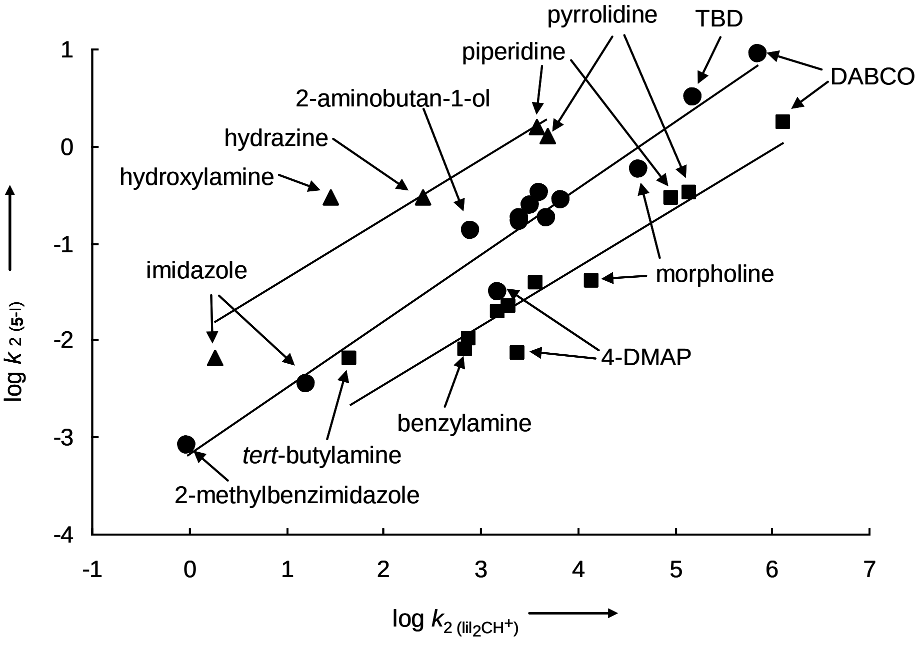

▲ In methanol, ● in DMSO and ■ in acetonitrile

Figure 2.9. Correlation of log k_2 for the reactions of various N-nucleophiles with **5**-I versus log k_2 of their reactions with the lil$_2$CH$^+$ cation in different solvents. The rate constants are listed in Tables 2.S5.9.1 (in DMSO), 2.S5.9.2 (in acetonitrile) and 2.S5.9.3 (in methanol) in section 2.S.5.9.

2.2.5. The Effect of the Substrate Structure on the S_N2 Reactivity of the Electrophile

In the series of the reactions of benzyl halides with amines in DMSO and acetonitrile, attachment of a methoxy substituent at the para position was found to have always a mild rate accelerating effect (a factor of 2-6). The effect of a cyano substituent is also slightly rate enhancing, but it is much smaller than the influence of a methoxy group. The fact that para substituents of the benzyl halides have a very small effect on the rates of the substitution reactions indicates that only little positive charge is developed on the benzyl carbon in the transition state.

A plot of log k_2 for the reactions of benzyl chlorides with DABCO, piperidine, and *n*-propylamine versus the Hammett's substituent constants σ_p is represented in Figure 2.10. Though the limited number of data inhibits a detailed analysis, Figure 2.10 indicates a curved Hammett plot, because electron-donating as well as electron-accepting substituents cause a slight acceleration. The poor correlation of the logarithms of aminolysis rate constants for benzyl halides with Hammett's substituent constants[14] is in line with the previous observations for the S_N2 reactions of substituted benzyl chlorides.[7a,15]

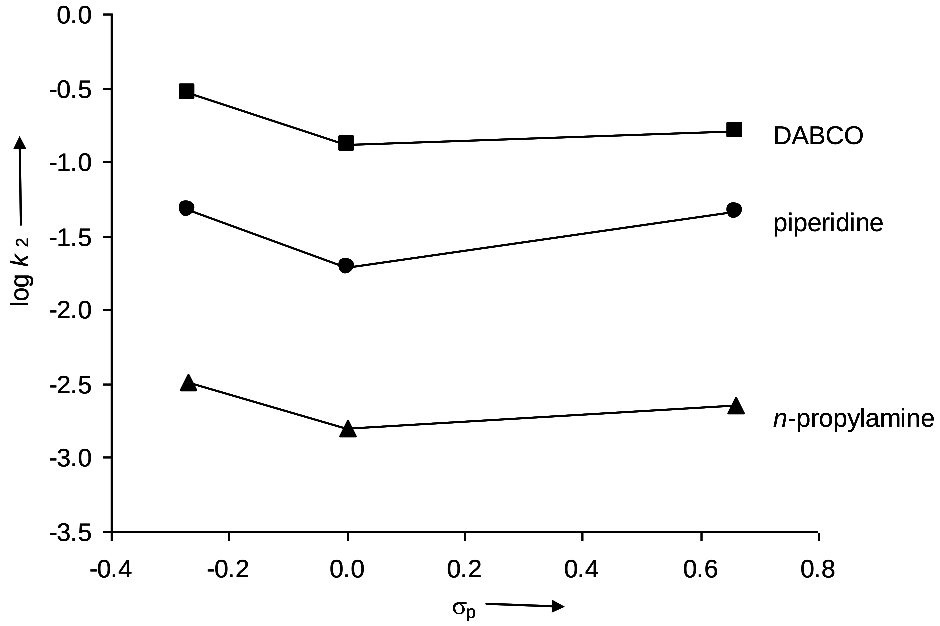

Figure 2.10. Plot of log k_2 of the reactions of *para*-substituted benzyl chlorides with amines at 20 ºC in DMSO versus Hammett's substituent constants σ_p.

The influence of the carbonyl group in the α-position to the reactive center on the S_N2 reactivity of the substrate has long been surrounded by much contradiction. In reactions with potassium iodide in acetone, phenacyl halides were reported to be significantly more electrophilic than benzyl analogs.[16] However, the inverted reactivity order towards amines in chloroform was found by Ross et al.[17] Pearson et al. observed similar reactivities of benzyl and phenacyl bromides towards pyridine in methanol solution, while in the same solvent phenacyl bromide was found to react with thiourea ca. 35 times faster than benzyl bromide.[18] Halvorsen and Songstad, who compared the S_N2 reactivities of phenacyl bromide (**4**-Br) and methyl iodide (**5**-I) towards different types of nucleophiles in acetonitrile, came to the conclusion that the ratio $k_{\mathbf{4}\text{-Br}}/k_{\mathbf{5}\text{-I}}$ is only large for the reactions with powerful ionic nucleophiles and is smaller than 1 with less nucleophilic reaction partners.[19]

Shaik's valence bond approach towards the reactivity effects of the α- and β-carbon substituents on the the S_N2 reactivity of the substrate suggested a reasonable rationalization for the reactivity crossovers mentioned above.[20] According to this approach, the reaction barrier E is seen to be a fraction f of the energy gap ($I_{N:}$ - A_{RX}) between two curves which intersect to form the reaction profile minus the avoided crossing B (Figure 2.11); $I_{N:}$ is the ionization potential of the nucleophile (N:), A_{RX} is the electron affinity of the substrate (RX). Attachment of a π-acceptor substituent to the α-carbon atom in the substrate RX (like in phenacyl halides) leads to an improvement of the acceptor ability of the substrate A_{RX}, and thus makes the energy gap ($I_{N:}$ - A_{RX}) smaller. On the other hand, the fraction f of the energy gap, which enters the reaction barrier E, increases for the reasons discussed in detail in Ref. 20. Thus, when the reaction is gap-controlled, i.e. when $I_{\mathrm{N:}}$ is relatively low, one can expect a higher rate constant for the reaction with the acceptor-substituted substrate than with the unsubstituted one. On the contrary, when $I_{\mathrm{N:}}$ is high (for relatively weak nucleophiles), the height of f controls the overall reaction barrier, and the reaction with the unsubstituted substrate occurs more rapidly than with the acceptor-substituted one.

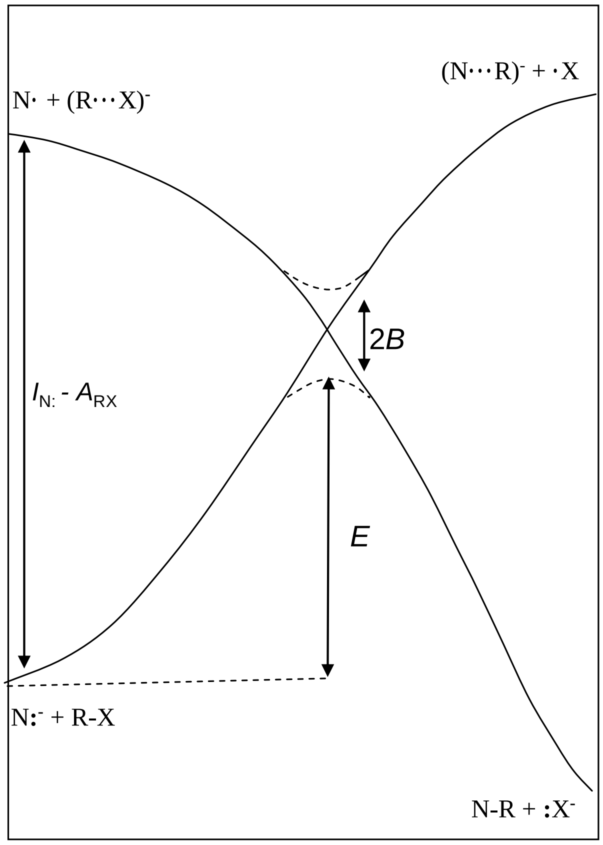

Figure 2.11. Correlation diagram describing the formation of the energy profile for the reaction $N^-: + R\text{-}X \rightarrow N\text{-}R + :X^-$.

We found that phenacyl halides are about one order of magnitude more reactive towards neutral N-nucleophiles in DMSO than benzyl halides. Figure 2.12a shows the correlations of log k_{S_N2} for the reactions of benzyl- and phenacyl chlorides with N-nucleophiles versus log $k_{\mathrm{lil_2CH^+}}$ for the corresponding amines.

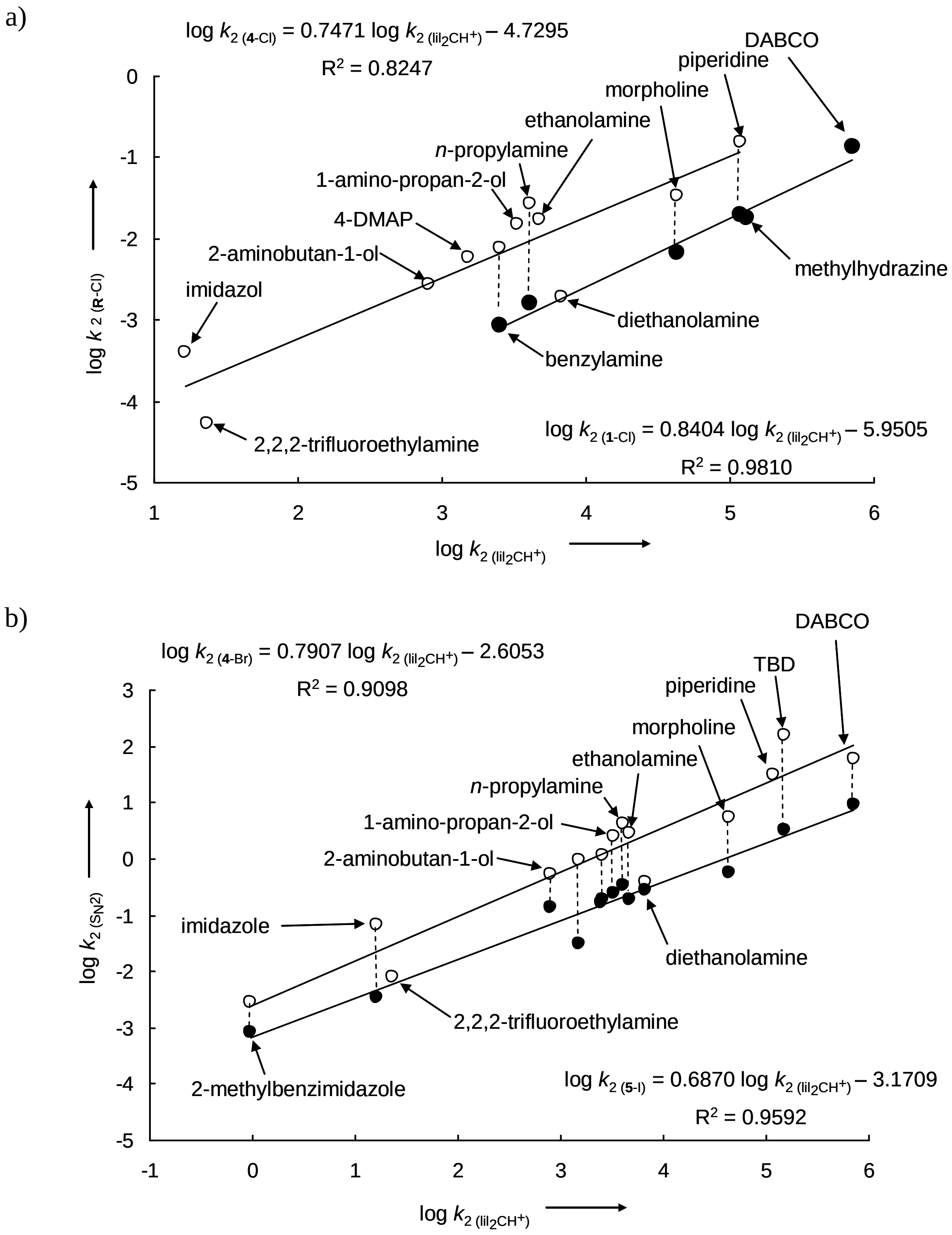

Figure 2.12. Comparison of selectivities of phenacyl halides in aminolysis reaction with those of benzyl halides and methyl iodide. Correlations of log k_2 for the reactions of various N-nucleophiles with (a) **4**-Cl (○) and **1**-Cl (●) and (b) **4**-Br (○) and **5**-I (●) versus log k_2 for their reactions with the lil$_2$CH$^+$ cation in DMSO. b)

The relatively small ratio $k_{\mathbf{4}\text{-Cl}}/k_{\mathbf{1}\text{-Cl}}$ for the reactions with neutral nitrogen nucleophiles (compared to that towards iodide ion in acetone) is in agreement with Shaik's model of the S$_N$2 reactivity.[20]

However, from this model one would also expect a higher slope of the correlation line for phenacyl chloride (**4**-Cl) than that for benzyl chloride (**1**-Cl) in Figure 2.12a, which we do not observe. On the other hand, a higher slope for the correlation line for **4**-Br than that for **5**-I in Figure 2.12b is in line with the data of Halvorsen and Songstad[19] and with Shaik's model.

2.2.6. The Effect of the Leaving Group on the Reactivity of the Substrate in the S_N2 Reactions

The S_N2 aminolysis reactions of benzyl bromides in DMSO were found to proceed ca. 100-200 times faster than similar reactions of benzyl chlorides. The $k_{\text{R-Br}}/k_{\text{R-Cl}}$ ratios for the reactions studied in this work are thus comparable to those reported by Bordwell et al. for the reactions of benzyl chloride and benzyl bromide with 9-substituted fluorenyl anions in DMSO.[15b] Figure 2.13a shows that the slopes of the correlations of log k_{S_N2} versus log $k_{\text{lil}_2\text{CH}^+}$ for the aminolysis reactions of **2**-Br and **2**-Cl are almost the same.

A similar situation is also observed with phenacyl halides: **4**-Br is ca. 150-200 times more reactive than **4**-Cl, and the slopes of both correlations of log k_{S_N2} versus log $k_{\text{lil}_2\text{CH}^+}$ for the reactions of phenacyl halides with amines in DMSO are very similar (Figure 2.13b).

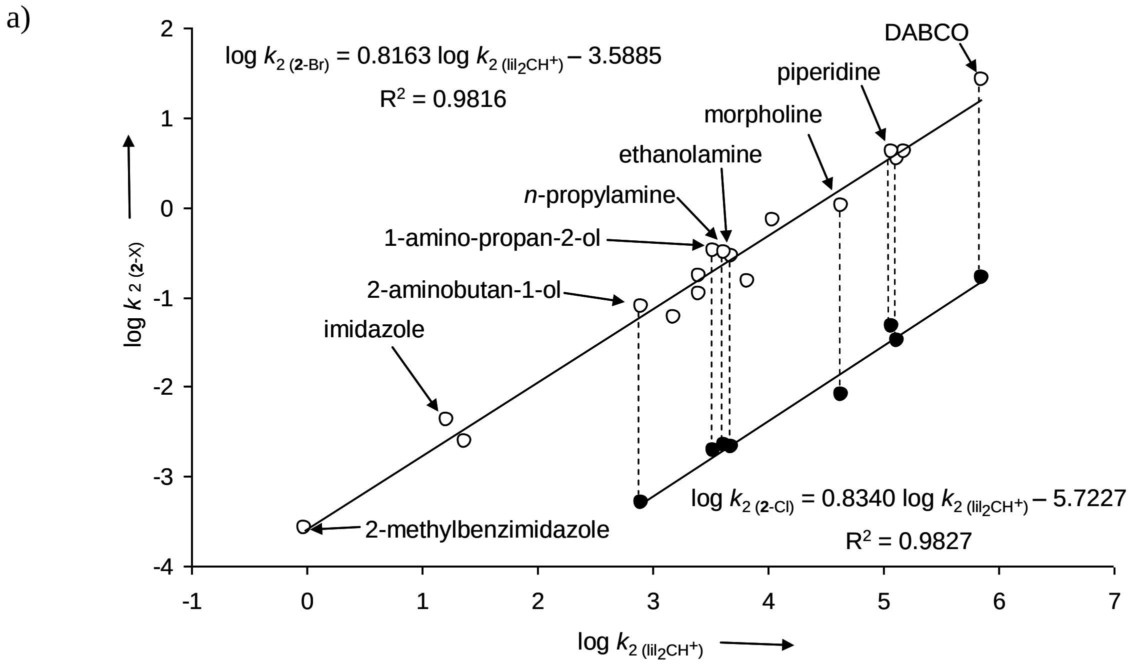

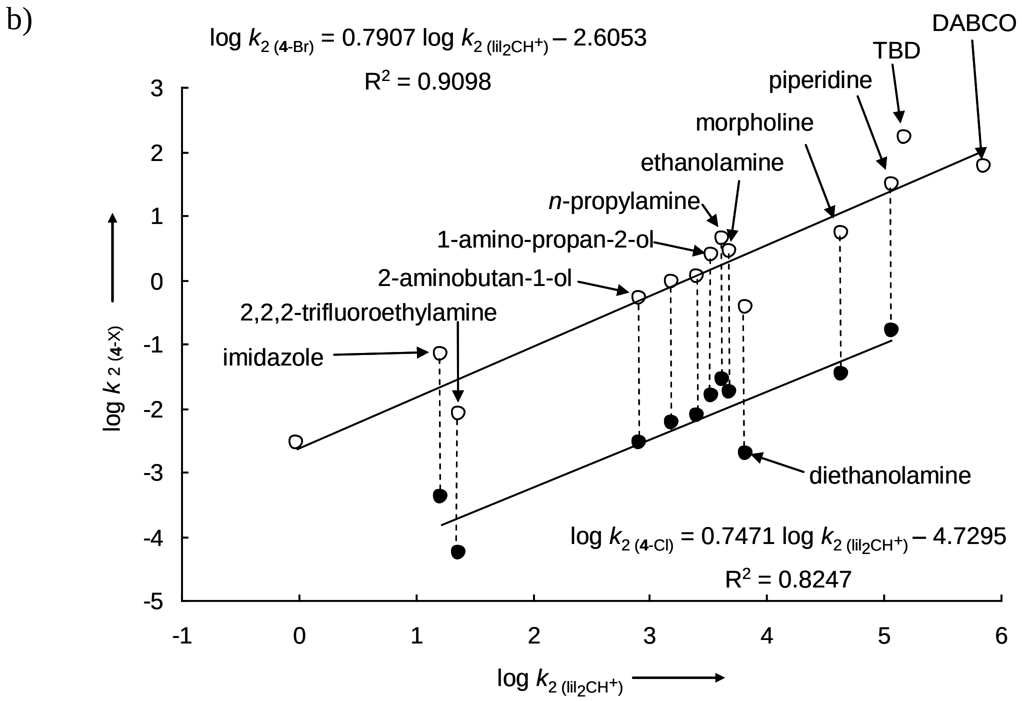

Figure 2.13. Influence of the leaving group on the S_N2 reactivity of benzyl and phenacyl halides: correlations of log k_2 for the reactions of various N-nucleophiles with (a) **2**-Br (○) and **2**-Cl (●) and (b) with **4**-Br (○) and **4**-Cl (●) versus log k_2 for their reactions with the lil_2CH^+ cation in DMSO.

Methyl tosylate was found to be half an order to one order of magnitude less reactive and showed a smaller selectivity than methyl iodide in the reactions with N-nucleophiles in DMSO (Figure 2.14). It is interesting to note that some studies on the aminolysis of benzhydryl derivatives in DMSO, made in our group,[21] and other reports[22] indicate that tosylate can even be a weaker leaving group than bromide in some S_N2 reactions, although it is a better nucleofuge in S_N1 processes.[21,23]

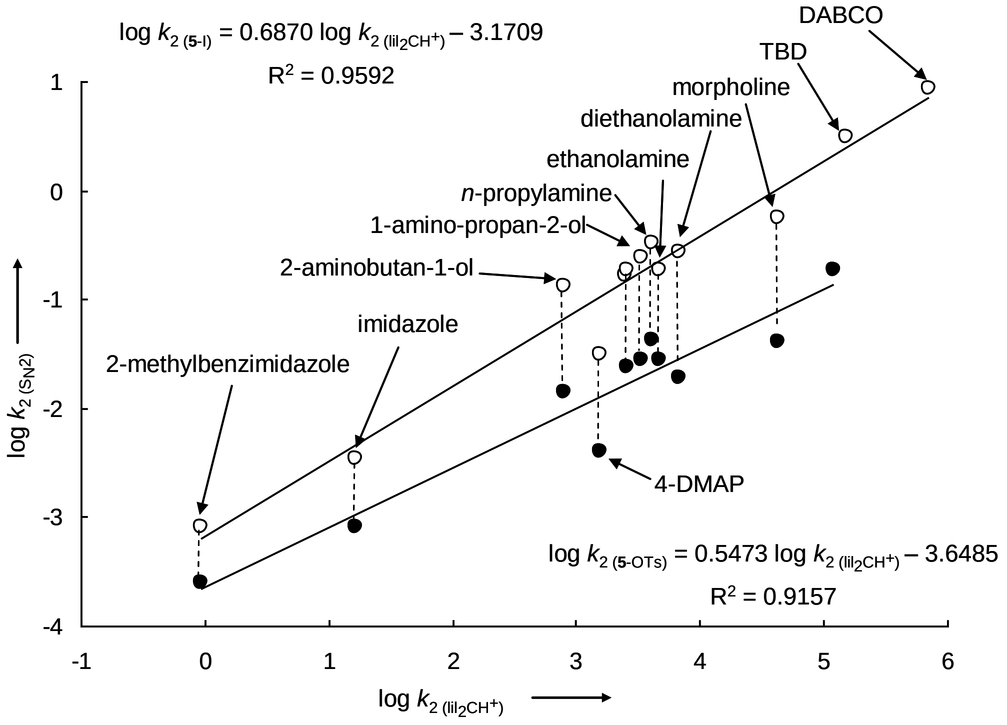

Figure 2.14. Correlations of log k_2 for the reactions of various N-nucleophiles with **5**-I (○) and **5**-OTs (●) versus log k_2 for their reactions with the lil$_2$CH$^+$ cation in DMSO.

The ratio $k_{5\text{-I}}/k_{5\text{-OTs}}$ depends on the reactivity of the reaction partner varying between 3 for the reaction with relatively weakly nucleophilic and 15 for the most reactive ones. The observation that the ratio $k_{5\text{-I}}/k_{5\text{-OTs}}$ increases for the S_N2 reactions with increasing reactivity of the nucleophile (Figure 2.14) is in line with earlier reports.[22a,24]

2.3. Conclusion

The rate constants for the reactions of a series of nitrogen nucleophiles with several neutral S_N2 substrates in DMSO and acetonitrile correlate linearly with the calculated rate constants for their reactions with lil$_2$CH$^+$ in the same solvents. This observation indicates a close relationship between the nucleophilic reactivities of N-nucleophiles towards Csp^2 and Csp^3 electrophilic centers. The rate constants for the reactions of tertiary amines (except DABCO) and triarylphosphanes with S_N2 substrates deviate downwards from the correlations of log k_{S_N2} versus log $k_{\text{lil}_2\text{CH}^+}$, probably due to steric effects.

In contrast to good linear correlations of the logarithms of the rate constants, the plots of log k_{S_N2}/s_N versus N for the reactions studied in this work show much scatter. Eq. 2 thus appears to be less reliable for accurate prediction of the rate constants for S_N2 processes compared to the direct correlation with log k_2 values for the reactions with benzhydrylium ion lil_2CH^+, calculated from s_N and N parameters.

The correlations of log k_{S_N2} for the reactions of uncharged electrophiles with neutral nitrogen nucleophiles versus log $k_{lil_2CH^+}$ make separate lines in different solvents indicating different solvent effects on the electrophilic reactivities of neutral S_N2 substrates and benzhydrylium ions.

Phenacyl halides are about one order of magnitude more reactive towards amines in DMSO than the corresponding benzyl halides. Substitution of the *para*-position of the phenyl ring of benzyl halide has only marginal effect on its electrophilic reactivity, indicating only little charge on the benzyl carbon in the transition state.

The ratio k^{Br}/k^{Cl} for the reactions of phenacyl and benzyl halides with N-nucleophiles varies between 91 and 199. Methyl iodide shows a higher reactivity towards amines in DMSO than methyl tosylate. The ratio k^{I}/k^{OTs} gets larger with increasing reactivity of the reaction partner.

2.S. Supplementary Data and Experimental Section

2.S.1. General.

Materials. Commercially available DMSO and acetonitrile were used without further purification for all experiments.

Liquid amines were distilled twice prior to use, DABCO and TBD were purified by sublimation. Commercially available phosphanes were used for the measurements without further purification.

The substrates were purchased (with the exception of 4-cyanobenzyl chloride and 4-methoxybenzyl bromide) and used without further purification.

4-Cyanobenzyl chloride (**2**-Cl) was obtained using the following two-step synthesis. 4-Cyanobenzyldehyde (2.60 g, 19.8 mmol) was dissolved in methanol (30 mL) and sodium borohydrate (1.48 g, 39.1 mmol) was added to the solution in small portions. The reaction mixture was stirred at 20°C overnight. After quenching with water (50 mL) and extraction with ether (7 × 20 mL), combined organic layers were dried over sodium sulfate and evaporated. The oily residue was purified using column chromatography (silica gel, ethyl ether/hexane = 1:1) yielding p-cyanobenzyl alcohol (2.30 g, 17.3 mmol, 87%). Thus obtained alcohol was added to a solution of Ph_3P (4.50 g, 17.2 mmol) in tetrachloromethane (70 mL). The mixture was refluxed for 24 h, filtered through silica gel and evaporated. The residue was recrystallized from heptane to yield **2**-Cl (1.56 g, 10.3 mmol, 60%).

4-Methoxybenzyl bromide (**3**-Br) was synthesized from 4-methoxybenzyl alcohol (obtained using the procedure described for p-cyanobenzyl alcohol). To a solution of CBr_4 (12.3 g, 37.1 mmol) and the alcohol (4.83 g, 35.0 mmol) in benzene (70 mL), Ph_3P (10.4 g, 39.7 mmol) was added under stirring in small portions. The reaction mixture was kept at 20°C overnight and then filtered off a colourless precipitate. The filtrate was concentrated using the rotary evaporator, and the residue was distilled under reduced pressure (bp 89-93°C at 1.3 mbar) to yield (5.21 g, 25.9 mmol, 74%) of **3**-Br as colourless oil. As the product is relatively unstable, it could only be kept in the fridge for several days before being used for kinetic measurements.

Kinetic measurements. The reactions of the neutral substrates, mentioned in the chapter, with amines and phosphanes in DMSO and acetonitrile were followed by conductometry (conductometers: Radiometer Analytical CDM 230 or Tacussel CD 810, Pt electrode: WTW LTA 1/NS). For the study of solvolysis reactions with half-lives of 10^{-2} s < $\tau 1/2$ < 10 s, a standard stopped-flow conductometer (Hi-Tech Scientific SF-61 DX2, platinum electrodes, cell volume: 21 µL, cell constant 4.24 cm-1, minimum dead time 2.2 ms) was used in single-mixing mode. The temperature of the solutions during all kinetic studies was kept constant (20 ± 0.1 °C) by using a circulating bath thermostat.

For the study of slow reactions, the solution of the nucleophile in acetonitrile or DMSO was thermostated (20 ± 0.1 °C) for 5 min prior to adding the substrate. Typically, a certain amount of the substrate was dissolved in acetonitrile (in a 2.00 or 5.00 mL volumetric flask), then a small amount of it (100-500 μL) was injected into the nucleophile solution, and the conductance (*G*) was recorded at given time intervals. When the stopped-flow equipment was used, the substrates were dissolved in acetonitrile or DMSO and mixed in the conductivity cell with the solution of the nucleophile. When the stopped-flow technique was used for the measurement of the rate constants in DMSO, the solutions of the substrates in DMSO were prepared prior to measurements and used immediately, to avoid the side reaction with the solvent. The first-order rate constants k_{obs} (s^{-1}) were obtained by least squares fitting of the increasing conductance to a single-exponential equation. Second-order rate constants k_2 (M^{-1} s^{-1}) were obtained from the slopes of linear plots of k_{obs} versus the concentrations of the amines [Nu].

2.S.2. Rate constants in DMSO.

2.S.2.1. Rate constants for the reactions of benzyl chloride (1-Cl) in DMSO.

Table 2.S2.1.1. Rate constants for the reaction of benzyl chloride (**1**-Cl) with DABCO at 20˚C in DMSO (conventional conductometer).

No	$[E]_0/M^1$	$[Nu]_0/M$	$[Nu]_0/[E]_0$	k_{obs}/s^{-1}
1	3.01×10^{-3}	3.74×10^{-2}	12	4.11×10^{-3}
2	3.01×10^{-3}	5.37×10^{-2}	18	6.56×10^{-3}
3	2.99×10^{-3}	8.18×10^{-2}	27	1.00×10^{-2}
4	2.90×10^{-3}	1.08×10^{-1}	37	1.31×10^{-2}
5	2.91×10^{-3}	1.29×10^{-1}	44	1.64×10^{-2}
$k_2 = 1.31 \times 10^{-1}$ $M^{-1}s^{-1}$				

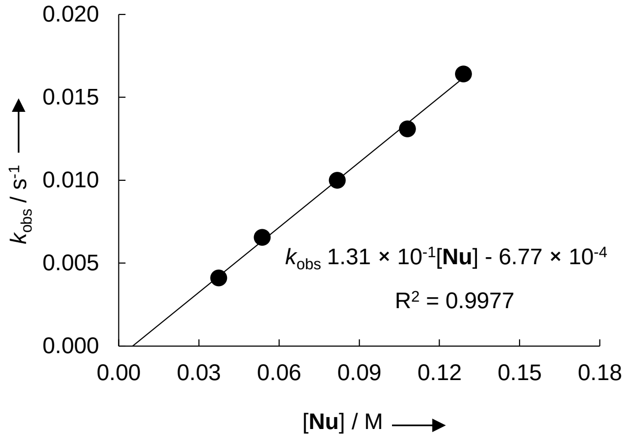

Table 2.S2.1.2. Rate constants for the reaction of benzyl chloride (**1**-Cl) with 1,1-dimethylhydrazine at 20˚C in DMSO (conventional conductometer).

No	$[E]_0$/M^1	$[Nu]_0$/M	$[Nu]_0$/ $[E]_0$	k_{obs}/s^{-1}
1	3.85×10^{-3}	7.48×10^{-2}	19	1.83×10^{-3}
2	4.47×10^{-3}	1.01×10^{-1}	23	2.41×10^{-3}
3	3.91×10^{-3}	1.18×10^{-1}	30	2.90×10^{-3}
4	3.78×10^{-3}	1.54×10^{-1}	41	3.70×10^{-3}
5	3.76×10^{-3}	1.92×10^{-1}	51	4.49×10^{-3}
		$k_2 = 2.29 \times 10^{-2}$ M^{-1}s^{-1}		

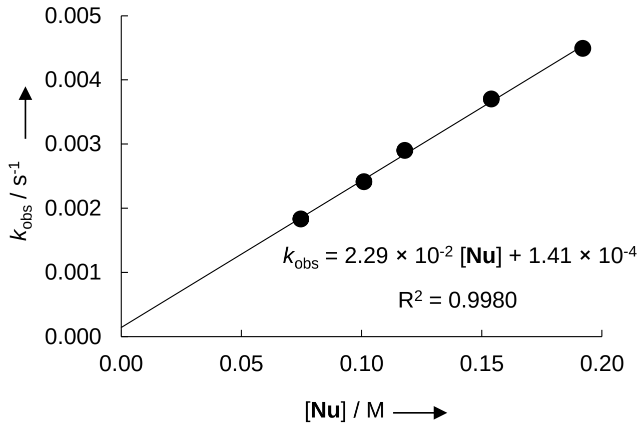

Table 2.S2.1.3. Rate constants for the reaction of benzyl chloride (**1**-Cl) with methylhydrazine at 20˚C in DMSO (conventional conductometer).

No	$[E]_0$/M^1	$[Nu]_0$/M	$[Nu]_0$/ $[E]_0$	k_{obs}/s^{-1}
1	2.95×10^{-3}	5.98×10^{-2}	20	1.03×10^{-3}
2	2.99×10^{-3}	8.10×10^{-2}	27	1.50×10^{-3}
3	2.95×10^{-3}	1.39×10^{-1}	47	2.58×10^{-3}
4	2.91×10^{-3}	1.61×10^{-1}	55	2.86×10^{-3}
5	2.99×10^{-3}	2.03×10^{-1}	68	3.58×10^{-3}
		$k_2 = 1.77 \times 10^{-2}$ M^{-1}s^{-1}		

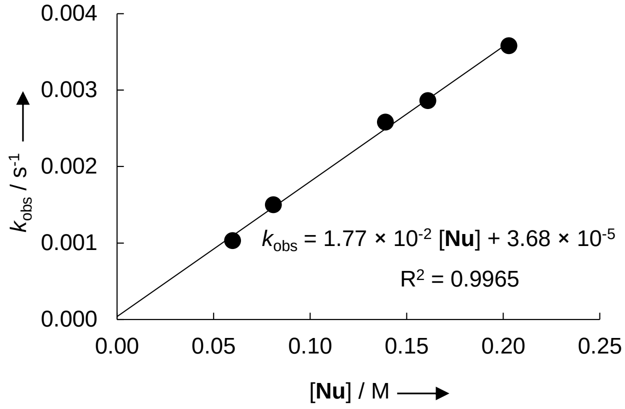

Table 2.S2.1.4. Rate constants for the reaction of benzyl chloride (**1**-Cl) with piperidine at 20˚C in DMSO (conventional conductometer).

No	$[E]_0/M^1$	$[Nu]_0/M$	$[Nu]_0/[E]_0$	k_{obs}/s^{-1}
1	2.78×10^{-3}	1.54×10^{-1}	55	3.41×10^{-3}
2	2.79×10^{-3}	2.04×10^{-1}	73	4.23×10^{-3}
3	2.67×10^{-3}	2.48×10^{-1}	93	5.28×10^{-3}
4	2.64×10^{-3}	2.78×10^{-1}	105	5.90×10^{-3}
5	2.67×10^{-3}	3.58×10^{-1}	134	7.29×10^{-3}
$k_2 = 1.94 \times 10^{-2}\ M^{-1}s^{-1}$				

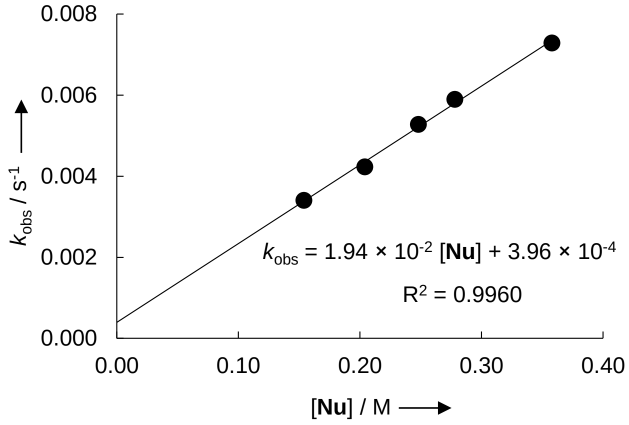

Table 2.S2.1.5. Rate constants for the reaction of benzyl chloride (**1**-Cl) with morpholine at 20˚C in DMSO (conventional conductometer).

No	$[E]_0/M^1$	$[Nu]_0/M$	$[Nu]_0/[E]_0$	k_{obs}/s^{-1}
1	2.69×10^{-3}	1.25×10^{-1}	46	7.52×10^{-4}
2	2.65×10^{-3}	2.04×10^{-1}	77	1.30×10^{-3}
3	2.70×10^{-3}	2.78×10^{-1}	103	1.76×10^{-3}
4	2.60×10^{-3}	3.62×10^{-1}	139	2.26×10^{-3}
5	2.57×10^{-3}	4.58×10^{-1}	178	3.01×10^{-3}
$k_2 = 6.66 \times 10^{-3}\ M^{-1}s^{-1}$				

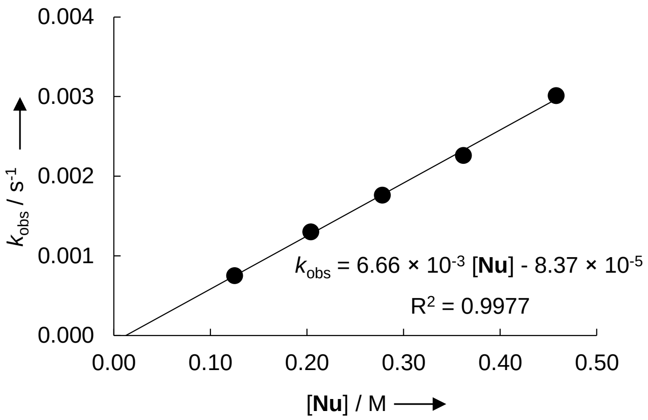

Table 2.S2.1.6. Rate constants for the reaction of benzyl chloride (**1**-Cl) with *n*-propylamine at 20˚C in DMSO (conventional conductometer).

No	$[E]_0/M^1$	$[Nu]_0/M$	$[Nu]_0/[E]_0$	k_{obs}/s^{-1}
1	2.90×10^{-3}	1.79×10^{-1}	62	2.94×10^{-4}
2	2.97×10^{-3}	2.39×10^{-1}	80	4.22×10^{-4}
3	2.85×10^{-3}	3.46×10^{-1}	121	5.62×10^{-4}
4	2.87×10^{-3}	4.60×10^{-1}	160	7.53×10^{-4}
$k_2 = 1.59 \times 10^{-3}\ M^{-1}s^{-1}$				

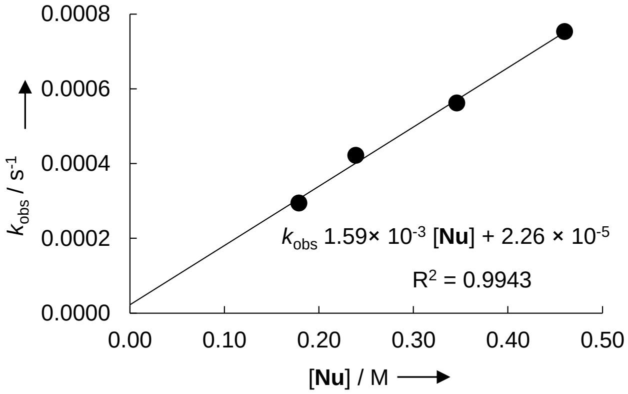

Table 2.S2.1.7. Rate constants for the reaction of benzyl chloride (**1**-Cl) with benzylamine at 20˚C in DMSO (conventional conductometer).

No	$[E]_0/M^1$	$[Nu]_0/M$	$[Nu]_0/[E]_0$	k_{obs}/s^{-1}
1	2.89×10^{-3}	1.97×10^{-1}	68	1.58×10^{-4}
2	2.78×10^{-3}	2.36×10^{-1}	85	1.92×10^{-4}
3	2.82×10^{-3}	3.10×10^{-1}	110	2.52×10^{-4}
$k_2 = 8.29 \times 10^{-4}\ M^{-1}s^{-1}$				

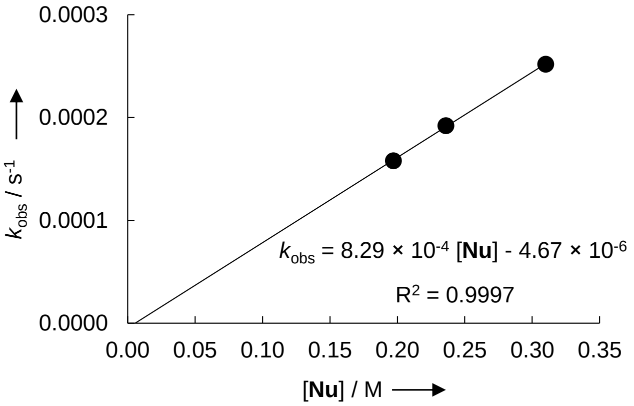

2.S.2.2. Rate constants for the reactions of 4-cyanobenzyl chloride (2-Cl) in DMSO

Table 2.S2.2.1. Rate constants for the reaction of 4-cyanobenzyl chloride (**2**-Cl) with DABCO at 20˚C in DMSO (conventional conductometer).

No	$[E]_0/M^1$	$[Nu]_0/M$	$[Nu]_0/ [E]_0$	k_{obs}/s^{-1}
1	1.88×10^{-3}	3.15×10^{-2}	17	4.58×10^{-3}
2	1.85×10^{-3}	4.29×10^{-2}	23	6.03×10^{-3}
3	1.82×10^{-3}	4.39×10^{-2}	24	6.93×10^{-3}
4	1.89×10^{-3}	5.65×10^{-2}	30	8.63×10^{-3}
5	1.91×10^{-3}	6.38×10^{-2}	33	9.86×10^{-3}
$k_2 = 1.64 \times 10^{-1}$ M^{-1}s^{-1}				

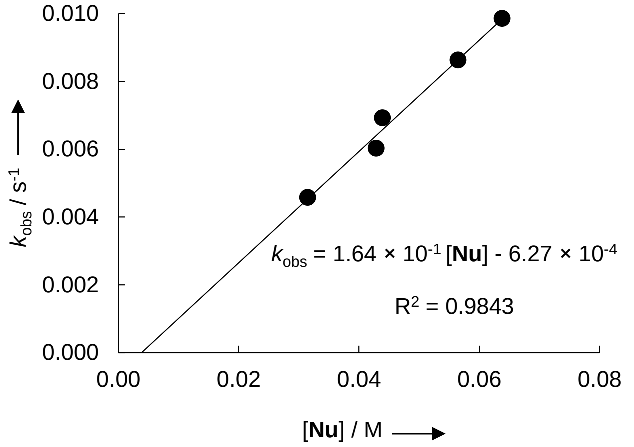

Table 2.S2.2.2. Rate constants for the reaction of 4-cyanobenzyl chloride (**2**-Cl) with 1,1-dimethylhydrazine at 20˚C in DMSO (conventional conductometer).

No	$[E]_0$/M^1	$[Nu]_0$/M	$[Nu]_0$/ $[E]_0$	k_{obs}/s^{-1}
1	1.88×10^{-3}	3.15×10^{-2}	17	4.58×10^{-3}
2	1.85×10^{-3}	4.29×10^{-2}	23	6.03×10^{-3}
3	1.82×10^{-3}	4.39×10^{-2}	24	6.93×10^{-3}
4	1.89×10^{-3}	5.65×10^{-2}	30	8.63×10^{-3}
5	1.91×10^{-3}	6.38×10^{-2}	33	9.86×10^{-3}
$k_2 = 3.43 \times 10^{-2}$ M^{-1}s^{-1}				

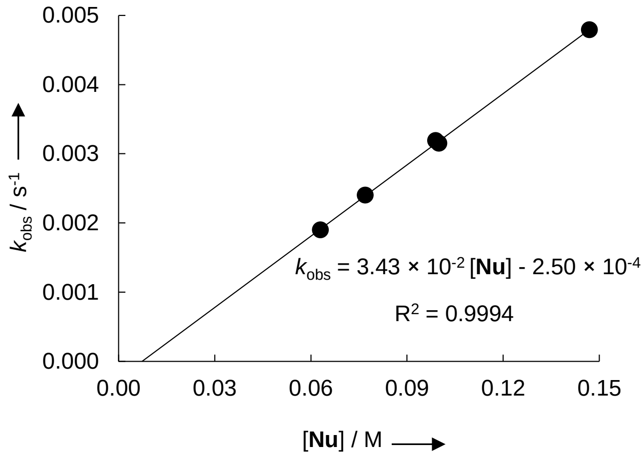

Table 2.S2.2.3. Rate constants for the reaction of 4-cyanobenzyl chloride (**2**-Cl) with methylhydrazine at 20˚C in DMSO (conventional conductometer).

No	$[E]_0$/M^1	$[Nu]_0$/M	$[Nu]_0$/ $[E]_0$	k_{obs}/s^{-1}
1	2.29×10^{-3}	1.14×10^{-1}	50	3.35×10^{-3}
2	2.35×10^{-3}	1.81×10^{-1}	77	5.65×10^{-3}
3	2.20×10^{-3}	1.95×10^{-1}	89	5.87×10^{-3}
4	2.25×10^{-3}	2.41×10^{-1}	107	7.69×10^{-3}
5	2.27×10^{-3}	3.14×10^{-1}	138	9.66×10^{-3}
$k_2 = 3.18 \times 10^{-2}$ M^{-1}s^{-1}				

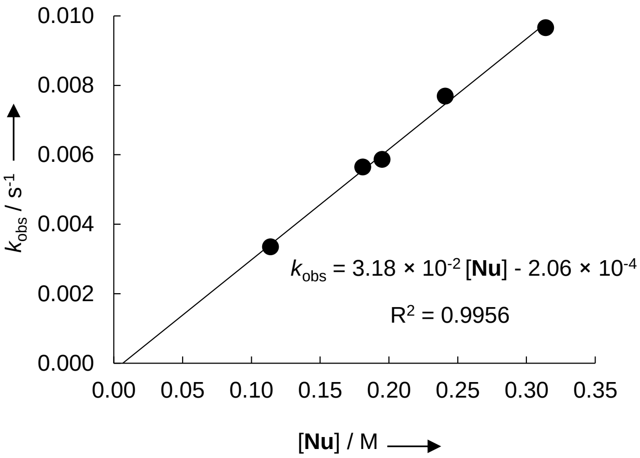

Table 2.S2.2.4. Rate constants for the reaction of 4-cyanobenzyl chloride (**2**-Cl) with piperidine at 20˚C in DMSO (conventional conductometer).

No	$[E]_0/M^1$	$[Nu]_0/M$	$[Nu]_0/[E]_0$	k_{obs}/s^{-1}
1	1.91×10^{-3}	1.05×10^{-1}	55	3.90×10^{-3}
2	1.92×10^{-3}	1.21×10^{-1}	63	4.52×10^{-3}
3	1.76×10^{-3}	1.40×10^{-1}	80	5.46×10^{-3}
4	1.88×10^{-3}	1.81×10^{-1}	96	7.06×10^{-3}
5	1.88×10^{-3}	2.33×10^{-1}	124	9.75×10^{-3}
$k_2 = 4.54 \times 10^{-2}\ M^{-1}s^{-1}$				

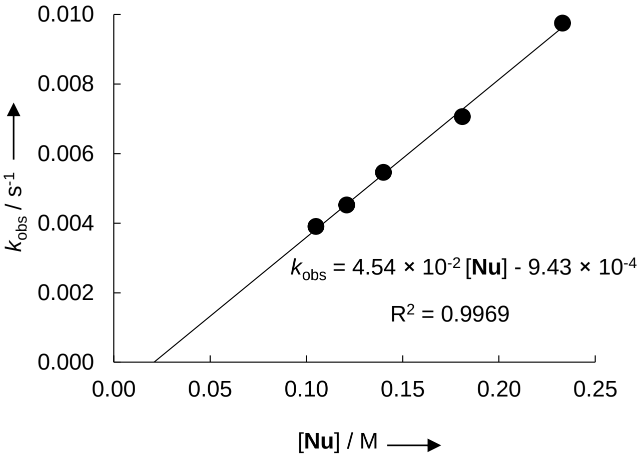

Table 2.S2.2.5. Rate constants for the reaction of 4-cyanobenzyl chloride (**2**-Cl) with morpholine at 20˚C in DMSO (conventional conductometer).

No	$[E]_0$/M^1	$[Nu]_0$/M	$[Nu]_0$/ $[E]_0$	k_{obs}/s^{-1}
1	1.86×10^{-3}	2.16×10^{-1}	116	2.03×10^{-3}
2	1.89×10^{-3}	2.76×10^{-1}	146	2.54×10^{-3}
3	1.89×10^{-3}	3.12×10^{-1}	165	2.77×10^{-3}
4	1.81×10^{-3}	4.69×10^{-1}	259	4.07×10^{-3}
$k_2 = 8.04 \times 10^{-3}$ M^{-1}s^{-1}				

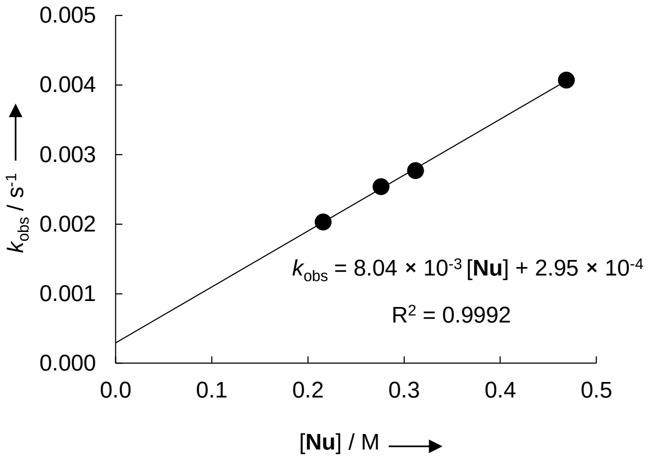

Table 2.S2.2.6. Rate constants for the reaction of 4-cyanobenzyl chloride (**2**-Cl) with aminoethanol at 20˚C in DMSO (conventional conductometer).

No	$[E]_0$/M^1	$[Nu]_0$/M	$[Nu]_0$/ $[E]_0$	k_{obs}/s^{-1}
1	2.70×10^{-3}	1.94×10^{-1}	72	4.77×10^{-4}
2	2.71×10^{-3}	2.85×10^{-1}	105	6.91×10^{-4}
3	2.68×10^{-3}	3.92×10^{-1}	146	8.93×10^{-4}
4	2.66×10^{-3}	4.48×10^{-1}	168	1.04×10^{-3}
5	2.69×10^{-3}	5.61×10^{-1}	209	1.27×10^{-3}
$k_2 = 2.15 \times 10^{-3}$ M^{-1}s^{-1}				

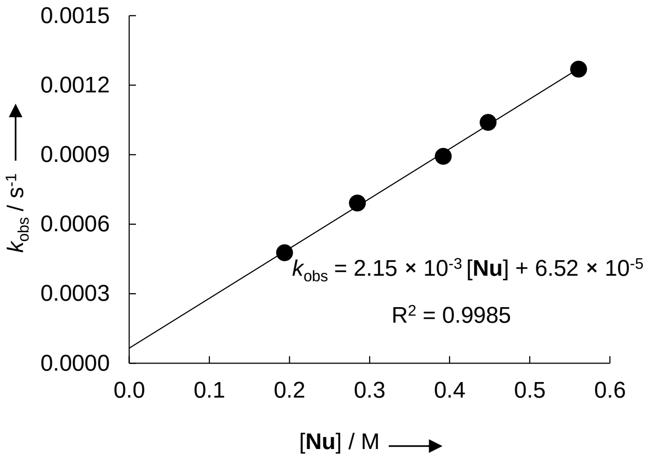

Table 2.S2.2.7. Rate constants for the reaction of 4-cyanobenzyl chloride (**2**-Cl) with 1-aminopropan-2-ol at 20˚C in DMSO (conventional conductometer).

No	$[E]_0/M^1$	$[Nu]_0$/M	$[Nu]_0$/ $[E]_0$	k_{obs}/s^{-1}
1	2.74×10^{-3}	1.54×10^{-1}	56	3.33×10^{-4}
2	2.71×10^{-3}	1.79×10^{-1}	66	3.75×10^{-4}
3	1.87×10^{-3}	2.24×10^{-1}	120	4.49×10^{-4}
4	2.64×10^{-3}	3.95×10^{-1}	150	7.75×10^{-4}
5	1.82×10^{-3}	4.63×10^{-1}	254	9.16×10^{-4}
$k_2 = 1.90 \times 10^{-3}\ M^{-1}s^{-1}$				

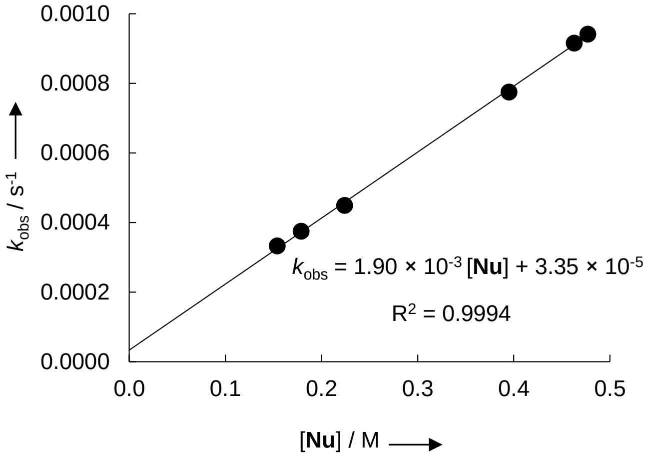

Table 2.S2.2.8. Rate constants for the reaction of 4-cyanobenzyl chloride (**2**-Cl) with propylamine at 20˚C in DMSO (conventional conductometer).

No	$[E]_0/M^1$	$[Nu]_0/M$	$[Nu]_0/[E]_0$	k_{obs}/s^{-1}
1	1.88×10^{-3}	2.00×10^{-1}	106	5.74×10^{-4}
2	1.92×10^{-3}	2.93×10^{-1}	153	7.48×10^{-4}
3	1.82×10^{-3}	3.90×10^{-1}	214	1.03×10^{-3}
4	1.78×10^{-3}	5.59×10^{-1}	314	1.37×10^{-3}
$k_2 = 2.26 \times 10^{-3}\ M^{-1}s^{-1}$				

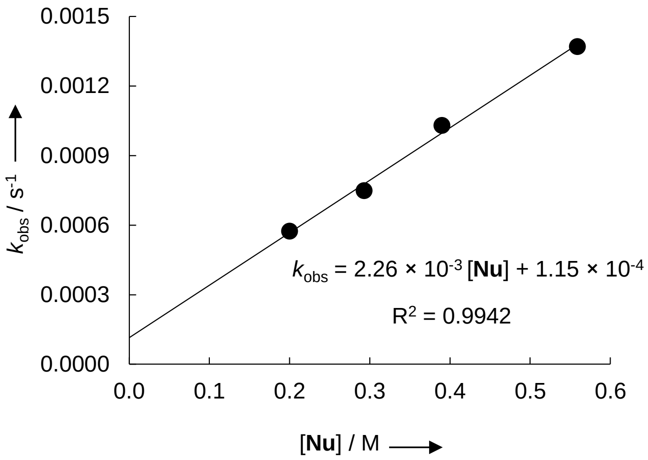

Table 2.S2.2.9. Rate constants for the reaction of 4-cyanobenzyl chloride (**2**-Cl) with 2-aminobutan-1-ol at 20˚C in DMSO (conventional conductometer).

No	$[E]_0/M^1$	$[Nu]_0/M$	$[Nu]_0/[E]_0$	k_{obs}/s^{-1}
1	2.86×10^{-3}	1.18×10^{-1}	41	7.08×10^{-5}
2	2.80×10^{-3}	1.73×10^{-1}	62	1.01×10^{-4}
3	2.84×10^{-3}	2.23×10^{-1}	79	1.26×10^{-4}
4	2.77×10^{-3}	3.45×10^{-1}	125	1.86×10^{-4}
5	2.73×10^{-3}	5.31×10^{-1}	195	2.81×10^{-4}
$k_2 = 5.06 \times 10^{-4}\ M^{-1}s^{-1}$				

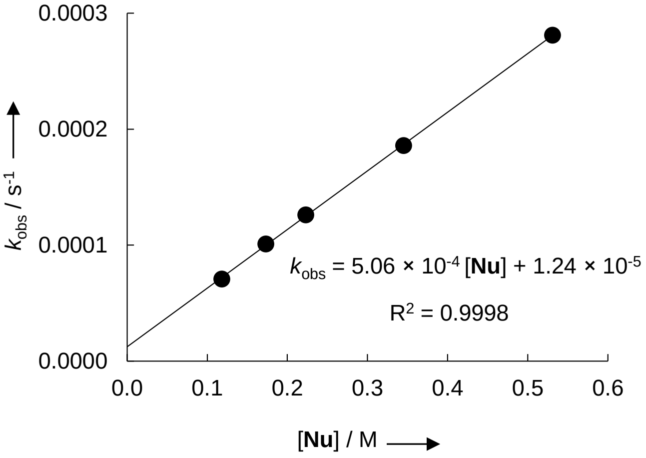

2.S.2.3. Rate constants for the reactions of 4-methoxybenzyl chloride (3-Cl) in DMSO.

Table 2.S2.3.1. Rate constants for the reaction of 4-methoxybenzyl chloride (**3**-Cl) with DABCO at 20˚C in DMSO (stopped-flow technique).

No	$[E]_0/M^1$	$[Nu]_0/M$	$[Nu]_0/ [E]_0$	k_{obs}/s^{-1}
1	5.02×10^{-4}	1.49×10^{-1}	297	4.58×10^{-2}
2	5.02×10^{-4}	1.95×10^{-1}	388	5.86×10^{-2}
3	5.02×10^{-4}	2.46×10^{-1}	490	7.52×10^{-2}
4	5.02×10^{-4}	2.98×10^{-1}	594	9.00×10^{-2}
5	5.02×10^{-4}	3.30×10^{-1}	657	9.88×10^{-2}
$k_2 = 2.96 \times 10^{-1}\ M^{-1}s^{-1}$				

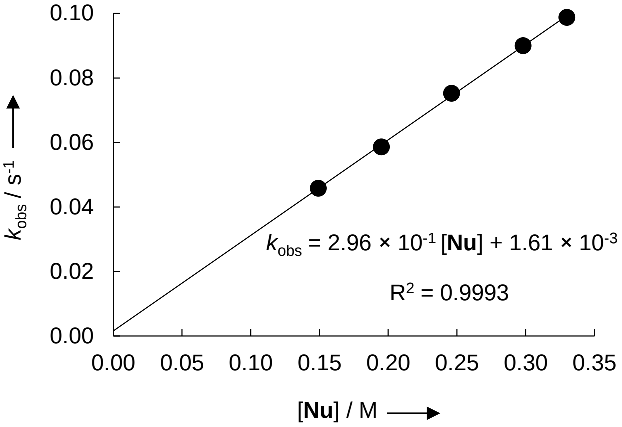

Table 2.S2.3.2. Rate constants for the reaction of 4-methoxybenzyl chloride (**3**-Cl) with 1,1-dimethylhydrazine at 20˚C in DMSO (conventional conductometer).

No	$[E]_0/M^1$	$[Nu]_0/M$	$[Nu]_0/[E]_0$	k_{obs}/s^{-1}
1	2.60×10^{-3}	8.20×10^{-2}	32	5.60×10^{-3}
2	2.55×10^{-3}	1.04×10^{-1}	41	6.92×10^{-3}
3	2.55×10^{-3}	1.18×10^{-1}	46	7.74×10^{-3}
4	2.56×10^{-3}	1.56×10^{-1}	61	1.04×10^{-2}
		$k_2 = 6.51 \times 10^{-2}\ M^{-1}s^{-1}$		

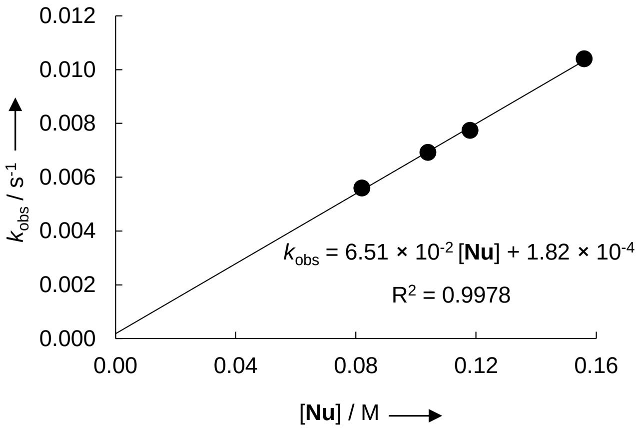

Table 2.S2.3.3. Rate constants for the reaction of 4-methoxybenzyl chloride (**3**-Cl) with methylhydrazine at 20˚C in DMSO (conventional conductometer).

No	$[E]_0/M^1$	$[Nu]_0/M$	$[Nu]_0/[E]_0$	k_{obs}/s^{-1}
1	2.53×10^{-3}	8.60×10^{-2}	34	3.26×10^{-3}
2	2.51×10^{-3}	1.15×10^{-1}	46	4.10×10^{-3}
3	2.54×10^{-3}	1.49×10^{-1}	58	5.47×10^{-3}
4	2.51×10^{-3}	2.13×10^{-1}	85	7.90×10^{-3}
5	2.30×10^{-3}	2.23×10^{-1}	97	8.03×10^{-3}
		$k_2 = 3.62 \times 10^{-2}\ M^{-1}s^{-1}$		

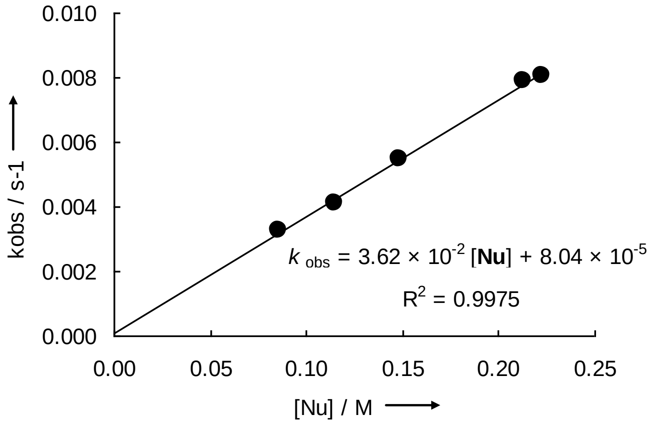

Table 2.S2.3.4. Rate constants for the reaction of 4-methoxybenzyl chloride (**3**-Cl) with piperidine at 20˚C in DMSO (stopped-flow technique).

No	$[E]_0/M^1$	$[Nu]_0/M$	$[Nu]_0/[E]_0$	k_{obs}/s^{-1}
1	3.00×10^{-3}	1.36×10^{-1}	46	6.74×10^{-3}
2	2.97×10^{-3}	2.00×10^{-1}	67	9.98×10^{-3}
3	2.93×10^{-3}	2.31×10^{-1}	79	1.21×10^{-2}
4	2.92×10^{-3}	2.83×10^{-1}	97	1.40×10^{-2}
5	2.85×10^{-3}	3.11×10^{-1}	109	1.51×10^{-2}
$k_2 = 4.82 \times 10^{-2}\ M^{-1}s^{-1}$				

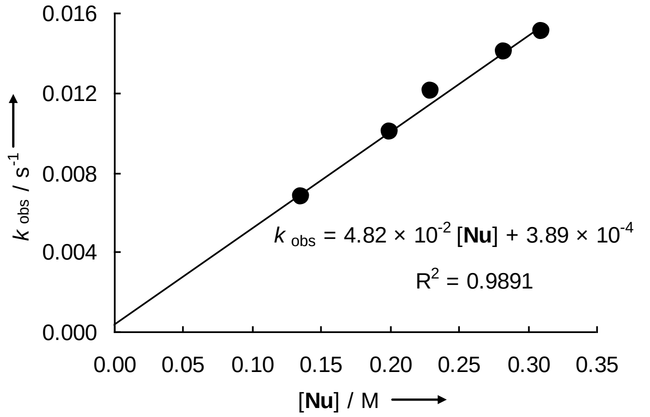

Table 2.S2.3.5. Rate constants for the reaction of 4-methoxybenzyl chloride (**3**-Cl) with propylamine at 20˚C in DMSO (stopped-flow technique).

No	$[E]_0/M^1$	$[Nu]_0/M$	$[Nu]_0/[E]_0$	k_{obs}/s^{-1}
1	2.75×10^{-3}	1.80×10^{-1}	65	6.41×10^{-4}
2	2.68×10^{-3}	2.78×10^{-1}	104	9.90×10^{-4}
3	2.67×10^{-3}	3.43×10^{-1}	128	1.18×10^{-3}
4	2.63×10^{-3}	4.00×10^{-1}	152	1.35×10^{-3}
5	2.57×10^{-3}	4.55×10^{-1}	177	1.55×10^{-3}
$k_2 = 3.25 \times 10^{-3}\ M^{-1}s^{-1}$				

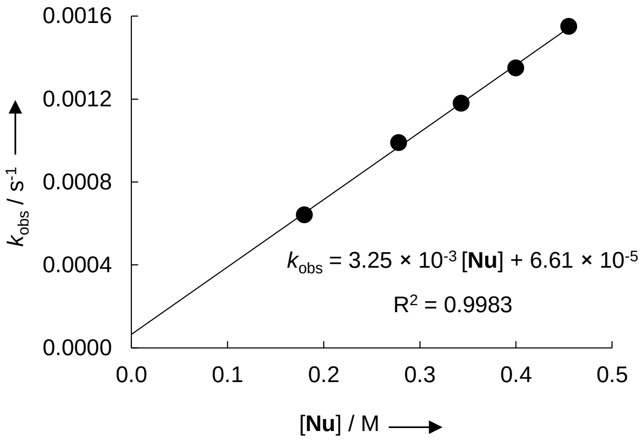

Table 2.S2.3.6. Rate constants for the reaction of 4-methoxybenzyl chloride (**3**-Cl) with benzylamine at 20˚C in DMSO (stopped-flow technique).

No	$[E]_0/M^1$	$[Nu]_0/M$	$[Nu]_0/[E]_0$	k_{obs}/s^{-1}
1	2.73×10^{-3}	1.85×10^{-1}	68	3.59×10^{-4}
2	2.71×10^{-3}	2.42×10^{-1}	89	4.46×10^{-4}
3	2.64×10^{-3}	2.90×10^{-1}	110	5.35×10^{-4}
4	2.68×10^{-3}	3.39×10^{-1}	126	6.22×10^{-4}
$k_2 = 1.72 \times 10^{-3}\ M^{-1}s^{-1}$				

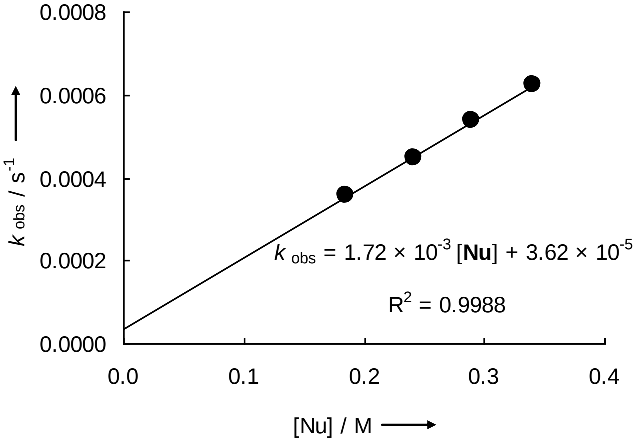

Table 2.S2.3.7. Rate constants for the reaction of 4-methoxybenzyl chloride (**3**-Cl) with imidazole at 20˚C in DMSO (stopped-flow technique).

No	$[E]_0$/M^1	$[Nu]_0$/M	$[Nu]_0$/ $[E]_0$	k_{obs}/s^{-1}
1	1.65×10^{-3}	2.71×10^{-1}	164	1.80×10^{-5}
2	1.67×10^{-3}	4.09×10^{-1}	245	2.46×10^{-5}
3	1.34×10^{-3}	4.36×10^{-1}	326	2.58×10^{-5}
$k_2 = 4.75 \times 10^{-5}$ M^{-1}s^{-1}				

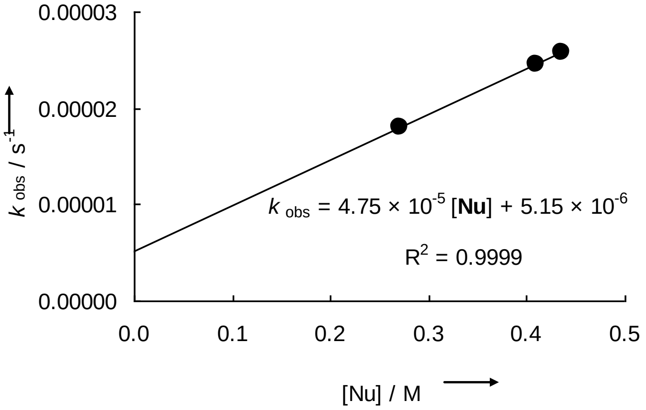

2.S.2.4. Rate constants for the reactions of phenacyl chloride (4-Cl) in DMSO.

Table 2.S2.4.1. Rate constants for the reaction of phenacyl chloride (**4**-Cl) with piperidine at 20˚C in DMSO (conventional conductometer).

No	$[E]_0/M^1$	$[Nu]_0/M$	$[Nu]_0/[E]_0$	k_{obs}/s^{-1}
1	6.78×10^{-4}	2.18×10^{-2}	32	5.19×10^{-3}
2	6.77×10^{-4}	3.21×10^{-2}	47	6.87×10^{-3}
3	6.79×10^{-4}	7.34×10^{-2}	108	1.31×10^{-2}
4	6.81×10^{-4}	9.75×10^{-2}	143	1.68×10^{-2}
5	6.95×10^{-4}	1.66×10^{-1}	239	2.75×10^{-2}
$k_2 = 1.54 \times 10^{-1}\ M^{-1}s^{-1}$				

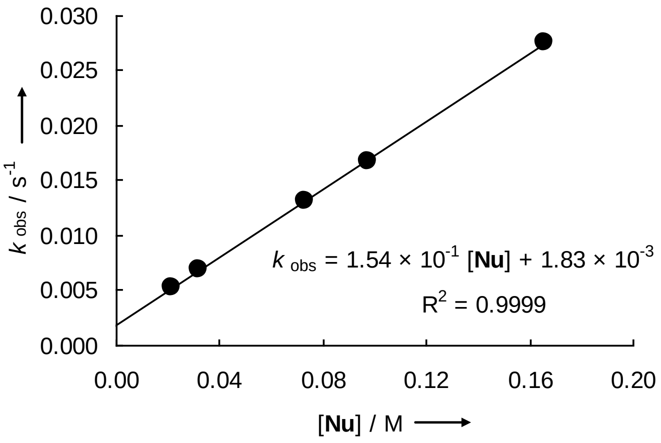

Table 2.S2.4.2. Rate constants for the reaction of phenacyl chloride (**4**-Cl) with morpholine at 20˚C in DMSO (conventional conductometer).

No	$[E]_0/M^1$	$[Nu]_0/M$	$[Nu]_0/[E]_0$	k_{obs}/s^{-1}
1	7.04×10^{-4}	1.24×10^{-1}	176	4.36×10^{-3}
2	6.80×10^{-4}	8.21×10^{-2}	121	2.84×10^{-3}
3	7.12×10^{-4}	5.30×10^{-2}	74	1.90×10^{-3}
4	6.89×10^{-4}	3.01×10^{-2}	44	1.27×10^{-3}
5	6.74×10^{-4}	1.39×10^{-1}	206	4.80×10^{-3}
$k_2 = 3.31 \times 10^{-2}\ M^{-1}s^{-1}$				

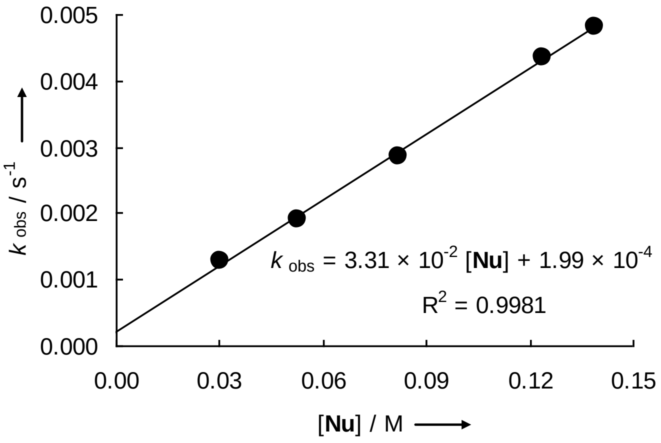

Table 2.S2.4.3. Rate constants for the reaction of phenacyl chloride (**4**-Cl) with 2-aminoethanol at 20˚C in DMSO (stopped-flow technique).

No	$[E]_0/M^1$	$[Nu]_0/M$	$[Nu]_0/ [E]_0$	k_{obs}/s^{-1}
1	6.37×10^{-4}	7.04×10^{-2}	111	1.46×10^{-3}
2	6.55×10^{-4}	1.06×10^{-1}	162	1.97×10^{-3}
3	6.32×10^{-4}	1.99×10^{-1}	315	3.65×10^{-3}
4	6.32×10^{-4}	1.72×10^{-1}	272	3.12×10^{-3}
5	6.43×10^{-4}	2.51×10^{-1}	390	4.50×10^{-3}
$k_2 = 1.71 \times 10^{-2}$ $M^{-1}s^{-1}$				

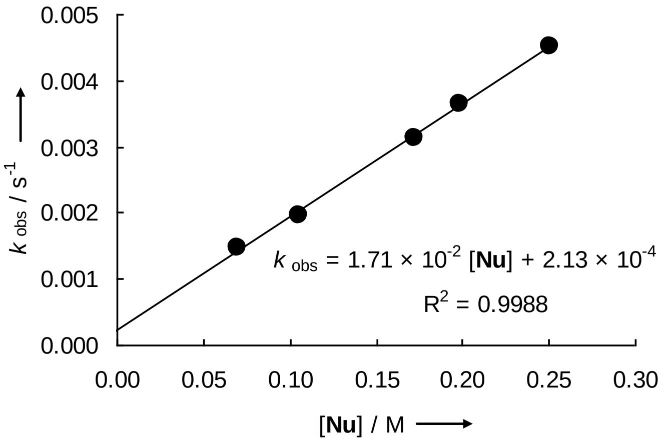

Table 2.S2.4.4. Rate constants for the reaction of phenacyl chloride (**4**-Cl) with 1-aminopropan-2-ol at 20˚C in DMSO (conventional conductometer).

No	$[E]_0/M^1$	$[Nu]_0/M$	$[Nu]_0/ [E]_0$	k_{obs}/s^{-1}
1	6.86×10^{-4}	7.98×10^{-2}	116	1.32×10^{-3}
2	6.78×10^{-4}	1.02×10^{-1}	150	1.66×10^{-3}
3	7.02×10^{-4}	1.40×10^{-1}	199	2.23×10^{-3}
$k_2 = 1.51 \times 10^{-2}$ $M^{-1}s^{-1}$				

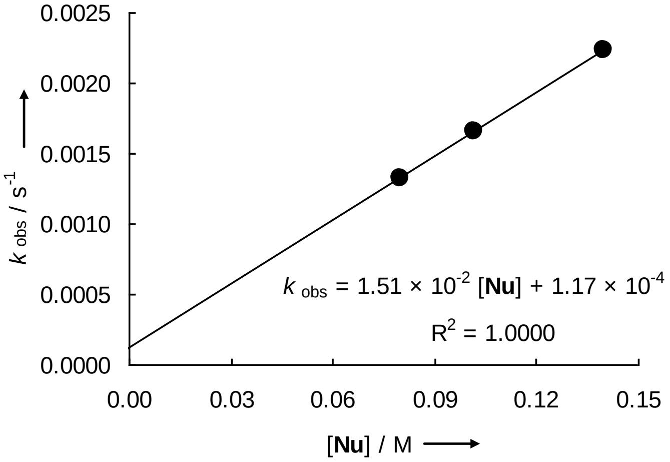

Table 2.S2.4.5. Rate constants for the reaction of phenacyl chloride (**4**-Cl) with *n*-propylamine at 20˚C in DMSO (conventional conductometer).

No	$[E]_0/M^1$	$[Nu]_0/M$	$[Nu]_0/ [E]_0$	k_{obs}/s^{-1}
1	6.98×10^{-4}	5.95×10^{-2}	85	1.45×10^{-3}
2	6.62×10^{-4}	9.50×10^{-2}	144	2.50×10^{-3}
3	6.72×10^{-4}	1.10×10^{-1}	164	2.87×10^{-3}
4	6.58×10^{-4}	1.65×10^{-1}	251	4.34×10^{-3}
$k_2 = 2.72 \times 10^{-2}\ M^{-1}s^{-1}$				

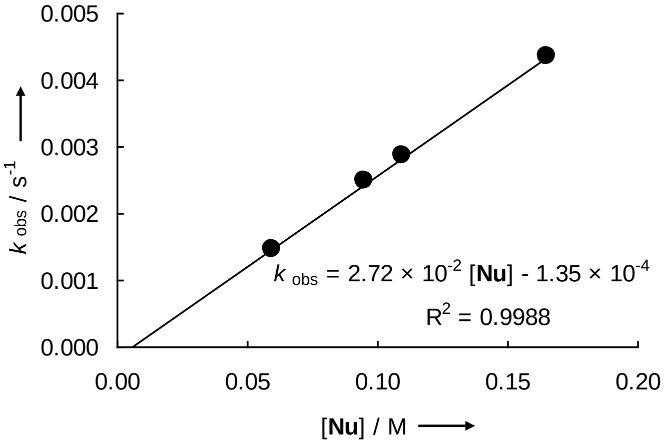

Table 2.S2.4.6. Rate constants for the reaction of phenacyl chloride (**4**-Cl) with benzylamine at 20˚C in DMSO (conventional conductometer).

No	$[E]_0/M^1$	$[Nu]_0/M$	$[Nu]_0/[E]_0$	k_{obs}/s^{-1}
1	6.74×10^{-4}	5.45×10^{-2}	81	5.23×10^{-4}
2	6.87×10^{-4}	8.72×10^{-2}	127	7.63×10^{-4}
3	6.46×10^{-4}	1.06×10^{-1}	164	9.25×10^{-4}
4	6.82×10^{-4}	1.39×10^{-1}	204	1.15×10^{-3}
$k_2 = 7.48 \times 10^{-3}\ M^{-1}s^{-1}$				

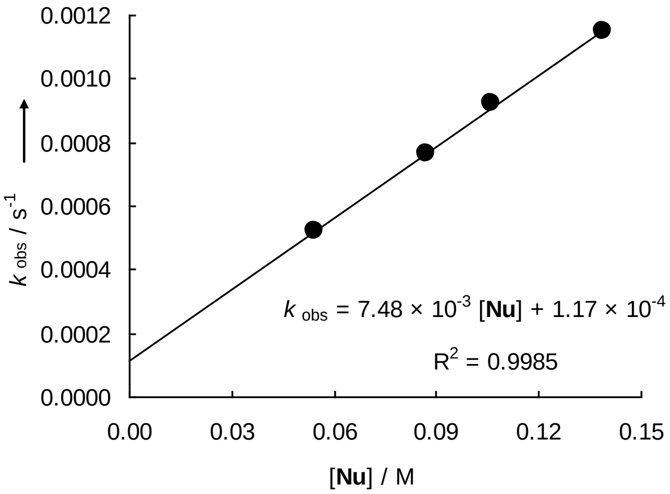

Table 2.S2.4.7. Rate constants for the reaction of phenacyl chloride (**4**-Cl) with 4-dimethylaminopyridine at 20˚C in DMSO (conventional conductometer).

No	$[E]_0/M^1$	$[Nu]_0/M$	$[Nu]_0/[E]_0$	k_{obs}/s^{-1}
1	6.63×10^{-4}	3.69×10^{-2}	56	2.24×10^{-4}
2	6.79×10^{-4}	6.94×10^{-2}	102	4.20×10^{-4}
3	6.68×10^{-4}	8.51×10^{-2}	127	5.17×10^{-4}
4	6.75×10^{-4}	1.07×10^{-1}	159	6.41×10^{-4}
5	6.88×10^{-4}	1.35×10^{-1}	196	8.01×10^{-4}
$k_2 = 5.88 \times 10^{-3}\ M^{-1}s^{-1}$				

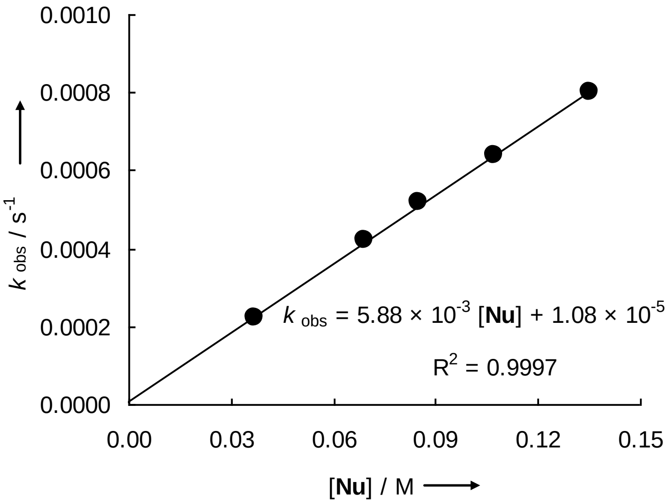

Table 2.S2.4.8. Rate constants for the reaction of phenacyl chloride (**4**-Cl) with 2-aminobutan-1-ol at 20˚C in DMSO (conventional conductometer).

No	$[E]_0/M^1$	$[Nu]_0/M$	$[Nu]_0/ [E]_0$	k_{obs}/s^{-1}
1	6.81×10^{-4}	9.71×10^{-2}	143	2.90×10^{-4}
2	6.79×10^{-4}	1.39×10^{-1}	205	4.03×10^{-4}
3	6.68×10^{-4}	1.75×10^{-1}	262	5.03×10^{-4}
4	6.70×10^{-4}	2.21×10^{-1}	330	6.34×10^{-4}
$k_2 = 2.78 \times 10^{-3}\ M^{-1}s^{-1}$				

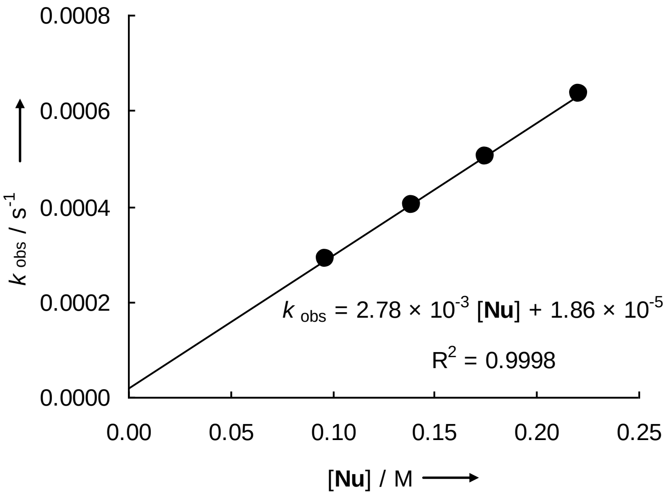

Table 2.S2.4.9. Rate constants for the reaction of phenacyl chloride (**4**-Cl) with diethanolamine at 20˚C in DMSO (conventional conductometer).

No	$[E]_0/M^1$	$[Nu]_0/M$	$[Nu]_0/[E]_0$	k_{obs}/s^{-1}
1	6.34×10^{-4}	7.92×10^{-2}	125	1.60×10^{-4}
2	6.37×10^{-4}	1.15×10^{-1}	181	2.42×10^{-4}
3	6.56×10^{-4}	1.61×10^{-1}	245	3.24×10^{-4}
4	6.28×10^{-4}	1.93×10^{-1}	307	3.81×10^{-4}
5	6.32×10^{-4}	2.44×10^{-1}	386	4.76×10^{-4}
		$k_2 = 1.89 \times 10^{-3}\ M^{-1}s^{-1}$		

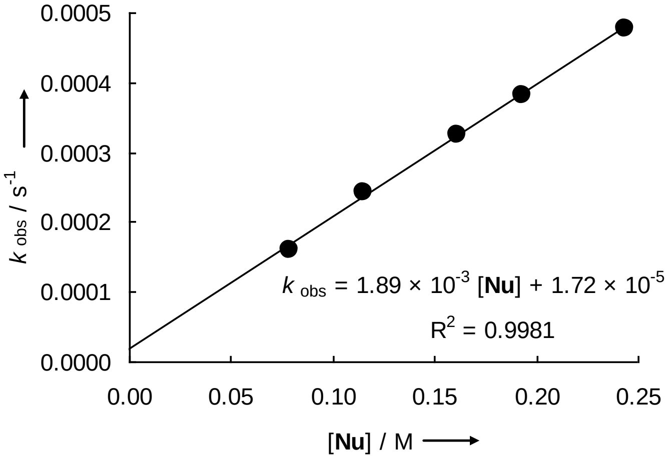

Table 2.S2.4.10. Rate constants for the reaction of phenacyl chloride (**4**-Cl) with imidazole at 20˚C in DMSO (conventional conductometer).

No	$[E]_0/M^1$	$[Nu]_0/M$	$[Nu]_0/[E]_0$	k_{obs}/s^{-1}
1	6.80×10^{-4}	1.37×10^{-1}	201	5.96×10^{-5}
2	6.85×10^{-4}	2.64×10^{-1}	385	1.10×10^{-4}
3	6.79×10^{-4}	3.08×10^{-1}	454	1.28×10^{-4}
4	6.87×10^{-4}	3.67×10^{-1}	534	1.51×10^{-4}
		$k_2 = 3.98 \times 10^{-4}\ M^{-1}s^{-1}$		

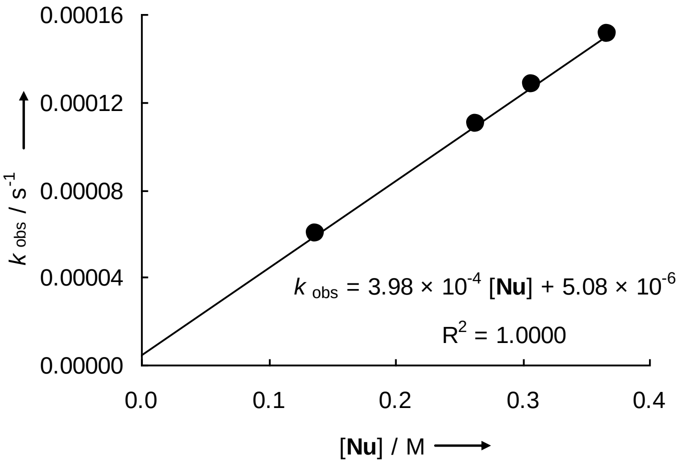

Table 2.S2.4.11. Rate constants for the reaction of phenacyl chloride (**4**-Cl) with 2,2,2-trifluoroethylamine at 20˚C in DMSO (conventional conductometer).

No	$[E]_0/M^1$	$[Nu]_0/M$	$[Nu]_0/ [E]_0$	k_{obs}/s^{-1}
1	6.33×10^{-4}	1.23×10^{-1}	194	6.05×10^{-6}
2	6.31×10^{-4}	1.53×10^{-1}	242	7.41×10^{-6}
3	6.60×10^{-4}	1.87×10^{-1}	283	9.43×10^{-6}
$k_2 = 5.30 \times 10^{-5}$ M^{-1}s^{-1}				

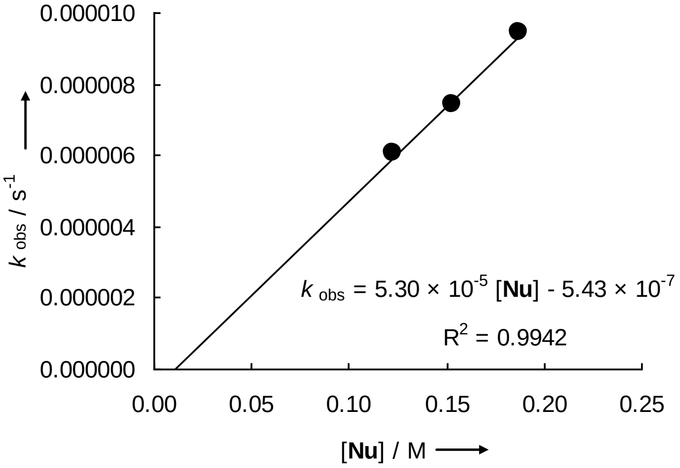

2.S.2.5. Rate constants for the reactions of benzyl bromide (1-Br) in DMSO.

Table 2.S2.5.1. Rate constants for the reaction of benzyl bromide (**1**-Br) with TBD (1,5,7-triazabicyclo[4.4.0]dec-5-ene) at 20˚C in DMSO (conventional conductometer).

No	$[E]_0/M^1$	$[Nu]_0/M$	$[Nu]_0/ [E]_0$	k_{obs}/s^{-1}
1	6.84×10^{-4}	8.22×10^{-3}	12	1.50×10^{-2}
2	8.87×10^{-4}	1.53×10^{-2}	17	2.71×10^{-2}
3	6.12×10^{-4}	1.19×10^{-2}	19	2.17×10^{-2}
4	8.61×10^{-4}	1.85×10^{-2}	21	3.27×10^{-2}
$k_2 = 1.71\ M^{-1}s^{-1}$				

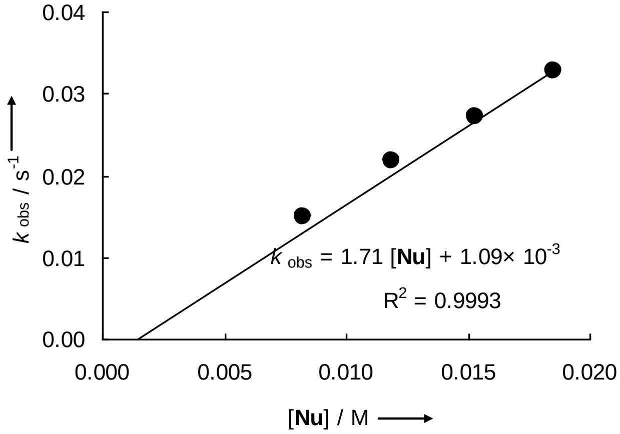

Table 2.S2.5.2. Rate constants for the reaction of benzyl bromide (**1**-Br) with 1,1-dimethylhydrazine at 20˚C in DMSO (stopped-flow).

No	$[E]_0/M^1$	$[Nu]_0/M$	$[Nu]_0/ [E]_0$	k_{obs}/s^{-1}
1	4.43×10^{-3}	7.71×10^{-2}	17	2.94×10^{-1}
2	4.43×10^{-3}	1.60×10^{-1}	36	6.13×10^{-1}
3	4.43×10^{-3}	1.98×10^{-1}	45	7.66×10^{-1}
4	4.43×10^{-3}	2.75×10^{-1}	62	1.04
5	4.43×10^{-3}	3.09×10^{-1}	70	1.16
$k_2 = 3.73\ M^{-1}s^{-1}$				

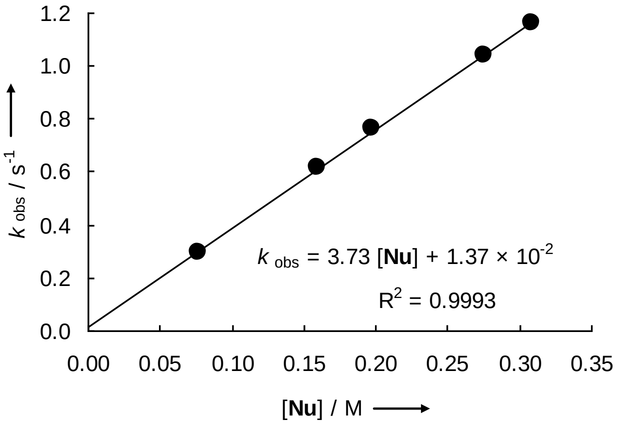

Table 2.S2.5.3. Rate constants for the reaction of benzyl bromide (**1**-Br) with methylhydrazine at 20˚C in DMSO (stopped-flow).

No	$[E]_0/M^1$	$[Nu]_0/M$	$[Nu]_0/ [E]_0$	k_{obs}/s^{-1}
1	1.75×10^{-3}	8.23×10^{-2}	47	1.45×10^{-1}
2	1.75×10^{-3}	1.21×10^{-1}	69	2.20×10^{-1}
3	1.75×10^{-3}	1.43×10^{-1}	82	2.63×10^{-1}
4	1.75×10^{-3}	2.57×10^{-1}	147	4.81×10^{-1}
		$k_2 = 1.92\ M^{-1}s^{-1}$		

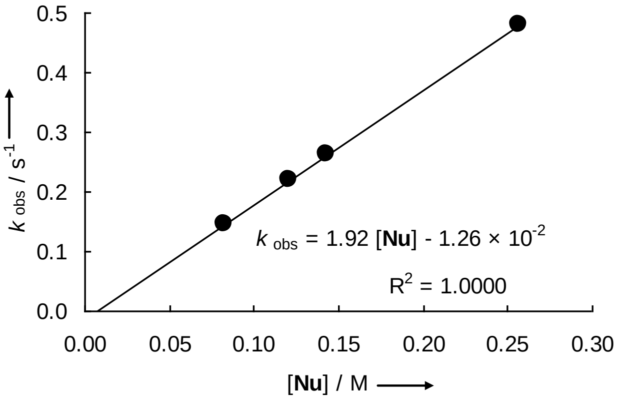

Table 2.S2.5.4. Rate constants for the reaction of benzyl bromide (**1**-Br) with DBN (1,5-diazabicyclo[4.3.0]non-5-ene) at 20˚C in DMSO (conventional conductometer).

No	$[E]_0/M^1$	$[Nu]_0/M$	$[Nu]_0/[E]_0$	k_{obs}/s^{-1}
1	7.19×10^{-4}	8.60×10^{-3}	12	3.93×10^{-3}
2	7.07×10^{-4}	1.52×10^{-2}	21	6.76×10^{-3}
3	6.77×10^{-4}	2.27×10^{-2}	34	1.01×10^{-2}
4	7.08×10^{-4}	3.22×10^{-2}	45	1.46×10^{-2}
$k_2 = 4.52 \times 10^{-1}\ M^{-1}s^{-1}$				

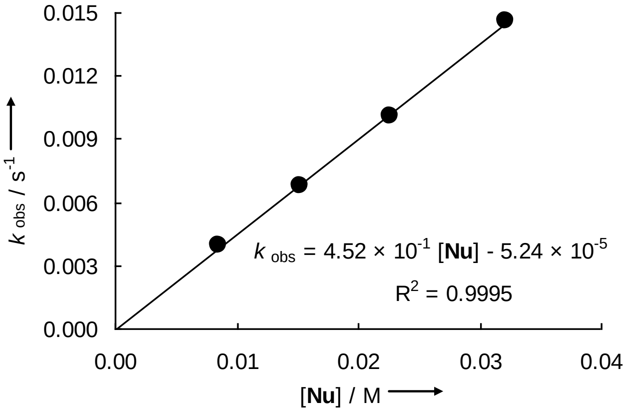

Table 2.S2.5.5. Rate constants for the reaction of benzyl bromide (**1**-Br) with TMG (1,1,3,3-tetramethylguanidine) at 20˚C in DMSO (conventional conductometer).

No	$[E]_0/M^1$	$[Nu]_0/M$	$[Nu]_0/[E]_0$	k_{obs}/s^{-1}
1	1.01×10^{-3}	4.60×10^{-2}	46	6.26×10^{-4}
2	1.07×10^{-3}	7.59×10^{-2}	71	1.02×10^{-3}
3	1.06×10^{-3}	1.02×10^{-1}	96	1.32×10^{-3}
4	1.03×10^{-3}	1.25×10^{-1}	121	1.60×10^{-3}
5	1.00×10^{-3}	1.48×10^{-1}	148	1.87×10^{-3}
$k_2 = 1.21 \times 10^{-2}\ M^{-1}s^{-1}$				

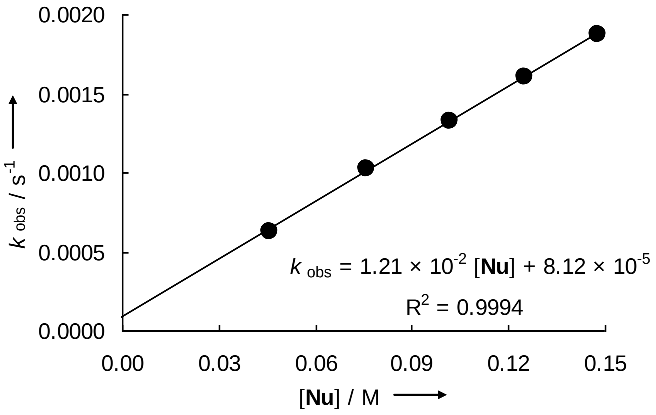

2.S.2.6. Rate constants for the reactions of 4-cyanobenzyl bromide (2-Br) in DMSO.

Table 2.S2.6.1. Rate constants for the reaction of 4-cyanobenzyl bromide (**2**-Br) with DABCO at 20˚C in DMSO (stopped-flow).

No	$[E]_0/M^1$	$[Nu]_0/M$	$[Nu]_0/[E]_0$	k_{obs}/s^{-1}
1	7.42×10^{-4}	1.19×10^{-2}	16	2.97×10^{-1}
2	7.42×10^{-4}	1.43×10^{-2}	19	3.56×10^{-1}
3	7.42×10^{-4}	1.67×10^{-2}	23	4.17×10^{-1}
4	7.42×10^{-4}	1.91×10^{-2}	26	4.78×10^{-1}
5	7.42×10^{-4}	2.14×10^{-2}	29	5.40×10^{-1}
$k_2 = 2.55 \times 10^1\ M^{-1}s^{-1}$				

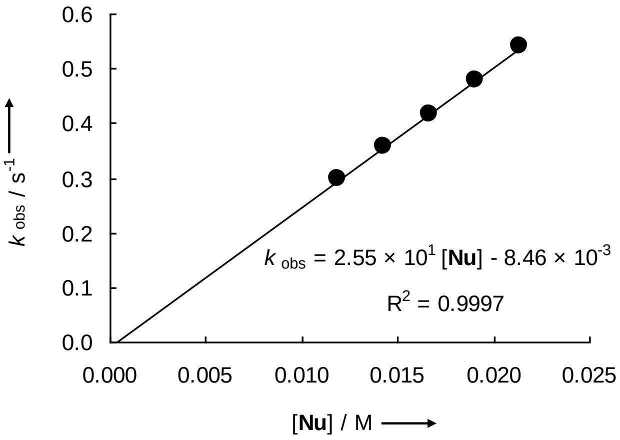

Table 2.S2.6.2. Rate constants for the reaction of 4-cyanobenzyl bromide (**2**-Br) with TBD (1,5,7-triazabicyclo[4.4.0]dec-5-ene) at 20˚C in DMSO (stopped-flow).

No	$[E]_0/M^1$	$[Nu]_0/M$	$[Nu]_0/[E]_0$	k_{obs}/s^{-1}
1	7.42×10^{-4}	2.13×10^{-2}	29	9.60×10^{-2}
2	7.42×10^{-4}	3.19×10^{-2}	43	1.39×10^{-1}
3	7.42×10^{-4}	3.72×10^{-2}	50	1.63×10^{-1}
$k_2 = 4.19\ M^{-1}s^{-1}$				

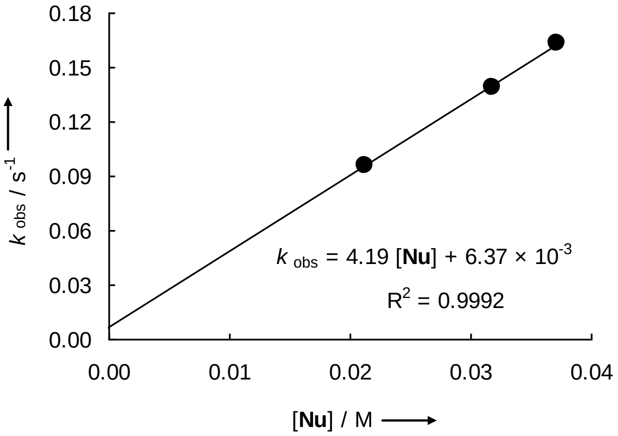

Table 2.S2.6.3. Rate constants for the reaction of 4-cyanobenzyl bromide (**2**-Br) with 1,1-dimethylhydrazine at 20˚C in DMSO (stopped-flow).

No	$[E]_0/M^1$	$[Nu]_0/M$	$[Nu]_0/ [E]_0$	k_{obs}/s^{-1}
1	5.66×10^{-4}	7.71×10^{-2}	136	3.63×10^{-1}
2	5.66×10^{-4}	1.60×10^{-1}	283	7.54×10^{-1}
3	5.66×10^{-4}	1.98×10^{-1}	350	9.49×10^{-1}
4	5.66×10^{-4}	2.75×10^{-1}	486	1.28
5	5.66×10^{-4}	3.09×10^{-1}	546	1.45
$k_2 = 4.66\,M^{-1}s^{-1}$				

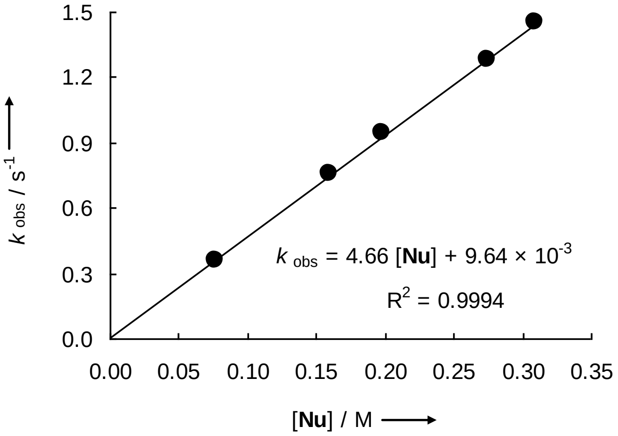

Table 2.S2.6.4. Rate constants for the reaction of 4-cyanobenzyl bromide (**2**-Br) with methylhydrazine at 20˚C in DMSO (stopped-flow).

No	$[E]_0/M^1$	$[Nu]_0/M$	$[Nu]_0/ [E]_0$	k_{obs}/s^{-1}
1	5.66×10^{-4}	1.09×10^{-1}	193	3.55×10^{-1}
2	5.66×10^{-4}	1.80×10^{-1}	318	5.98×10^{-1}
3	5.66×10^{-4}	2.19×10^{-1}	387	7.58×10^{-1}
4	5.66×10^{-4}	2.88×10^{-1}	509	9.53×10^{-1}
5	5.66×10^{-4}	3.89×10^{-1}	687	1.31
$k_2 = 3.38\ M^{-1}s^{-1}$				

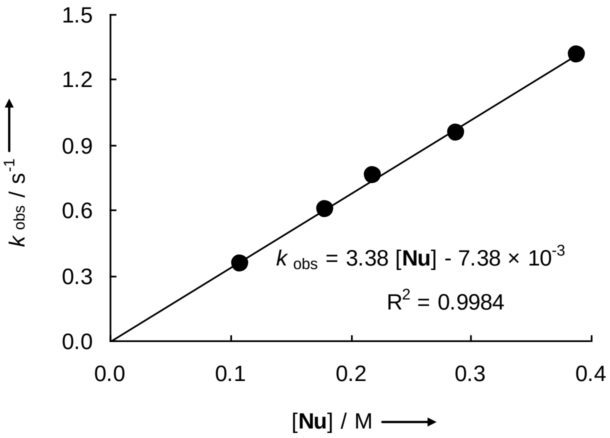

Table 2.S2.6.5. Rate constants for the reaction of 4-cyanobenzyl bromide (**2**-Br) with DBN (1,5-diazabicyclo[4.3.0]non-5-ene) at 20˚C in DMSO (conventional conductometer).

No	$[E]_0/M^1$	$[Nu]_0/M$	$[Nu]_0/ [E]_0$	k_{obs}/s^{-1}
1	6.17×10^{-4}	6.11×10^{-3}	10	4.51×10^{-3}
2	6.13×10^{-4}	1.21×10^{-2}	20	8.84×10^{-3}
3	4.87×10^{-4}	1.81×10^{-2}	37	1.26×10^{-2}
4	4.77×10^{-4}	2.36×10^{-2}	49	1.72×10^{-2}
$k_2 = 7.15 \times 10^{-2}\ M^{-1}s^{-1}$				

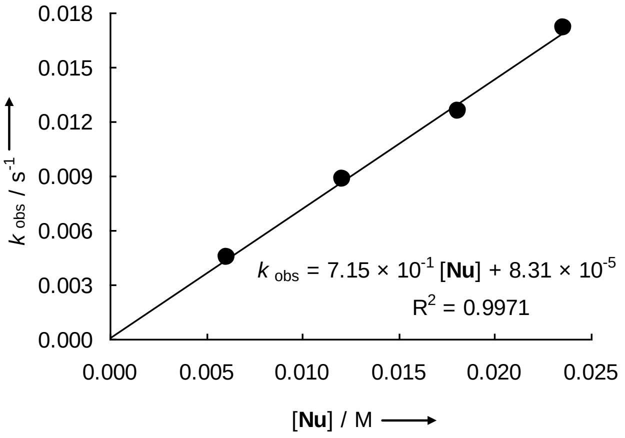

Table 2.S2.6.6. Rate constants for the reaction of 4-cyanobenzyl bromide (**2**-Br) with DBU (1,8-diazabicyclo[5.4.0]undec-7-ene) at 20˚C in DMSO (conventional conductometer).

No	$[E]_0/M^1$	$[Nu]_0/M$	$[Nu]_0/[E]_0$	k_{obs}/s^{-1}
1	1.86×10^{-4}	9.39×10^{-3}	50	9.82×10^{-4}
2	1.82×10^{-4}	1.83×10^{-2}	101	1.88×10^{-3}
3	1.81×10^{-4}	2.74×10^{-2}	151	3.09×10^{-3}
4	1.81×10^{-4}	3.65×10^{-2}	202	3.84×10^{-3}
5	1.74×10^{-4}	4.37×10^{-2}	251	4.80×10^{-3}
$k_2 = 1.10 \times 10^{-1}\ M^{-1}s^{-1}$				

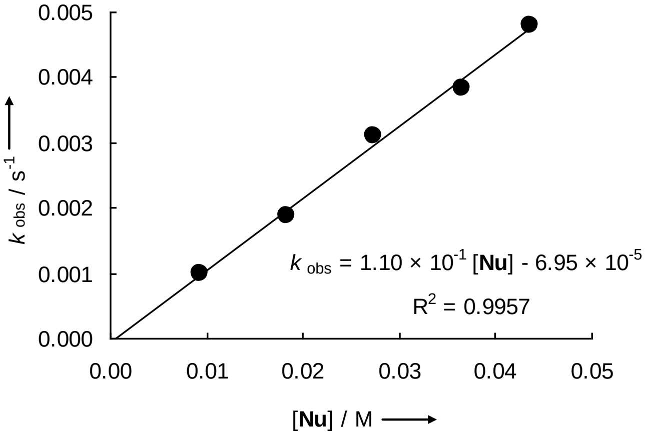

Table 2.S2.6.7. Rate constants for the reaction of 4-cyanobenzyl bromide (**2**-Br) with TMG (1,1,3,3-tetramethylguanidine) at 20˚C in DMSO (conventional conductometer).

No	$[E]_0/M^1$	$[Nu]_0/M$	$[Nu]_0/[E]_0$	k_{obs}/s^{-1}
1	6.11×10^{-4}	1.26×10^{-2}	21	2.56×10^{-4}
2	6.07×10^{-4}	3.75×10^{-2}	62	6.92×10^{-4}
3	6.40×10^{-4}	6.59×10^{-2}	103	1.22×10^{-3}
$k_2 = 1.81 \times 10^{-2}\ M^{-1}s^{-1}$				

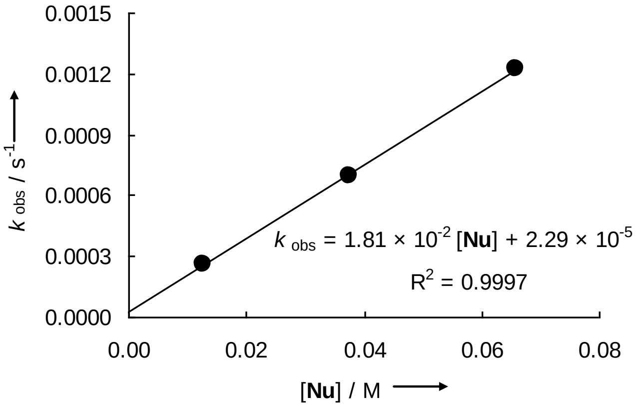

Table 2.S2.6.8. Rate constants for the reaction of 4-cyanobenzyl bromide (**2**-Br) with piperidine at 20˚C in DMSO (stopped-flow).

No	$[E]_0/M^1$	$[Nu]_0/M$	$[Nu]_0/[E]_0$	k_{obs}/s^{-1}
1	4.64×10^{-4}	9.18×10^{-2}	198	3.73×10^{-1}
2	4.64×10^{-4}	1.32×10^{-1}	284	5.59×10^{-1}
3	4.64×10^{-4}	1.81×10^{-1}	390	7.69×10^{-1}
4	4.64×10^{-4}	2.33×10^{-1}	502	9.61×10^{-1}
5	4.64×10^{-4}	2.62×10^{-1}	565	1.09
$k_2 = 4.15\ M^{-1}s^{-1}$				

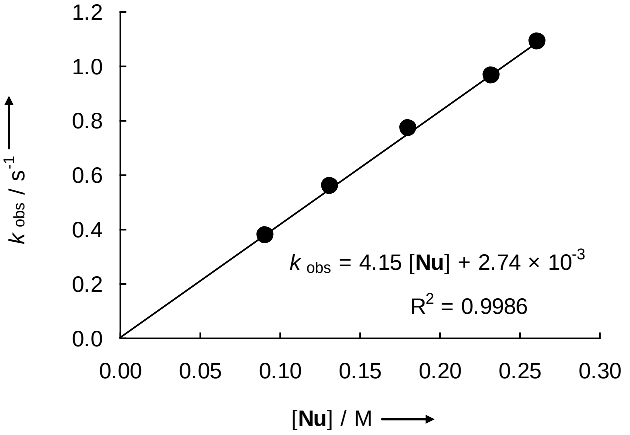

Table 2.S2.6.9. Rate constants for the reaction of 4-cyanobenzyl bromide (**2**-Br) with morpholine at 20˚C in DMSO (stopped-flow).

No	$[E]_0/M^1$	$[Nu]_0/M$	$[Nu]_0/[E]_0$	k_{obs}/s^{-1}
1	4.83×10^{-4}	1.03×10^{-1}	213	1.10×10^{-1}
2	4.83×10^{-4}	1.45×10^{-1}	300	1.56×10^{-1}
3	4.83×10^{-4}	1.77×10^{-1}	366	1.92×10^{-1}
4	4.83×10^{-4}	2.39×10^{-1}	495	2.53×10^{-1}
$k_2 = 1.05\ M^{-1}s^{-1}$				

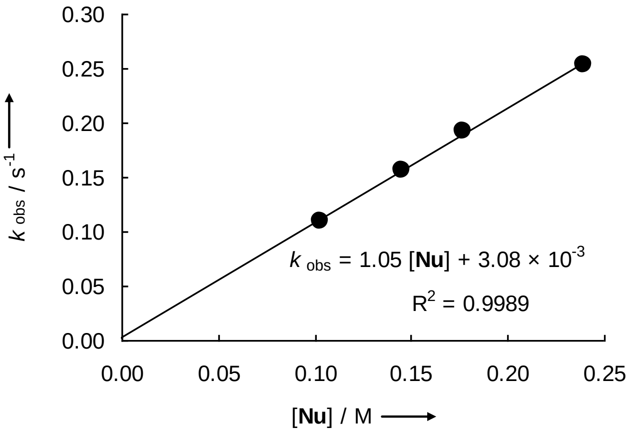

Table 2.S2.6.10. Rate constants for the reaction of 4-cyanobenzyl bromide (**2**-Br) with 2-aminoethanol at 20˚C in DMSO (conventional conductometer).

No	$[E]_0/M^1$	$[Nu]_0/M$	$[Nu]_0/[E]_0$	k_{obs}/s^{-1}
1	7.37×10^{-4}	1.28×10^{-2}	17	3.91×10^{-3}
2	7.19×10^{-4}	1.87×10^{-2}	26	5.52×10^{-3}
3	7.11×10^{-4}	2.47×10^{-2}	35	7.32×10^{-3}
4	7.06×10^{-4}	3.07×10^{-2}	43	8.98×10^{-3}
$k_2 = 2.85 \times 10^{-1}\ M^{-1}s^{-1}$				

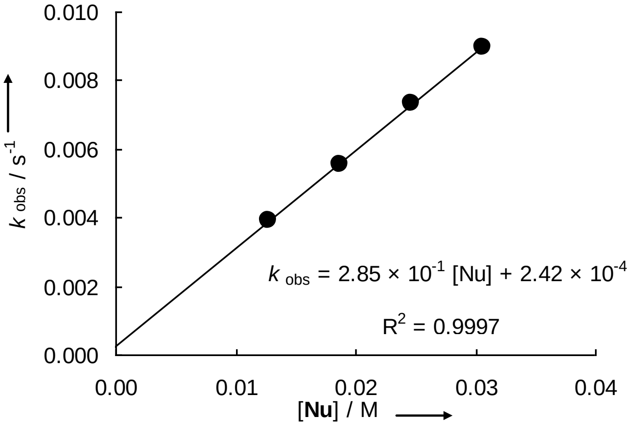

Table 2.S2.6.11. Rate constants for the reaction of 4-cyanobenzyl bromide (**2**-Br) with 1-aminopropan-2-ol at 20˚C in DMSO (conventional conductometer).

No	$[E]_0/M^1$	$[Nu]_0$/M	$[Nu]_0/ [E]_0$	k_{obs}/s^{-1}
1	1.01×10^{-3}	4.57×10^{-2}	45	1.20×10^{-2}
2	1.02×10^{-3}	6.12×10^{-2}	60	1.72×10^{-2}
3	1.03×10^{-3}	7.94×10^{-2}	77	2.31×10^{-2}
		$k_2 = 3.29 \times 10^{-1}$ M^{-1}s^{-1}		

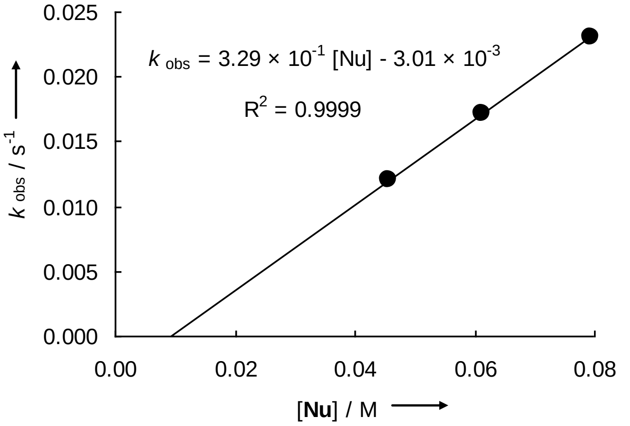

Table 2.S2.6.12. Rate constants for the reaction of 4-cyanobenzyl bromide (**2**-Br) with *n*-propylamine at 20˚C in DMSO (conventional conductometer).

No	$[E]_0/M^1$	$[Nu]_0$/M	$[Nu]_0/ [E]_0$	k_{obs}/s^{-1}
1	1.03×10^{-3}	5.99×10^{-2}	58	1.91×10^{-2}
2	1.01×10^{-3}	8.59×10^{-2}	85	2.74×10^{-2}
3	1.00×10^{-3}	1.05×10^{-1}	105	3.29×10^{-2}
		$k_2 = 3.07 \times 10^{-1}$ M^{-1}s^{-1}		

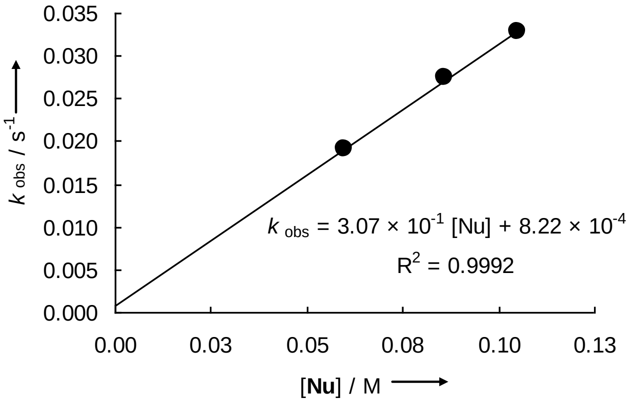

Table 2.S2.6.13. Rate constants for the reaction of 4-cyanobenzyl bromide (**2**-Br) with benzylamine at 20˚C in DMSO (conventional conductometer).

No	$[E]_0/M^1$	$[Nu]_0/M$	$[Nu]_0/ [E]_0$	k_{obs}/s^{-1}
1	1.01×10^{-3}	2.09×10^{-2}	21	3.62×10^{-3}
2	9.70×10^{-4}	3.02×10^{-2}	31	5.14×10^{-3}
3	9.50×10^{-4}	3.94×10^{-2}	41	6.75×10^{-3}
4	9.40×10^{-4}	4.87×10^{-2}	52	8.36×10^{-3}
$k_2 = 1.71 \times 10^{-1}\ M^{-1}s^{-1}$				

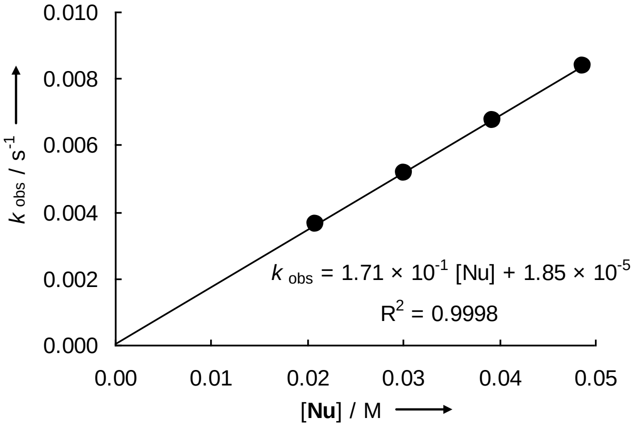

Table 2.S2.6.14. Rate constants for the reaction of 4-cyanobenzyl bromide (**2**-Br) with 4-DMAP at 20˚C in DMSO (conventional conductometer).

No	$[E]_0/M^1$	$[Nu]_0/M$	$[Nu]_0/[E]_0$	k_{obs}/s^{-1}
1	9.39×10^{-4}	1.62×10^{-2}	17	1.05×10^{-3}
2	9.21×10^{-4}	2.11×10^{-2}	23	1.35×10^{-3}
3	6.99×10^{-4}	2.57×10^{-2}	37	1.60×10^{-3}
4	6.90×10^{-4}	3.04×10^{-2}	44	1.88×10^{-3}
$k_2 = 5.81 \times 10^{-2}\ M^{-1}s^{-1}$				

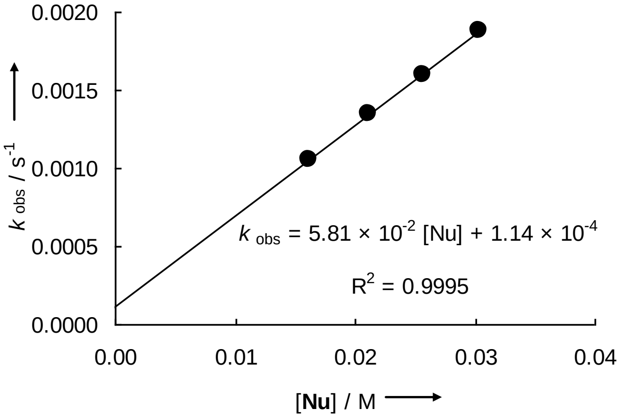

Table 2.S2.6.15. Rate constants for the reaction of 4-cyanobenzyl bromide (**2**-Br) with 2-aminobutan-1-ol at 20˚C in DMSO (conventional conductometer).

No	$[E]_0/M^1$	$[Nu]_0/M$	$[Nu]_0/[E]_0$	k_{obs}/s^{-1}
1	2.56×10^{-3}	6.54×10^{-2}	26	5.53×10^{-3}
2	2.54×10^{-3}	1.24×10^{-1}	49	1.01×10^{-2}
3	2.56×10^{-3}	1.69×10^{-1}	66	1.35×10^{-2}
4	2.56×10^{-3}	1.86×10^{-1}	73	1.47×10^{-2}
$k_2 = 7.62 \times 10^{-2}\ M^{-1}s^{-1}$				

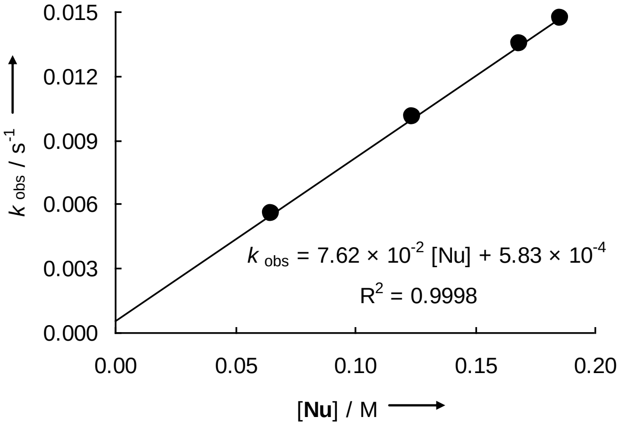

Table 2.S2.6.16. Rate constants for the reaction of 4-cyanobenzyl bromide (**2**-Br) with diethanolamine at 20˚C in DMSO (conventional conductometer).

No	$[E]_0/M^1$	$[Nu]_0/M$	$[Nu]_0/[E]_0$	k_{obs}/s^{-1}
1	9.32×10^{-4}	1.50×10^{-2}	16	2.46×10^{-3}
2	9.13×10^{-4}	1.96×10^{-2}	21	3.16×10^{-3}
3	9.10×10^{-4}	2.45×10^{-2}	27	3.91×10^{-3}
4	9.07×10^{-4}	3.06×10^{-2}	34	4.78×10^{-3}
5	8.81×10^{-4}	3.56×10^{-2}	40	5.56×10^{-3}
$k_2 = 1.50 \times 10^{-1}\ M^{-1}s^{-1}$				

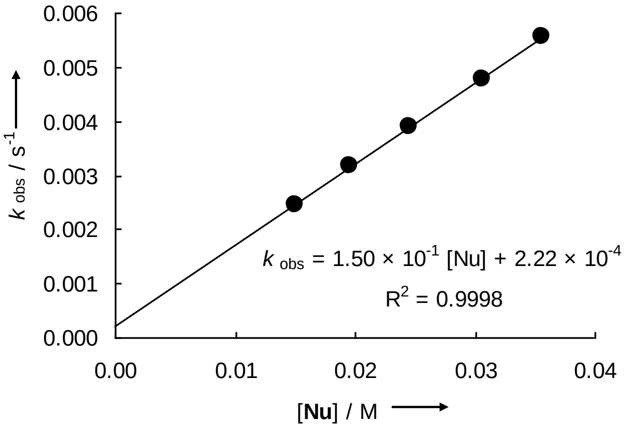

Table 2.S2.6.17 Rate constants for the reaction of 4-cyanobenzyl bromide (**2**-Br) with imidazole at 20˚C in DMSO (conventional conductometer).

No	$[E]_0/M^1$	$[Nu]_0/M$	$[Nu]_0/[E]_0$	k_{obs}/s^{-1}
1	7.19×10^{-4}	1.81×10^{-2}	25	1.12×10^{-4}
2	6.98×10^{-4}	2.63×10^{-2}	38	1.46×10^{-4}
3	6.99×10^{-4}	3.51×10^{-2}	50	1.86×10^{-4}
4	6.70×10^{-4}	4.21×10^{-2}	63	2.13×10^{-4}
$k_2 = 4.25 \times 10^{-3}\ M^{-1}s^{-1}$				

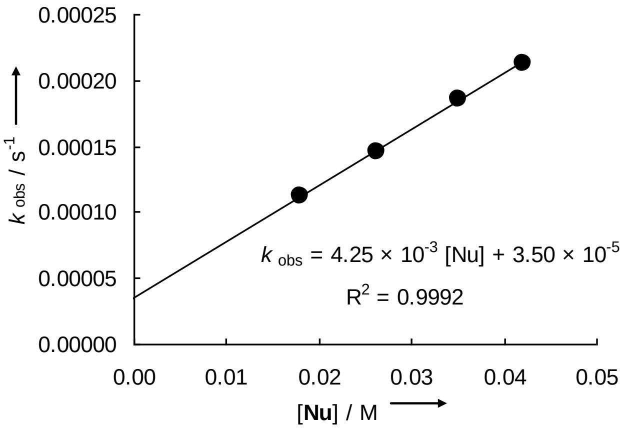

Table 2.S2.6.18. Rate constants for the reaction of 4-cyanobenzyl bromide (**2**-Br) with 2-methylbenzimidazole at 20˚C in DMSO (conventional conductometer).

No	$[E]_0/M^1$	$[Nu]_0/M$	$[Nu]_0/ [E]_0$	k_{obs}/s^{-1}
1	6.89×10^{-4}	2.48×10^{-2}	36	3.67×10^{-5}
2	7.39×10^{-4}	5.84×10^{-2}	79	4.56×10^{-5}
3	4.67×10^{-4}	7.93×10^{-2}	170	5.21×10^{-5}
4	4.31×10^{-4}	1.02×10^{-1}	239	5.78×10^{-5}
5	7.41×10^{-4}	1.62×10^{-1}	219	7.31×10^{-5}
$k_2 = 2.66 \times 10^{-4}$ $M^{-1}s^{-1}$				

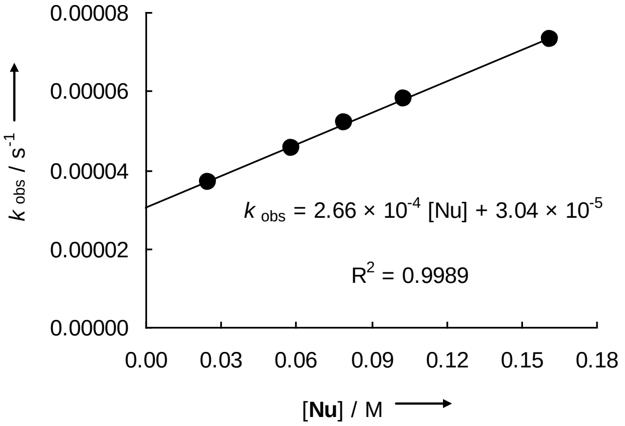

Table 2.S2.6.19. Rate constants for the reaction of 4-cyanobenzyl bromide (**2**-Br) with 2,2,2-trifluoroethylamine at 20˚C in DMSO (conventional conductometer).

No	$[E]_0/M^1$	$[Nu]_0/M$	$[Nu]_0/ [E]_0$	k_{obs}/s^{-1}
1	2.60×10^{-3}	9.88×10^{-2}	38	2.74×10^{-4}
2	2.52×10^{-3}	1.41×10^{-1}	56	3.70×10^{-4}
3	2.55×10^{-3}	3.62×10^{-1}	142	9.03×10^{-4}
$k_2 = 2.40 \times 10^{-3}$ $M^{-1}s^{-1}$				

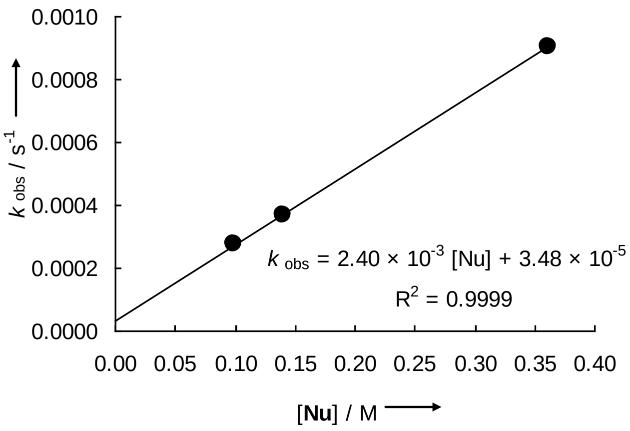

2.S.2.7. Rate constants for the reactions of 4methoxybenzyl bromide (3-Br) in DMSO.

Table 2.S2.7.1. Rate constants for the reaction of 4-methoxybenzyl bromide (**3**-Br) with 1,1-dimethylhydrazine at 20˚C in DMSO (stopped-flow).

No	$[E]_0/M^1$	$[Nu]_0/M$	$[Nu]_0/[E]_0$	k_{obs}/s^{-1}
1	1.31×10^{-3}	4.17×10^{-2}	32	3.97×10^{-1}
2	1.31×10^{-3}	7.09×10^{-2}	54	6.92×10^{-1}
3	1.31×10^{-3}	8.92×10^{-2}	68	8.43×10^{-1}
4	1.31×10^{-3}	1.27×10^{-1}	92	1.12
5	1.31×10^{-3}	1.36×10^{-1}	104	1.28
		$k_2 = 9.19\ M^{-1}s^{-1}$		

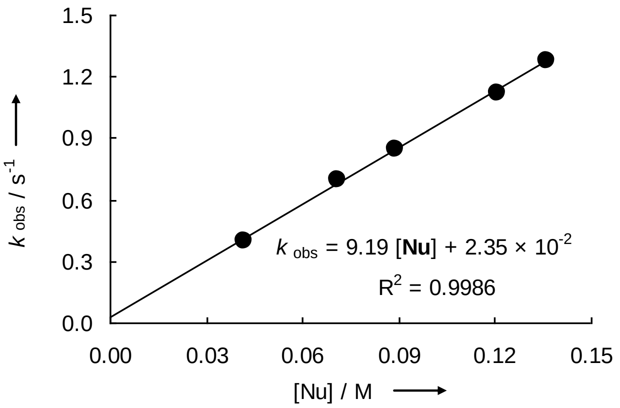

Table 2.S2.7.2. Rate constants for the reaction of 4-methoxybenzyl bromide (**3**-Br) with methylhydrazine at 20˚C in DMSO (stopped-flow).

No	$[E]_0$/M^1	$[Nu]_0$/M	$[Nu]_0$/ $[E]_0$	k_{obs}/s^{-1}
1	2.08×10^{-3}	8.01×10^{-2}	39	3.92×10^{-1}
2	2.08×10^{-3}	1.09×10^{-1}	52	5.27×10^{-1}
3	2.08×10^{-3}	1.83×10^{-1}	88	9.11×10^{-1}
4	2.08×10^{-3}	2.30×10^{-1}	110	1.13
5	2.08×10^{-3}	3.43×10^{-1}	165	1.71
$k_2 = 5.02\ M^{-1}s^{-1}$				

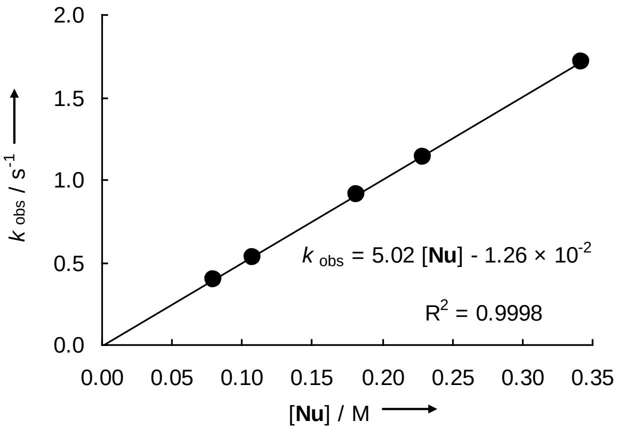

Table 2.S2.7.3. Rate constants for the reaction of 4-methoxybenzyl bromide (**3**-Br) with piperidine at 20˚C in DMSO (stopped-flow).

No	$[E]_0$/M^1	$[Nu]_0$/M	$[Nu]_0$/ $[E]_0$	k_{obs}/s^{-1}
1	4.49×10^{-4}	9.18×10^{-2}	204	5.92×10^{-1}
2	4.49×10^{-4}	1.32×10^{-1}	294	8.61×10^{-1}
3	4.49×10^{-4}	1.81×10^{-1}	403	1.14
4	4.49×10^{-4}	2.33×10^{-1}	519	1.47
5	4.49×10^{-4}	2.62×10^{-1}	584	1.64
$k_2 = 6.13\ M^{-1}s^{-1}$				

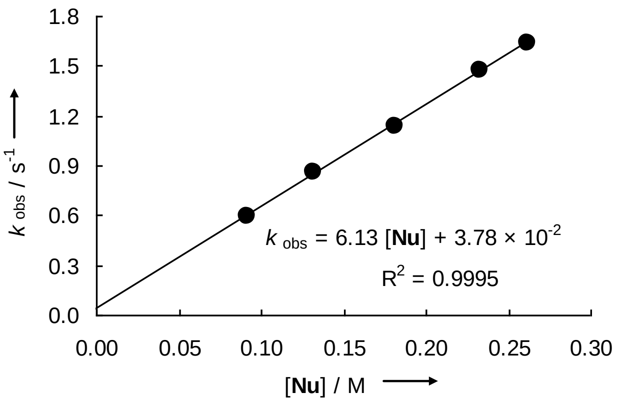

Table 2.S2.7.4. Rate constants for the reaction of 4-methoxybenzyl bromide (**3**-Br) with morpholine at 20˚C in DMSO (stopped-flow).

No	$[E]_0$/M^1	$[Nu]_0$/M	$[Nu]_0$/ $[E]_0$	k_{obs}/s^{-1}
1	8.97×10^{-4}	1.13×10^{-1}	126	2.41×10^{-1}
2	8.97×10^{-4}	1.53×10^{-1}	171	3.34×10^{-1}
3	8.97×10^{-4}	2.10×10^{-1}	234	4.47×10^{-1}
4	8.97×10^{-4}	2.57×10^{-1}	287	5.40×10^{-1}
5	8.97×10^{-4}	3.19×10^{-1}	356	6.64×10^{-1}
$k_2 = 2.04$ M^{-1}s^{-1}				

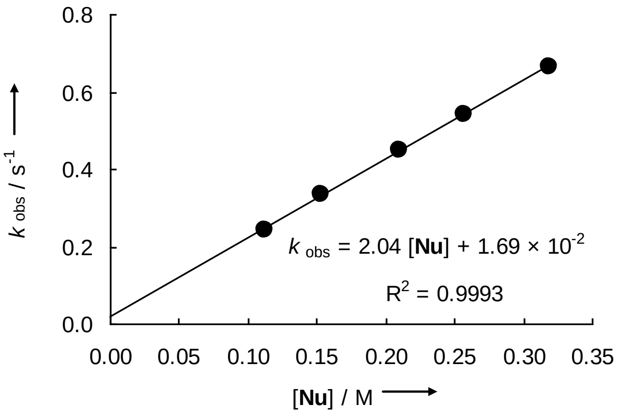

Table 2.S2.7.5. Rate constants for the reaction of 4-methoxybenzyl bromide (**3**-Br) with 2,2,2-trifluoroethylamine at 20˚C in DMSO (conventional conductometer).

No	$[E]_0$/M^1	$[Nu]_0$/M	$[Nu]_0$/ $[E]_0$	k_{obs}/s^{-1}
1	2.51×10^{-3}	1.22×10^{-1}	49	1.94×10^{-3}
2	2.54×10^{-3}	1.94×10^{-1}	76	2.61×10^{-3}
3	2.49×10^{-3}	2.56×10^{-1}	103	3.22×10^{-3}
4	2.50×10^{-3}	3.39×10^{-1}	136	4.01×10^{-3}
$k_2 = 9.56 \times 10^{-3}$ M^{-1}s^{-1}				

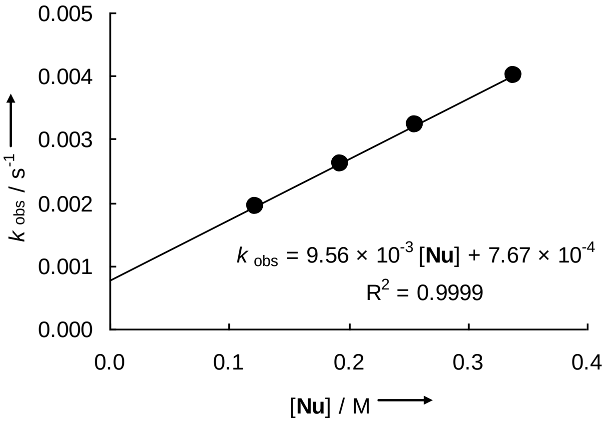

2.S.2.8. Rate constants for the reactions of phenacyl bromide (4-Br) in DMSO.

Table 2.S2.8.1. Rate constants for the reaction of phenacyl bromide (**4**-Br) with DABCO at 20˚C in DMSO (stopped-flow).

No	$[E]_0/M^1$	$[Nu]_0/M$	$[Nu]_0/[E]_0$	k_{obs}/s^{-1}
1	1.40×10^{-3}	1.70×10^{-2}	12	9.32×10^{-1}
2	1.40×10^{-3}	2.64×10^{-2}	19	1.44
3	1.40×10^{-3}	3.59×10^{-2}	26	1.97
4	1.40×10^{-3}	4.53×10^{-2}	32	2.53
5	1.40×10^{-3}	5.48×10^{-2}	39	3.12
		$k_2 = 5.78 \times 10^1\ M^{-1}s^{-1}$		

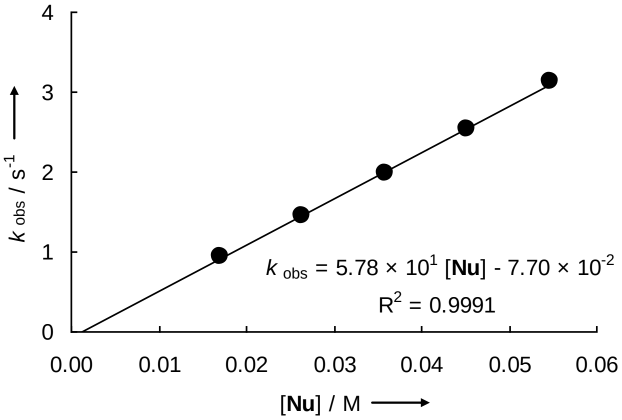

Table 2.S2.8.2. Rate constants for the reaction of phenacyl bromide (**4**-Br) with TBD (1,5,7-triazabicyclo[4.4.0]dec-5-ene) at 20˚C in DMSO (stopped-flow).

No	$[E]_0$/M^1	$[Nu]_0$/M	$[Nu]_0$/ $[E]_0$	k_{obs}/s^{-1}
1	1.52×10^{-3}	2.36×10^{-2}	16	4.23
2	1.52×10^{-4}	3.67×10^{-2}	24	6.35
3	1.52×10^{-5}	4.98×10^{-2}	33	8.35
4	1.52×10^{-6}	6.29×10^{-2}	41	1.05×10^{1}
$k_2 = 1.59 \times 10^2$ M^{-1}s^{-1}				

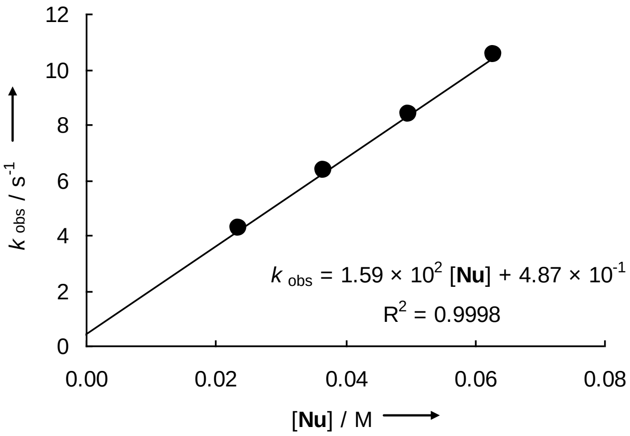

Table 2.S2.8.3. Rate constants for the reaction of phenacyl bromide (**4**-Br) with piperidine at 20˚C in DMSO (stopped-flow).

No	$[E]_0$/M^1	$[Nu]_0$/M	$[Nu]_0$/ $[E]_0$	k_{obs}/s^{-1}
1	2.38×10^{-3}	7.47×10^{-2}	31	2.18
2	2.38×10^{-4}	1.32×10^{-1}	55	3.98
3	2.38×10^{-5}	1.76×10^{-1}	74	5.33
4	2.38×10^{-6}	2.34×10^{-1}	98	7.06
5	2.38×10^{-7}	2.81×10^{-1}	118	8.54
$k_2 = 3.07 \times 10^1$ M^{-1}s^{-1}				

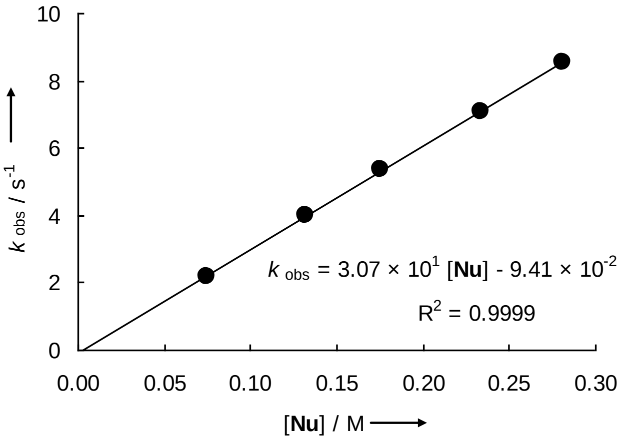

Table 2.S2.8.4. Rate constants for the reaction of phenacyl bromide (**4**-Br) with morpholine at 20˚C in DMSO (stopped-flow).

No	$[E]_0/M^1$	$[Nu]_0/M$	$[Nu]_0/[E]_0$	k_{obs}/s^{-1}
1	2.06×10^{-3}	1.15×10^{-1}	56	6.61×10^{-1}
2	2.06×10^{-6}	1.52×10^{-1}	74	8.86×10^{-1}
3	2.06×10^{-4}	2.02×10^{-1}	98	1.12
4	2.06×10^{-7}	2.63×10^{-1}	128	1.47
5	2.06×10^{-5}	3.12×10^{-1}	151	1.74
$k_2 = 5.43\,M^{-1}s^{-1}$				

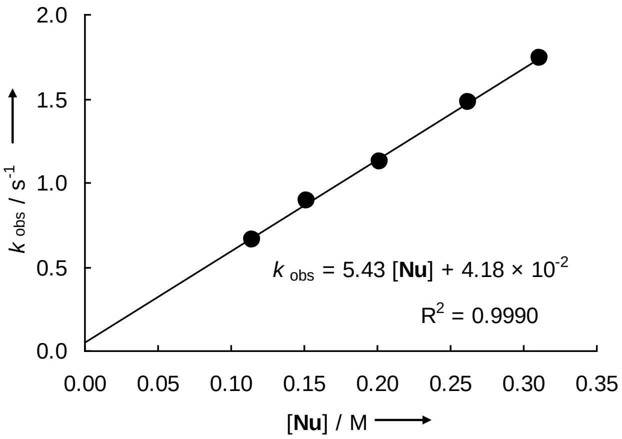

Table 2.S2.8.5. Rate constants for the reaction of phenacyl bromide (**4**-Br) with 2-aminoethanol at 20˚C in DMSO (stopped-flow).

No	$[E]_0/M^1$	$[Nu]_0/M$	$[Nu]_0/[E]_0$	k_{obs}/s^{-1}
1	2.28×10^{-3}	1.52×10^{-1}	67	4.48×10^{-1}
2	2.28×10^{-4}	2.23×10^{-1}	98	6.42×10^{-1}
3	2.28×10^{-5}	3.08×10^{-1}	135	8.90×10^{-1}
4	2.28×10^{-6}	3.83×10^{-1}	168	1.1
5	2.28×10^{-7}	4.75×10^{-1}	208	1.32
$k_2 = 2.73\,M^{-1}s^{-1}$				

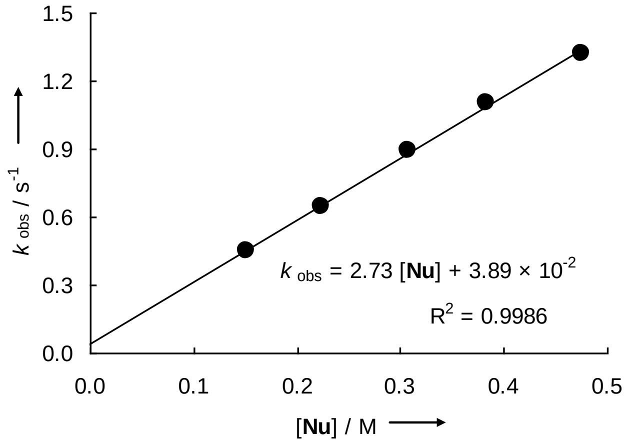

Table 2.S2.8.6. Rate constants for the reaction of phenacyl bromide (**4**-Br) with 1-aminopropan-2-ol at 20˚C in DMSO (stopped-flow).

No	$[E]_0$/M^1	$[Nu]_0$/M	$[Nu]_0$/ $[E]_0$	k_{obs}/s^{-1}
1	2.28×10^{-3}	1.44×10^{-1}	63	3.75×10^{-1}
2	2.28×10^{-3}	1.88×10^{-1}	82	4.89×10^{-1}
3	2.28×10^{-3}	2.65×10^{-1}	116	6.82×10^{-1}
4	2.28×10^{-3}	3.21×10^{-1}	141	8.06×10^{-1}
5	2.28×10^{-3}	3.78×10^{-1}	166	9.61×10^{-1}
k_2 = 2.48 M^{-1}s^{-1}				

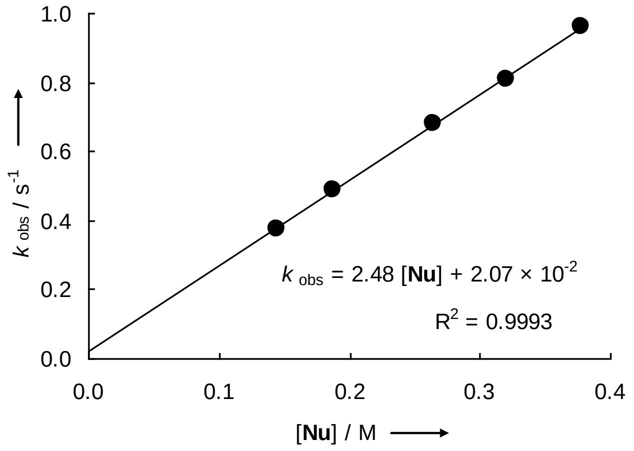

Table 2.S2.8.7. Rate constants for the reaction of phenacyl bromide (**4**-Br) with *n*-propylamine at 20˚C in DMSO (stopped-flow).

No	$[E]_0/M^1$	$[Nu]_0/M$	$[Nu]_0/ [E]_0$	k_{obs}/s^{-1}
1	2.56×10^{-3}	1.49×10^{-1}	58	6.18×10^{-1}
2	2.56×10^{-4}	2.11×10^{-1}	82	8.78×10^{-1}
3	2.56×10^{-5}	2.65×10^{-1}	104	1.1
4	2.56×10^{-6}	3.14×10^{-1}	123	1.3
$k_2 = 4.13\ M^{-1}s^{-1}$				

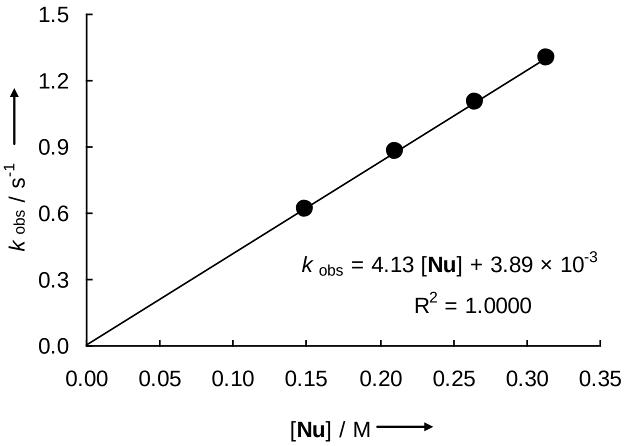

Table 2.S2.8.8. Rate constants for the reaction of phenacyl bromide (**4**-Br) with benzylamine at 20˚C in DMSO (stopped-flow).

No	$[E]_0/M^1$	$[Nu]_0/M$	$[Nu]_0/ [E]_0$	k_{obs}/s^{-1}
1	2.92×10^{-3}	1.49×10^{-1}	51	1.69×10^{-1}
2	2.92×10^{-4}	3.04×10^{-1}	104	3.39×10^{-1}
3	2.92×10^{-5}	4.56×10^{-1}	156	5.06×10^{-1}
4	2.92×10^{-6}	6.01×10^{-1}	206	6.63×10^{-1}
5	2.92×10^{-7}	7.13×10^{-1}	244	7.81×10^{-1}
$k_2 = 1.09\ M^{-1}s^{-1}$				

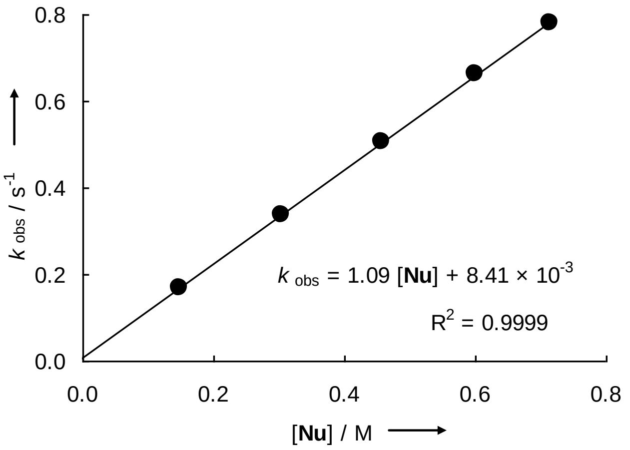

Table 2.S2.8.9. Rate constants for the reaction of phenacyl bromide (**4**-Br) with 4-DMAP at 20˚C in DMSO (stopped-flow).

No	$[E]_0/M^1$	$[Nu]_0/M$	$[Nu]_0/[E]_0$	k_{obs}/s^{-1}
1	2.65×10^{-3}	6.40×10^{-2}	24	6.46×10^{-2}
2	2.65×10^{-4}	1.19×10^{-1}	45	1.15×10^{-1}
3	2.65×10^{-5}	1.73×10^{-1}	65	1.66×10^{-1}
4	2.65×10^{-6}	2.06×10^{-1}	78	1.96×10^{-1}
		$k_2 = 9.28 \times 10^{-1}\ M^{-1}s^{-1}$		

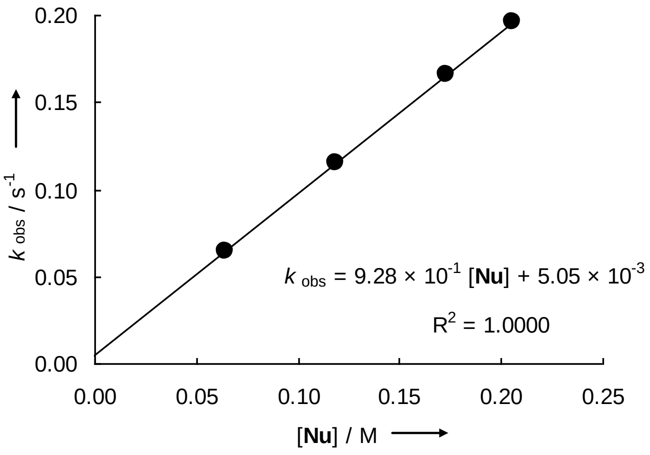

Table 2.S2.8.10. Rate constants for the reaction of phenacyl bromide (**4**-Br) with 2-aminobutan-1-ol at 20˚C in DMSO (conventional conductometer).

No	$[E]_0/M^1$	$[Nu]_0/M$	$[Nu]_0/ [E]_0$	k_{obs}/s^{-1}
1	7.83×10^{-4}	7.65×10^{-3}	10	4.29×10^{-3}
2	7.88×10^{-4}	1.03×10^{-2}	13	5.58×10^{-3}
3	7.90×10^{-4}	1.29×10^{-2}	16	6.86×10^{-3}
4	7.64×10^{-4}	1.49×10^{-2}	20	7.95×10^{-3}
5	7.46×10^{-4}	1.95×10^{-2}	26	1.03×10^{-2}
$k_2 = 5.09 \times 10^{-1}\ M^{-1}s^{-1}$				

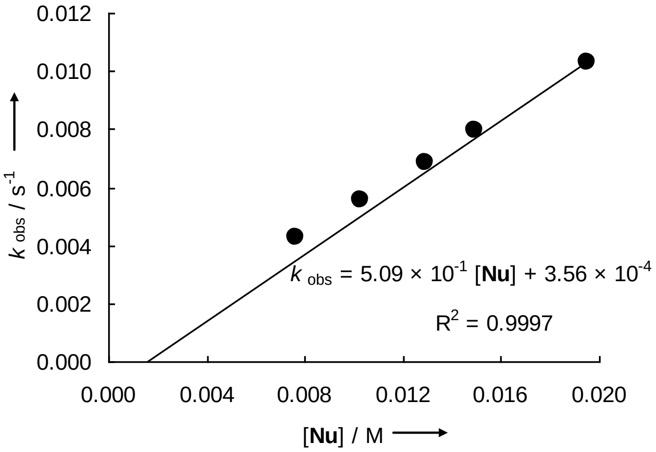

Table 2.S2.8.11. Rate constants for the reaction of phenacyl bromide (**4**-Br) with diethanolamine at 20˚C in DMSO (conventional conductometer).

No	$[E]_0/M^1$	$[Nu]_0/M$	$[Nu]_0/ [E]_0$	k_{obs}/s^{-1}
1	5.52×10^{-4}	9.59×10^{-3}	17	3.98×10^{-3}
2	5.44×10^{-4}	1.89×10^{-2}	35	7.49×10^{-3}
3	5.38×10^{-4}	2.80×10^{-2}	52	1.11×10^{-2}
4	5.18×10^{-4}	3.60×10^{-2}	69	1.38×10^{-2}
$k_2 = 3.75 \times 10^{-1}\ M^{-1}s^{-1}$				

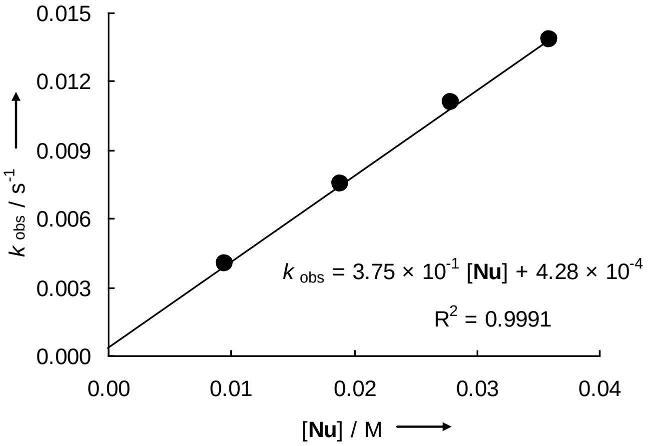

Table 2.S2.8.12. Rate constants for the reaction of phenacyl bromide (**4**-Br) with imidazole at 20˚C in DMSO (conventional conductometer).

No	$[E]_0/M^1$	$[Nu]_0/M$	$[Nu]_0/ [E]_0$	k_{obs}/s^{-1}
1	7.71×10^{-4}	2.01×10^{-2}	26	1.40×10^{-3}
2	8.43×10^{-4}	2.51×10^{-2}	30	1.73×10^{-3}
3	7.58×10^{-4}	2.96×10^{-2}	39	2.05×10^{-3}
4	8.26×10^{-4}	3.69×10^{-2}	45	2.50×10^{-3}
5	7.63×10^{-4}	3.98×10^{-2}	52	2.71×10^{-3}
$k_2 = 6.61 \times 10^{-2}\ M^{-1}s^{-1}$				

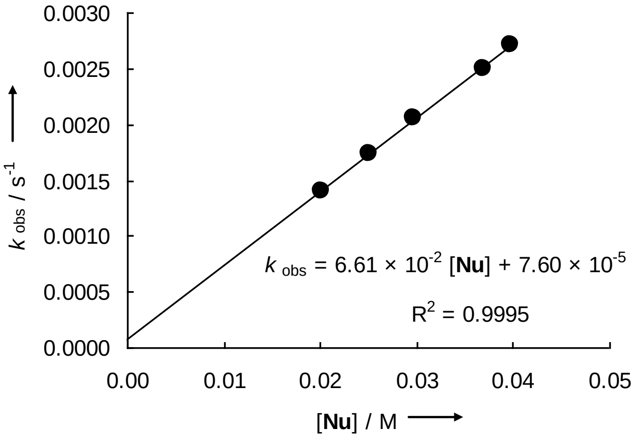

Table 2.S2.8.13. Rate constants for the reaction of phenacyl bromide (**4**-Br) with 2-methylbenzimidazole at 20˚C in DMSO (conventional conductometer).

No	$[E]_0/M^1$	$[Nu]_0/M$	$[Nu]_0/[E]_0$	k_{obs}/s^{-1}
1	8.43×10^{-4}	1.66×10^{-2}	20	8.82×10^{-5}
2	8.96×10^{-4}	2.48×10^{-2}	28	1.10×10^{-4}
3	8.78×10^{-4}	3.24×10^{-2}	37	1.34×10^{-4}
4	8.12×10^{-4}	4.49×10^{-2}	55	1.67×10^{-4}
5	8.01×10^{-4}	5.54×10^{-2}	69	1.98×10^{-4}
		$k_2 = 2.83 \times 10^{-3}\ M^{-1}s^{-1}$		

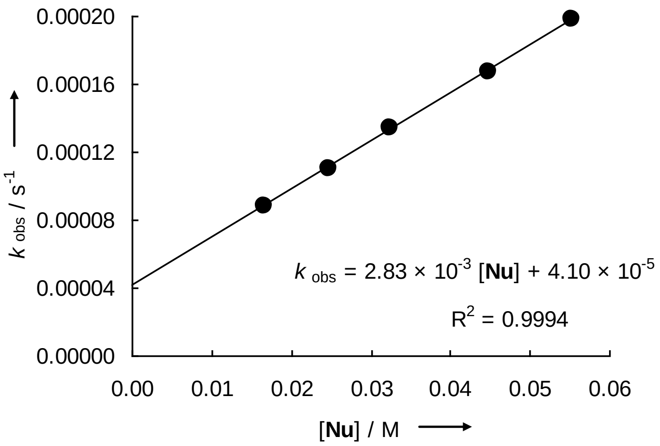

Table 2.S2.8.14. Rate constants for the reaction of phenacyl bromide (**4**-Br) with 2,2,2-trifluoroethylamine at 20˚C in DMSO (conventional conductometer).

No	$[E]_0/M^1$	$[Nu]_0/M$	$[Nu]_0/[E]_0$	k_{obs}/s^{-1}
1	8.24×10^{-4}	5.05×10^{-2}	61	3.73×10^{-4}
2	8.06×10^{-4}	1.14×10^{-1}	141	8.34×10^{-4}
3	7.99×10^{-4}	1.70×10^{-1}	213	1.26×10^{-3}
4	7.74×10^{-4}	2.20×10^{-1}	284	1.68×10^{-3}
5	7.71×10^{-4}	2.74×10^{-1}	355	2.14×10^{-3}
		$k_2 = 7.91 \times 10^{-3}\ M^{-1}s^{-1}$		

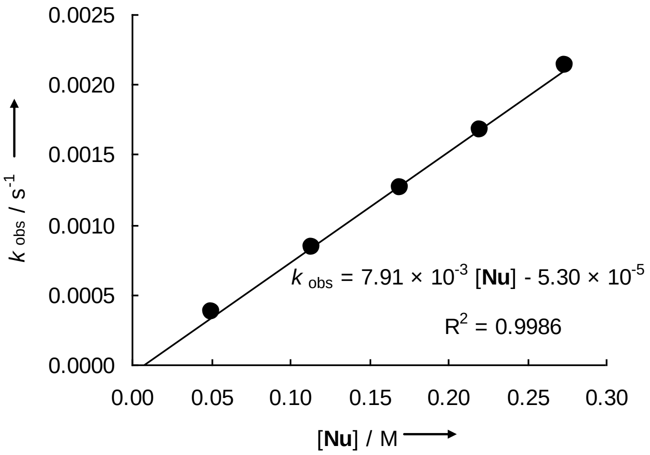

2.S.2.9. Rate constants for the reactions of methyl iodide (5-I) in DMSO.

Table 2.S2.9.1. Rate constants for the reaction of methyl iodide (**5**-I) with DABCO at 20˚C in DMSO (stopped-flow).

No	$[E]_0/M^1$	$[Nu]_0/M$	$[Nu]_0/ [E]_0$	k_{obs}/s^{-1}
1	1.08×10^{-3}	1.70×10^{-2}	16	1.56×10^{-1}
2	1.08×10^{-3}	2.64×10^{-2}	24	2.33×10^{-1}
3	1.08×10^{-3}	3.59×10^{-2}	33	3.18×10^{-1}
4	1.08×10^{-3}	4.53×10^{-2}	42	4.03×10^{-1}
5	1.08×10^{-3}	5.48×10^{-2}	51	4.86×10^{-1}
$k_2 = 8.79\ M^{-1}s^{-1}$				

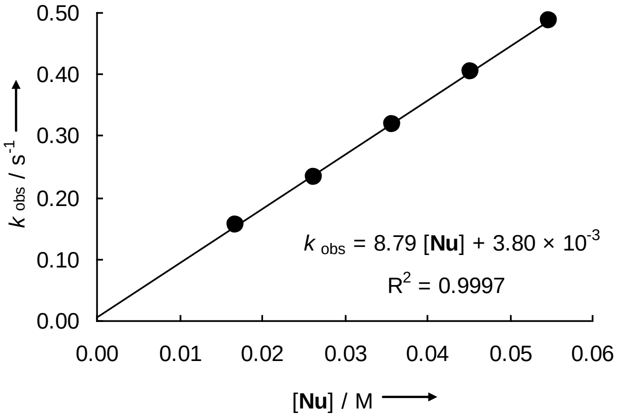

Table 2.S2.9.2. Rate constants for the reaction of methyl iodide (**5**-I) with TBD (1,5,7-triazabicyclo[4.4.0]dec-5-ene) at 20˚C in DMSO (stopped-flow).

No	$[E]_0/M^1$	$[Nu]_0/M$	$[Nu]_0/[E]_0$	k_{obs}/s^{-1}
1	1.10×10^{-3}	2.36×10^{-2}	21	8.10×10^{-2}
2	1.10×10^{-3}	3.67×10^{-2}	33	1.24×10^{-1}
3	1.10×10^{-3}	4.98×10^{-2}	45	1.64×10^{-1}
4	1.10×10^{-3}	6.29×10^{-2}	57	2.02×10^{-1}
$k_2 = 3.07\ M^{-1}s^{-1}$				

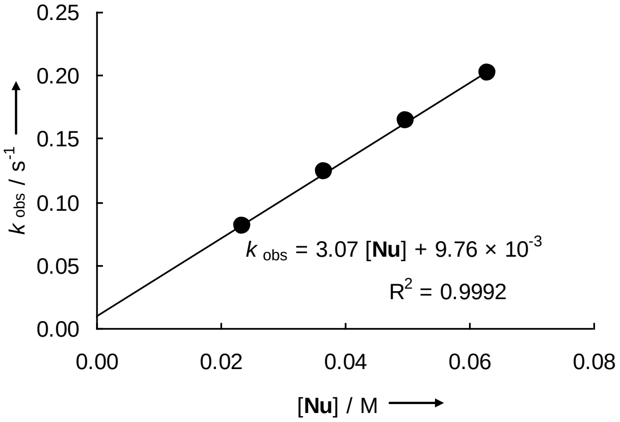

Table 2.S2.9.3. Rate constants for the reaction of methyl iodide (**5**-I) with DBU (1,8-diazabicyclo[5.4.0]undec-7-ene) at 20˚C in DMSO (conventional conductometer).

No	$[E]_0/M^1$	$[Nu]_0/M$	$[Nu]_0/[E]_0$	k_{obs}/s^{-1}
1	1.22×10^{-4}	9.17×10^{-3}	75	1.52×10^{-3}
2	1.21×10^{-4}	1.81×10^{-2}	150	2.90×10^{-3}
3	1.18×10^{-4}	2.65×10^{-2}	225	4.35×10^{-3}
4	1.16×10^{-4}	3.48×10^{-2}	300	5.67×10^{-3}
5	1.14×10^{-4}	4.28×10^{-2}	375	6.97×10^{-3}
$k_2 = 1.63 \times 10^{-1}\ M^{-1}s^{-1}$				

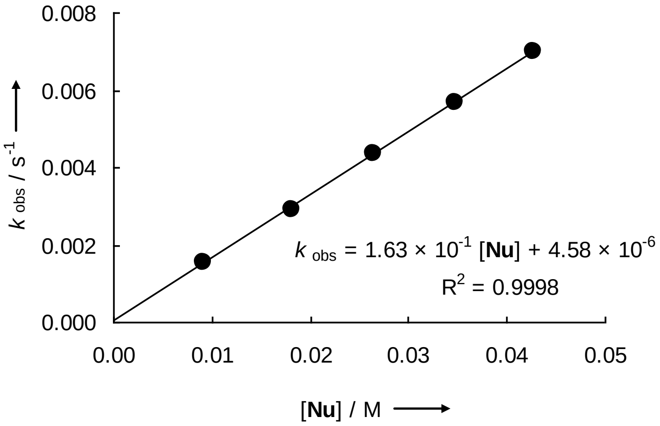

Table 2.S2.9.4. Rate constants for the reaction of methyl iodide (**5**-I) with morpholine at 20˚C in DMSO (conventional conductometer).

No	$[E]_0$/M^1	$[Nu]_0$/M	$[Nu]_0$/ $[E]_0$	k_{obs}/s^{-1}
1	1.53×10^{-3}	1.58×10^{-2}	10	8.26×10^{-3}
2	1.55×10^{-3}	2.41×10^{-2}	16	1.25×10^{-2}
3	1.55×10^{-3}	3.21×10^{-2}	21	1.74×10^{-2}
$k_2 = 5.63 \times 10^{-1}$ M^{-1}s^{-1}				

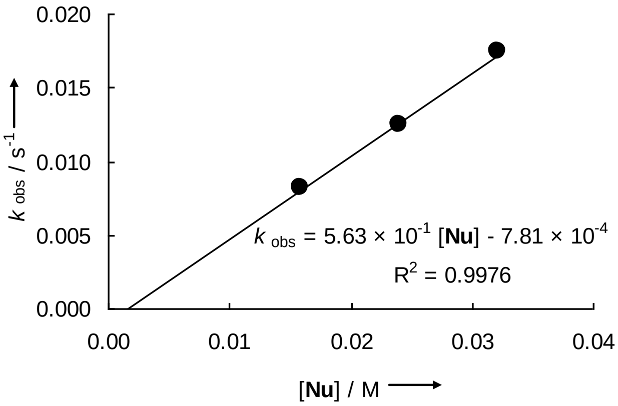

Table 2.S2.9.5. Rate constants for the reaction of methyl iodide (**5**-I) with 2-aminoethanol at 20˚C in DMSO (conventional conductometer).

No	$[E]_0$/M^1	$[Nu]_0$/M	$[Nu]_0$/ $[E]_0$	k_{obs}/s^{-1}
1	3.20×10^{-3}	7.64×10^{-1}	238	1.63×10^{-1}
2	3.20×10^{-3}	9.14×10^{-1}	285	1.95×10^{-1}
3	3.20×10^{-3}	1.06	330	2.19×10^{-1}
4	3.20×10^{-3}	1.21	378	2.47×10^{-1}
5	3.20×10^{-3}	1.36	425	2.73×10^{-1}
$k_2 = 1.83 \times 10^{-1}$ M^{-1}s^{-1}				

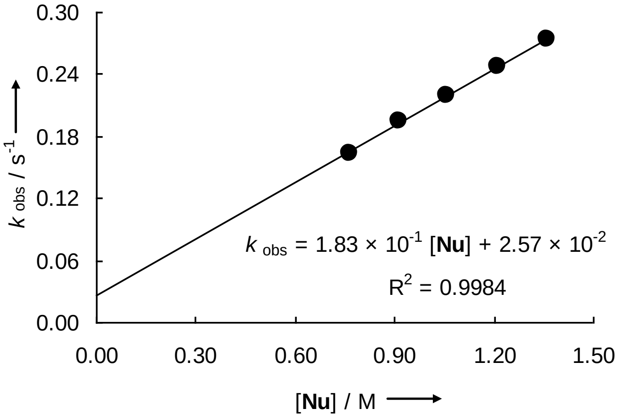

Table 2.S2.9.6. Rate constants for the reaction of methyl iodide (**5**-I) with 1-aminopropan-2-ol at 20˚C in DMSO (conventional conductometer).

No	$[E]_0/M^1$	$[Nu]_0/M$	$[Nu]_0/ [E]_0$	k_{obs}/s^{-1}
1	2.10×10^{-3}	2.18×10^{-2}	10	5.39×10^{-3}
2	2.03×10^{-3}	3.58×10^{-2}	18	8.64×10^{-3}
3	1.99×10^{-3}	5.28×10^{-2}	26	1.26×10^{-2}
4	2.00×10^{-3}	7.05×10^{-2}	35	1.70×10^{-2}
5	1.95×10^{-3}	8.61×10^{-2}	44	2.11×10^{-2}
$k_2 = 2.44 \times 10^{-1}\ M^{-1}s^{-1}$				

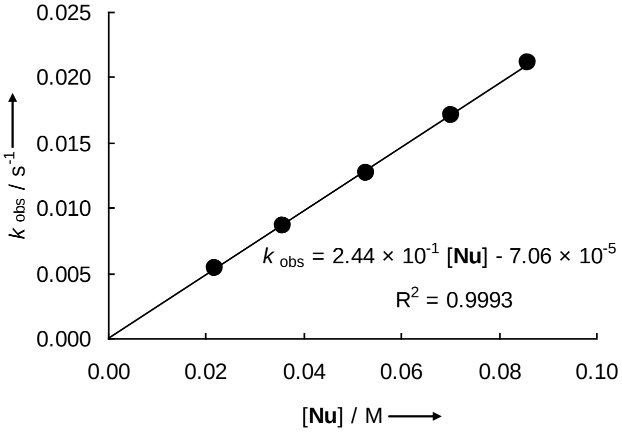

Table 2.S2.9.7. Rate constants for the reaction of methyl iodide (**5**-I) with *n*-propylamine at 20˚C in DMSO (conventional conductometer).

No	$[E]_0/M^1$	$[Nu]_0/M$	$[Nu]_0/ [E]_0$	k_{obs}/s^{-1}
1	1.54×10^{-3}	2.61×10^{-2}	17	9.08×10^{-3}
2	1.58×10^{-3}	3.21×10^{-2}	20	1.10×10^{-2}
3	1.50×10^{-3}	4.24×10^{-2}	28	1.40×10^{-2}
4	1.56×10^{-3}	5.30×10^{-2}	34	1.86×10^{-2}
5	1.50×10^{-3}	6.79×10^{-2}	45	2.26×10^{-2}
$k_2 = 3.31 \times 10^{-1}\ M^{-1}s^{-1}$				

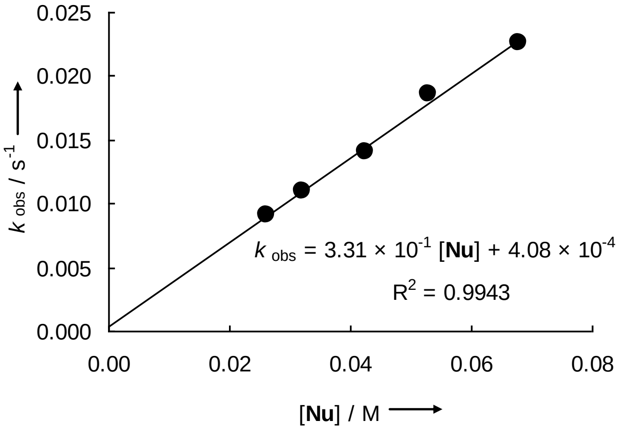

Table 2.S2.9.8. Rate constants for the reaction of methyl iodide (**5**-I) with benzylamine at 20˚C in DMSO (conventional conductometer).

No	$[E]_0$/M^1	$[Nu]_0$/M	$[Nu]_0$/ $[E]_0$	k_{obs}/s^{-1}
1	1.70×10^{-3}	2.61×10^{-2}	15	4.78×10^{-3}
2	1.68×10^{-3}	3.18×10^{-2}	19	6.27×10^{-3}
3	1.63×10^{-3}	3.87×10^{-2}	24	7.15×10^{-3}
4	1.61×10^{-3}	4.34×10^{-2}	27	8.33×10^{-3}
5	1.65×10^{-3}	5.32×10^{-2}	32	9.88×10^{-3}
6	1.61×10^{-3}	6.02×10^{-2}	37	1.12×10^{-2}
$k_2 = 1.83 \times 10^{-1}$ M^{-1}s^{-1}				

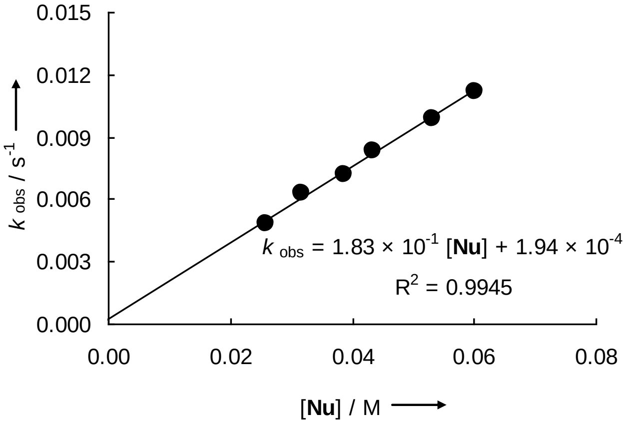

Table 2.S2.9.9. Rate constants for the reaction of methyl iodide (**5**-I) with 4-DMAP at 20˚C in DMSO (conventional conductometer).

No	$[E]_0$/M^1	$[Nu]_0$/M	$[Nu]_0$/ $[E]_0$	k_{obs}/s^{-1}
1	1.27×10^{-3}	1.62×10^{-2}	13	4.80×10^{-4}
2	1.80×10^{-3}	2.99×10^{-2}	17	9.17×10^{-4}
3	1.80×10^{-3}	3.38×10^{-2}	19	1.02×10^{-3}
4	1.78×10^{-3}	4.99×10^{-2}	28	1.52×10^{-3}
$k_2 = 3.08 \times 10^{-2}$ M^{-1}s^{-1}				

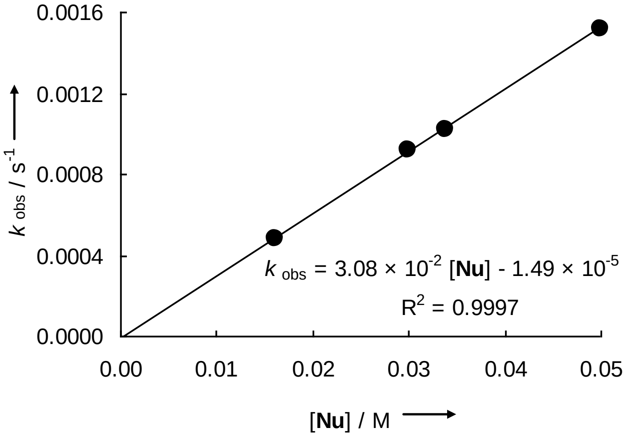

Table 2.S2.9.10. Rate constants for the reaction of methyl iodide (**5**-I) with 2-aminobutan-1-ol at 20˚C in DMSO (conventional conductometer).

No	$[E]_0/M^1$	$[Nu]_0/M$	$[Nu]_0/[E]_0$	k_{obs}/s^{-1}
1	1.76×10^{-3}	3.04×10^{-2}	17	3.88×10^{-3}
2	1.77×10^{-3}	4.35×10^{-2}	25	5.54×10^{-3}
3	1.84×10^{-3}	6.03×10^{-2}	33	7.64×10^{-3}
4	1.81×10^{-3}	7.20×10^{-2}	40	9.22×10^{-3}
5	1.77×10^{-3}	8.69×10^{-2}	49	1.14×10^{-2}
$k_2 = 1.32 \times 10^{-1}\ M^{-1}s^{-1}$				

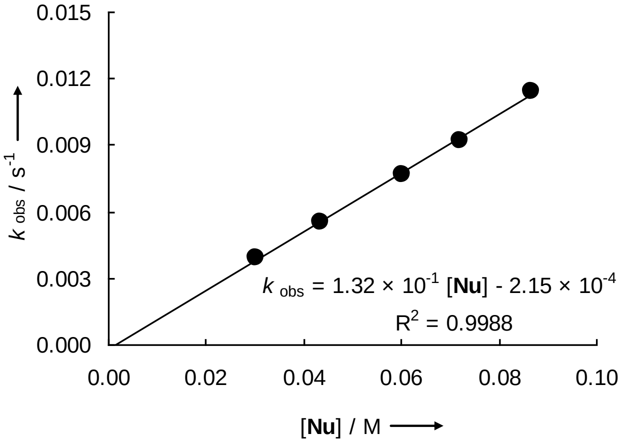

Table 2.S2.9.11. Rate constants for the reaction of methyl iodide (**5**-I) with diethanolamine at 20˚C in DMSO (conventional conductometer).

No	$[E]_0/M^1$	$[Nu]_0/M$	$[Nu]_0/[E]_0$	k_{obs}/s^{-1}
1	1.79×10^{-3}	2.01×10^{-2}	11	5.70×10^{-3}
2	1.63×10^{-3}	3.42×10^{-2}	19	9.48×10^{-3}
3	1.71×10^{-3}	4.81×10^{-2}	30	1.33×10^{-2}
4	1.68×10^{-3}	6.53×10^{-2}	38	1.82×10^{-2}
5	1.75×10^{-3}	8.03×10^{-2}	48	2.22×10^{-2}
$k_2 = 2.75 \times 10^{-1}\ M^{-1}s^{-1}$				

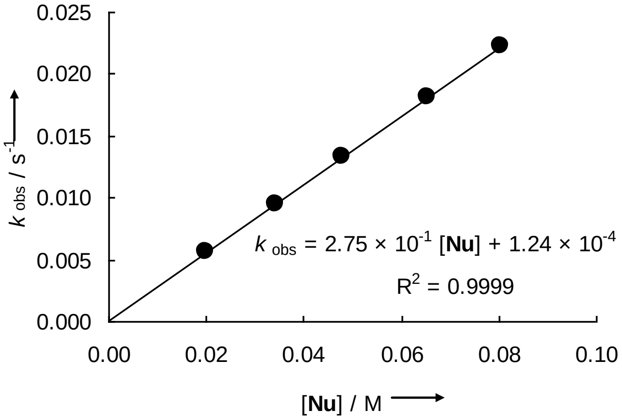

Table 2.S2.9.12. Rate constants for the reaction of methyl iodide (**5**-I) with imidazole at 20˚C in DMSO (conventional conductometer).

No	$[E]_0/M^1$	$[Nu]_0/M$	$[Nu]_0/[E]_0$	k_{obs}/s^{-1}
1	2.02×10^{-3}	6.94×10^{-2}	34	2.73×10^{-4}
2	2.14×10^{-3}	1.49×10^{-1}	70	5.36×10^{-4}
3	2.08×10^{-3}	2.36×10^{-1}	113	8.23×10^{-4}
4	2.37×10^{-3}	3.66×10^{-1}	154	1.29×10^{-3}
$k_2 = 3.43 \times 10^{-3}\ M^{-1}s^{-1}$				

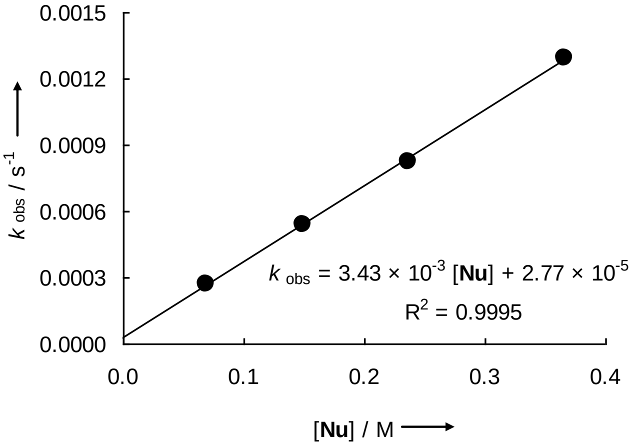

Table 2.S2.9.13. Rate constants for the reaction of methyl iodide (**5**-I) with 2-methylbenzimidazole at 20˚C in DMSO (conventional conductometer).

No	$[E]_0/M^1$	$[Nu]_0/M$	$[Nu]_0/[E]_0$	k_{obs}/s^{-1}
1	2.00×10^{-3}	5.57×10^{-2}	28	6.82×10^{-5}
2	2.08×10^{-3}	1.43×10^{-1}	69	1.40×10^{-4}
3	2.17×10^{-3}	2.46×10^{-1}	113	2.23×10^{-4}
4	2.01×10^{-3}	3.29×10^{-1}	164	2.91×10^{-4}
		$k_2 = 8.14 \times 10^{-4}\ M^{-1}s^{-1}$		

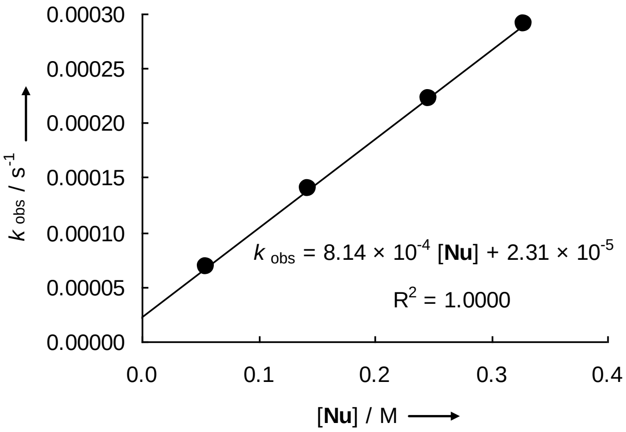

2.S.2.10. Rate constants for the reactions of methyl tosylate (5-OTs) in DMSO.

Table 2.S2.10.1. Rate constants for the reaction of methyl tosylate (**5**-OTs) with piperidine at 20˚C in DMSO (conventional conductometer).

No	$[E]_0/M^1$	$[Nu]_0/M$	$[Nu]_0/[E]_0$	k_{obs}/s^{-1}
1	1.48×10^{-3}	1.43×10^{-2}	10	2.61×10^{-3}
2	1.60×10^{-3}	2.79×10^{-2}	17	5.03×10^{-3}
3	1.59×10^{-3}	4.14×10^{-2}	26	7.60×10^{-3}
4	1.53×10^{-3}	5.47×10^{-2}	36	9.56×10^{-3}
5	1.53×10^{-3}	6.86×10^{-2}	45	1.25×10^{-2}
		$k_2 = 1.80 \times 10^{-1}\ M^{-1}s^{-1}$		

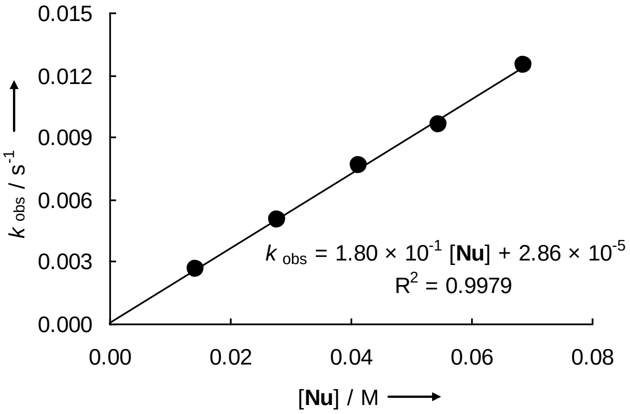

Table 2.S2.10.2. Rate constants for the reaction of methyl tosylate (**5**-OTs) with morpholine at 20˚C in DMSO (conventional conductometer).

No	$[E]_0/M^1$	$[Nu]_0/M$	$[Nu]_0/ [E]_0$	k_{obs}/s^{-1}
1	1.54×10^{-3}	1.69×10^{-2}	11	7.22×10^{-4}
2	1.55×10^{-3}	3.40×10^{-2}	22	1.38×10^{-3}
3	1.57×10^{-3}	4.84×10^{-2}	31	2.05×10^{-3}
4	1.48×10^{-3}	6.06×10^{-2}	41	2.50×10^{-3}
5	1.47×10^{-3}	7.93×10^{-2}	54	3.25×10^{-3}
$k_2 = 4.08 \times 10^{-2}$ $M^{-1}s^{-1}$				

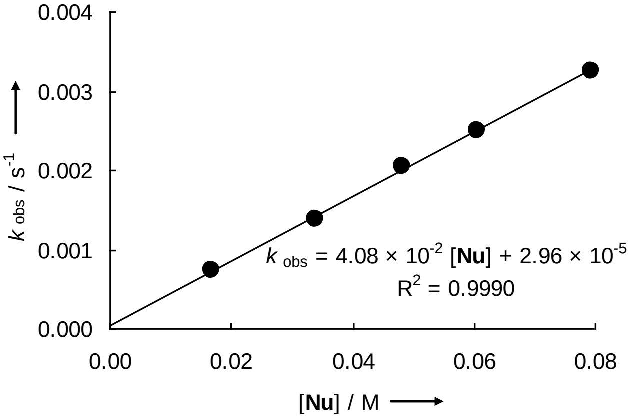

Table 2.S2.10.3. Rate constants for the reaction of methyl tosylate (**5**-OTs) with 2-aminoethanol at 20˚C in DMSO (conventional conductometer).

No	$[E]_0/M^1$	$[Nu]_0/M$	$[Nu]_0/[E]_0$	k_{obs}/s^{-1}
1	1.53×10^{-3}	2.19×10^{-2}	14	7.73×10^{-4}
2	1.42×10^{-3}	3.12×10^{-2}	22	1.06×10^{-3}
3	1.50×10^{-3}	4.48×10^{-2}	30	1.40×10^{-3}
4	1.53×10^{-3}	5.61×10^{-2}	37	1.70×10^{-3}
5	1.54×10^{-3}	6.77×10^{-2}	44	2.06×10^{-3}
$k_2 = 2.76 \times 10^{-2}\ M^{-1}s^{-1}$				

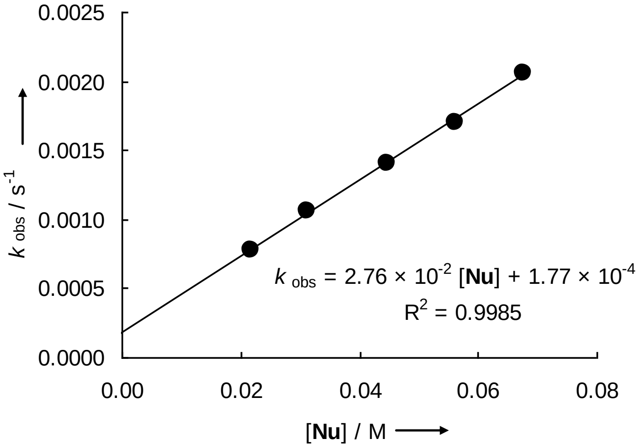

Table 2.S2.10.4. Rate constants for the reaction of methyl tosylate (**5**-OTs) with 1-aminopropan-2-ol at 20˚C in DMSO (conventional conductometer).

No	$[E]_0/M^1$	$[Nu]_0/M$	$[Nu]_0/[E]_0$	k_{obs}/s^{-1}
1	1.54×10^{-3}	3.63×10^{-2}	24	1.06×10^{-3}
2	1.55×10^{-3}	5.34×10^{-2}	34	1.55×10^{-3}
3	1.51×10^{-3}	6.95×10^{-2}	46	1.98×10^{-3}
4	1.46×10^{-3}	8.71×10^{-2}	60	2.49×10^{-3}
5	1.55×10^{-3}	9.68×10^{-2}	62	2.79×10^{-3}
$k_2 = 2.84 \times 10^{-2}\ M^{-1}s^{-1}$				

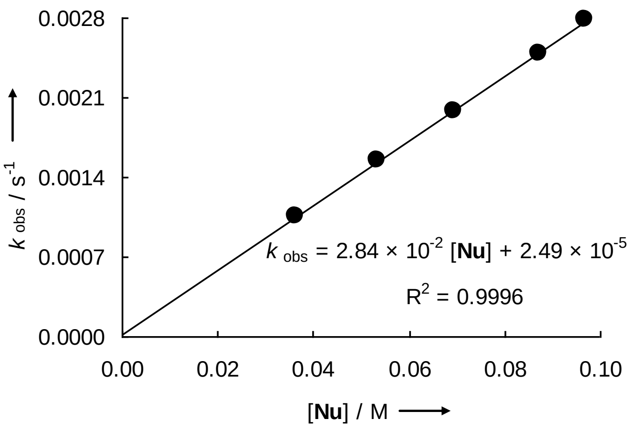

Table 2.S2.10.5. Rate constants for the reaction of methyl tosylate (**5**-OTs) with *n*-propylamine at 20˚C in DMSO (conventional conductometer).

No	$[E]_0/M^1$	$[Nu]_0/M$	$[Nu]_0/ [E]_0$	k_{obs}/s^{-1}
1	1.71×10^{-3}	3.46×10^{-2}	20	1.52×10^{-3}
2	1.50×10^{-3}	5.02×10^{-2}	33	2.14×10^{-3}
3	1.46×10^{-3}	6.49×10^{-2}	44	2.79×10^{-3}
4	1.50×10^{-3}	8.33×10^{-2}	56	3.59×10^{-3}
$k_2 = 4.27 \times 10^{-2}\ M^{-1}s^{-1}$				

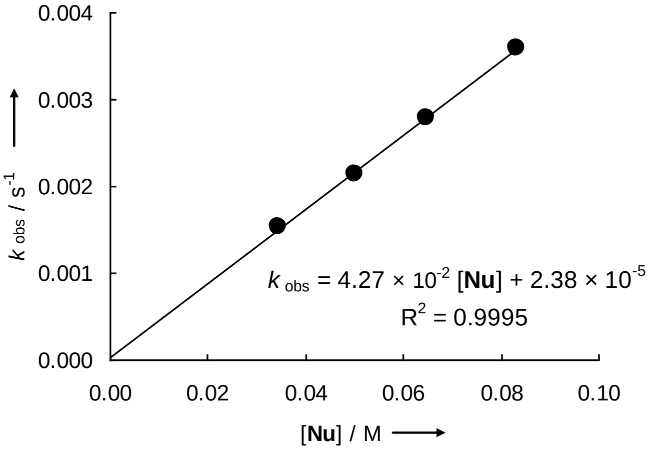

Table 2.S2.10.6. Rate constants for the reaction of methyl tosylate (**5**-OTs) with benzylamine at 20˚C in DMSO (conventional conductometer).

No	$[E]_0/M^1$	$[Nu]_0/M$	$[Nu]_0/ [E]_0$	k_{obs}/s^{-1}
1	1.58×10^{-3}	3.80×10^{-2}	24	8.25×10^{-4}
2	1.45×10^{-3}	4.93×10^{-2}	34	1.09×10^{-3}
3	1.56×10^{-3}	5.95×10^{-2}	38	1.34×10^{-3}
4	1.55×10^{-3}	7.53×10^{-2}	49	1.68×10^{-3}
5	1.48×10^{-3}	8.23×10^{-2}	56	1.90×10^{-3}
$k_2 = 2.38 \times 10^{-2}\ M^{-1}s^{-1}$				

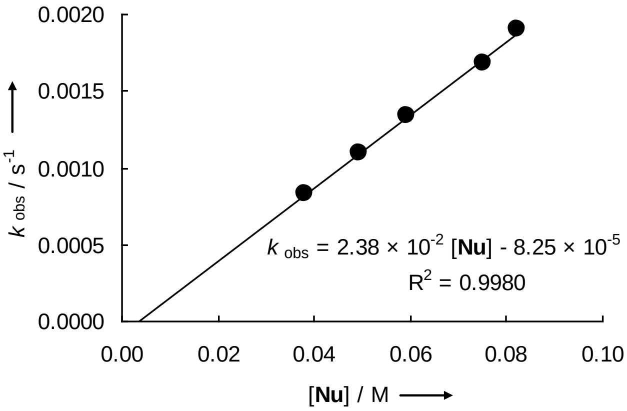

Table 2.S2.10.7. Rate constants for the reaction of methyl tosylate (**5**-OTs) with 4-DMAP at 20˚C in DMSO (conventional conductometer).

No	$[E]_0/M^1$	$[Nu]_0/M$	$[Nu]_0/ [E]_0$	k_{obs}/s^{-1}
1	1.73×10^{-3}	1.71×10^{-2}	10	7.20×10^{-5}
2	1.53×10^{-3}	3.18×10^{-2}	21	1.37×10^{-4}
3	1.63×10^{-3}	4.90×10^{-2}	30	2.01×10^{-4}
4	1.69×10^{-3}	6.79×10^{-2}	40	2.76×10^{-4}
$k_2 = 3.98 \times 10^{-3}\ M^{-1}s^{-1}$				

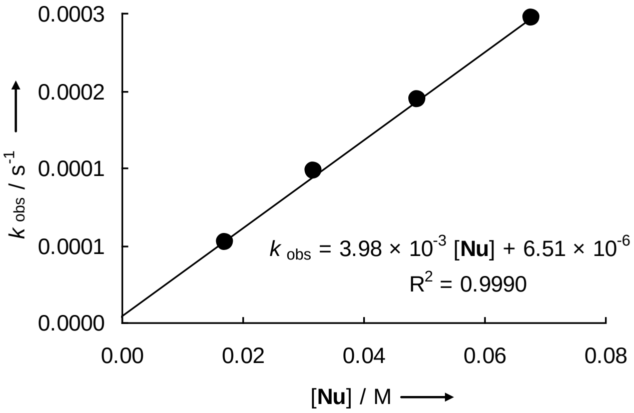

Table 2.S2.10.8. Rate constants for the reaction of methyl tosylate (**5**-OTs) with 2-aminobutan-1-ol at 20˚C in DMSO (conventional conductometer).

No	$[E]_0$/M^1	$[Nu]_0$/M	$[Nu]_0$/ $[E]_0$	k_{obs}/s^{-1}
1	1.61×10^{-3}	1.81×10^{-2}	11	2.41×10^{-4}
2	1.57×10^{-3}	3.52×10^{-2}	22	4.80×10^{-4}
3	1.62×10^{-3}	5.29×10^{-2}	33	7.29×10^{-4}
4	1.42×10^{-3}	6.80×10^{-2}	48	9.44×10^{-4}
5	1.38×10^{-3}	8.29×10^{-2}	60	1.13×10^{-3}
$k_2 = 1.38 \times 10^{-2}$ M^{-1}s^{-1}				

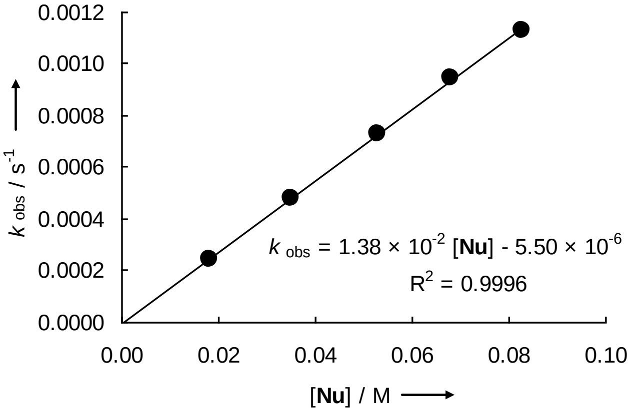

Table 2.S2.10.9. Rate constants for the reaction of methyl tosylate (**5**-OTs) with diethanolamine at 20˚C in DMSO (conventional conductometer).

No	$[E]_0$/M^1	$[Nu]_0$/M	$[Nu]_0$/ $[E]_0$	k_{obs}/s^{-1}
1	1.53×10^{-3}	1.97×10^{-2}	13	4.09×10^{-4}
2	1.50×10^{-3}	2.76×10^{-2}	18	5.59×10^{-4}
3	1.52×10^{-3}	3.26×10^{-2}	21	6.44×10^{-4}
4	1.64×10^{-3}	4.16×10^{-2}	25	8.21×10^{-4}
$k_2 = 1.87 \times 10^{-2}$ M^{-1}s^{-1}				

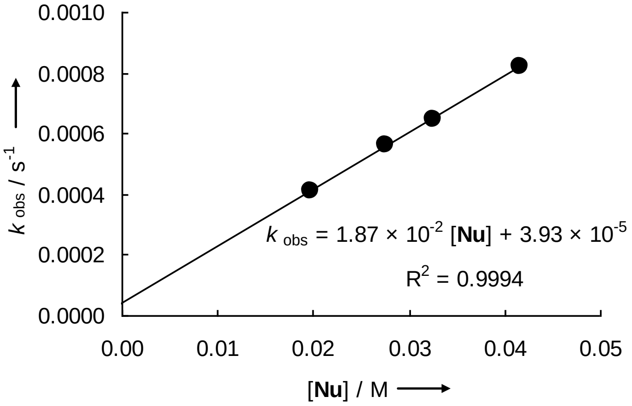

Table 2.S2.10.10. Rate constants for the reaction of methyl tosylate (**5**-OTs) with imidazole at 20˚C in DMSO (conventional conductometer).

No	$[E]_0/M^1$	$[Nu]_0/M$	$[Nu]_0/[E]_0$	k_{obs}/s^{-1}
1	1.49×10^{-3}	8.79×10^{-2}	59	1.01×10^{-4}
2	1.57×10^{-3}	1.80×10^{-1}	115	1.61×10^{-4}
3	1.67×10^{-3}	2.73×10^{-1}	163	2.69×10^{-4}
4	1.62×10^{-3}	4.09×10^{-1}	252	3.55×10^{-4}
5	1.56×10^{-3}	5.75×10^{-1}	369	4.87×10^{-4}
$k_2 = 7.99 \times 10^{-4}$ M^{-1}s^{-1}				

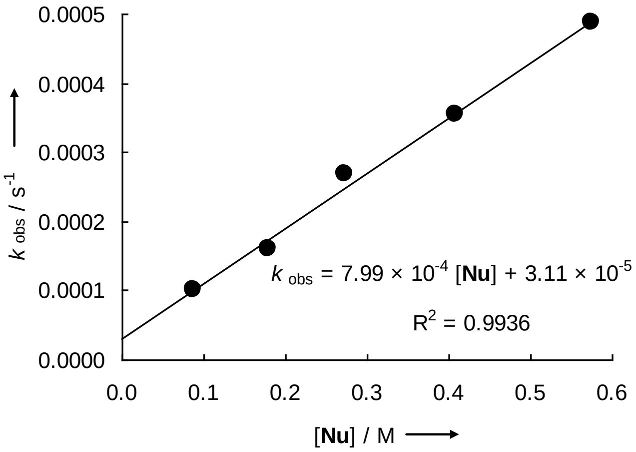

Table 2.S2.10.11. Rate constants for the reaction of methyl iodide with 2-methylbenzimidazole at 20˚C in DMSO (conventional conductometer).

No	$[E]_0/M^1$	$[Nu]_0/M$	$[Nu]_0/[E]_0$	k_{obs}/s^{-1}
1	1.65×10^{-3}	1.40×10^{-1}	85	3.49×10^{-5}
2	1.69×10^{-3}	2.06×10^{-1}	122	5.22×10^{-5}
3	1.58×10^{-3}	2.70×10^{-1}	171	6.70×10^{-5}
$k_2 = 2.47 \times 10^{-4}$ M^{-1}s^{-1}				

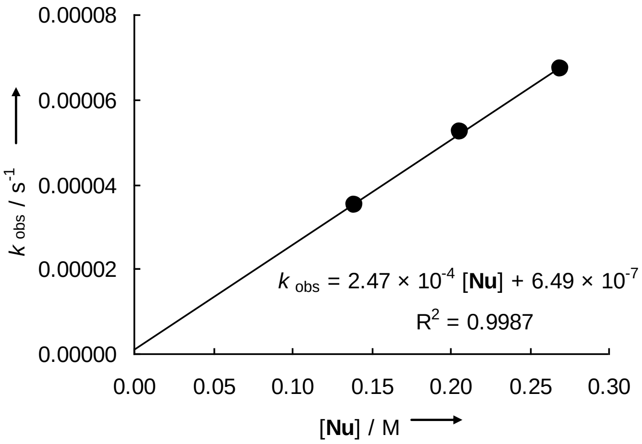

2.S.3. Rate constants in acetonitrile.

2.S.3.1. Rate constants for the reactions of benzyl bromide (1-Br) in acetonitrile.

Table 2.S3.1.1. Rate constants for the reaction of benzyl bromide (**1**-Br) with DABCO at 20˚C in acetonitrile (conventional conductometer).

No	$[E]_0/M^1$	$[Nu]_0/M$	$[Nu]_0/ [E]_0$	k_{obs}/s^{-1}
1	1.91×10^{-4}	2.14×10^{-3}	11	9.45×10^{-3}
2	1.93×10^{-4}	2.79×10^{-3}	14	1.24×10^{-2}
3	1.90×10^{-4}	3.35×10^{-3}	18	1.51×10^{-2}
4	1.89×10^{-4}	3.92×10^{-3}	21	1.74×10^{-2}
5	1.89×10^{-4}	4.53×10^{-3}	24	2.01×10^{-2}
$k_2 = 4.45\ M^{-1}s^{-1}$				

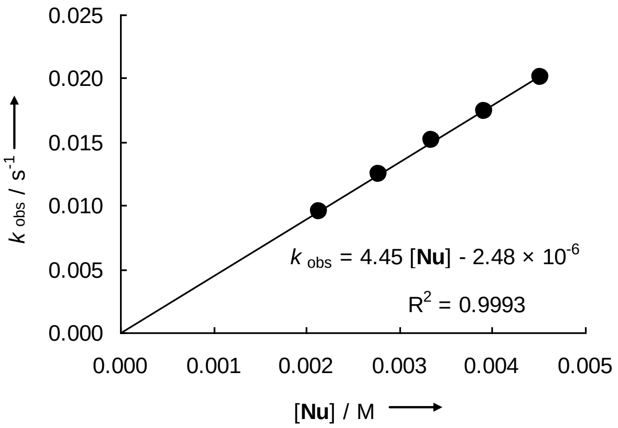

Table 2.S3.1.2. Rate constants for the reaction of benzyl bromide (**1**-Br) with methylhydrazine at 20˚C in acetonitrile (conventional conductometer).

No	$[E]_0/M^1$	$[Nu]_0/M$	$[Nu]_0/ [E]_0$	k_{obs}/s^{-1}
1	2.12×10^{-4}	1.81×10^{-2}	85	3.41×10^{-3}
2	2.12×10^{-4}	2.42×10^{-2}	114	4.53×10^{-3}
3	2.08×10^{-4}	2.97×10^{-2}	143	5.68×10^{-3}
4	2.07×10^{-4}	3.54×10^{-2}	171	6.50×10^{-3}
5	2.05×10^{-4}	4.10×10^{-2}	200	7.38×10^{-3}
$k_2 = 1.74 \times 10^{-1}\ M^{-1}s^{-1}$				

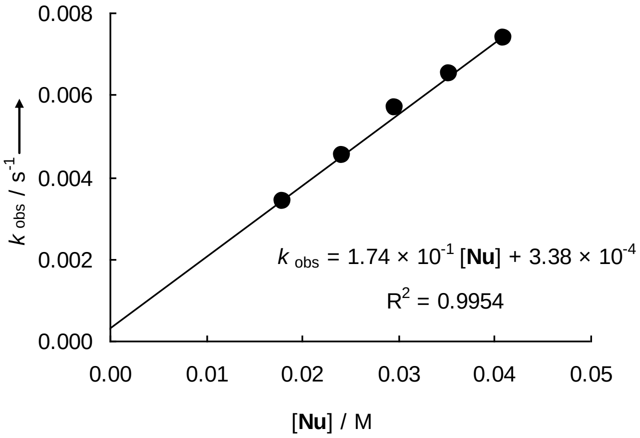

Table 2.S3.1.3. Rate constants for the reaction of benzyl bromide (**1**-Br) with piperidine at 20˚C in acetonitrile (conventional conductometer).

No	$[E]_0/M^1$	$[Nu]_0/M$	$[Nu]_0/[E]_0$	k_{obs}/s^{-1}
1	2.44×10^{-4}	3.73×10^{-3}	15	2.83×10^{-3}
2	2.40×10^{-4}	5.51×10^{-3}	23	4.11×10^{-3}
3	2.41×10^{-4}	7.38×10^{-3}	31	5.31×10^{-3}
4	2.40×10^{-4}	9.16×10^{-3}	38	6.71×10^{-3}
5	2.38×10^{-4}	1.09×10^{-2}	46	8.01×10^{-3}
$k_2 = 7.20 \times 10^{-1}$ M^{-1}s^{-1}				

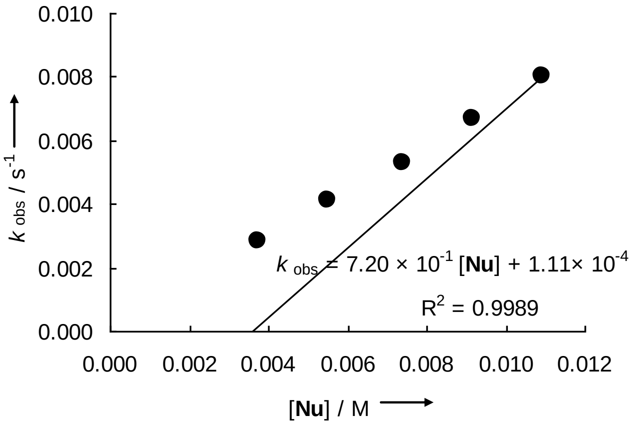

Table 2.S3.1.4. Rate constants for the reaction of benzyl bromide (**1**-Br) with morpholine at 20˚C in acetonitrile (conventional conductometer).

No	$[E]_0/M^1$	$[Nu]_0/M$	$[Nu]_0/[E]_0$	k_{obs}/s^{-1}
1	2.14×10^{-4}	7.40×10^{-3}	35	1.06×10^{-3}
2	2.10×10^{-4}	9.77×10^{-3}	47	1.38×10^{-3}
3	2.09×10^{-4}	1.45×10^{-2}	69	2.01×10^{-3}
4	2.88×10^{-4}	2.08×10^{-2}	72	2.85×10^{-3}
$k_2 = 1.33 \times 10^{-1}$ M^{-1}s^{-1}				

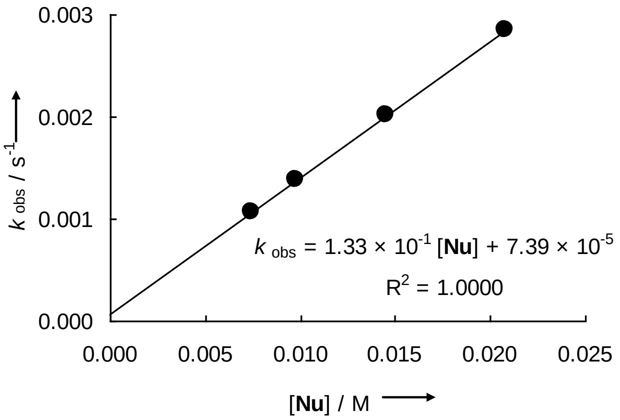

Table 2.S3.1.5. Rate constants for the reaction of benzyl bromide (**1**-Br) with 2-aminoethanol at 20˚C in acetonitrile (conventional conductometer).

No	$[E]_0/M^1$	$[Nu]_0/M$	$[Nu]_0/[E]_0$	k_{obs}/s^{-1}
1	5.02×10^{-4}	5.85×10^{-2}	117	1.09×10^{-3}
2	5.06×10^{-4}	7.22×10^{-2}	143	1.39×10^{-3}
3	5.00×10^{-4}	9.77×10^{-2}	195	1.87×10^{-3}
		$k_2 = 1.98 \times 10^{-2}\ M^{-1}s^{-1}$		

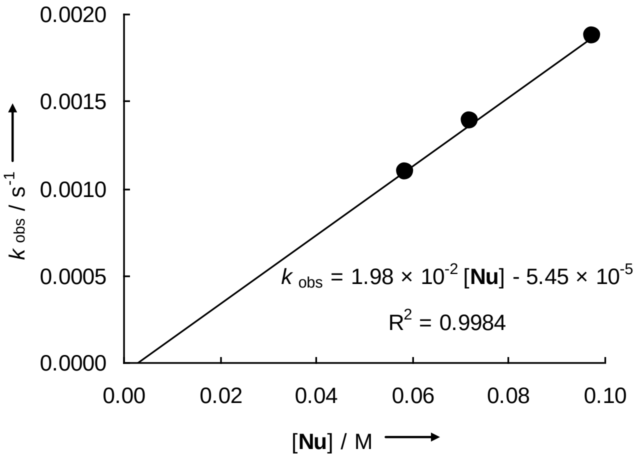

Table 2.S3.1.6. Rate constants for the reaction of benzyl bromide (**1**-Br) with *n*-butylamine at 20˚C in acetonitrile (conventional conductometer).

No	$[E]_0/M^1$	$[Nu]_0/M$	$[Nu]_0/[E]_0$	k_{obs}/s^{-1}
1	5.01×10^{-4}	4.69×10^{-2}	94	1.73×10^{-3}
2	4.97×10^{-4}	7.48×10^{-2}	151	2.77×10^{-3}
3	5.00×10^{-4}	9.49×10^{-2}	190	3.49×10^{-3}
		$k_2 = 3.67 \times 10^{-2}\ M^{-1}s^{-1}$		

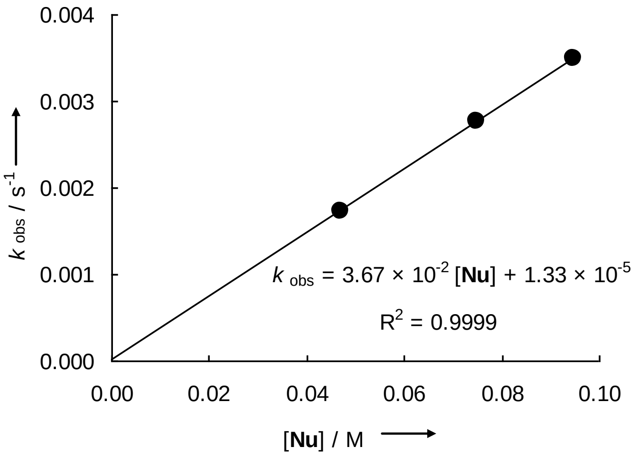

Table 2.S3.1.7. Rate constants for the reaction of benzyl bromide (**1**-Br) with *n*-propylamine at 20˚C in acetonitrile (conventional conductometer).

No	$[E]_0/M^1$	$[Nu]_0/M$	$[Nu]_0/[E]_0$	k_{obs}/s^{-1}
1	5.46×10^{-4}	4.35×10^{-2}	80	1.24×10^{-3}
2	5.61×10^{-4}	5.79×10^{-2}	103	1.69×10^{-3}
3	5.53×10^{-4}	7.43×10^{-2}	134	2.33×10^{-3}
4	5.53×10^{-4}	1.02×10^{-1}	184	3.24×10^{-3}
5	5.55×10^{-4}	1.25×10^{-1}	225	3.61×10^{-3}
6	5.58×10^{-4}	1.39×10^{-1}	249	3.81×10^{-3}
7	5.44×10^{-4}	1.50×10^{-1}	276	4.50×10^{-3}
$k_2 = 2.86 \times 10^{-2}\ M^{-1}s^{-1}$				

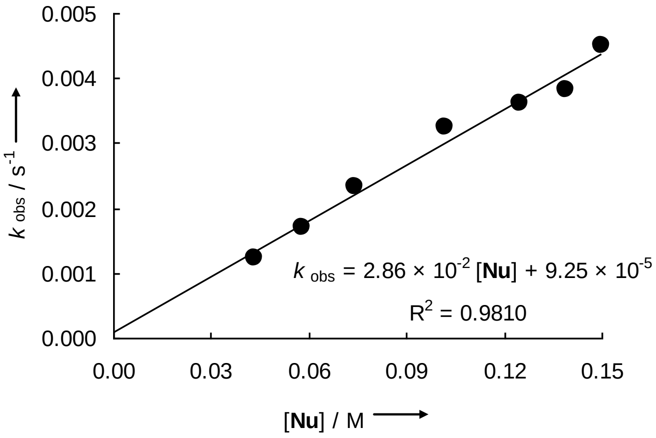

2.S.3.2. Rate constants for the reactions of 4-cyanobenzyl bromide (2-Br) in acetonitrile.

Table 2.S3.2.1. Rate constants for the reaction of 4-cyanobenzyl bromide (**2**-Br) with DABCO at 20˚C in acetonitrile (conventional conductometer).

No	$[E]_0/M^1$	$[Nu]_0/M$	$[Nu]_0/[E]_0$	k_{obs}/s^{-1}
1	1.97×10^{-4}	2.03×10^{-3}	10	8.08×10^{-3}
2	1.93×10^{-4}	2.27×10^{-3}	12	8.98×10^{-3}
3	1.93×10^{-4}	2.56×10^{-3}	13	9.92×10^{-3}
4	1.97×10^{-4}	2.90×10^{-3}	15	1.14×10^{-2}
5	1.92×10^{-4}	3.40×10^{-3}	18	1.31×10^{-2}
$k_2 = 3.69\ M^{-1}s^{-1}$				

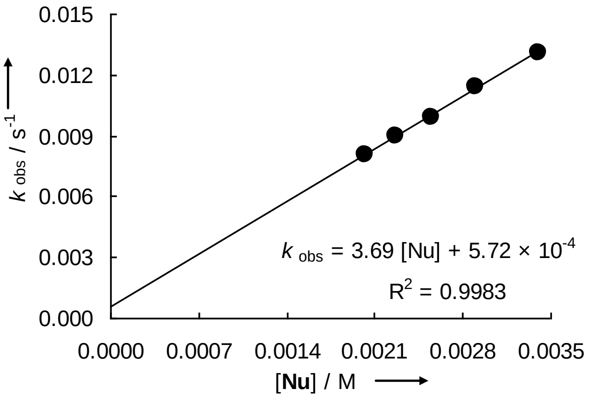

Table 2.S3.2.2. Rate constants for the reaction of 4-cyanobenzyl bromide (**2**-Br) with methylhydrazine at 20˚C in acetonitrile (conventional conductometer).

No	$[E]_0/M^1$	$[Nu]_0/M$	$[Nu]_0/[E]_0$	k_{obs}/s^{-1}
1	1.81×10^{-4}	5.88×10^{-3}	32	1.21×10^{-3}
2	1.80×10^{-4}	7.00×10^{-3}	39	1.45×10^{-3}
3	1.80×10^{-4}	8.17×10^{-3}	45	1.69×10^{-3}
4	1.79×10^{-4}	1.06×10^{-2}	59	2.25×10^{-3}
$k_2 = 2.20 \times 10^{-1}\ M^{-1}s^{-1}$				

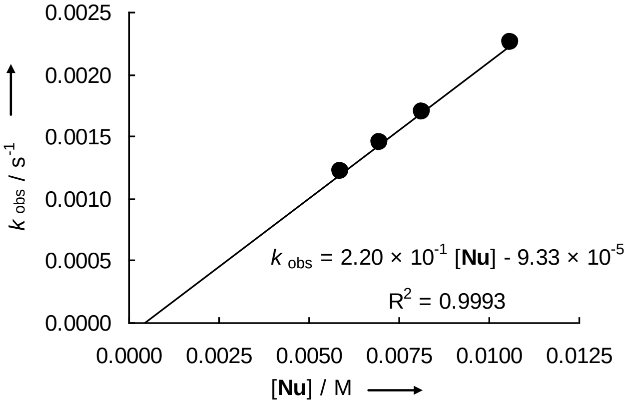

Table 2.S3.2.3. Rate constants for the reaction of 4-cyanobenzyl bromide (**2**-Br) with N-methylpyrrolidine at 20˚C in acetonitrile (conventional conductometer).

No	$[E]_0/M^1$	$[Nu]_0/M$	$[Nu]_0/ [E]_0$	k_{obs}/s^{-1}
1	2.12×10^{-5}	1.62×10^{-3}	76	4.13×10^{-4}
2	2.97×10^{-5}	3.24×10^{-3}	109	8.29×10^{-4}
3	2.97×10^{-5}	4.87×10^{-3}	164	1.20×10^{-3}
4	2.91×10^{-5}	6.36×10^{-3}	219	1.62×10^{-3}
5	2.89×10^{-5}	7.88×10^{-3}	273	2.01×10^{-3}
$k_2 = 2.55 \times 10^{-1}\ M^{-1}s^{-1}$				

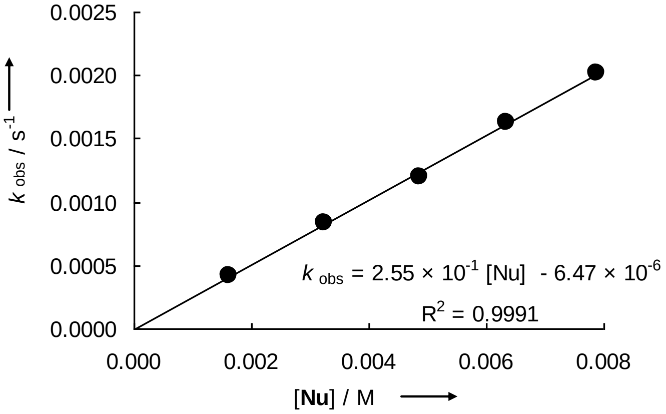

Table 2.S3.2.4. Rate constants for the reaction of 4-cyanobenzyl bromide (**2**-Br) with triethylamine at 20˚C in acetonitrile (conventional conductometer).

No	$[E]_0/M^1$	$[Nu]_0/M$	$[Nu]_0/ [E]_0$	k_{obs}/s^{-1}
1	1.86×10^{-5}	1.11×10^{-2}	597	2.98×10^{-5}
2	2.06×10^{-5}	2.04×10^{-2}	990	5.21×10^{-5}
3	1.96×10^{-5}	2.91×10^{-2}	1485	7.06×10^{-5}
$k_2 = 2.27 \times 10^{-3}\ M^{-1}s^{-1}$				

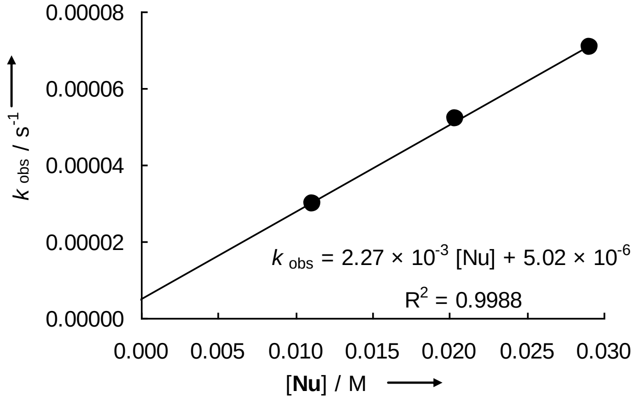

Table 2.S3.2.5. Rate constants for the reaction of 4-cyanobenzyl bromide (**2**-Br) with tri-*n*-butylamine at 20˚C in acetonitrile (conventional conductometer).

No	$[E]_0/M^1$	$[Nu]_0/M$	$[Nu]_0/ [E]_0$	k_{obs}/s^{-1}
1	2.93×10^{-5}	1.25×10^{-2}	427	2.02×10^{-5}
2	4.02×10^{-5}	1.66×10^{-2}	413	2.77×10^{-5}
3	3.23×10^{-5}	2.74×10^{-2}	848	4.60×10^{-5}
4	2.79×10^{-5}	5.13×10^{-2}	1839	8.30×10^{-5}
		$k_2 = 1.61 \times 10^{-3}\ M^{-1}s^{-1}$		

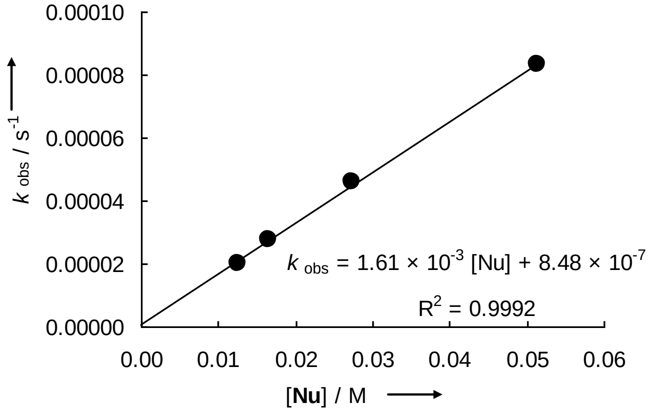

Table 2.S3.2.6. Rate constants for the reaction of 4-cyanobenzyl bromide (**2**-Br) with pyrrolidine at 20˚C in acetonitrile (conventional conductometer).

No	$[E]_0/M^1$	$[Nu]_0/M$	$[Nu]_0/[E]_0$	k_{obs}/s^{-1}
1	1.03×10^{-4}	1.36×10^{-3}	13	1.18×10^{-3}
2	1.03×10^{-4}	2.71×10^{-3}	26	2.23×10^{-3}
3	1.03×10^{-4}	4.07×10^{-3}	40	3.29×10^{-3}
4	1.01×10^{-4}	5.33×10^{-3}	53	4.24×10^{-3}
5	1.01×10^{-4}	6.67×10^{-3}	66	5.17×10^{-3}
$k_2 = 7.55 \times 10^{-1}\ M^{-1}s^{-1}$				

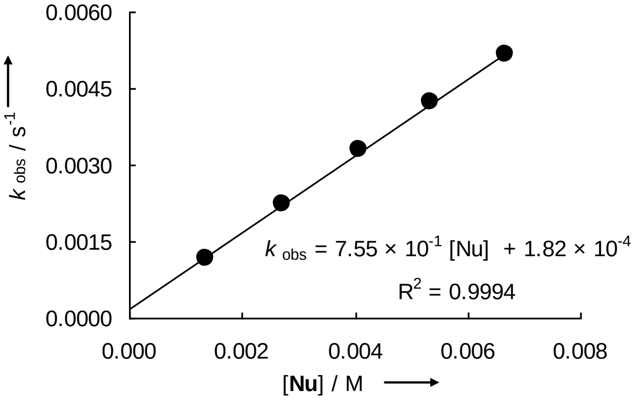

Table 2.S3.2.7. Rate constants for the reaction of 4-cyanobenzyl bromide (**2**-Br) with piperidine at 20˚C in acetonitrile (conventional conductometer).

No	$[E]_0/M^1$	$[Nu]_0/M$	$[Nu]_0/[E]_0$	k_{obs}/s^{-1}
1	2.19×10^{-4}	3.96×10^{-3}	18	3.39×10^{-3}
2	2.18×10^{-4}	5.92×10^{-3}	27	4.94×10^{-3}
3	2.15×10^{-4}	7.78×10^{-3}	36	6.28×10^{-3}
4	2.14×10^{-4}	9.66×10^{-3}	45	7.67×10^{-3}
5	2.14×10^{-4}	1.16×10^{-2}	54	9.35×10^{-3}
$k_2 = 7.70 \times 10^{-1}\ M^{-1}s^{-1}$				

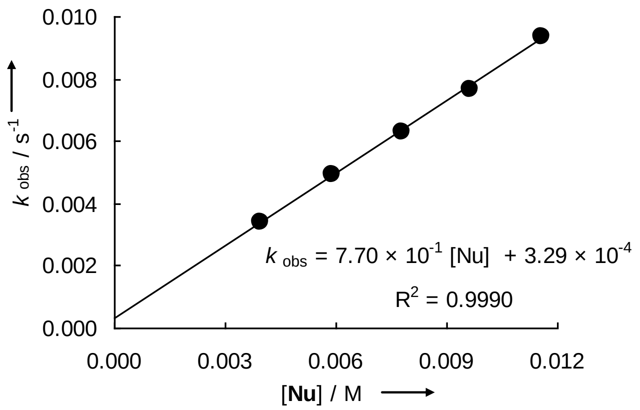

Table 2.S3.2.8. Rate constants for the reaction of 4-cyanobenzyl bromide (**2**-Br) with morpholine at 20˚C in acetonitrile (conventional conductometer).

No	$[E]_0/M^1$	$[Nu]_0/M$	$[Nu]_0/[E]_0$	k_{obs}/s^{-1}
1	1.68×10^{-4}	4.78×10^{-3}	28	5.49×10^{-4}
2	1.70×10^{-4}	7.22×10^{-3}	42	8.01×10^{-4}
3	1.68×10^{-4}	9.55×10^{-3}	57	1.10×10^{-3}
4	1.65×10^{-4}	1.17×10^{-2}	71	1.29×10^{-3}
5	1.64×10^{-4}	1.39×10^{-2}	85	1.54×10^{-3}
$k_2 = 1.09 \times 10^{-1}$ $M^{-1}s^{-1}$				

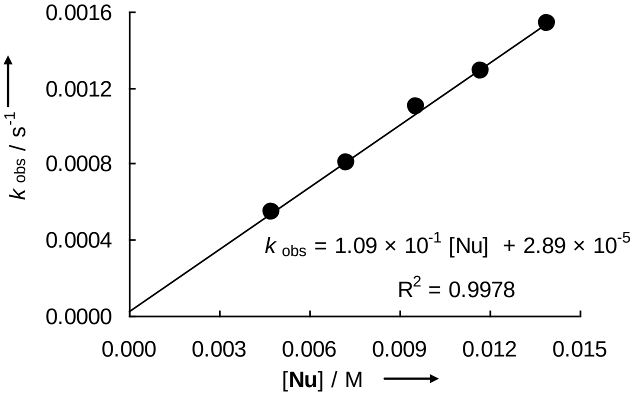

Table 2.S3.2.9. Rate constants for the reaction of 4-cyanobenzyl bromide (**2**-Br) with 2-aminoethanol at 20˚C in acetonitrile (conventional conductometer).

No	$[E]_0/M^1$	$[Nu]_0/M$	$[Nu]_0/[E]_0$	k_{obs}/s^{-1}
1	2.08×10^{-5}	4.56×10^{-3}	219	6.67×10^{-5}
2	2.95×10^{-5}	9.04×10^{-3}	306	1.28×10^{-4}
3	2.91×10^{-5}	1.34×10^{-2}	460	1.91×10^{-4}
4	2.86×10^{-5}	1.75×10^{-2}	612	2.55×10^{-4}
5	2.77×10^{-5}	2.12×10^{-2}	765	3.13×10^{-4}
$k_2 = 1.48 \times 10^{-2}\ M^{-1}s^{-1}$				

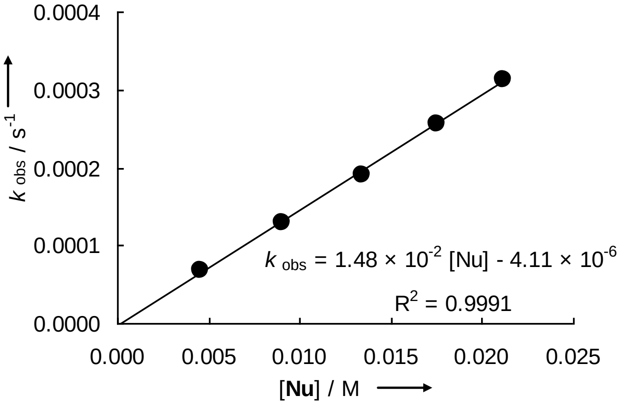

Table 2.S3.2.10. Rate constants for the reaction of 4-cyanobenzyl bromide (**2**-Br) with di-*n*-propylamine at 20˚C in acetonitrile (conventional conductometer).

No	$[E]_0/M^1$	$[Nu]_0/M$	$[Nu]_0/[E]_0$	k_{obs}/s^{-1}
1	2.91×10^{-5}	8.30×10^{-3}	285	2.26×10^{-4}
2	4.06×10^{-5}	1.26×10^{-2}	310	3.42×10^{-4}
3	3.97×10^{-5}	1.67×10^{-2}	421	4.67×10^{-4}
4	2.71×10^{-5}	2.06×10^{-2}	760	5.70×10^{-4}
$k_2 = 2.82 \times 10^{-2}\ M^{-1}s^{-1}$				

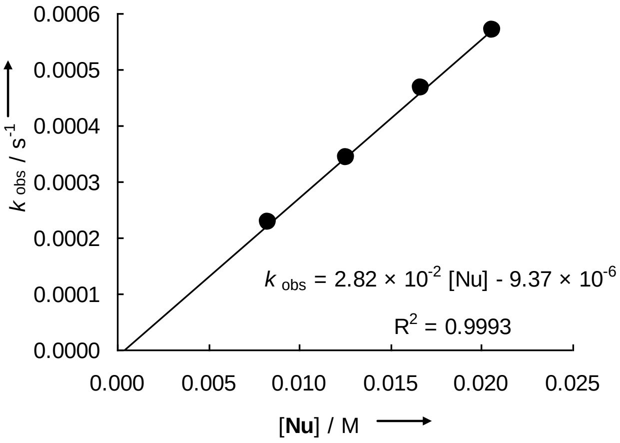

Table 2.S3.2.11. Rate constants for the reaction of 4-cyanobenzyl bromide (**2**-Br) with *n*-propylamine at 20˚C in acetonitrile (conventional conductometer).

No	$[E]_0/M^1$	$[Nu]_0/M$	$[Nu]_0/[E]_0$	k_{obs}/s^{-1}
1	4.13×10^{-4}	3.53×10^{-2}	85	1.23×10^{-3}
2	4.16×10^{-4}	5.33×10^{-2}	128	1.82×10^{-3}
3	4.08×10^{-4}	6.98×10^{-2}	171	2.40×10^{-3}
4	4.04×10^{-4}	8.64×10^{-2}	214	2.88×10^{-3}
5	4.07×10^{-4}	1.05×10^{-1}	258	3.46×10^{-3}
$k_2 = 3.20 \times 10^{-2}\ M^{-1}s^{-1}$				

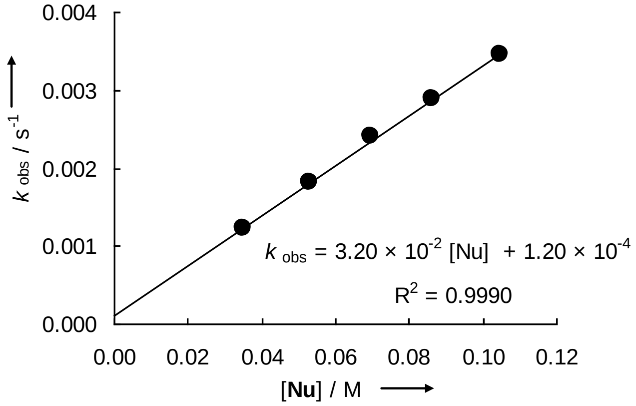

Table 2.S3.2.12. Rate constants for the reaction of 4-cyanobenzyl bromide (**2**-Br) with benzylamine at 20˚C in acetonitrile (conventional conductometer).

No	$[E]_0$/M^1	$[Nu]_0$/M	$[Nu]_0$/ $[E]_0$	k_{obs}/s^{-1}
1	1.04×10^{-4}	1.09×10^{-2}	105	1.06×10^{-4}
2	1.02×10^{-4}	2.14×10^{-2}	210	2.15×10^{-4}
3	1.02×10^{-4}	3.22×10^{-2}	316	3.20×10^{-4}
4	1.02×10^{-4}	4.26×10^{-2}	418	4.17×10^{-4}
5	9.89×10^{-5}	5.17×10^{-2}	523	4.95×10^{-4}
		$k_2 = 9.54 \times 10^{-3}$ M^{-1}s^{-1}		

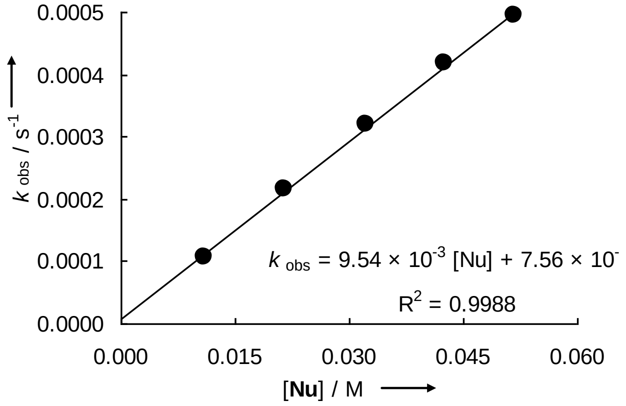

Table 2.S3.2.13. Rate constants for the reaction of 4-cyanobenzyl bromide (**2**-Br) with 4-DMAP at 20˚C in acetonitrile (conventional conductometer).

No	$[E]_0$/M^1	$[Nu]_0$/M	$[Nu]_0$/ $[E]_0$	k_{obs}/s^{-1}
1	2.34×10^{-5}	2.90×10^{-3}	124	5.04×10^{-5}
2	2.22×10^{-5}	5.78×10^{-3}	260	9.59×10^{-5}
3	1.79×10^{-5}	7.93×10^{-3}	443	1.32×10^{-4}
4	1.81×10^{-5}	1.08×10^{-2}	597	1.82×10^{-4}
		$k_2 = 1.67 \times 10^{-2}$ M^{-1}s^{-1}		

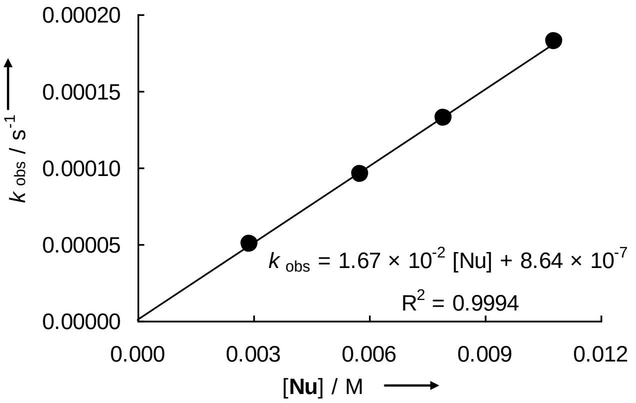

Table 2.S3.2.14. Rate constants for the reaction of 4-cyanobenzyl bromide (**2**-Br) with *tert*-butylamine at 20˚C in acetonitrile (conventional conductometer).

No	$[E]_0/M^1$	$[Nu]_0/M$	$[Nu]_0/[E]_0$	k_{obs}/s^{-1}
1	1.97×10^{-5}	1.90×10^{-2}	964	5.99×10^{-5}
2	1.93×10^{-5}	2.55×10^{-2}	1321	7.87×10^{-5}
3	1.82×10^{-5}	3.23×10^{-2}	1775	1.01×10^{-4}
		$k_2 = 3.09 \times 10^{-3}\ M^{-1}s^{-1}$		

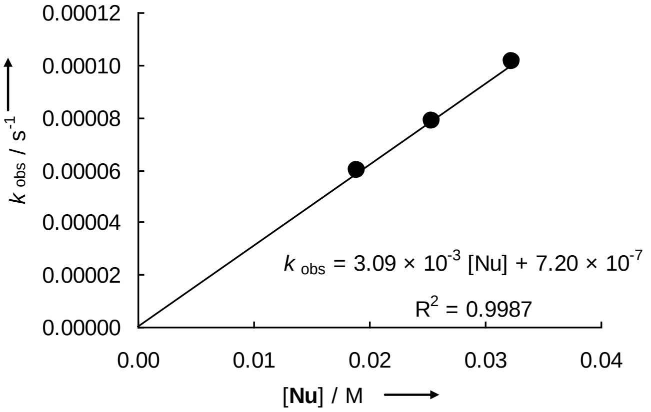

Table 2.S3.2.15. Rate constants for the reaction of 4-cyanobenzyl bromide (**2**-Br) with imidazole at 20˚C in acetonitrile (conventional conductometer).

No	$[E]_0/M^1$	$[Nu]_0/M$	$[Nu]_0/[E]_0$	k_{obs}/s^{-1}
1	6.07×10^{-4}	9.00×10^{-2}	148	6.64×10^{-5}
2	5.92×10^{-4}	1.34×10^{-1}	227	9.58×10^{-5}
3	5.79×10^{-4}	1.75×10^{-1}	302	1.25×10^{-4}
4	5.57×10^{-4}	2.53×10^{-1}	454	1.75×10^{-4}
5	6.19×10^{-4}	3.48×10^{-1}	562	2.33×10^{-4}
		$k_2 = 6.46 \times 10^{-4}\ M^{-1}s^{-1}$		

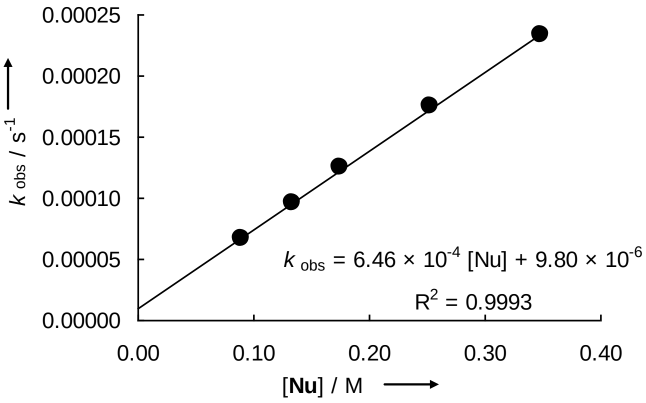

Table 2.S3.2.16. Rate constants for the reaction of 4-cyanobenzyl bromide (**2**-Br) with tri-*n*-butylphosphane at 20˚C in acetonitrile (conventional conductometer).

No	$[E]_0/M^1$	$[Nu]_0/M$	$[Nu]_0/ [E]_0$	k_{obs}/s^{-1}
1	4.82×10^{-4}	1.05×10^{-2}	22	2.72×10^{-3}
2	5.31×10^{-4}	1.78×10^{-2}	34	4.65×10^{-3}
3	4.81×10^{-4}	2.46×10^{-2}	51	6.50×10^{-3}
4	4.85×10^{-4}	3.26×10^{-2}	67	8.75×10^{-3}
$k_2 = 2.73 \times 10^{-1}$ $M^{-1}s^{-1}$				

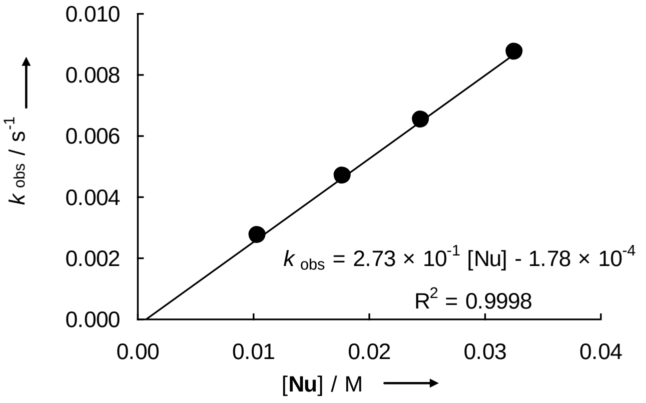

Table 2.S3.2.17. Rate constants for the reaction of 4-cyanobenzyl bromide (**2**-Br) with tris(4-methoxyphenyl)phosphane at 20˚C in acetonitrile (conventional conductometer).

No	$[E]_0/M^1$	$[Nu]_0/M$	$[Nu]_0/ [E]_0$	k_{obs}/s^{-1}
1	3.89×10^{-4}	6.90×10^{-3}	18	9.10×10^{-5}
2	3.84×10^{-4}	1.07×10^{-2}	28	1.43×10^{-4}
3	3.93×10^{-4}	1.70×10^{-2}	43	2.26×10^{-4}
$k_2 = 1.33 \times 10^{-2} M^{-1}s^{-1}$				

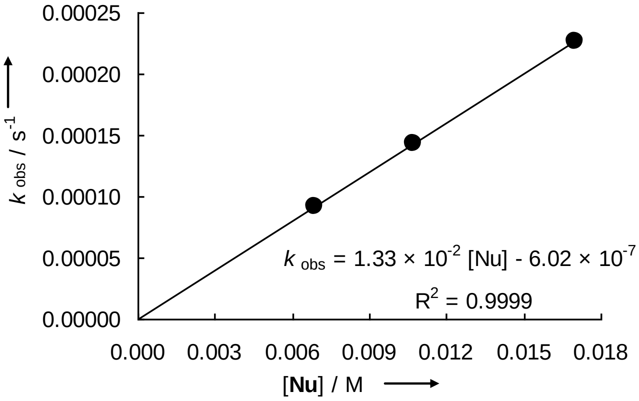

Table 2.S3.2.18. Rate constants for the reaction of 4-cyanobenzyl bromide (**2**-Br) with triphenylphosphane at 20˚C in acetonitrile (conventional conductometer).

No	$[E]_0/M^1$	$[Nu]_0/M$	$[Nu]_0/ [E]_0$	k_{obs}/s^{-1}
1	5.33×10^{-4}	1.25×10^{-2}	23	2.17×10^{-5}
2	5.17×10^{-4}	2.02×10^{-2}	39	3.49×10^{-5}
3	5.74×10^{-4}	2.63×10^{-2}	46	4.48×10^{-5}
$k_2 = 1.68 \times 10^{-3}$ M^{-1}s^{-1}				

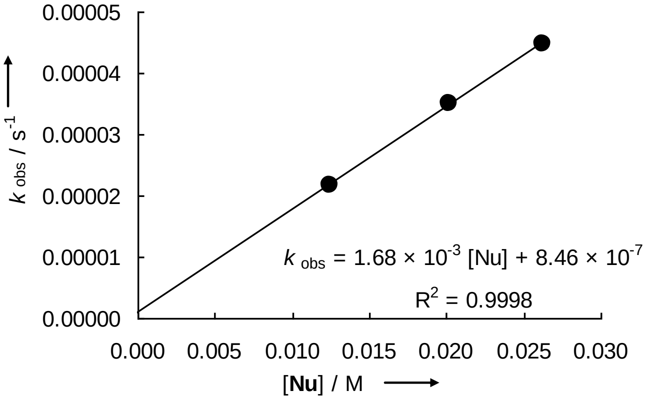

2.S.3.3. Rate constants for the reactions of 4-methoxybenzyl bromide (3-Br) in acetonitrile.

Table 2.S3.3.1. Rate constants for the reaction of 4-cyanobenzyl bromide (**3**-Br) with DABCO at 20˚C in acetonitrile (conventional conductometer).

No	$[E]_0/M^1$	$[Nu]_0/M$	$[Nu]_0/ [E]_0$	k_{obs}/s^{-1}
1	1.38×10^{-4}	1.75×10^{-3}	13	2.36×10^{-2}
2	1.96×10^{-4}	2.03×10^{-3}	10	2.75×10^{-2}
3	1.96×10^{-4}	2.32×10^{-3}	12	3.23×10^{-2}
4	1.94×10^{-4}	2.58×10^{-3}	13	3.56×10^{-2}
$k_2 = 1.47 \times 10^{1}$ M^{-1}s^{-1}				

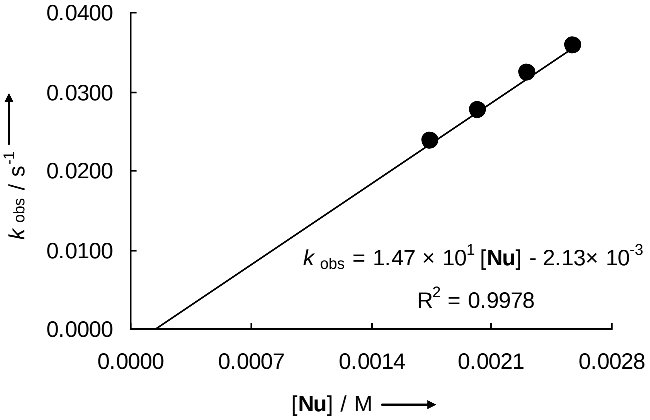

Table 2.S3.3.2. Rate constants for the reaction of 4-cyanobenzyl bromide (**3**-Br) with methylhydrazine at 20˚C in acetonitrile (conventional conductometer).

No	$[E]_0/M^1$	$[Nu]_0/M$	$[Nu]_0/ [E]_0$	k_{obs}/s^{-1}
1	1.86×10^{-4}	2.82×10^{-3}	15	1.42×10^{-3}
2	1.87×10^{-4}	3.78×10^{-3}	20	1.88×10^{-3}
3	1.87×10^{-4}	4.25×10^{-3}	23	2.07×10^{-3}
4	1.96×10^{-4}	5.70×10^{-3}	29	2.73×10^{-3}
$k_2 = 4.53 \times 10^{-1}\ M^{-1}s^{-1}$				

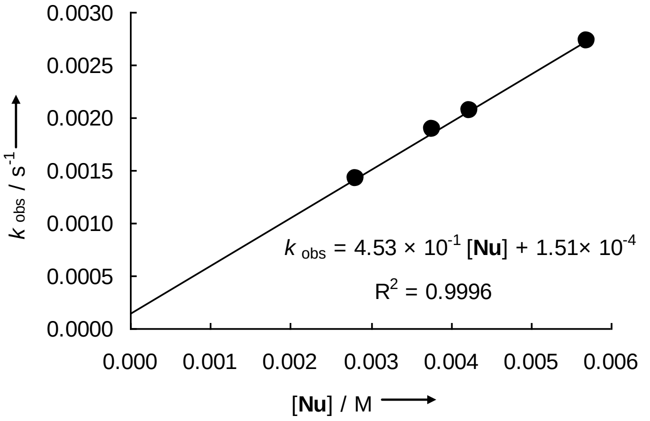

Table 2.S3.3.3. Rate constants for the reaction of 4-cyanobenzyl bromide (**3**-Br) with piperidine at 20˚C in acetonitrile (conventional conductometer).

No	$[E]_0/M^1$	$[Nu]_0/M$	$[Nu]_0/[E]_0$	k_{obs}/s^{-1}
1	1.81×10^{-4}	3.54×10^{-3}	20	6.42×10^{-3}
2	1.89×10^{-4}	7.38×10^{-3}	39	1.31×10^{-2}
3	1.84×10^{-4}	8.99×10^{-3}	49	1.60×10^{-2}
4	1.82×10^{-4}	1.07×10^{-2}	59	1.90×10^{-2}
5	1.81×10^{-4}	3.54×10^{-3}	20	6.42×10^{-3}
$k_2 = 1.76\ M^{-1}s^{-1}$				

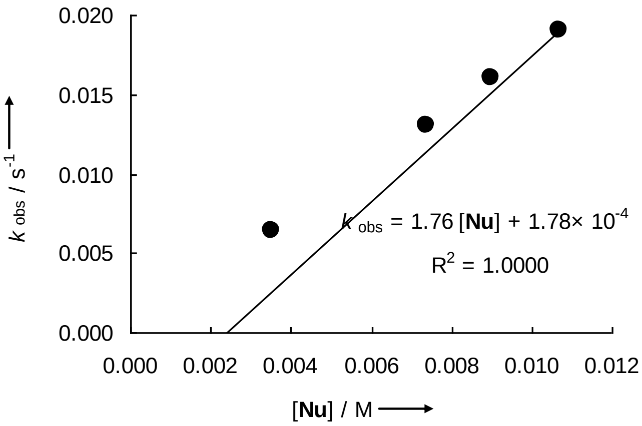

Table 2.S3.3.4. Rate constants for the reaction of 4-cyanobenzyl bromide (**3**-Br) with morpholine at 20˚C in acetonitrile (conventional conductometer).

No	$[E]_0/M^1$	$[Nu]_0/M$	$[Nu]_0/[E]_0$	k_{obs}/s^{-1}
1	1.86×10^{-4}	7.35×10^{-3}	40	2.96×10^{-3}
2	1.85×10^{-4}	9.73×10^{-3}	53	3.95×10^{-3}
3	1.83×10^{-4}	1.33×10^{-2}	73	5.40×10^{-3}
4	1.82×10^{-4}	1.68×10^{-2}	92	6.72×10^{-3}
5	1.80×10^{-4}	1.89×10^{-2}	105	7.53×10^{-3}
$k_2 = 3.95 \times 10^{-1}\ M^{-1}s^{-1}$				

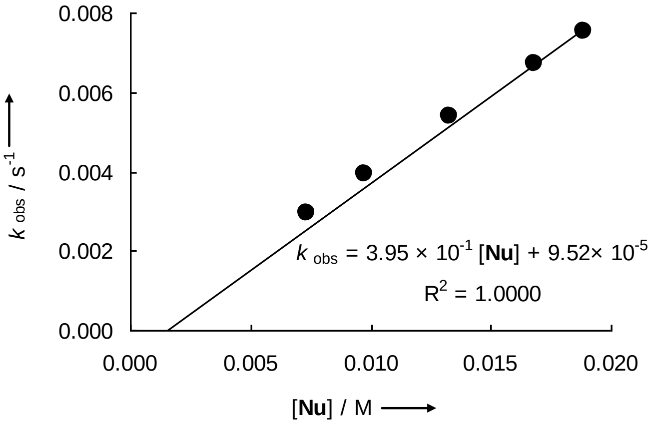

Table 2.S3.3.5. Rate constants for the reaction of 4-cyanobenzyl bromide (**3**-Br) with 2-aminoethanol at 20˚C in acetonitrile (conventional conductometer).

No	$[E]_0/M^1$	$[Nu]_0/M$	$[Nu]_0/[E]_0$	k_{obs}/s^{-1}
1	4.63×10^{-4}	3.56×10^{-2}	77	1.96×10^{-3}
2	4.69×10^{-4}	5.90×10^{-2}	126	3.08×10^{-3}
3	4.74×10^{-4}	8.18×10^{-2}	173	4.25×10^{-3}
4	4.75×10^{-4}	1.02×10^{-1}	215	5.18×10^{-3}
$k_2 = 4.88 \times 10^{-2}\ M^{-1}s^{-1}$				

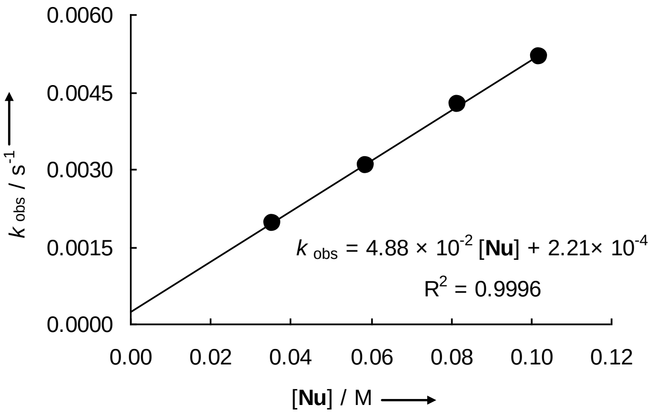

Table 2.S3.3.6. Rate constants for the reaction of 4-cyanobenzyl bromide (**3**-Br) with di-*n*-propylamine at 20˚C in acetonitrile (conventional conductometer).

No	$[E]_0/M^1$	$[Nu]_0/M$	$[Nu]_0/[E]_0$	k_{obs}/s^{-1}
1	4.87×10^{-4}	3.71×10^{-2}	76	6.99×10^{-3}
2	4.80×10^{-4}	4.28×10^{-2}	89	7.99×10^{-3}
3	4.91×10^{-4}	5.98×10^{-2}	122	1.16×10^{-2}
4	4.75×10^{-4}	6.55×10^{-2}	138	1.24×10^{-2}
5	4.66×10^{-4}	7.82×10^{-2}	168	1.50×10^{-2}
$k_2 = 1.96 \times 10^{-1}\ M^{-1}s^{-1}$				

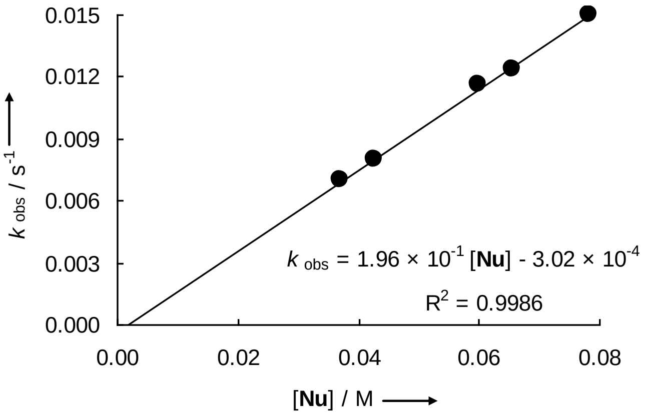

Table 2.S3.3.7. Rate constants for the reaction of 4-cyanobenzyl bromide (**3**-Br) with *n*-butylamine at 20˚C in acetonitrile (conventional conductometer).

No	$[E]_0/M^1$	$[Nu]_0/M$	$[Nu]_0/ [E]_0$	k_{obs}/s^{-1}
1	4.38×10^{-4}	4.68×10^{-2}	107	4.68×10^{-3}
2	4.47×10^{-4}	5.87×10^{-2}	131	5.75×10^{-3}
3	4.48×10^{-4}	8.02×10^{-2}	179	7.97×10^{-3}
$k_2 = 1.04 \times 10^{-1}$ $M^{-1}s^{-1}$				

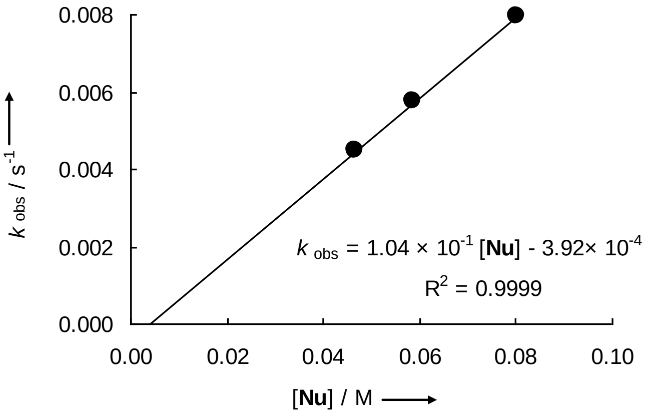

Table 2.S3.3.8. Rate constants for the reaction of 4-cyanobenzyl bromide (**3**-Br) with *n*-propylamine at 20˚C in acetonitrile (conventional conductometer).

No	$[E]_0/M^1$	$[Nu]_0/M$	$[Nu]_0/ [E]_0$	k_{obs}/s^{-1}
1	4.07×10^{-4}	3.60×10^{-2}	88	3.14×10^{-3}
2	4.03×10^{-4}	5.35×10^{-2}	133	4.61×10^{-3}
3	4.02×10^{-4}	7.11×10^{-2}	177	5.93×10^{-3}
4	3.96×10^{-4}	8.41×10^{-2}	212	6.92×10^{-3}
5	3.90×10^{-4}	1.03×10^{-1}	264	8.43×10^{-3}
$k_2 = 7.83 \times 10^{-2}$ $M^{-1}s^{-1}$				

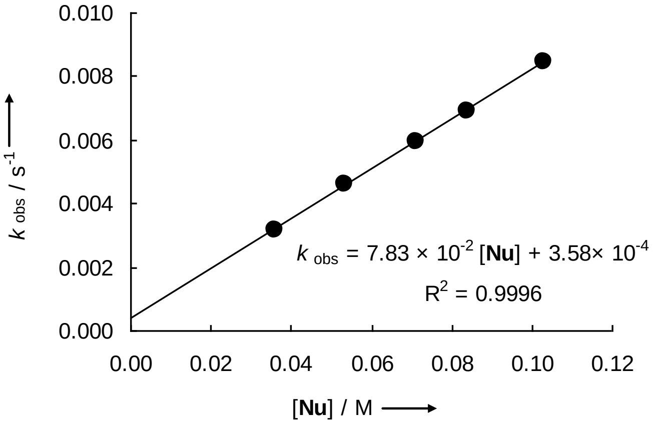

Table 2.S3.3.9. Rate constants for the reaction of 4-cyanobenzyl bromide (**3**-Br) with benzylamine at 20˚C in acetonitrile (conventional conductometer).

No	$[E]_0/M^1$	$[Nu]_0/M$	$[Nu]_0/[E]_0$	k_{obs}/s^{-1}
1	2.95×10^{-4}	3.08×10^{-2}	104	1.07×10^{-3}
2	2.93×10^{-4}	3.67×10^{-2}	125	1.31×10^{-3}
3	2.94×10^{-4}	4.29×10^{-2}	146	1.50×10^{-3}
4	2.91×10^{-4}	4.85×10^{-2}	167	1.62×10^{-3}
5	2.86×10^{-4}	5.96×10^{-2}	208	2.03×10^{-3}
$k_2 = 3.23 \times 10^{-2}$ M^{-1}s^{-1}				

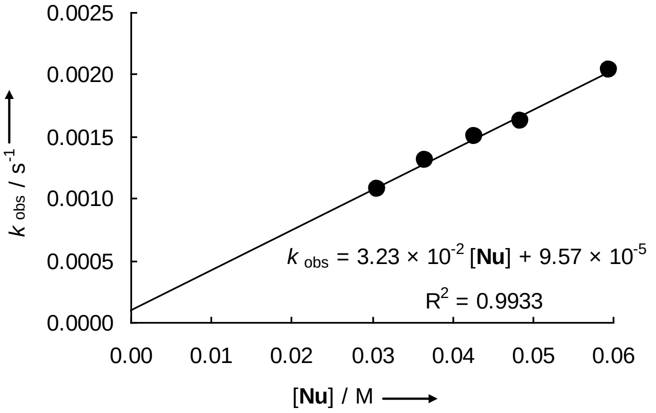

Table 2.S3.3.10. Rate constants for the reaction of 4-cyanobenzyl bromide (**3**-Br) with 2,2,2-trifluoroethylamine at 20˚C in acetonitrile (conventional conductometer).

No	$[E]_0/M^1$	$[Nu]_0/M$	$[Nu]_0/[E]_0$	k_{obs}/s^{-1}
1	3.64×10^{-4}	3.40×10^{-2}	93	2.15×10^{-5}
2	3.87×10^{-4}	6.87×10^{-2}	178	5.29×10^{-5}
3	3.57×10^{-4}	8.67×10^{-2}	243	6.95×10^{-5}
$k_2 = 9.10 \times 10^{-4}$ M^{-1}s^{-1}				

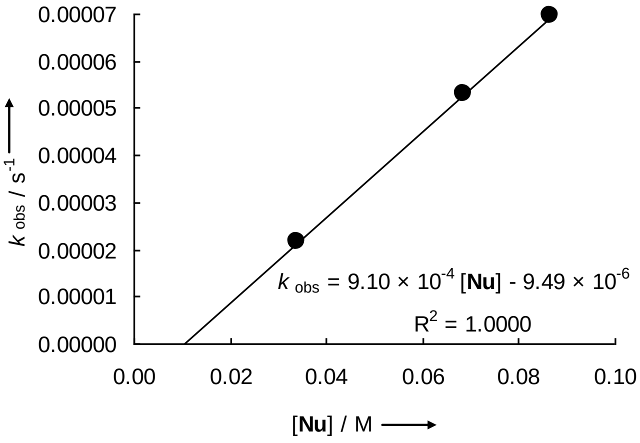

2.S.3.4. Rate constants for the reactions of methyl iodide (5-I) in acetonitrile.

Table 2.S3.4.1. Rate constants for the reaction of methyl iodide (**5**-I) with DABCO at 20˚C in acetonitrile (conventional conductometer).

No	$[E]_0/M^1$	$[Nu]_0/M$	$[Nu]_0/[E]_0$	k_{obs}/s^{-1}
1	7.75×10^{-3}	8.43×10^{-2}	11	1.37×10^{-1}
2	7.75×10^{-4}	1.06×10^{-1}	14	1.75×10^{-1}
3	7.75×10^{-5}	1.34×10^{-1}	17	2.21×10^{-1}
4	7.75×10^{-6}	1.54×10^{-1}	20	2.58×10^{-1}
5	7.75×10^{-7}	1.74×10^{-1}	22	2.92×10^{-1}
		$k_2 = 1.73\ M^{-1}s^{-1}$		

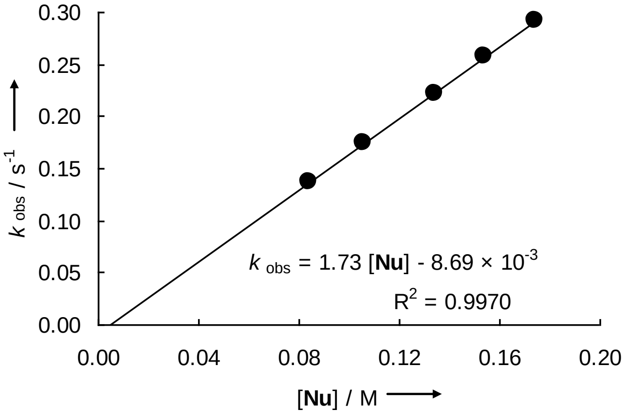

Table 2.S3.4.2. Rate constants for the reaction of methyl iodide (**5**-I) with N-methylpyrrolidine at 20˚C in acetonitrile (conventional conductometer).

No	$[E]_0/M^1$	$[Nu]_0/M$	$[Nu]_0/ [E]_0$	k_{obs}/s^{-1}
1	2.85×10^{-5}	7.80×10^{-4}	27	2.65×10^{-4}
2	2.79×10^{-5}	2.29×10^{-3}	82	7.49×10^{-4}
3	2.77×10^{-5}	3.02×10^{-3}	109	9.85×10^{-4}
4	2.77×10^{-5}	3.79×10^{-3}	137	1.24×10^{-3}
		$k_2 = 3.23 \times 10^{-1}\ M^{-1}s^{-1}$		

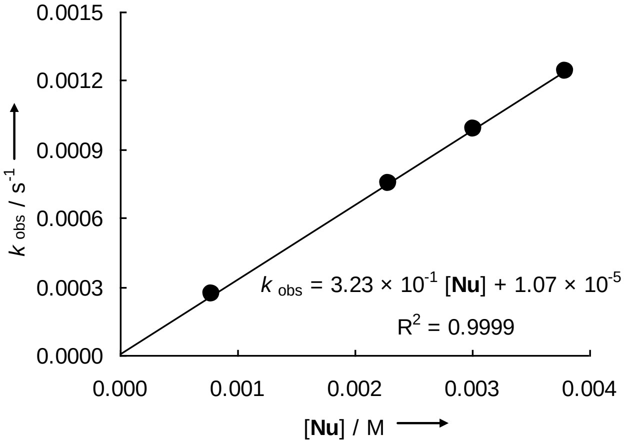

Table 2.S3.4.3. Rate constants for the reaction of methyl iodide (**5**-I) with N-methylpiperidine at 20˚C in acetonitrile (conventional conductometer).

No	$[E]_0/M^1$	$[Nu]_0/M$	$[Nu]_0/ [E]_0$	k_{obs}/s^{-1}
1	4.39×10^{-5}	3.97×10^{-3}	90	3.23×10^{-4}
2	4.13×10^{-5}	1.68×10^{-2}	407	1.26×10^{-3}
3	4.08×10^{-5}	2.21×10^{-2}	542	1.65×10^{-3}
4	3.98×10^{-5}	2.61×10^{-2}	656	1.94×10^{-3}
		$k_2 = 7.31 \times 10^{-2}\ M^{-1}s^{-1}$		

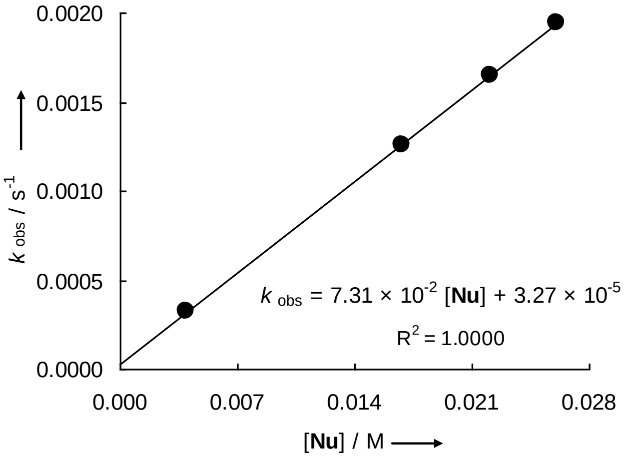

Table 2.S3.4.4. Rate constants for the reaction of methyl iodide (**5**-I) with triethylamine at 20˚C in acetonitrile (conventional conductometer).

No	$[E]_0$/M^1	$[Nu]_0$/M	$[Nu]_0$/ $[E]_0$	k_{obs}/s^{-1}
1	4.72×10^{-5}	1.26×10^{-2}	267	4.13×10^{-4}
2	4.62×10^{-5}	1.85×10^{-2}	400	5.87×10^{-4}
3	4.76×10^{-5}	2.54×10^{-2}	534	8.15×10^{-4}
4	4.65×10^{-5}	3.11×10^{-2}	669	9.73×10^{-4}
$k_2 = 3.06 \times 10^{-2}$ M^{-1}s^{-1}				

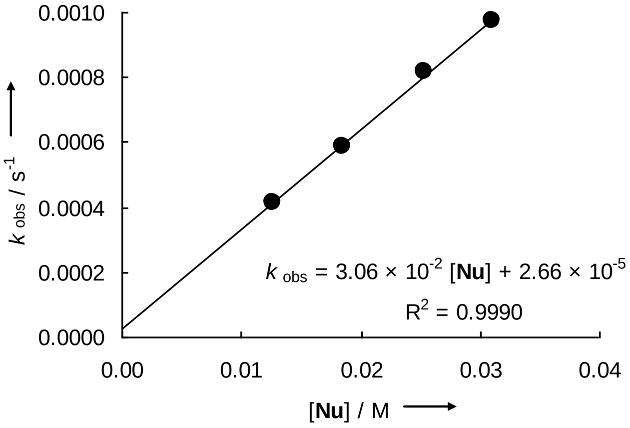

Table 2.S3.4.5. Rate constants for the reaction of methyl iodide (**5**-I) with pyrrolidine at 20˚C in acetonitrile (conventional conductometer).

No	$[E]_0/M^1$	$[Nu]_0/M$	$[Nu]_0/ [E]_0$	k_{obs}/s^{-1}
1	2.99×10^{-5}	2.10×10^{-3}	70	6.94×10^{-4}
2	2.67×10^{-5}	3.75×10^{-3}	140	1.22×10^{-3}
3	2.93×10^{-5}	6.17×10^{-3}	211	2.01×10^{-3}
4	2.87×10^{-5}	8.06×10^{-3}	281	2.61×10^{-3}
$k_2 = 3.22 \times 10^{-1}\ M^{-1}s^{-1}$				

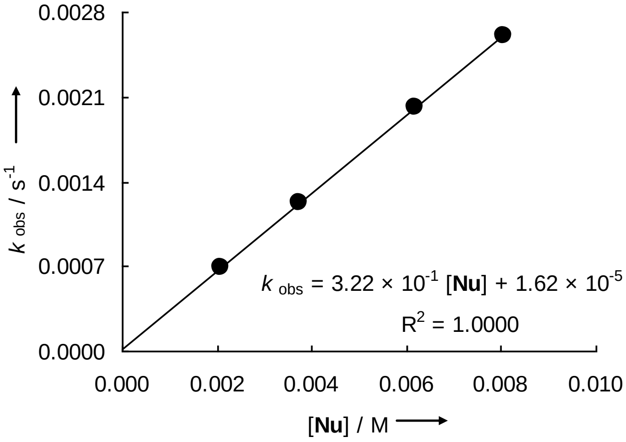

Table 2.S3.4.6. Rate constants for the reaction of methyl iodide (**5**-I) with piperidine at 20˚C in acetonitrile (conventional conductometer).

No	$[E]_0/M^1$	$[Nu]_0/M$	$[Nu]_0/ [E]_0$	k_{obs}/s^{-1}
1	2.47×10^{-4}	5.83×10^{-3}	24	1.68×10^{-3}
2	2.37×10^{-4}	1.12×10^{-2}	47	3.27×10^{-3}
3	2.39×10^{-4}	1.69×10^{-2}	71	4.86×10^{-3}
4	2.27×10^{-4}	2.14×10^{-2}	94	6.13×10^{-3}
5	2.25×10^{-4}	2.65×10^{-2}	118	7.61×10^{-3}
$k_2 = 2.86 \times 10^{-1}\ M^{-1}s^{-1}$				

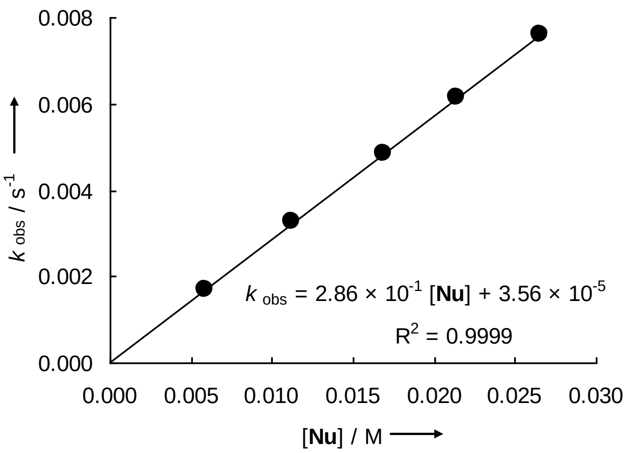

Table 2.S3.4.7. Rate constants for the reaction of methyl iodide (**5**-I) with morpholine at 20˚C in acetonitrile (conventional conductometer).

No	$[E]_0$/M^1	$[Nu]_0$/M	$[Nu]_0$/ $[E]_0$	k_{obs}/s^{-1}
1	2.45×10^{-4}	4.54×10^{-2}	185	2.02×10^{-3}
2	2.39×10^{-4}	6.66×10^{-2}	279	2.86×10^{-3}
3	2.46×10^{-4}	9.14×10^{-2}	372	3.89×10^{-3}
4	2.30×10^{-4}	1.06×10^{-1}	461	4.52×10^{-3}
		$k_2 = 4.12 \times 10^{-2}$ M^{-1}s^{-1}		

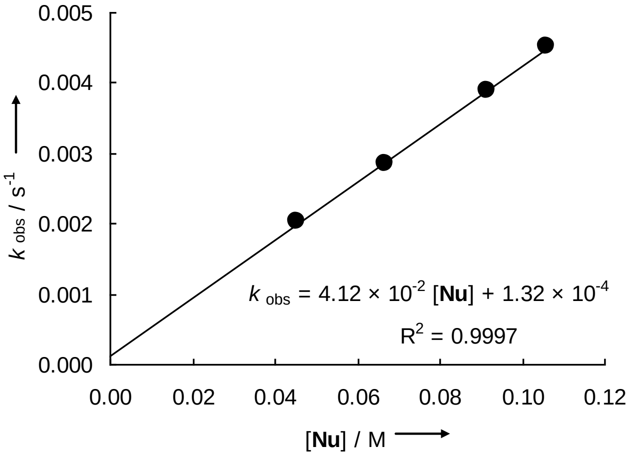

Table 2.S3.4.8. Rate constants for the reaction of methyl iodide (**5**-I) with 2-aminoethanol at 20˚C in acetonitrile (conventional conductometer).

No	$[E]_0$/M^1	$[Nu]_0$/M	$[Nu]_0$/ $[E]_0$	k_{obs}/s^{-1}
1	2.83×10^{-5}	4.08×10^{-3}	144	4.42×10^{-5}
2	2.81×10^{-5}	6.08×10^{-3}	216	6.50×10^{-5}
3	2.80×10^{-5}	8.07×10^{-3}	288	8.53×10^{-5}
		$k_2 = 1.03 \times 10^{-2}$ M^{-1}s^{-1}		

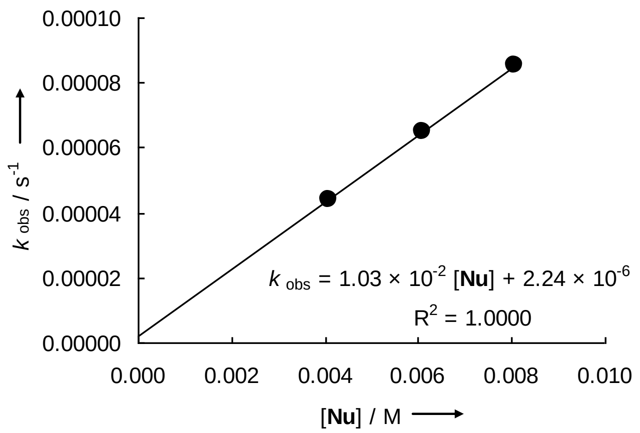

Table 2.S3.4.9. Rate constants for the reaction of methyl iodide (**5**-I) with di-*n*-propylamine at 20˚C in acetonitrile (conventional conductometer).

No	$[E]_0/M^1$	$[Nu]_0/M$	$[Nu]_0/[E]_0$	k_{obs}/s^{-1}
1	1.61×10^{-4}	6.05×10^{-3}	38	2.49×10^{-4}
2	1.57×10^{-4}	1.16×10^{-2}	74	4.50×10^{-4}
3	1.53×10^{-4}	1.69×10^{-2}	110	7.01×10^{-4}
4	1.52×10^{-4}	2.27×10^{-2}	149	9.06×10^{-4}
5	1.50×10^{-4}	2.76×10^{-2}	184	1.08×10^{-3}

$k_2 = 3.91 \times 10^{-2}\ M^{-1}s^{-1}$

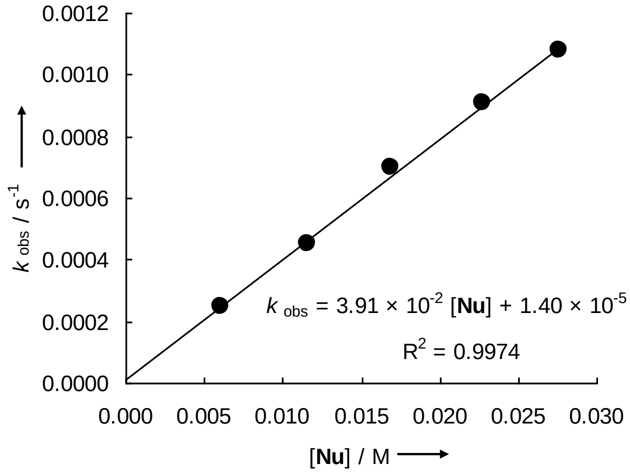

Table 2.S3.4.10. Rate constants for the reaction of methyl iodide (**5**-I) with *n*-butylamine at 20˚C in acetonitrile (conventional conductometer).

No	$[E]_0/M^1$	$[Nu]_0/M$	$[Nu]_0/[E]_0$	k_{obs}/s^{-1}
1	2.76×10^{-4}	1.43×10^{-2}	52	3.17×10^{-4}
2	2.73×10^{-4}	2.82×10^{-2}	103	6.00×10^{-4}
3	2.62×10^{-4}	4.07×10^{-2}	155	8.77×10^{-4}
4	2.56×10^{-4}	5.29×10^{-2}	207	1.15×10^{-3}
5	2.55×10^{-4}	6.59×10^{-2}	258	1.44×10^{-3}
		$k_2 = 2.19 \times 10^{-2}\ M^{-1}s^{-1}$		

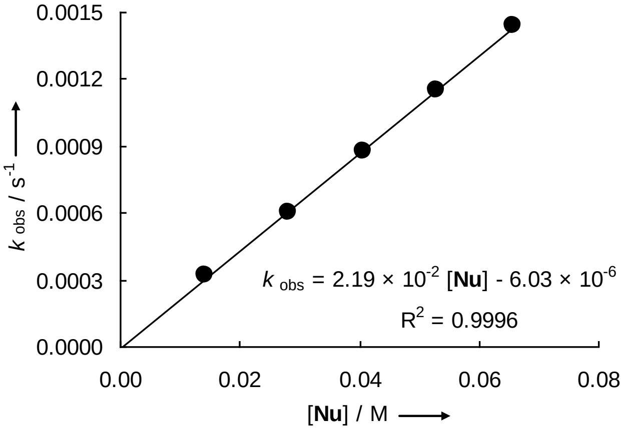

Table 2.S3.4.11. Rate constants for the reaction of methyl iodide (**5**-I) with *n*-propylamine at 20˚C in acetonitrile (conventional conductometer).

No	$[E]_0/M^1$	$[Nu]_0/M$	$[Nu]_0/[E]_0$	k_{obs}/s^{-1}
1	2.68×10^{-4}	1.10×10^{-2}	41	2.13×10^{-4}
2	2.62×10^{-4}	2.40×10^{-2}	92	4.74×10^{-4}
3	2.58×10^{-4}	3.56×10^{-2}	138	6.95×10^{-4}
4	2.49×10^{-4}	5.10×10^{-2}	205	9.85×10^{-4}
		$k_2 = 1.93 \times 10^{-2}\ M^{-1}s^{-1}$		

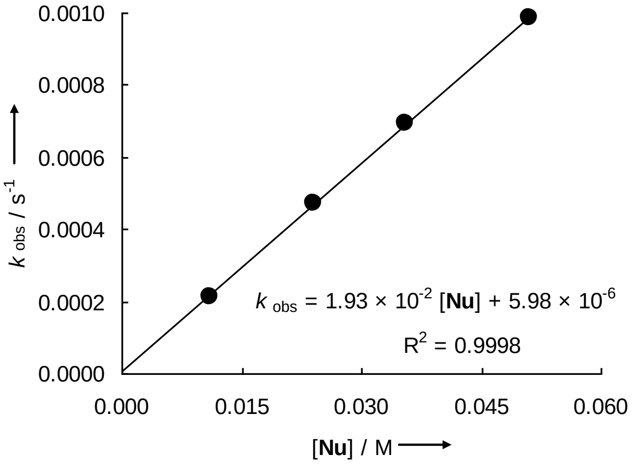

Table 2.S3.4.12. Rate constants for the reaction of methyl iodide (**5**-I) with benzylamine at 20˚C in acetonitrile (conventional conductometer).

No	$[E]_0/M^1$	$[Nu]_0/M$	$[Nu]_0/[E]_0$	k_{obs}/s^{-1}
1	2.52×10^{-4}	2.06×10^{-2}	82	1.64×10^{-4}
2	2.49×10^{-4}	4.07×10^{-2}	163	3.28×10^{-4}
3	2.47×10^{-4}	6.07×10^{-2}	246	4.81×10^{-4}
4	2.38×10^{-4}	9.73×10^{-2}	409	7.69×10^{-4}
$k_2 = 7.87 \times 10^{-3}\ M^{-1}s^{-1}$				

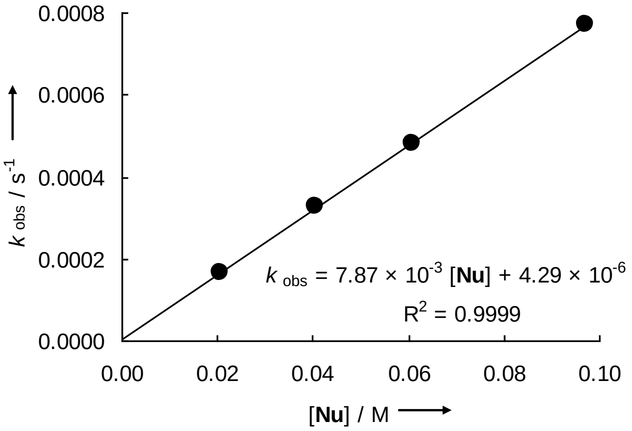

Table 2.S3.4.13. Rate constants for the reaction of methyl iodide (**5**-I) with 4-DMAP at 20˚C in acetonitrile (conventional conductometer).

No	$[E]_0/M^1$	$[Nu]_0/M$	$[Nu]_0/[E]_0$	k_{obs}/s^{-1}
1	2.05×10^{-5}	7.50×10^{-3}	366	5.89×10^{-5}
2	1.99×10^{-5}	1.09×10^{-2}	548	8.26×10^{-5}
3	1.91×10^{-5}	1.40×10^{-2}	733	1.06×10^{-4}
$k_2 = 7.24 \times 10^{-3}\ M^{-1}s^{-1}$				

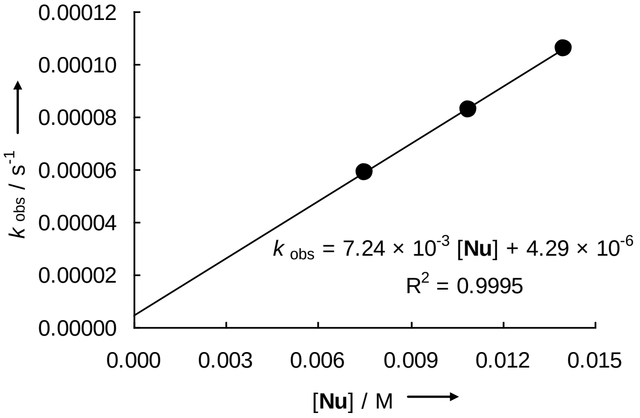

Table 2.S3.4.14. Rate constants for the reaction of methyl iodide (**5**-I) with *tert*-butylamine at 20˚C in acetonitrile (conventional conductometer).

No	$[E]_0/M^1$	$[Nu]_0/M$	$[Nu]_0/[E]_0$	k_{obs}/s^{-1}
1	2.73×10^{-5}	5.50×10^{-3}	201	3.44×10^{-5}
2	2.69×10^{-5}	1.08×10^{-2}	401	6.64×10^{-5}
3	2.64×10^{-5}	1.59×10^{-2}	602	1.01×10^{-4}
$k_2 = 6.40 \times 10^{-3}\ M^{-1}s^{-1}$				

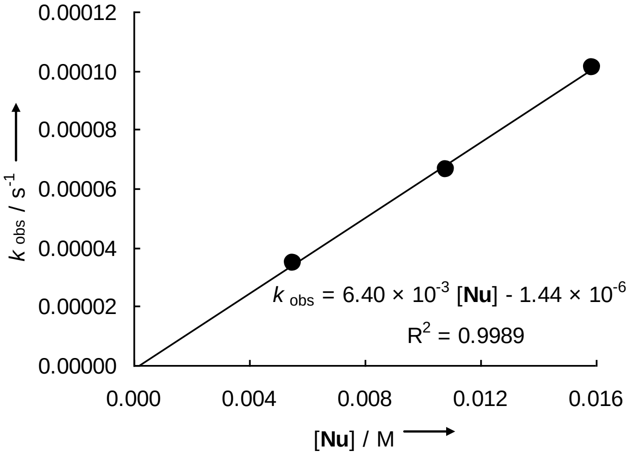

Table 2.S3.4.15. Rate constants for the reaction of methyl iodide (**5**-I) with tri-*n*-butylphosphane at 20˚C in acetonitrile (conventional conductometer).

No	$[E]_0/M^1$	$[Nu]_0/M$	$[Nu]_0/[E]_0$	k_{obs}/s^{-1}
1	2.07×10^{-5}	3.34×10^{-3}	161	1.05×10^{-3}
2	2.06×10^{-5}	5.82×10^{-3}	283	2.19×10^{-3}
3	2.15×10^{-5}	8.79×10^{-3}	409	3.43×10^{-3}
$k_2 = 4.36 \times 10^{-1}\ M^{-1}s^{-1}$				

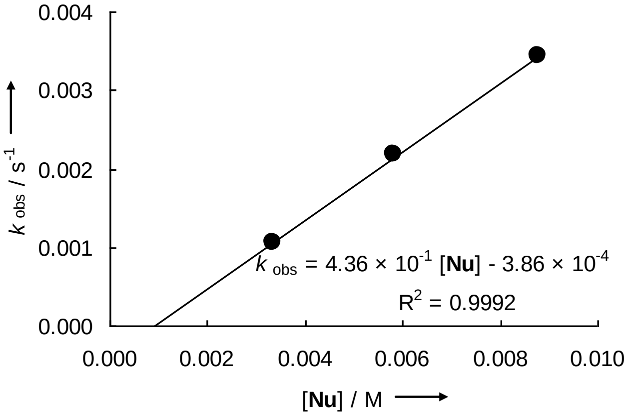

Table 2.S3.4.16. Rate constants for the reaction of methyl iodide (**5**-I) with tris(4-methoxyphenyl)phosphane at 20˚C in acetonitrile (conventional conductometer).

No	$[E]_0/M^1$	$[Nu]_0/M$	$[Nu]_0/[E]_0$	k_{obs}/s^{-1}
1	3.25×10^{-4}	4.15×10^{-3}	13	8.83×10^{-5}
2	3.41×10^{-4}	7.02×10^{-3}	21	1.51×10^{-4}
$k_2 = 2.18 \times 10^{-2}\ M^{-1}s^{-1}$				

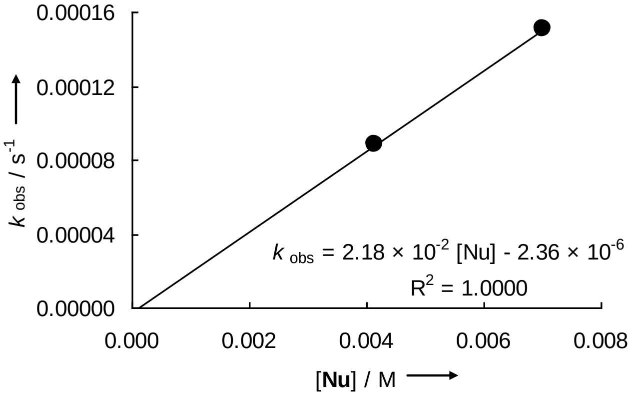

Table 2.S3.4.17. Rate constants for the reaction of methyl iodide (**5**-I) with triphenylphosphane at 20˚C in acetonitrile (conventional conductometer).

No	$[E]_0/M^1$	$[Nu]_0/M$	$[Nu]_0/ [E]_0$	k_{obs}/s^{-1}
1	8.00×10^{-5}	1.37×10^{-2}	171	6.05×10^{-5}
2	1.02×10^{-4}	2.22×10^{-2}	218	9.24×10^{-5}
3	2.52×10^{-4}	3.93×10^{-2}	156	1.92×10^{-4}
$k_2 = 5.24 \times 10^{-3}\ M^{-1}s^{-1}$				

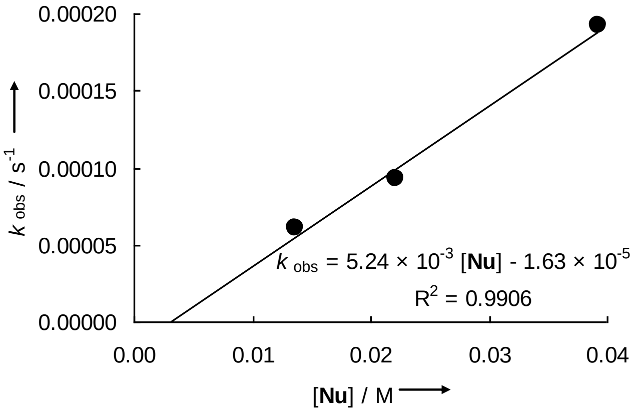

2.S.4. Rate constants for the reaction of amines and phosphanes with lil$_2$CH$^+$ in DMSO and acetonitrile.

Table 2.S.4.1. Calculated and experimental rate constants for the reactions of N-nucleophiles with lil$_2$CH$^+$ in DMSO.

Nucleophile	N	s_N	log $k_{2\text{ (lil)}_2\text{CH}^+\text{ calc.}}$ [a]	log $k_{2\text{ (lil)}_2\text{CH}^+\text{ exp.}}$
DBN	20.40	0.39	4.04	3.99[b]
methylhydrazine	19.89	0.52	5.12	4.96[b]
TBD	19.15	0.57	5.19	4.99[b]
piperidine	17.19	0.71	5.08	5.05[c]
morpholine	16.96	0.67	4.64	4.66[c]
DABCO	16.62	0.89	5.86	n/a[d]
2-aminoethanol	16.07	0.61	3.68	3.67[e]
n-propylamine	15.70	0.64	3.62	3.59[c]
diethanolamine	15.51	0.70	3.83	3.79[e]
1-aminopropan-2-ol	15.47	0.65	3.53	3.52[e]
benzylamine	15.28	0.65	3.41	3.40[e]
DBU	15.11	0.67	3.4	3.41[b]
4-DMAP	14.80	0.67	3.19	n/a[f]
2-aminobutan-1-ol	14.39	0.67	2.91	2.92[e]
2,2,2-trifluoroethylamine	12.15	0.65	1.37	1.35[c]
imidazole	11.58	0.79	1.22	n/a[f]
2-methylbenzimidazole	10.02	0.85	-0.02	n/a[f]

(a) Calculated using Equation 1. (b) The values are taken from Chapter 1 of this thesis. (c) From Ref. 25. (d) The value couldn't be measured for thermodynamic reasons. (e) From Ref. 7a. (f) The value was not determined.

Table 2.S.4.2. Calculated second-order rate constants for the reactions of N- and P-nucleophiles with lil$_2$CH$^+$ in acetonitrile.

Nucleophile	N	s_N	log $k_{2\ (\mathrm{lil})_2\mathrm{CH}^+\ \mathrm{calc.}}$ [a]	log $k_{2\ (\mathrm{lil})_2\mathrm{CH}^+\ \mathrm{exp.}}$
DABCO	18.80	0.70	6.13	n/a[b]
methylhydrazine	17.73	0.58	4.46	4.52
N-methylpyrrolidine	20.59	0.52	5.49	n/a[b]
N-methylpiperidine	18.72	0.52	4.51	n/a[b]
triethylamine	17.10	0.52	3.67	n/a[b]
pyrrolidine	18.64	0.60	5.16	5.07[c]
piperidine	17.35	0.68	4.97	4.89[c]
morpholine	15.65	0.74	4.15	4.06[c]
2-aminoethanol	14.11	0.71	2.89	2.77[c]
dipropylamine	14.51	0.80	3.58	3.60[c]
n-butylamine	15.27	0.63	3.29	n/a[b]
n-propylamine	15.11	0.63	3.19	3.14[c]
benzylamine	14.29	0.67	2.85	2.81[c]
4-DMAP	15.51	0.62	3.39	3.32[d]
tert-butylamine	12.35	0.72	1.66	1.62 [c]
imidazole	11.47	0.79	1.13	n/a[b]
2,2,2-trifluoroethylamine	10.13	0.75	0.07	n/a[b]
tributylphosphane	17.94	0.54	4.27	n/a[b]
tris(4-methoxyphenyl)phosphane	17.14	0.55	3.91	3.80[e]
triphenylphosphane	15.43	0.54	2.91	2.84[e]

(a) Calculated using Equation 1. (b) The value was not determined. (c) From Ref. 26. (d) From Ref. 27. (e) The values are taken from Chapter 1 of this thesis.

Table 2.S.4.3. Calculated rate constants (second-order, if not mentioned otherwise) for the reactions of the nucleophiles used in Ref. 6 with lil_2CH^+ in methanol.

Nucleophile	*N*	s_N	log $k_{(\text{lil})_2\text{CH}^+\ \text{calc.}}$ [a]	log $k_{(\text{lil})_2\text{CH}^+\ \text{exp.}}$
$(\text{MeO}_2\text{C})_2\text{CH}^-$	18.24	0.64	5.25	5.26 [b]
$(\text{NC})_2\text{CH}^-$	18.21	0.68	5.56	5.64 [b]
pyrrolidine	15.97 [c,d]	0.62 [c,d]	3.68	3.71 [c,d]
piperidine	15.63 [c,d]	0.64 [c,d]	3.58	3.58 [c,d]
morpholine	15.40 [c,d]	0.64 [c,d]	3.43	3.42 [c,d]
azide	14.54 [c,e]	0.82	3.69	3.72 [c,e]
methoxide	14.51	0.68	3.04	3.07 [c,f]
diethanolamine	13.71 [c,d]	0.67 [c,d]	2.46	2.48 [c,d]
hydrazine	13.47 [c,d]	0.7 [c,d]	2.40	2.42 [c,d]
benzylamine	13.46 [c,d]	0.62 [c,d]	2.12	2.13 [c,d]
n-propylamine	13.41 [c,d]	0.65 [c,d]	2.19	2.24 [c,d]
ethanolamine	13.23 [c,d]	0.64 [c,d]	2.04	2.05 [c,d]
hydroxylamine	12.23 [c,d]	0.66 [c,d]	1.45	1.47 [c,d]
imidazole	10.41 [c,d]	0.69 [c,d]	0.26	0.27 [c,d]
2,2,2-trifluoroethylamine	10.20 [c,d]	0.91 [c,d]	0.15	n/a [g]
trimethylphosphite	9.04 [c,d]	0.69 [c,d]	-0.69	-0.70 [c,d]
methanol	7.54 [h,i]	0.92 [h]	-2.30 [j]	-2.21 [i,j]
ethanol	7.44 [h,i]	0.90 [h]	-2.34 [j]	-2.24 [i,j]
propan-1-ol	7.05 [h,k]	0.80 [h,k]	-2.39 [j]	-2.44 [f,j]
80E20W [l]	6.68 [h]	0.85 [h]	-2.86 [j]	-2.78 [i,j]
propan-2-ol	6.49 [h,k]	0.96 [h,k]	-3.41 [j]	n/a [g]
60E40W [l]	6.28 [h,i]	0.87 [h]	-3.27 [j]	-3.15 [i,j]
40E60W [l]	5.81 [h,i]	0.90 [h]	-3.81 [j]	n/a [g]
80A20W [l]	5.77 [h,m]	0.87 [h]	-3.71 [j]	-3.72 [j,m]
90A10W [l]	5.70 [h,m]	0.85 [h]	-3.69 [j]	-3.66 [j,m]
20E80W [l]	5.54 [h,i]	0.94 [h]	-4.23 [j]	n/a [g]
water	5.20 [h,i]	0.89 [h]	-4.31 [j]	n/a [g]
40T60W [l]	3.77 [h,i]	0.88 [h]	-5.52 [j]	n/a [g]
60T40W [l]	3.42 [h,i]	0.90 [h]	-5.96 [j]	n/a [g]
90T10W [l]	2.93 [h,i]	0.88 [h]	-6.26 [j]	n/a [g]
T	1.23 [h,i]	0.92 [h]	-8.11 [j]	n/a [g]

(a) Calculated using Equation 1. (b) From Ref. 28. (c) Reactivity parameters refer to 91/9 (v/v) methanol/acetonitrile. (d) from Ref. 6. (e) From Ref. 29. (f) From Ref. 30. (g) The value was not determined. (h) Reactivity parameters *N* and s_N refer to first-order rate constants. (i) From Ref. 31. (j) First-order rate constant. (k) Reactivity parameters *N* and s_N and log $k_{(\text{lil})_2\text{CH}^+}$ refer to 91/9 (v/v) alcohol/acetonitrile mixtures, from Ref. 30. (l) Mixtures of solvents are given as (v/v); solvents: A=acetone, E=ethanol, T=2,2,2-trifluoroethanol, W=water. (m) From Ref. 32.

2.S.5. Correlations of log k_2/s_N versus N for S_N2 reactions and of log $k_{2(S_N2)}$ versus log $k_{(lil_2CH^+)}$.

2.S.5.1. Correlations for benzyl chloride (1-Cl).

Table 2.S5.1. Rate constants for the reactions of **1**-Cl and $(lil)_2CH^+$ with amines at 20˚C in DMSO.

Nucleophile	N	s_N	$k_{2\,(\mathbf{1}\text{-Cl})}$	log $k_{2\,(\mathbf{1}\text{-Cl})}$	log $k_{2\,(lil)2CH+}$ [a]
DABCO	16.62	0.89	1.31×10^{-1}	-0.88	5.86
methylhydrazine	19.89	0.52	1.77×10^{-2}	-1.75	5.12
piperidine	17.19	0.71	1.94×10^{-2}	-1.71	5.08
morpholine	16.96	0.67	6.66×10^{-3}	-2.18	4.64
n-propylamine	15.70	0.64	1.59×10^{-3}	-2.80	3.62
benzylamine	15.28	0.65	8.29×10^{-4}	-3.08	3.41

(a) Calculated using Equation 1.

A)

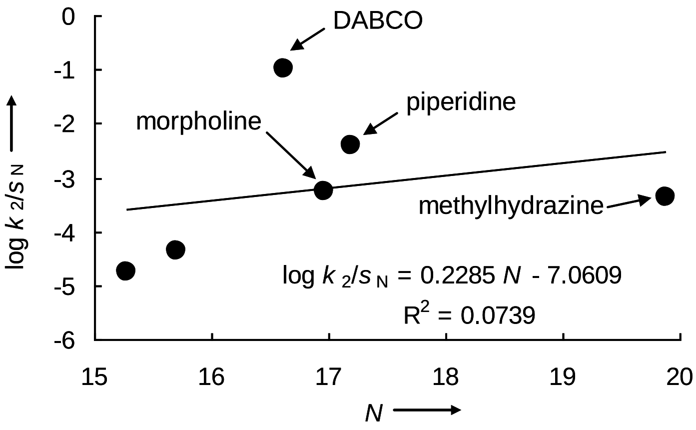

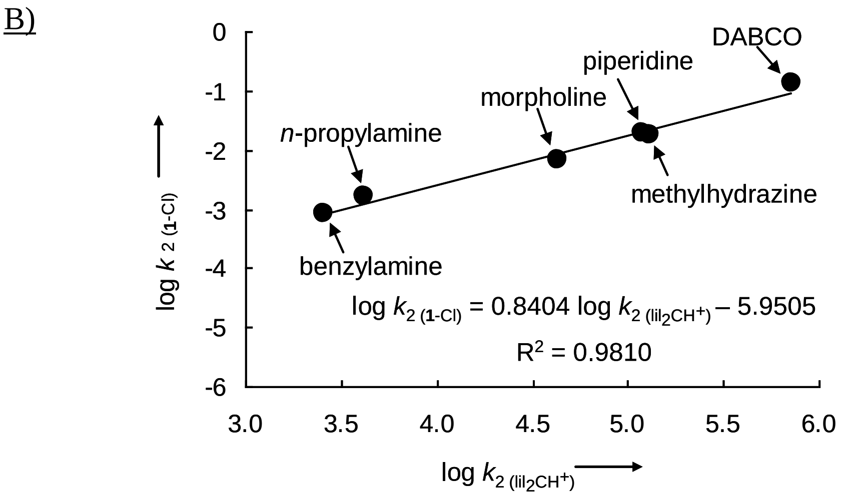

Figure 2.S5.1. A) Correlation of log k_2/s_N versus N for the reactions of **1**-Cl with amines at 20˚C in DMSO. B) Correlation of log k_2 for the reactions of amines with **1**-Cl versus log k_2 for their reactions with lil$_2$CH$^+$ at 20˚C in DMSO.

2.S.5.2. Correlations for 4-cyanobenzyl chloride (2-Cl).

Table 2.S5.2. Rate constants for the reactions of **2**-Cl and (lil)$_2$CH$^+$ with amines at 20˚C in DMSO.

Nucleophile	N	s_N	$k_{2\,(\mathbf{2}\text{-Cl})}$	log $k_{2\,(\mathbf{2}\text{-Cl})}$	log $k_{2\,(\text{lil})_2\text{CH}^+}$ [a]
DABCO	16.62	0.89	1.64×10^{-1}	-0.79	5.86
methylhydrazine	19.89	0.52	3.18×10^{-2}	-1.5	5.12
piperidine	17.19	0.71	4.54×10^{-2}	-1.34	5.08
morpholine	16.96	0.67	8.04×10^{-3}	-2.09	4.64
2-aminoethanol	16.07	0.61	2.15×10^{-3}	-2.67	3.68
1-aminopropan-2-ol	15.47	0.65	1.90×10^{-3}	-2.72	3.53
n-propylamine	15.70	0.64	2.26×10^{-3}	-2.65	3.62
2-aminobutan-1-ol	14.39	0.67	5.06×10^{-4}	-3.3	2.91

(a) Calculated using Equation 1.

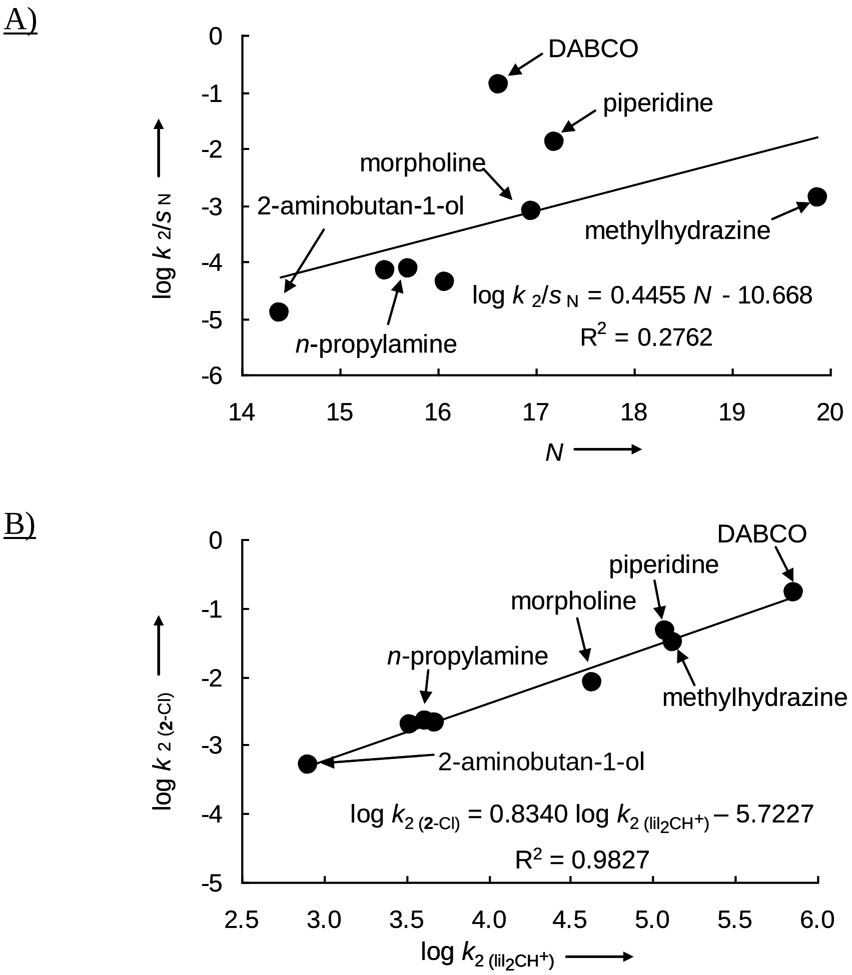

Figure 2.S5.2. A) Correlation of log k_2/s_N versus N for the reactions of **2**-Cl with amines at 20˚C in DMSO. B) Correlation of log k_2 for the reactions of amines with **2**-Cl versus log k_2 for their reactions with lil$_2$CH$^+$ at 20˚C in DMSO.

2.S.5.3. Correlations for 4-methoxybenzyl chloride (3-Cl).

Table 2.S5.3. Rate constants for the reactions of **3**-Cl and (lil)$_2$CH$^+$ with amines at 20˚C in DMSO.

Nucleophile	N	s_N	$k_{2\,(\mathbf{3}\text{-Cl})}$	log $k_{2\,(\mathbf{3}\text{-Cl})}$	log $k_{2\,(\text{lil})_2\text{CH}^+}$ [a]
DABCO	16.62	0.89	2.96×10^{-1}	-0.53	5.86
methylhydrazine	19.89	0.52	3.62×10^{-2}	-1.44	5.12
piperidine	17.19	0.71	4.82×10^{-2}	-1.32	5.08
n-propylamine	15.70	0.64	3.25×10^{-3}	-2.49	3.62
benzylamine	15.28	0.65	1.72×10^{-3}	-2.76	3.41
imidazole	11.58	0.79	4.75×10^{-5}	-4.32	1.22

(a) Calculated using Equation 1.

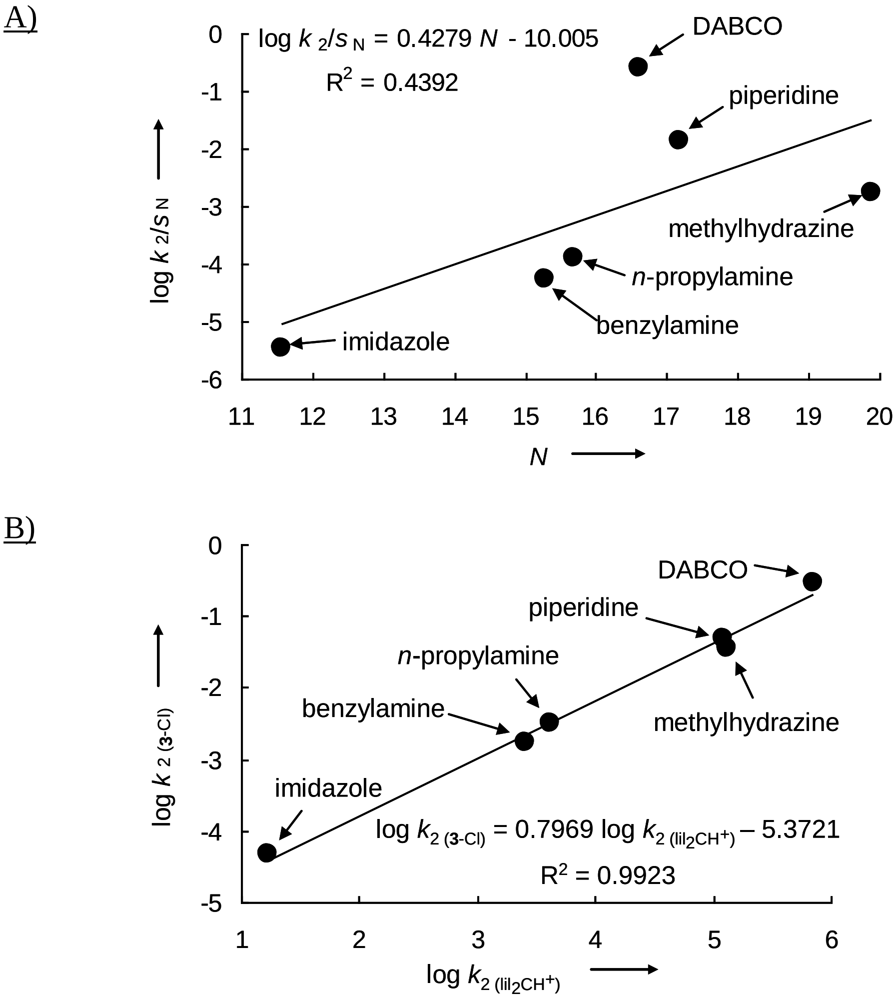

Figure 2.S5.3. A) Correlation of log k_2/s_N versus N for the reactions of 3-Cl with amines at 20˚C in DMSO. B) Correlation of log k_2 for the reactions of amines with **3**-Cl versus log k_2 for their reactions with lil_2CH^+ at 20˚C in DMSO.

2.S.5.4. Correlations for phenacyl chloride (4-Cl).

Table 2.S5.4. Rate constants for the reactions of **4**-Cl and (lil)$_2$CH$^+$ with amines at 20˚C in DMSO.

Nucleophile	*N*	s_N	$k_{2\,(\mathbf{4}\text{-Cl})}$	log $k_{2\,(\mathbf{4}\text{-Cl})}$	log $k_{2\,(\text{lil})_2\text{CH}^+}$ [a]
piperidine	17.19	0.71	1.54×10^{-1}	-0.81	5.08
morpholine	16.96	0.67	3.31×10^{-2}	-1.48	4.64
2-aminoethanol	16.07	0.61	1.71×10^{-2}	-1.77	3.68
1-aminopropan-2-ol	15.47	0.65	1.51×10^{-2}	-1.82	3.53
n-propylamine	15.70	0.64	2.72×10^{-2}	-1.57	3.62
benzylamine	15.28	0.65	7.48×10^{-3}	-2.13	3.41
2-aminobutan-1-ol	14.39	0.67	2.78×10^{-3}	-2.56	2.91
4-DMAP	14.80	0.67	5.88×10^{-3}	-2.23	3.19
diethanolamine	15.51	0.70	1.89×10^{-3}	-2.72	3.83
2,2,2-trifluoroethylamine	12.15	0.65	5.30×10^{-5}	-4.28	1.37
imidazole	11.58	0.79	3.98×10^{-4}	-3.4	1.22

(a) Calculated using Equation 1.

A)

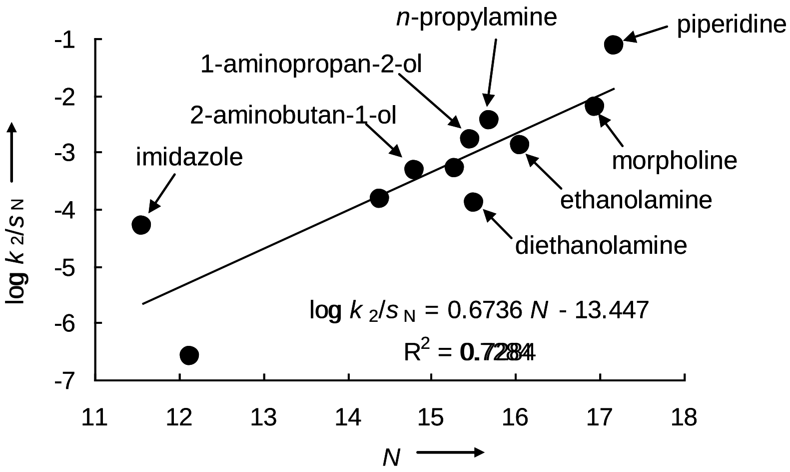

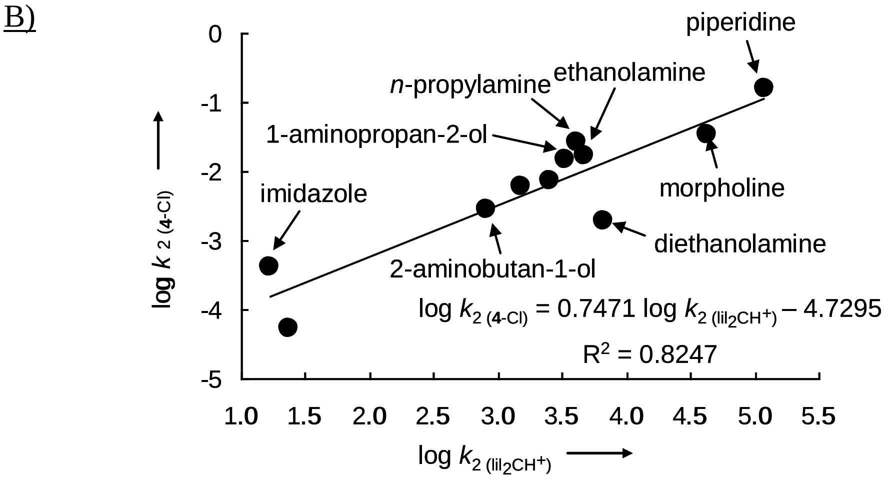

Figure 2.S5.4. A) Correlation of log k_2/s_N versus N for the reactions of 4-Cl with amines at 20˚C in DMSO. B) Correlation of log k_2 for the reactions of amines with 4-Cl versus log k_2 for their reactions with lil_2CH^+ at 20˚C in DMS

2.S.5.5. Correlations for benzyl bromide (1-Br).

Table 2.S5.5.1. Rate constants for the reactions of **1**-Br and $(lil)_2CH^+$ with amines at 20˚C in DMSO.

Nucleophiles	N	s_N	$k_{2\,(\mathbf{1}\text{-Br})}$	log $k_{2\,(\mathbf{1}\text{-Br})}$	log $k_{2\,(lil)_2CH^+}$ [a]
1,1-dimethylhydrazine	-	-	3.73	0.57	-
methylhydrazine	19.89	0.52	1.92	0.28	5.12
TBD	19.15	0.57	1.71	0.23	5.19
DBN	20.40	0.39	4.52×10^{-1}	-0.34	4.04
TMG	-	-	1.21×10^{-2}	-1.92	-

(a) Calculated using Equation 1.

For the reactions of amines with **1**-Br at 20˚C in DMSO, correlations of log k_2/s_N versus N and of log $k_{2\,(S_N2)}$ versus log $k_{2\,(lil2CH+)}$ do not make sense because of the paucity of data and a narrow reactivity range.

Table 2.S5.5.2. Rate constants for the reactions of **1**-Br and $(\text{lil})_2\text{CH}^+$ with amines at 20˚C in acetonitrile.

Nucleophile	N	s_N	$k_{2\,(\mathbf{1}\text{-Br})}$	$\log k_{2\,(\mathbf{1}\text{-Br})}$	$\log k_{2\,(\text{lil})_2\text{CH}^+}$ [a]
DABCO	18.80	0.70	4.45	0.65	6.13
methylhydrazine	17.73	0.58	1.74×10^{-1}	-0.76	4.46
piperidine	17.35	0.68	7.20×10^{-1}	-0.14	4.97
morpholine	15.65	0.74	1.33×10^{-1}	-0.88	4.15
2-aminoethanol	14.11	0.71	1.98×10^{-2}	-1.70	2.89
n-butylamine	15.27	0.63	3.67×10^{-2}	-1.44	3.29
n-propylamine	15.11	0.63	2.86×10^{-2}	-1.54	3.19

(a) Calculated using Equation 1.

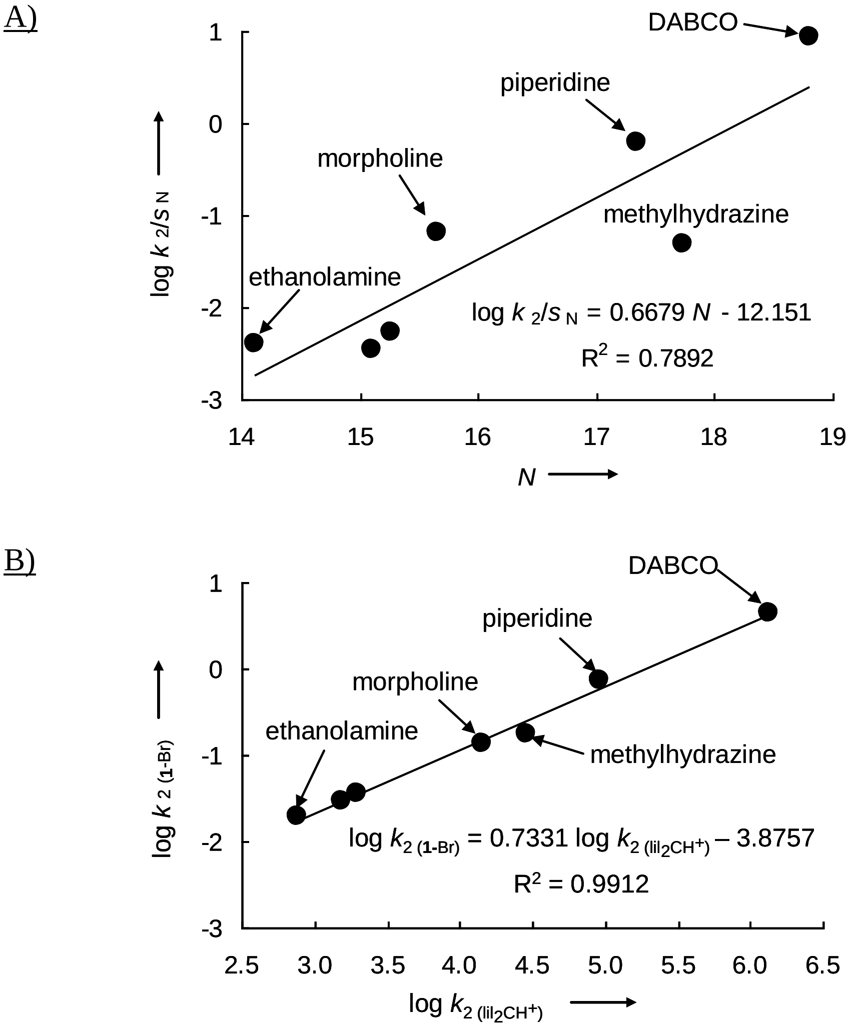

Figure 2.S5.5.2. A) Correlation of log k_2/s_N versus N for the reactions of **1**-Br with amines at 20˚C in acetonitrile. B) Correlation of log k_2 for the reactions of amines with **1**-Br versus log k_2 for their reactions with lil_2CH^+ at 20˚C in acetonitrile.

2.S.5.6. Correlations for 4-cyanobenzyl bromide (2-Br).

Table 2.S5.6.1. Rate constants for the reactions of **2**-Br and $(lil)_2CH^+$ with amines at 20˚C in DMSO.

Nucleophile	N	s_N	$k_{2\ (\mathbf{2}\text{-Br})}$	$\log k_{2\ (\mathbf{2}\text{-Br})}$	$\log k_{2\ (lil)_2CH^+}$ [a]
DABCO	16.62	0.89	2.55×10^{1}	1.41	5.86
1,1-dimethylhydrazine	-	-	4.66	0.67	-
methylhydrazine	19.89	0.52	3.38	0.53	5.12
TBD	19.15	0.57	4.19	0.62	5.19
piperidine	17.19	0.71	4.15	0.62	5.08
morpholine	16.96	0.67	1.05	0.02	4.64
DBN	20.40	0.39	7.15×10^{-1}	-0.15	4.04
DBU	15.11	0.67	1.10×10^{-1}	-0.96	3.4
2-aminoethanol	16.07	0.61	2.85×10^{-1}	-0.55	3.68
1-aminopropan-2-ol	15.47	0.65	3.29×10^{-1}	-0.48	3.53
n-propylamine	15.70	0.64	3.07×10^{-1}	-0.51	3.62
benzylamine	15.28	0.65	1.71×10^{-1}	-0.77	3.41
2-aminobutan-1-ol	14.39	0.67	7.62×10^{-2}	-1.12	2.91
4-DMAP	14.80	0.67	5.81×10^{-2}	-1.24	3.19
TMG	-	-	1.81×10^{-2}	-1.74	-
diethanolamine	15.51	0.70	1.50×10^{-1}	-0.82	3.83
2,2,2-trifluoroethylamine	12.15	0.65	2.40×10^{-3}	-2.62	1.37
imidazole	11.58	0.79	4.25×10^{-3}	-2.37	1.22
2-methylbenzimidazole	10.02	0.85	2.66×10^{-4}	-3.58	-0.02

(a) Calculated using Equation 1.

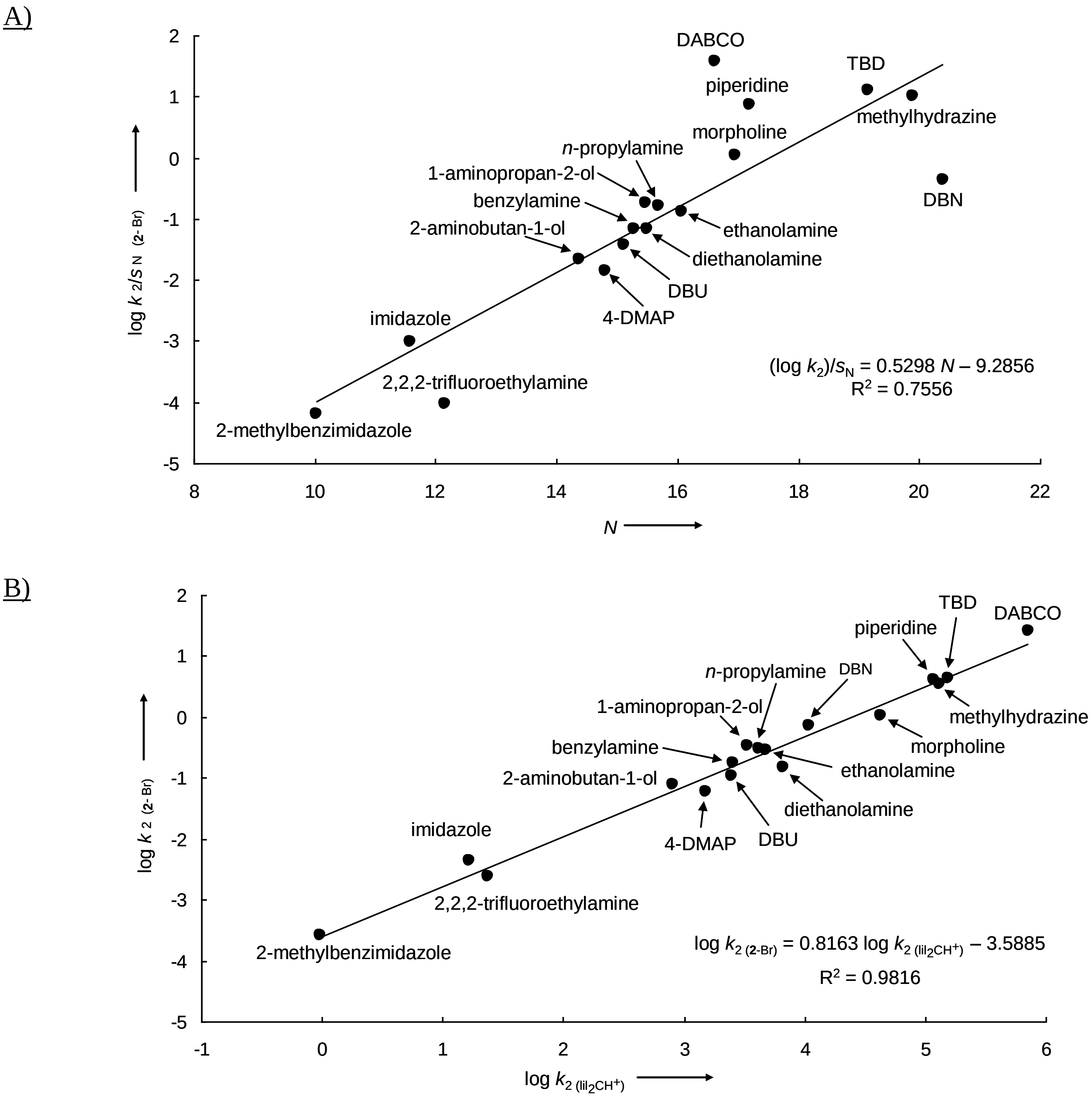

Figure 2.S5.6.1. A) Correlation of log k_2/s_N versus N for the reactions of **2**-Br with amines at 20°C in DMSO. B) Correlation of log k_2 for the reactions of amines with **2**-Br versus log k_2 for their reactions with lil$_2$CH$^+$ at 20°C in DMSO.

Table 2.S5.6.2. Rate constants for the reactions of **3**-Br and $(\text{lil})_2\text{CH}^+$ with amines and phosphanes at 20˚C in acetonitrile.

Nucleophile	N	s_N	$k_{2\,(\mathbf{2}\text{-Br})}$	log $k_{2\,(\mathbf{2}\text{-Br})}$	log $k_{2\,(\text{lil})_2\text{CH}^+}$ [a]
DABCO	18.80	0.70	3.69	0.57	6.13
methylhydrazine	17.73	0.58	2.20×10^{-1}	-0.66	4.46
N-methylpyrrolidine	20.59	0.52	2.55×10^{-1}	-0.59	5.49
triethylamine	17.10	0.52	2.27×10^{-3}	-2.64	3.67
tributylamine	-	-	1.61×10^{-3}	-2.79	-
pyrrolidine	18.64	0.60	7.55×10^{-1}	-0.12	5.16
piperidine	17.35	0.68	7.70×10^{-1}	-0.11	4.97
morpholine	15.65	0.74	1.09×10^{-1}	-0.96	4.15
2-aminoethanol	14.11	0.71	1.48×10^{-2}	-1.83	2.89
dipropylamine	14.51	0.80	2.82×10^{-2}	-1.55	3.58
n-propylamine	15.11	0.63	3.20×10^{-2}	-1.49	3.19
benzylamine	14.29	0.67	9.54×10^{-3}	-2.02	2.85
4-DMAP	15.51	0.62	1.67×10^{-2}	-1.78	3.39
tert-butylamine	12.35	0.72	3.09×10^{-3}	-2.51	1.66
imidazole	11.47	0.79	6.46×10^{-4}	-3.19	1.13
tributylphosphane	17.94	0.54	2.73×10^{-1}	-0.56	4.27
tris(4-methoxyphenyl)phosphane	17.14	0.55	1.33×10^{-2}	-1.88	3.91
triphenylphosphane	15.43	0.54	1.68×10^{-3}	-2.77	2.91

(a) Calculated using Equation 1.

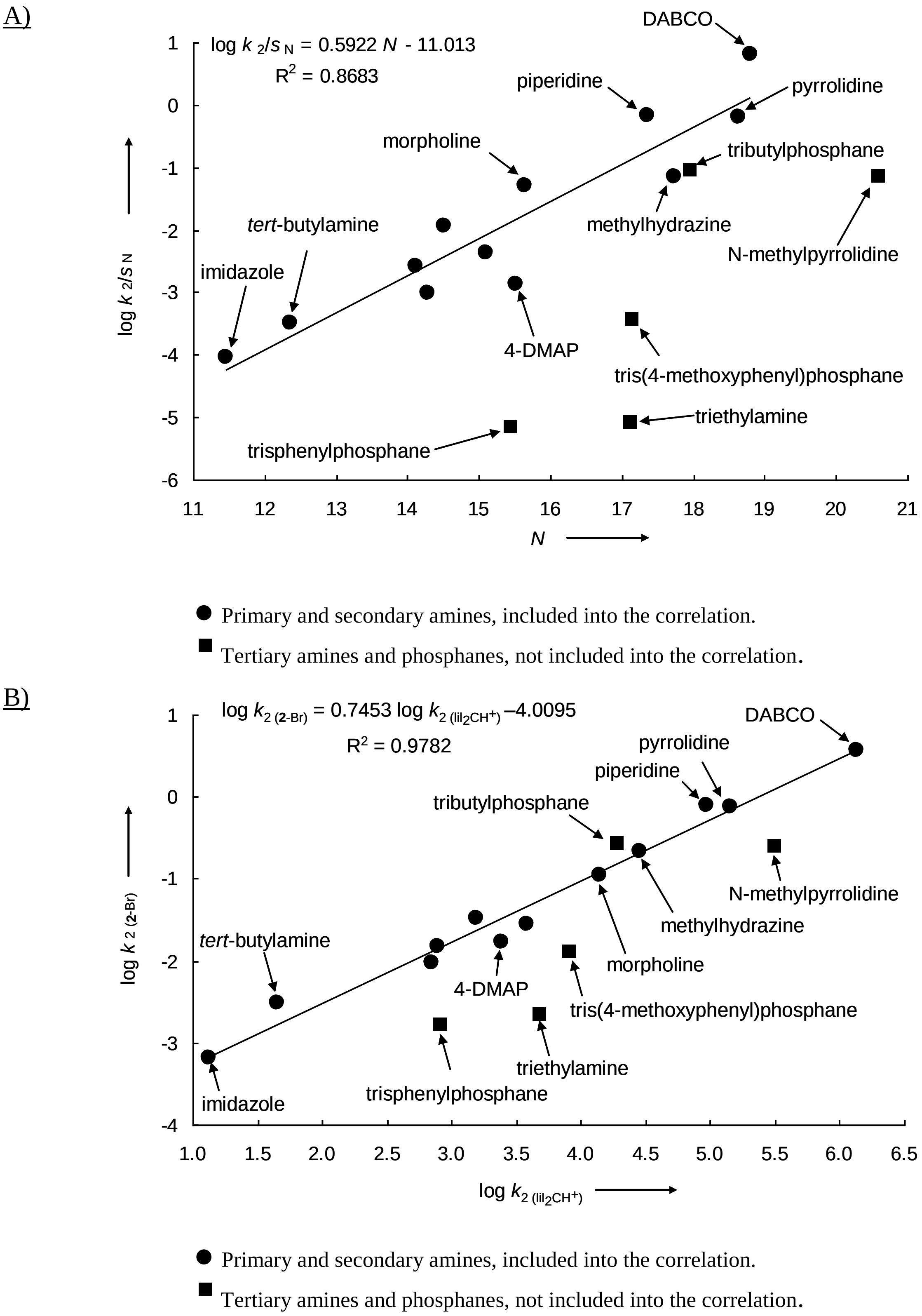

Figure 2.S5.6.2. A) Correlation of log k_2/s_N versus N for the reactions of **2**-Br of **2**-Br with amines and phosphanes at 20˚C in acetonitrile. B) Correlation of log k_2 for the reactions of amines and phosphanes with **2**-Br versus log k_2 for their reactions with lil$_2$CH$^+$ at 20˚C in acetonitrile.

2.S.5.7. Correlations for 4-methoxybenzyl bromide (3-Br).

Table 2.S5.7.1. Rate constants for the reactions of **3**-Br and $(lil)_2CH^+$ with amines at 20˚C in DMSO.

Nucleophile	N	s_N	$k_{2\,(\mathbf{3}\text{-Br})}$	$\log k_{2\,(\mathbf{3}\text{-Br})}$	$\log k_{2\,(\text{lil})_2\text{CH}^+}$ [a]
1,1-dimethylhydrazine	-	-	9.19	0.96	-
methylhydrazine	19.89	0.52	5.02	0.70	5.12
piperidine	17.19	0.71	6.13	0.79	5.08
morpholine	16.96	0.67	2.04	0.31	4.64
2,2,2-trifluoroethylamine	12.15	0.65	9.56×10^{-3}	-2.02	1.37

(a) Calculated using Equation 1.

A)

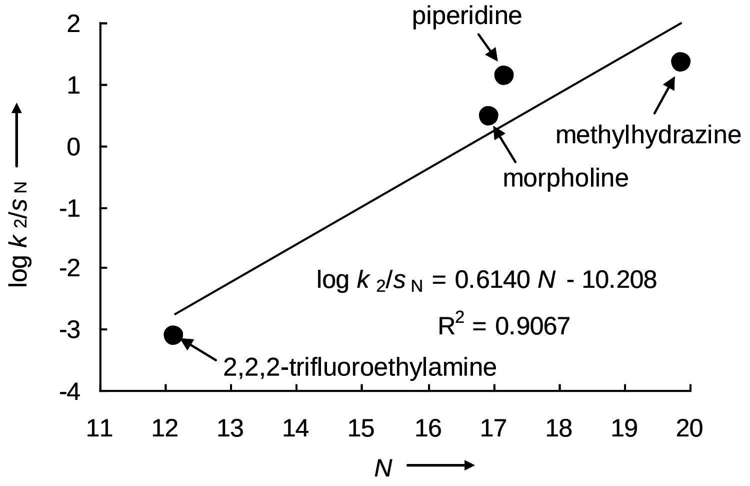

B)

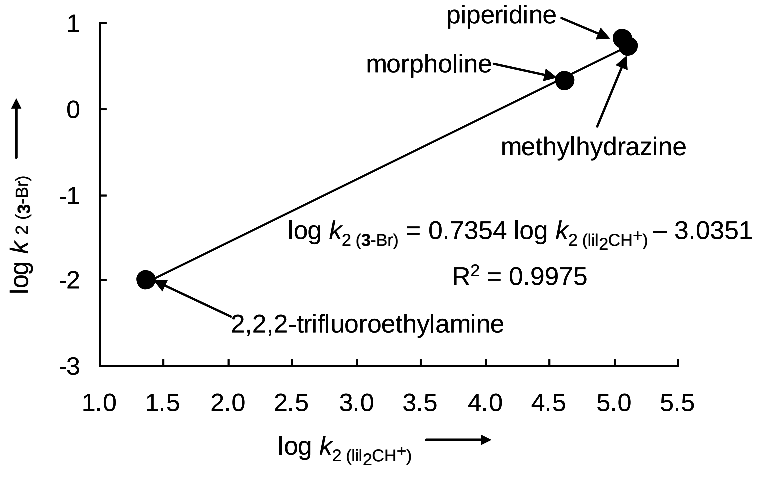

Figure 2.S5.7.1. A) Correlation of log k_2/s_N versus N for the reactions of **3**-Br with amines at 20˚C in DMSO. B) Correlation of log k_2 for the reactions of amines with **3**-Br versus log k_2 for their reactions with lil_2CH^+ at 20˚C in DMSO.

Table 2.S5.7.2. Rate constants for the reactions of **3**-Br and $(lil)_2CH^+$ with amines and phosphanes at 20˚C in acetonitrile.

Nucleophile	N	s_N	$k_{2\ (\mathbf{3}\text{-Br})}$	log $k_{2\ (\mathbf{3}\text{-Br})}$	log $k_{2\ (lil)_2CH^+}$ [a]
DABCO	18.80	0.70	1.47×10^{1}	1.17	6.13
methylhydrazine	17.73	0.58	4.53×10^{-1}	-0.34	4.46
piperidine	17.35	0.68	1.76	0.25	4.97
morpholine	15.65	0.74	3.95×10^{-1}	-0.4	4.15
2-aminoethanol	14.11	0.71	4.88×10^{-2}	-1.31	2.89
dipropylamine	14.51	0.80	1.96×10^{-1}	-0.71	3.58
n-butylamine	15.27	0.63	1.04×10^{-1}	-0.98	3.29
n-propylamine	15.11	0.63	7.83×10^{-2}	-1.11	3.19
benzylamine	14.29	0.67	3.23×10^{-2}	-1.49	2.85
2,2,2-trifluoroethylamine	10.13	0.75	9.10×10^{-4}	-3.04	0.07

(a) Calculated using Equation 1.

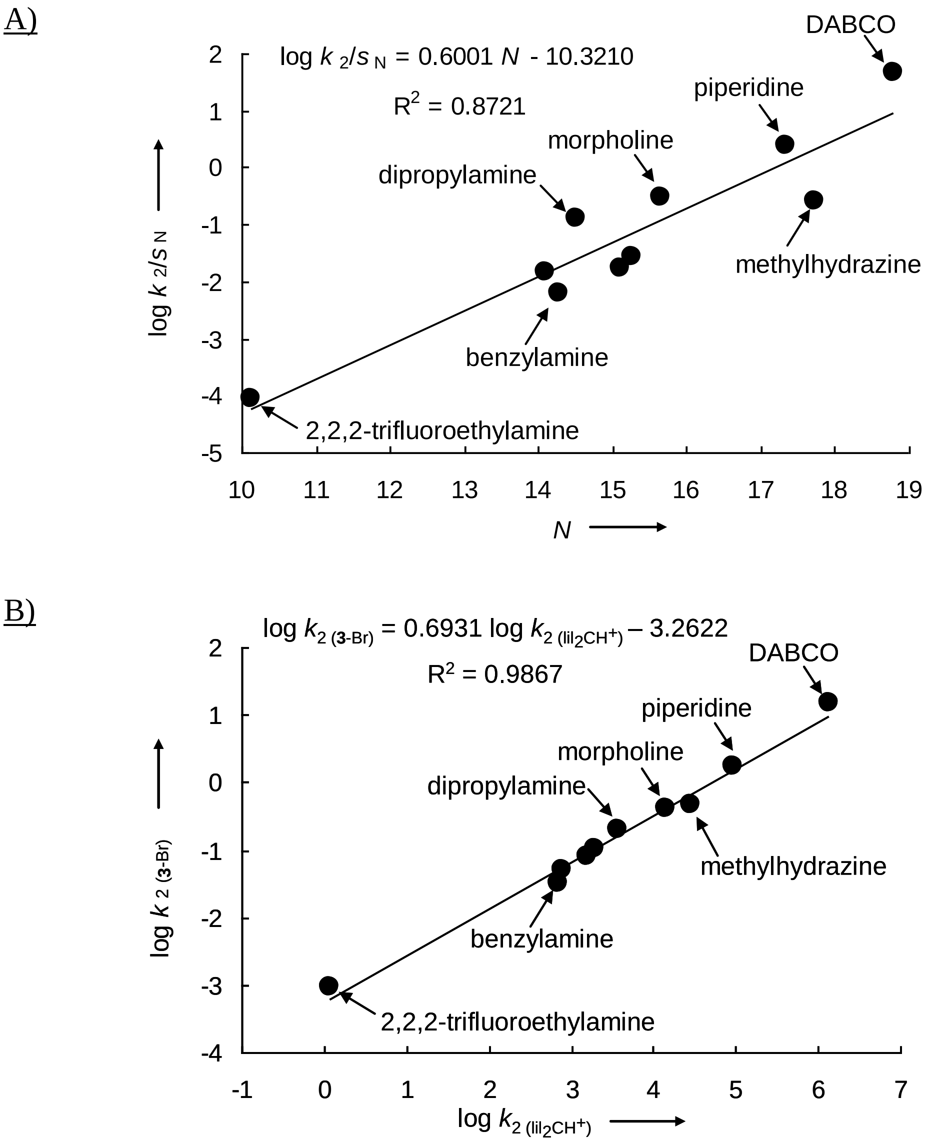

Figure 2.S5.7.2. A) Correlation of log k_2/s_N versus N for the reactions of **3**-Br with amines at 20˚C in acetonitrile. B) Correlation of log k_2 for the reactions of amines with **3**-Br versus log k_2 for their reactions with lil$_2$CH$^+$ at 20˚C in acetonitrile.

2.S.5.8. Correlations for phenacyl bromide (4-Br).

Table 2.S5.8. Rate constants for the reactions of **4**-Br and $(lil)_2CH^+$ with amines at 20˚C in DMSO.

Nucleophile	N	s_N	$k_{2\,(\mathbf{4}\text{-Br})}$	log $k_{2\,(\mathbf{4}\text{-Br})}$	log $k_{2\,(lil)_2CH^+}$ [a]
DABCO	16.62	0.89	5.78×10^{1}	1.76	5.86
TBD	19.15	0.57	1.59×10^{2}	2.20	5.19
piperidine	17.19	0.71	3.07×10^{1}	1.49	5.08
morpholine	16.96	0.67	5.43	0.73	4.64
2-aminoethanol	16.07	0.61	2.73	0.44	3.68
1-aminopropan-2-ol	15.47	0.65	2.48	0.39	3.53
n-propylamine	15.70	0.64	4.13	0.62	3.62
benzylamine	15.28	0.65	1.09	0.04	3.41
2-aminobutan-1-ol	14.39	0.67	5.09×10^{-1}	-0.29	2.91
4-DMAP	14.80	0.67	9.28×10^{-1}	-0.03	3.19
diethanolamine	15.51	0.70	3.75×10^{-1}	-0.43	3.83
2,2,2-trifluoroethylamine	12.15	0.65	7.91×10^{-3}	-2.10	1.37
imidazole	11.58	0.79	6.61×10^{-2}	-1.18	1.22
2-methylbenzimidazole	10.02	0.85	2.83×10^{-3}	-2.55	-0.02

(a) Calculated using Equation 1.

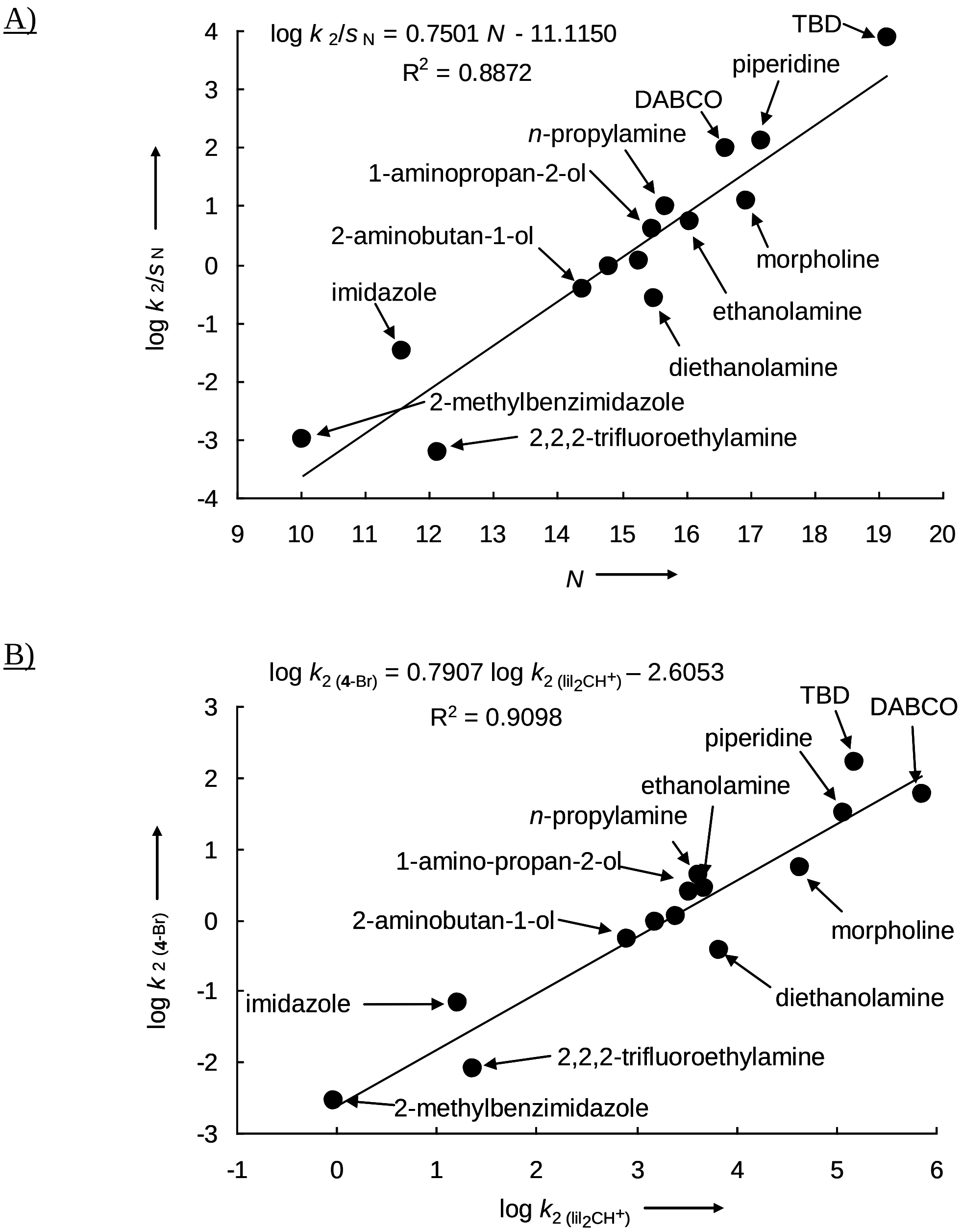

Figure 2.S5.8. A) Correlation of log k_2/s_N versus N for the reactions of **4**-Br with amines at 20°C in DMSO. B) Correlation of log k_2 for the reactions of amines with **4**-Br versus log k_2 for their reactions with lil_2CH^+ at 20°C in DMSO.

2.S.5.9. Correlations methyl iodide (5-I).

Table 2.S5.9.1. Rate constants for the reactions of **5**-I and $(lil)_2CH^+$ with amines at 20˚C in DMSO.

Nucleophile	N	s_N	$k_{2\,(\mathbf{5}\text{-I})}$	log $k_{2\,(\mathbf{5}\text{-I})}$	log $k_{2\,(lil)_2CH^+}$ [a]
DABCO	16.62	0.89	8.79	0.94	5.86
TBD	19.15	0.57	3.07	0.49	5.19
morpholine	16.96	0.67	5.63×10^{-1}	-0.25	4.64
DBU	15.11	0.67	1.63×10^{-1}	-0.79	3.4
2-aminoethanol	16.07	0.61	1.83×10^{-1}	-0.74	3.68
1-aminopropan-2-ol	15.47	0.65	2.44×10^{-1}	-0.61	3.53
n-propylamine	15.70	0.64	3.31×10^{-1}	-0.48	3.62
benzylamine	15.28	0.65	1.83×10^{-1}	-0.74	3.41
2-aminobutan-1-ol	14.39	0.67	1.32×10^{-1}	-0.88	2.91
4-DMAP	14.80	0.67	3.08×10^{-2}	-1.51	3.19
diethanolamine	15.51	0.70	2.75×10^{-1}	-0.56	3.83
imidazole	11.58	0.79	3.43×10^{-3}	-2.46	1.22
2-methylbenzimidazole	10.02	0.85	8.14×10^{-4}	-3.09	-0.02

(a) Calculated using Equation 1.

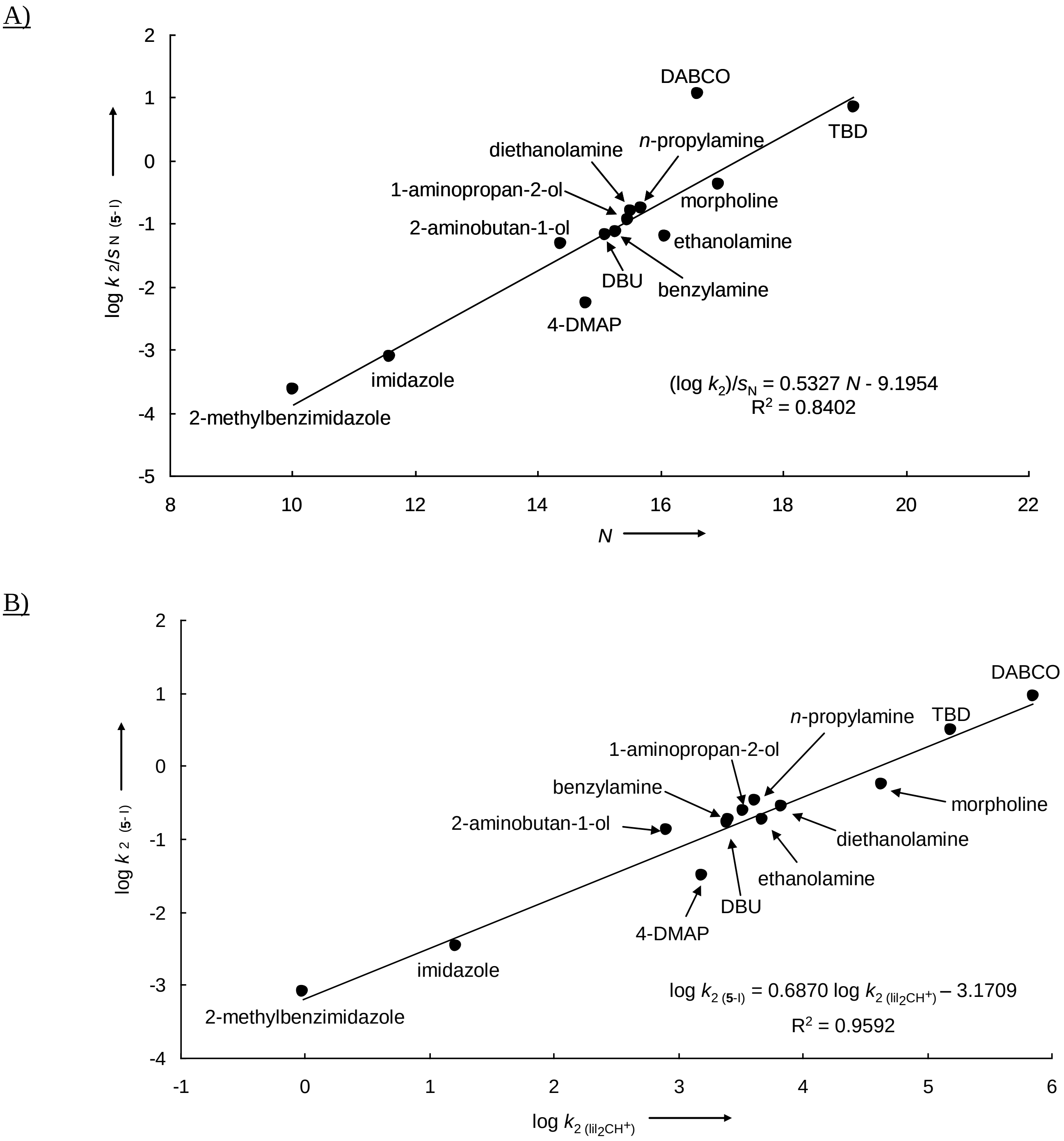

Figure 2.S5.9.1. A) Correlation of log k_2/s_N versus N for the reactions of **5**-I with amines at 20˚C in DMSO. B) Correlation of log k_2 for the reactions of amines with **5**-I versus log k_2 for their reactions with lil$_2$CH$^+$ at 20˚C in DMSO.

Table 2.S5.9.2. Rate constants for the reactions of **5**-I and $(\text{lil})_2\text{CH}^+$ with amines and phosphanes at 20˚C in acetonitrile.

Nucleophile	N	s_N	$k_{2\,(\mathbf{5}\text{-I})}$	log $k_{2\,(\mathbf{5}\text{-I})}$	log $k_{2\,(\text{lil})_2\text{CH}^+}$ [a]
DABCO	18.80	0.70	1.73	0.24	6.13
N-methylpyrrolidine	20.59	0.52	3.23×10^{-1}	-0.49	5.49
N-methylpiperidine	18.72	0.52	7.31×10^{-2}	-1.14	4.51
triethylamine	17.10	0.52	3.06×10^{-2}	-1.51	3.67
pyrrolidine	18.64	0.60	3.22×10^{-1}	-0.49	5.16
piperidine	17.35	0.68	2.86×10^{-1}	-0.54	4.97
morpholine	15.65	0.74	4.12×10^{-2}	-1.39	4.15
2-aminoethanol	14.11	0.71	1.03×10^{-2}	-1.99	2.89
dipropylamine	14.51	0.80	3.91×10^{-2}	-1.41	3.58
n-butylamine	15.27	0.63	2.19×10^{-2}	-1.66	3.29
n-propylamine	15.11	0.63	1.93×10^{-2}	-1.71	3.19
benzylamine	14.29	0.67	7.87×10^{-3}	-2.1	2.85
4-DMAP	15.51	0.62	7.24×10^{-3}	-2.14	3.39
tert-butylamine	12.35	0.72	6.40×10^{-3}	-2.19	1.66
tributylphosphane	17.94	0.54	4.36×10^{-1}	-0.36	4.27
tris(4-methoxyphenyl)phosphane	17.14	0.55	2.18×10^{-2}	-1.66	3.91
triphenylphosphane	15.43	0.54	5.24×10^{-3}	-2.28	2.91

(a) Calculated using Equation 1.

Table 2.S5.9.3. Rate constants for the reactions of **5**-I and $(\text{lil})_2\text{CH}^+$ with amines in methanol.

Nucleophile	N	s_N	$k_{2\,(\mathbf{5}\text{-I})}$ [a], 25°C	$k_{2\,(\mathbf{5}\text{-I})}$ [b], 20°C	log $k_{2\,(\mathbf{5}\text{-I})}$	log $k_{2\,(\text{lil})_2\text{CH}^+}$ [c]
pyrrolidine	15.97	0.62	2.2	1.3	0.34	3.68
piperidine	15.63	0.64	2.6	1.6	0.41	3.58
hydrazine	13.47	0.7	5.1×10^{-1}	3.0×10^{-1}	-0.29	2.4
hydroxylamine	12.23	0.66	5.0×10^{-1}	3.0×10^{-1}	-0.3	1.45
imidazole	10.41	0.69	1.2×10^{-2}	6.7×10^{-3}	-1.92	0.26

(a) The rate constants are measured at 25°C, the numbers are from Ref. 13. (b) Calculated from the rate constants at 25°C using the Eyring Equation. (c) Calculated using Equation 1.

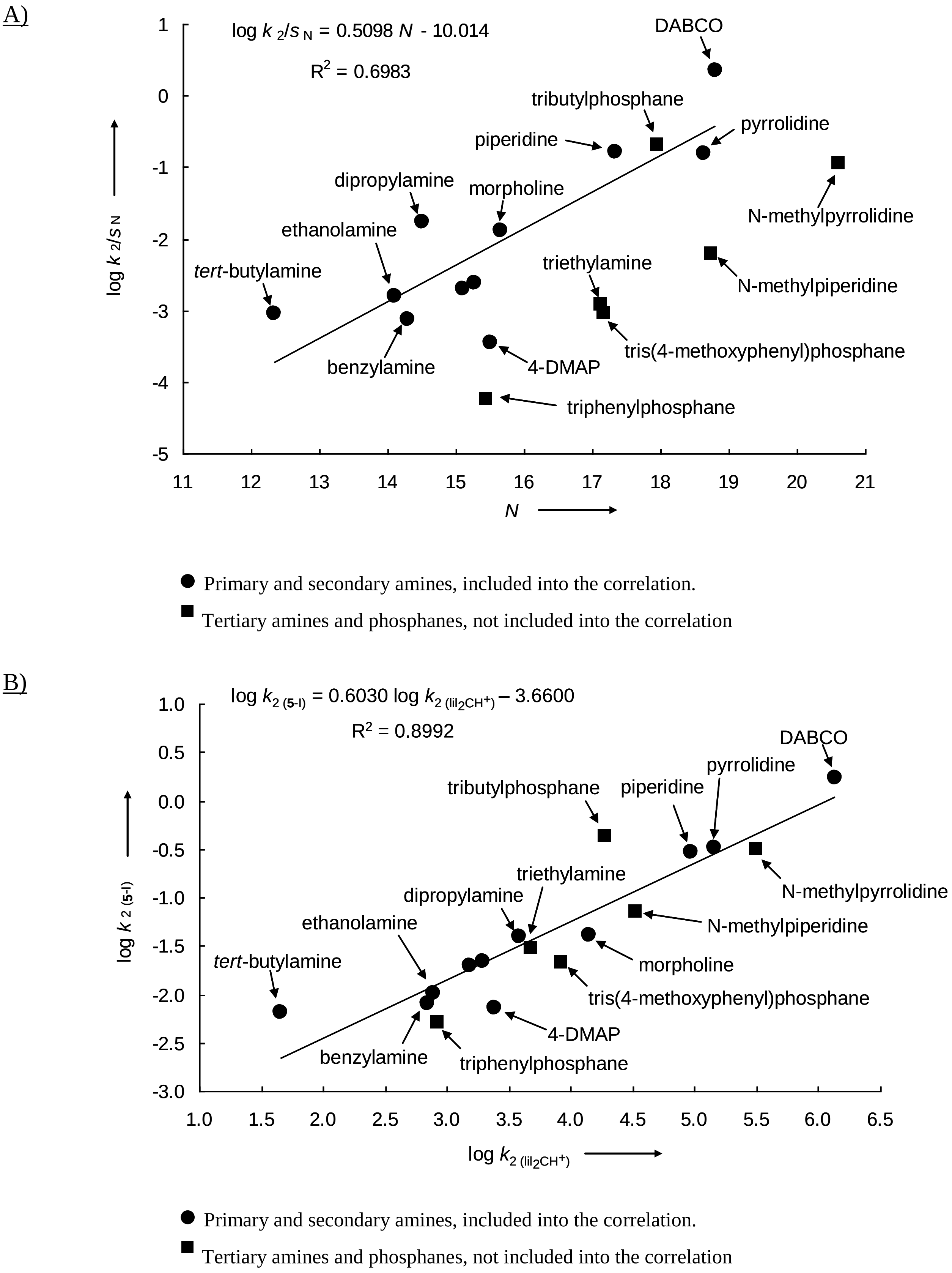

Figure 2.S5.9.2. A) Correlation of log k_2/s_N versus N for the reactions of **5**-I with amines and phosphanes at 20˚C in acetonitrile. B) Correlation of log k_2 for the reactions of amines and phosphanes with **5**-I versus log k_2 for their reactions with lil_2CH^+ at 20˚C in acetonitrile.

2.S.5.10. Correlations for methyl tosylate (5-OTs).

Table 2.S5.10. Rate constants for the reactions of **5**-OTs and $(\text{lil})_2\text{CH}^+$ with amines at 20˚C in DMSO.

Nucleophile	N	s_N	$k_{2\,(\mathbf{5}\text{-OTs})}$	log $k_{2\,(\mathbf{5}\text{-OTs})}$	log $k_{2\,(\text{lil})_2\text{CH}^+}$ [a]
piperidine	17.19	0.71	1.80×10^{-1}	-0.74	5.08
morpholine	16.96	0.67	4.08×10^{-2}	-1.39	4.64
2-aminoethanol	16.07	0.61	2.76×10^{-2}	-1.56	3.68
1-aminopropan-2-ol	15.47	0.65	2.84×10^{-2}	-1.55	3.53
n-propylamine	15.70	0.64	4.27×10^{-2}	-1.37	3.62
benzylamine	15.28	0.65	2.38×10^{-2}	-1.62	3.41
2-aminobutan-1-ol	14.39	0.67	1.38×10^{-2}	-1.86	2.91
4-DMAP	14.80	0.67	3.98×10^{-3}	-2.4	3.19
diethanolamine	15.51	0.70	1.87×10^{-2}	-1.73	3.83
imidazole	11.58	0.79	7.99×10^{-4}	-3.1	1.22
2-methylbenzimidazole	10.02	0.85	2.47×10^{-4}	-3.61	-0.02

(a) Calculated using Equation 1.

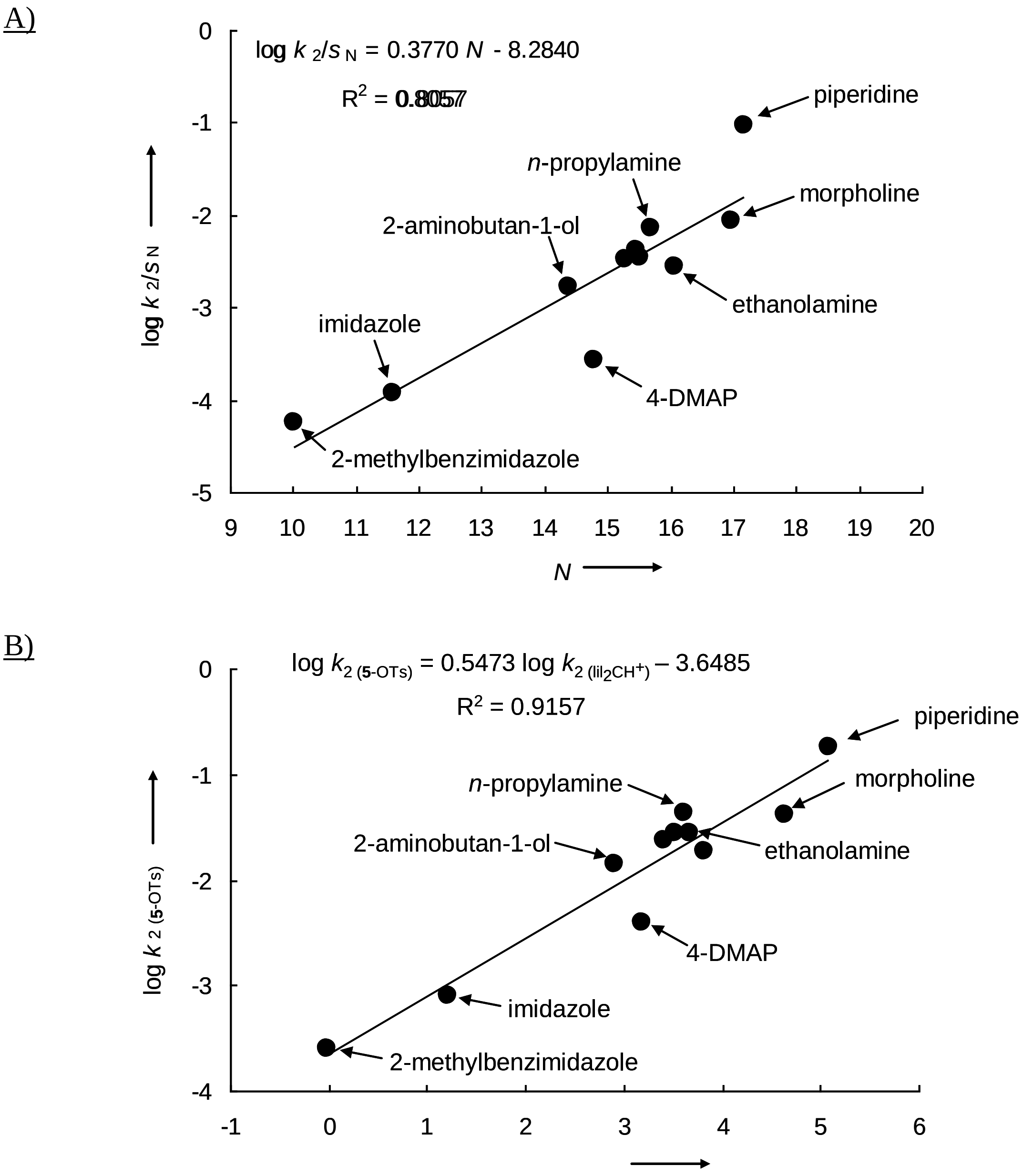

Figure 2.S5.10. A) Correlation of log k_2/s_N versus N for the reactions of **5**-OTs with amines at 20˚C in DMSO. B) Correlation of log k_2 for the reactions of amines with **5**-OTs versus log k_2 for their reactions with lil$_2$CH$^+$ at 20˚C in DMSO.

2.S.6. The relationship between the linearity of the plot of log k_{S_N2} versus log $k_{(\mathrm{lil})_2\mathrm{CH}^+}$, and the Equation log $k_{S_N2} = s_E s_N (N + E)$.

Figure 2.S6.1 shows the plot of s_N versus N for several different classes of nucleophiles in dichloromethane. The data are taken from the reactivity database[5h] and are compiled in Table 2.S6.1.

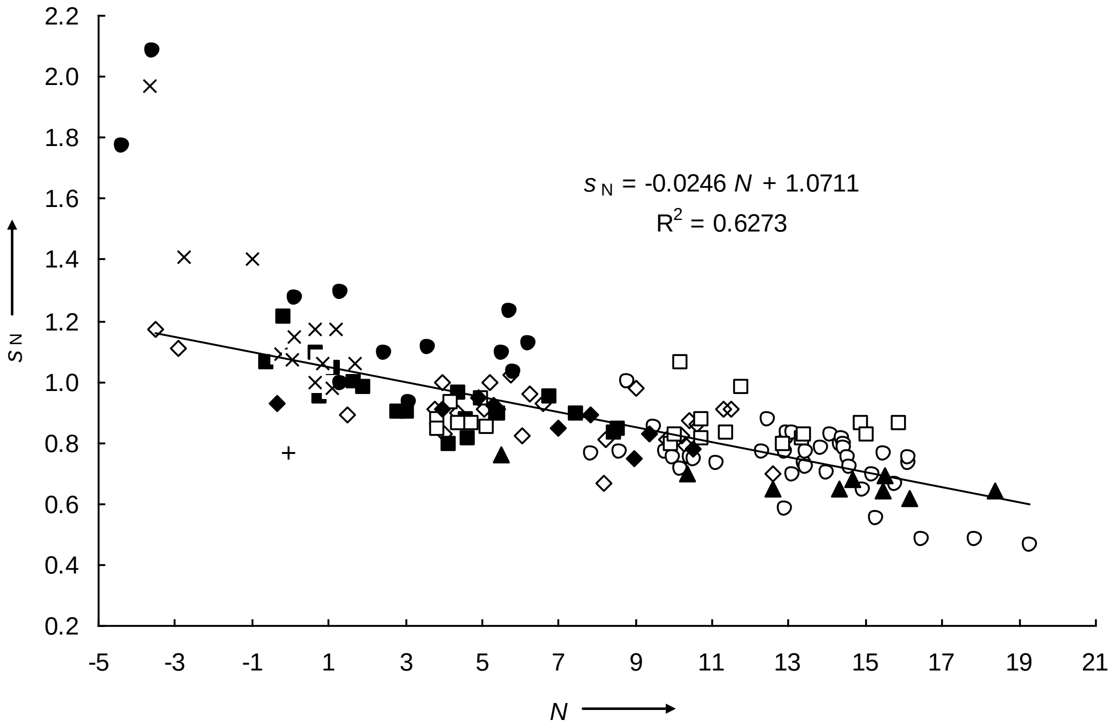

Figure 2.S6.1. Plot of s_N versus N for different classes of nucleophiles (determined in dichloromethane): ● arenes, × alkenes, ◇ enol ethers, ■ allyl element compounds, + alkynes, ◆ diazo compounds, ▲ P-nucleophiles, □ enamines, ○ N-nucleophiles. Three points deviate significantly from the trend line and are not used for the fit: toluene, m-xylene and 2-chloropropene.

Table 2.S6.1. The reactivity parameters N and s_N for different classes of nucleophiles in dichloromethane.

Class of the nucleophiles	Nucleophile	N	s_N
Arenes	toluene	-4.36	1.77
	m-xylene	-3.57	2.08
	3-methylanisole	0.13	1.27
	furan	1.33	1.29
	2-methylthiophene	1.35	0.99
	1,3-dimethoxybenzene	2.48	1.09
	N-(triisopropylsilyl)pyrrole	3.12	0.93
	2-methylfuran	3.61	1.11
	indole	5.55	1.09
	N-methylindole	5.75	1.23
	N-methylpyrrole	5.85	1.03
	5-methoxy-indole	6.22	1.12

Alkenes	2-chloropropene	-3.65	1.97
	1-hexene	-2.77	1.41
	tetramethylethylene	-1.00	1.40
	norbornene	-0.25	1.09
	2,3,3-trimethyl-but-1-ene	0.06	1.07
	1-methylcyclohexene	0.08	1.15
	2-methyl-but-2-ene	0.65	1.17
	2,3-dimethyl-but-1-ene	0.65	1.00
	2,4,4-trimethyl-pent-1-ene	0.79	1.07
	2-methyl-pent-1-ene	0.84	1.06
	2-methyl-buta-1,3-diene (isoprene)	1.10	0.98
	2-methylpropene (isobutylene)	1.11	0.98
	1-methylcyclopentene	1.18	1.17
	1-methyl-4-vinyl-benzene	1.70	1.06
	Danishefskys diene	8.57	0.84
Enol ethers	(3,3,4,4,5,5,6,6,7,7,7-undecafluoro)-2-(trimethylsiloxy)hept-1-ene	-3.52	1.17
	3,3,3-trifluoro-2-(trimethylsiloxy)propene	-2.94	1.11
	1-(perfluorophenyl)-1-(trimethylsiloxy)ethene	1.47	0.89
	n-butyl vinyl ether	3.76	0.91
	2-methyl-1-(trimethylsiloxy)propen	3.94	1.00
	(tris(trimethylsilyl)siloxy)ethene	4.01	0.83
	2,3-dihydrofuran	4.37	0.90
	1-(tris(trimethylsilyl)siloxy)cyclohexene	5.07	0.91
	1-(trimethylsiloxy)cyclohexene	5.21	1.00
	2-(trimethylsiloxy)propene	5.41	0.91
	1-(triphenylsiloxy)cyclopentene	5.76	1.02
	2-(tris(trimethylsilyl)siloxy)propene	6.04	0.82
	1-phenyl-1-(trimethylsiloxy)ethene	6.22	0.96
	1-(trimethylsiloxy)cyclopentene	6.57	0.93
	5-(tris(pentafluorophenyl)siloxy)-2,3-dihydrofuran	8.16	0.67
	1-phenoxy-1-(trimethylsiloxy)ethene	8.23	0.81
	1-methoxy-2-methyl-1-(trimethylsiloxy)propene	9.00	0.98
	1,1-diethoxyethene	9.81	0.81
	1-butoxy-1-(trimethylsiloxy)ethene	10.21	0.82
	1-butoxy-1-(t-butyl-dimethylsiloxy)ethene	10.32	0.79
	1,1-bis(trimethylsiloxy)propene	10.38	0.87
	2-(trimethylsiloxy)-5,6-dihydro-4H-pyran	10.61	0.86
	5-(triphenylsiloxy)-2,3-dihydrofuran	11.28	0.91
	4-methyl-5-(trimethylsiloxy)-2,3-dihydrofuran	11.50	0.91
	5-(trimethylsiloxy)-2,3-dihydrofuran	12.56	0.70

Allyl element compounds	allylchlorodimethylsilane	-0.57	1.06
	allyltriphenylsilane	-0.13	1.21
	2,4,6-trimethylstyrene	0.68	1.09
	styrene	0.78	0.95
	trimethyl(3-methyl-but-2-enyl)silane	0.90	1.17
	methylenecyclohexane	1.16	1.04
	allyltrimethylsilane	1.68	1.00
	allyltris(trimethylsilyl)silane	1.95	0.98
	methylenecyclopentane	2.82	0.90
	allyltriphenylstannane	3.09	0.90
	(2-methylallyl)triphenylsilane	4.17	0.79
	(2-methylallyl)trimethylsilane	4.41	0.96
	(2-methylallyl)tris(trimethylsilyl)silane	4.63	0.87
	(2-methylallyl)triphenylgermane	4.67	0.81
	2-phenyl-allyltrimethylsilane	5.38	0.89
	allyltributylstannane	5.46	0.89
	(allyl)dicarbonyl(cyclopentadienyl)iron(II)	6.78	0.95
	(2-methylallyl)tributylstannane	7.48	0.89
	(2-methylallyl)dicarbonyl(cyclopentadienyl)iron(II)	8.45	0.83
Alkynes	phenylacetylene	-0.04	0.77
Diazo compounds	diethyl diazomalonate	-0.35	0.93
	diazoacetone	3.96	0.91
	ethyl diazoacetate	4.91	0.95
	diphenyl-diazomethane	5.29	0.92
	1,1-dimethyl-2-methylenehydrazine	6.98	0.85
	N-methylenepyrrolidin-1-amine	7.84	0.89
	(trimethylsilyl)diazomethane	8.97	0.75
	phenyldiazomethane	9.35	0.83

	diazomethane	10.48	0.78
P-nucleophiles	triphenylphosphite	5.51	0.76
	tri-n-butylphosphite	10.36	0.70
	tris(4-chlorophenyl)phosphane	12.58	0.65
	triphenylphosphane	14.33	0.65
	tricyclohexylphosphane	14.64	0.68
	tri(4-methylphenyl)phosphane	15.44	0.64
	tri-n-butylphosphane	15.49	0.69
	tris(4-methoxyphenyl)phosphane	16.17	0.62
	tris(4-dimethylaminophenyl)phosphane	18.39	0.64
Enamines, enamides and ynamides	4-(bis(trimethylsiloxy)amino)pent-4-enoic acid methyl ester	3.84	0.87
	N-benzyl-4-methyl-N-(phenylethynyl)benzenesulfonamide	3.85	0.84
	2-(bis(tert-butyldimethylsiloxy)amino)propene	4.23	0.93
	N-benzyl-N-((2-methoxyphenyl)ethynyl)-4-methylbenzenesulfonamide	4.40	0.86
	2-(bis(trimethylsiloxy)amino)propene	4.76	0.86
	N-vinylcarbazole	5.02	0.94
	N-benzyl-N-(but-1-yn-1-yl)-4-methylbenzenesulfonamide	5.16	0.85
	alpha-(N-morpholino)styrene	9.96	0.79
	morpholinoisobutylene	10.04	0.82
	(E)-1-styryl-2-tritylpyrrolidine	10.19	1.06
	1-(phenylmethylamino)cyclohexene	10.73	0.81
	(E)-beta-(N-morpholino)styrene	10.76	0.87
	1-(N-morpholino)cyclohexene	11.40	0.83
	(E)-1-styryl-2-(triphenylsilyl)pyrrolidine	11.77	0.98
	1-(phenylmethylamino)cyclopentene	12.90	0.79
	1-(N-piperidino)cyclohexene	13.36	0.81
	1-(N-morpholino)cyclopentene	13.41	0.82
	1-(N-pyrrolidino)cyclohexene	14.91	0.86
	1-(N-piperidino)cyclopentene	15.06	0.82
	1-(N-pyrrolidino)cyclopentene	15.91	0.86
N-nucleophiles	(E)-N-benzylidene-1-phenylmethanamine	7.90	0.76
	(E)-N-benzylidenemethanamine	8.60	0.77
	N-cyclohexylideneaniline	8.80	1.00
	N-(propan-2-ylidene)aniline	9.53	0.85
	2-methyl-4,5-dihydrooxazole	9.81	0.77
	1-(2-methyl-4,5-dihydro-1H-imidazol-1-yl)ethanone	10.03	0.75
	2-methyl-4,5-dihydrothiazole	10.20	0.71
	quinine	10.46	0.75

	quinidine	10.54	0.74
	1-phenyl-N-(propan-2-ylidene)methanamine	11.13	0.73
	2-phenyl-4,5-dihydro-1H-imidazole	12.31	0.77
	1,3-dimethylimidazolidin-2-imine	12.46	0.87
	2-methyl-4,5-dihydro-1H-imidazole	12.92	0.77
	(R)-2-(tert-butyl)-3,4-dihydro-2H-benzo[4,5]thiazolo[3,2-a]pyrimidine	12.95	0.58
	2,3,5,6-tetrahydroimidazo[2,1-b]thiazole	12.98	0.81
	3,5,6,7-tetrahydro-2H-imidazo[2,1-b][1,3]thiazine	13.00	0.83
	1-benzyl-2-phenyl-4,5-dihydro-1H-imidazole	13.11	0.83
	5-methyl-3,4-dihydro-2H-pyrrole	13.12	0.69
	2,3-dihydrobenzo[d]imidazo[2,1-b]thiazole	13.42	0.73
	(S)-2-phenyl-3,4-dihydro-2H-benzo[4,5]thiazolo[3,2-a]pyrimidine	13.45	0.72
	1,1,3,3-tetramethylguanidine	13.48	0.77
	DHPB (3,4-dihydro-2H-benzo[4,5]thiazolo[3,2-a]pyrimidine)	13.86	0.78
	N-(1,3-dimethylimidazolidin-2-ylidene)-1-phenylmethanamine	14.00	0.70
	2,3,4,6,7,8-hexahydropyrimido[2,1-b][1,3]thiazine	14.10	0.82
	2-benzyl-1,1,3,3-tetramethylguanidine	14.36	0.79
	1-methyl-2,3,4,6,7,8-hexahydro-1H-pyrimido[1,2-a]pyrimidine (MeTBD)	14.43	0.81
	2,3,5,6-tetrahydro-1H-imidazo[1,2-a]imidazole (TBO)	14.44	0.79
	THTP (3,5,6,7-tetrahydro-2H-thiazolo[3,2-a]pyrimidine)	14.45	0.78
	4-(2-(fluorodiphenylmethyl)pyrrolidin-1-yl)pyridine	14.57	0.75
	2-phenyl-1,4,5,6-tetrahydropyrimidine	14.62	0.72
	(2S,3S)-3-isopropyl-2-phenyl-3,4-dihydro-2H-benzo[4,5]thiazolo[3,2-a]pyrimidine	14.96	0.64
	2-methyl-1,4,5,6-tetrahydropyrimidine	15.21	0.69
	(R)-2-benzhydryl-3,4-dihydro-2H-benzo[4,5]thiazolo[3,2-a]pyrimidine	15.30	0.55
	DBN	15.50	0.76
	4-(dimethylamino)pyridine	15.80	0.66
	1,2,3,5,6,7-hexahydroimidazo[1,2-a]pyrimidine (TBN)	16.15	0.73
	2,3,4,6,7,8-hexahydro-1H-pyrimido[1,2-a]pyrimidine	16.16	0.75
	(R)-2-isopropyl-3,4-dihydro-2H-benzo[4,5]thiazolo[3,2-a]pyrimidine	16.50	0.48

N-methylenepyrrolidin-1-amine	17.90	0.48
1,1-dimethyl-2-methylenehydrazine	19.31	0.46

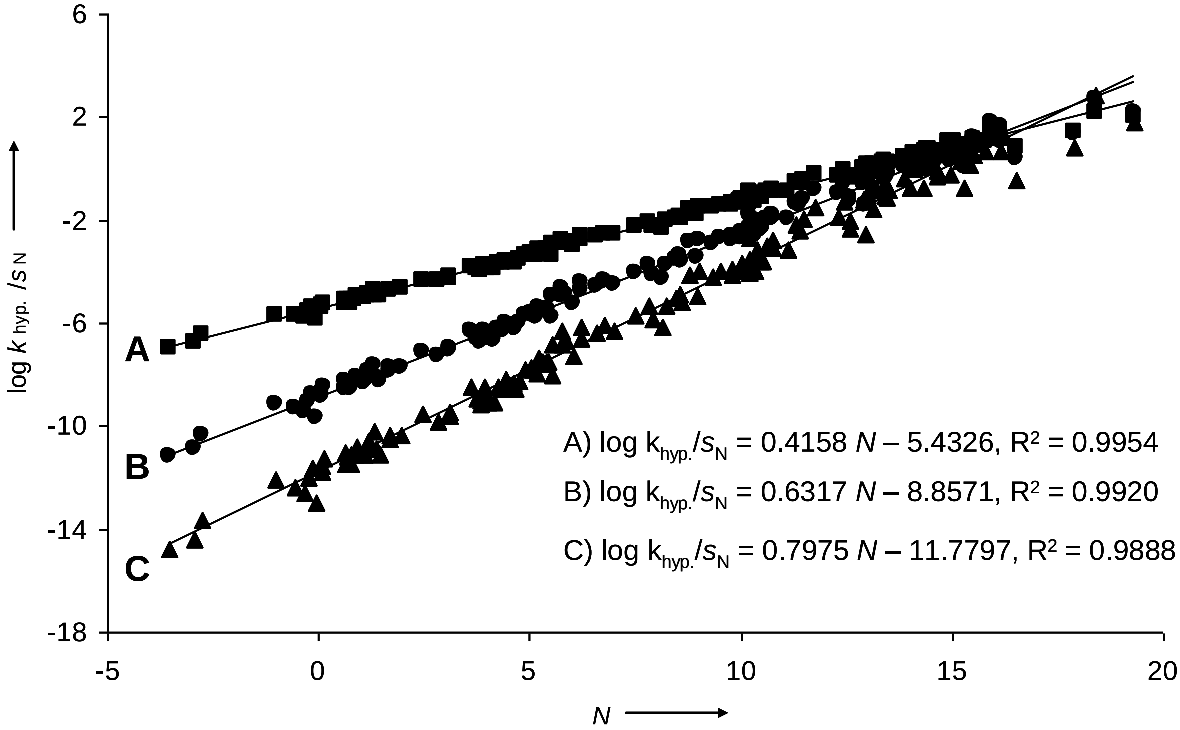

Figure 2.S6.2. Plots of log $k_{\mathrm{hyp.}}/s_{\mathrm{N}}$ versus N. Log $k_{\mathrm{hyp.}}$ (hypothetical rate constants which correlate linearly with those for the reaction with the lil$_2$CH$^+$ cation) were calculated using the following linear equations:

A) log $k_{\mathrm{hyp.}} = 0.45 * \log k_{\mathrm{lil_2CH^+}} - 1$; B) log $k_{\mathrm{hyp.}} = 0.7 * \log k_{\mathrm{lil_2CH^+}} - 2$; C) log $k_{\mathrm{hyp.}} = 0.9 * \log k_{\mathrm{lil_2CH^+}} - 3$. Log $k_{\mathrm{lil_2CH^+}}$ were calculated from s_{N} and N parameters for each nucleophile from Table 2.S6.1, except for those which deviate dramatically from the linear plot in Figure 2.S6.1 (toluene, m-xylene and 2-chloropropene), using Equation 1 and $E = -10.04$ for the lil$_2$CH$^+$ cation.

2.S.7. Correlations of log k_2 for the reactions of amines with 2-Br versus their calculated reactivities (log k_2) towards hypothetical electrophiles of different E parameters.

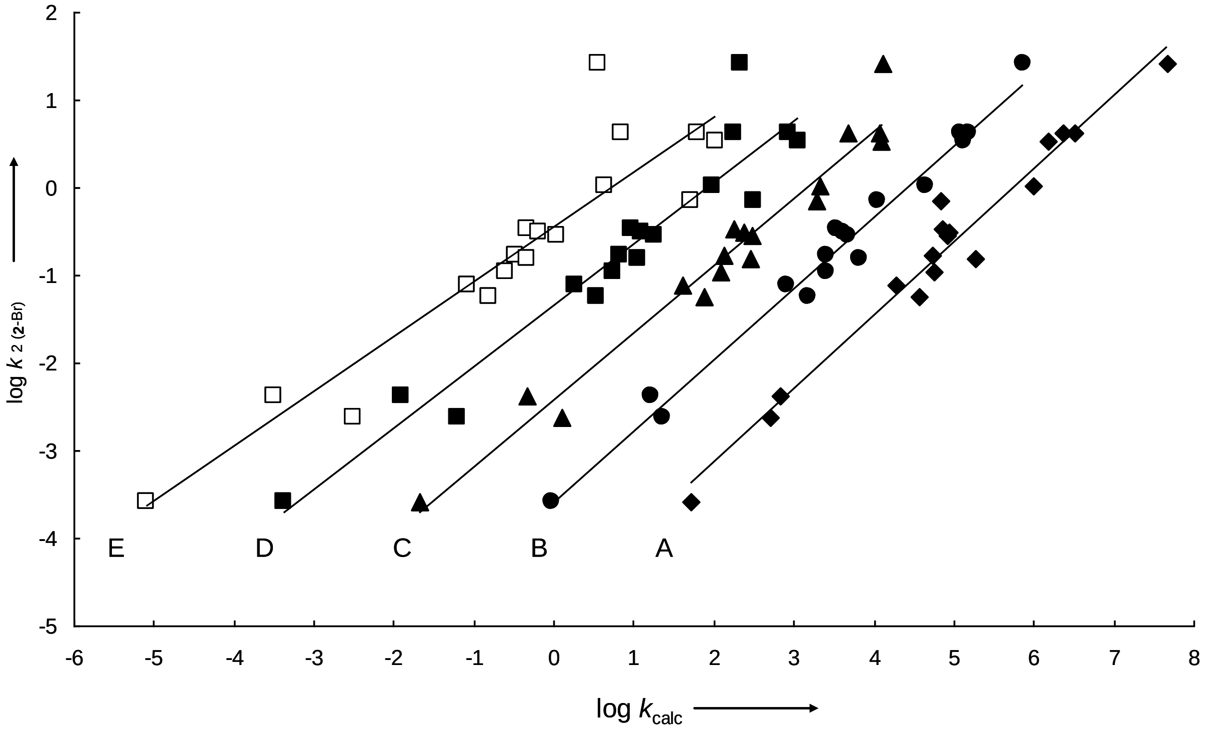

Figure 2.S7.1. Plots of log k_2 for the reactions of amines with **2**-Br versus the calculated reactivities of these amine towards hypothetical electrophiles of A) E = -8, B) E = -10.04 (the lil$_2$CH$^+$ cation), C) E = -12, D) E = -14, E) E = -16, calculated by Eq. 1 using their N and s_N parameters in DMSO. The amines and their reactivity parameters are listed in Table 2.S5.6.1.

The equations for the fits are:

A) $\log k_{2\,(\mathbf{2}\text{-Br})} = 0.8390 \log k_{\text{hyp}} - 4.8064$, $R^2 = 0.9640$,

B) $\log k_{2\,(\mathbf{2}\text{-Br})} = 0.8163 \log k_{\text{lil}_2\text{CH}^+} - 3.5885$, $R^2 = 0.9816$,

C) $\log k_{2\,(\mathbf{2}\text{-Br})} = 0.7671 \log k_{\text{hyp}} - 2.4153$, $R^2 = 0.9597$,

D) $\log k_{2\,(\mathbf{2}\text{-Br})} = 0.6996 \log k_{\text{hyp}} - 1.3345$, $R^2 = 0.9108$,

E) $\log k_{2\,(\mathbf{2}\text{-Br})} = 0.6269 \log k_{\text{hyp}} - 0.4357$, $R^2 = 0.8482$.

2.4. References

(1) C. G. Swain, C. B. Scott, *J. Am. Chem.* Soc. 1953, 75, 141 –147.

(2) a) C. D. Ritchie, *Acc. Chem. Res*. **1972**, *5*, 348 –354 ; b) C. D. Ritchie, P. O. I. Virtanen, *J. Am. Chem. Soc*. **1972**, *94*, 4966 –4971.

(3) J. W. Bunting, J. M. Mason, C. K. M. Heo**,** *J. Chem. Soc. Perkin Trans.* 2 **1994**, 2291-2300.

(4) J. P. Richard, M. M. Toteva, J. Crugeiras, *J. Am. Chem. Soc.* **2000**, *122*, 1664 –1674.

(5) a) H. Mayr, M. Patz, *Angew. Chem.* **1994**, *106*, 990-1010; *Angew. Chem. Int. Ed. Engl.* **1994**, *33*, 938–957; b) H. Mayr, T. Bug, M. F. Gotta, N. Hering, B. Irrgang, B. Janker, B. Kempf, R. Loos, A. R. Ofial, G. Remennikov, H. Schimmel, *J. Am. Chem. Soc.* **2001**, *123*, 9500–9512; c) R. Lucius, R. Loos, H. Mayr, *Angew. Chem.* **2002**, *114*, 97-102; *Angew. Chem. Int. Ed.* **2002**, *41*, 91–95; d) H. Mayr, B. Kempf, A. R. Ofial, *Acc. Chem. Res.* **2003**, *36*, 66–77; e) H. Mayr, A. R. Ofial, *Pure Appl. Chem.* **2005**, *77*, 1807–1821; f) H. Mayr, *Angew. Chem.* **2011**, *123*, 3692; *Angew. Chem. Int. Ed.* **2011**, *50*, 3612–3618; g) J. Ammer, C. Nolte, H. Mayr, *J. Am. Chem. Soc.* **2012**, *134*, 13902–13911; h) for a comprehensive listing of nucleophile-specific parameters N and s_N and electrophilicity parameters E, see http://www.cup.uni-muenchen.de/oc/mayr/DBintro.html.

(6) T. B. Phan, M. Breugst, H. Mayr, *Angew. Chem.* **2006**, *118*, 3954-3959; *Angew. Chem. Int. Ed.* **2006**, *45*, 3869 –3874.

(7) (a) T. B. Phan, C. Nolte, S. Kobayashi, A. R. Ofial, H. Mayr, *J. Am. Chem. Soc.* **2009**, *131*, 11392–11401; (b) N. Streidl, A. Antipova, H. Mayr, *J. Org. Chem.* **2009**, *74*, 7328-7334.

(8) H. Mayr, J. Ammer, M. Baidya, B. Maji, T. A. Nigst, A. R. Ofial, T. Singer, *J. Am. Chem. Soc.* **2015**, *137*, 2580-2599.

(9) F. G. Bordwell , W. T. Brannen, *J. Am. Chem. Soc.* **1964**, *86*, 4645–4650.

(10) F. G. Bordwell, D. L. Hughes, *J . Am. Chem. Soc.* **1986**, *108***,** 5991-5997.

(11) C. Reichardt, *Solvents and Solvent Effects in Organic Chemistry*, 3rd ed., Wiley-VCH, Weinheim, **2003**.

(12) T. Kanzian, T. A. Nigst, A. Maier, S. Pichl, H. Mayr**,** *Eur. J. Org. Chem.* **2009**, 6379–6385.

(13) R. G. Pearson, H. Sobel, J. Songstad, *J. Am. Chem. Soc.* **1968**, *90*, 319–326.

(14) C. Hansch, A. Leo, R. W. Taft, *Chem. Rev.* **1991**, *97*, 165-195.

(15) (a) P. R. Young, W. P. Jencks, *J. Am. Chem.* Soc. **1979,** *101*, 3288-3294, (b) F. G. Bordwell, D. L. Hughes, *J. Org. Chem.* **1980**, *45*, 3320-3325, (c) F. G. Bordwell, D. L. Hughes, *J. Am. Chem. Soc.* **1986**, *108*, 7300-7309.

(16) (a) J. B. Conant, W. R. Kirner, *J. Am. Chem. Soc.* **1924**, *46*, 232-252; (b) J. B. Conant, R. E. Hussey, *J. Am. Chem. Soc.* **1925**, *47*, 476-488; (c) J. B. Conant, W. R. Kirner, *J. Am. Chem. Soc.* **1925**, *47*, 488-501

(17) S. D. Ross, M. Finkelstein, R. C. Petersen, *J. Am. Chem. Soc.* **1968**, *90*, 6411-6415.

(18) R. G. Pearson, S.H. Langer, F. B. Williams, W. J. McGuire, *J. Am. Chem. Soc.* **1952**, *74*, 5130-5132.

(19) A. Halvorsen, J. Songstad, *J. Chem. Soc., Chem. Commun.* **1978**, 327-328.

(20) S. S. Shaik, *J. Am. Chem. Soc.* **1983**, *105*, 4359-4367.

(21) C. Nolte, PhD thesis, LMU München, 2012.

(22) (a) H. M. R. Hoffmann, *J. Chem. Soc.* **1965,** 6753-6761, (b) E. L. Eliel and R. G. Haber, *J . Am. Chem. Soc.* **1959,** *81*, 1249-1254.

(23) N. Streidl. B. Denegri, O. Kronja, H. Mayr, *Acc. Chem. Res.* **2010**, *43*, 1537-1549.

(24) L. B. Engemyr, J. Songstad, *Acta Chem. Scand.* **1972**, *26*, 4179-4180.

(25) S. Minegishi, H. Mayr, *J. Am. Chem. Soc.* **2003**, *125*, 286-295.

(26) T. A. Nigst, A. Antipova, H. Mayr, *J. Org. Chem.* **2012**, *77*, 8142-8155.

(27) M. Baidya, S. Kobayashi, F. Brotzel, U. Schmidhammer, E. Riedle, H. Mayr, *Angew. Chem.* **2007**, *119*, 6288-6292; *Angew. Chem. Int. Ed.* 2007, *46*, 6176-6179.

(28) T. B. Phan, H. Mayr, *Eur. J. Org. Chem.* **2006**, 2530-2537.

(29) T. B. Phan, H. Mayr, *J. Phys. Org. Chem.* **2006**, *19*, 706-713.

(30) T. B. Phan, H. Mayr, Can. J. Chem. 2005, 83, 1554 –1560.

(31) S. Minegishi, S. Kobayashi, H. Mayr, *J. Am. Chem. Soc.* **2004**, *126*, 5174-5181.

(32) B. Denegri, S. Minegishi, O. Kronja, H. Mayr, *Angew. Chem.* **2004**, *116*, 2353 –2356; *Angew. Chem. Int. Ed*. **2004**, *43*, 2302–2305.

CHAPTER 3

Reactivities of Stabilized 9-Substituted Fluorenyl Anions Towards Quinone Methides and Benzhydrylium Ions in Dimethyl Sulfoxide

3.1. Introduction

In chapter 1 of this thesis it was mentioned that this work is mainly focused on the investigation of the relationship between the reactivities of different types of nucleophiles towards C_{sp2} and C_{sp3} electrophilic centers.

Numerous studies on the nucleophilic reactivities of 9-substituted fluorenyl anions towards carbon electrophiles in various types of transformations, such as S_N2,[1] S_N2',[2] S_NAr [3] and e_T^- [4] prompted us to quantify the nucleophilicities of some of them using the method based on their reactivities towards benzhydrylium ions and structurally related quinone methides, which has extensively been used in our group[5].

On the one hand, by measuring the rate constants for the reactions of 9-substituted fluorenyl anions with our reference electrophiles, we will be able to compare the reactivity trend reported for their S_N2 reactions with benzyl halides in DMSO with that for addition reactions to the sp^2 carbon. On the other hand, we will be able to use the rate constants to derive the nucleophilicity parameters for these carbanions according to Eq. 1 and thus complement our set of coloured carbanions for systematic investigation of the reactivities of neutral electrophiles.

$$\log k_2 = s_N (E + N) \qquad (1)$$

In this chapter, we report on the reactivities of anions **1-3** towards benzhydrylium ions and quinone methides.

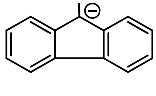

1

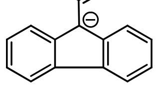

2

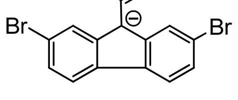

3

3.2. Results and Discussion

3.2.1. Synthesis of 9-Substituted Fluorenes.

9-Substituted fluorenes **(1-3)**-H were synthesized using procedures described in the literature[6] according to Scheme 3.1.

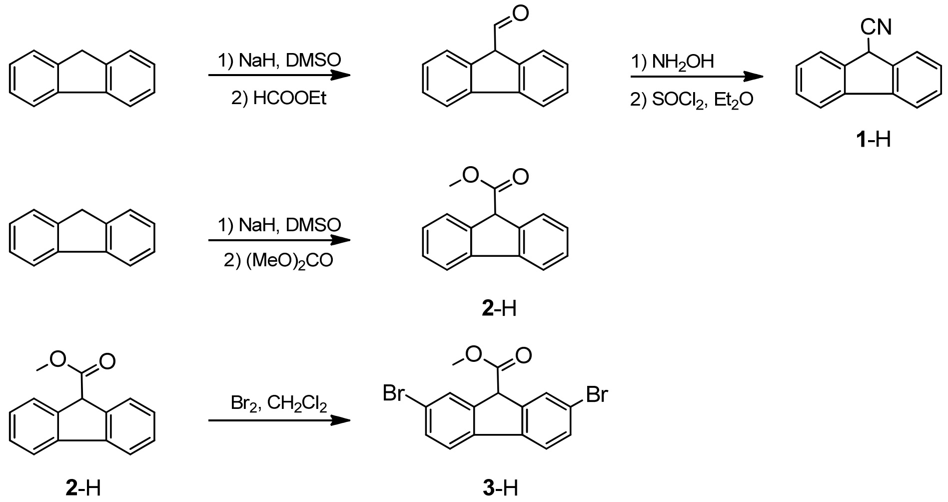

Scheme 3.1. Synthesis of the carbanion precursors (**1-3)**-H.

3.2.2. Kinetics of the Reactions of 9-Substituted Fluorenyl Anions with Benzhydrylium Ions and Quinone Methides

Methods employed for kinetic measurements

The kinetics of the reactions of fluorenyl anions **1-3** with the reference electrophiles **4a-j** (Table 3.1), were studied spectrophotometrically by following the time-dependent absorbances of the coloured electrophiles.

Conventional and stopped-flow methods, employed for studying kinetics of the reactions with quinone methides **4a-e,** have been described earlier.[5] To study the reactions of fluorenyl anions with quinone methides, fluorenes were deprotonated by mixing the solutions of the corresponding C-H acids with a base in DMSO. In case of more acidic 9-cyanofluorene **1**-H ($pK_a = 8.3$)[1a] and 2,7-dibromo-9-carbomethoxyfluorene **3**-H ($pK_a = 6.5$),[1a] deprotonation was achieved with tetrabutylammonium benzoate or 1,1,3,3-tetramethylguanidine (TMG). As benzoate is too weak to deprotonate 9-carbomethoxyfluorene **2**-H ($pK_a = 10.3$)[1a] quantitatively, TMG was always used as a base for the generation of **2**. To check whether the observed rate constants depend on the nature of the base, several experiments were also performed using potassium tert-butoxide as deprotonating agent.

Table 3.1. List of the reference electrophiles used in this study.

Reference electrophiles			E^{a}
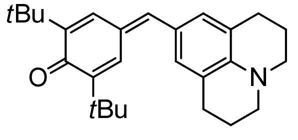		jul(*t*Bu)$_2$QM (**4a**)	-17.90
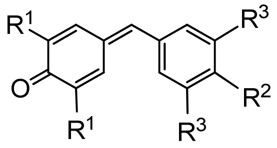	R^1 = *t*Bu, R^2 = NMe$_2$, R^3 = H	dma(*t*Bu)$_2$QM (**4b**)	-17.29
	R^1 = *t*Bu, R^2 = H, R^3 = F	*m*F$_2$(*t*Bu)$_2$QM (**4c**)	-14.50
	R^1 = Ph, R^2 = NMe$_2$, R^3 = H	dma(Ph)$_2$QM (**4d**)	-13.39
	R^1 = Ph, R^2 = OMe, R^3 = H	ani(Ph)$_2$QM (**4e**)	-12.18
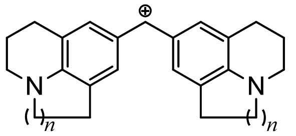	$n = 1$	(lil)$_2$CH$^+$(**4f**)	-10.04
	$n = 2$	(jul)$_2$CH$^+$ (**4g**)	-9.45
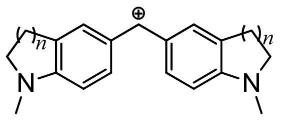	$n = 1$	(ind)$_2$CH$^+$ (**4h**)	-8.76
	$n = 2$	(thq)$_2$CH$^+$ (**4i**)	-8.22
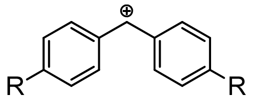	R = NMe$_2$	(dma)$_2$CH$^+$ (**4j**)	-7.02

(a) Electrophilicity parameters are taken from refs. 5b,c and 7.

Formation of the anions from the corresponding C-H acids after addition of the base was controlled by the UV-vis method following the absorbances of the carbanions between 350 and 450 nm. A typical result of deprotonation experiment is shown in Figure 3.1.

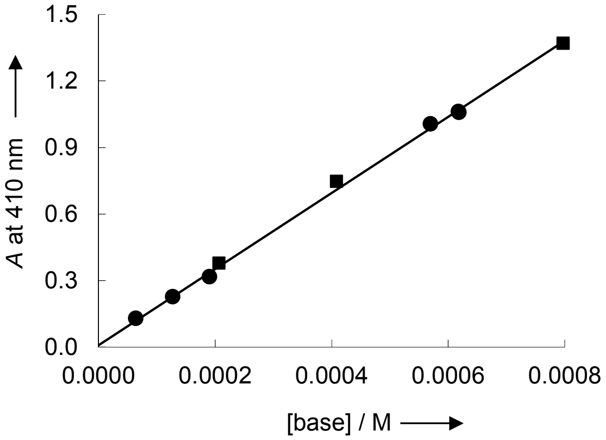

Figure 3.1. Correlation of the absorbance of **2** (at 410nm) with the concentrations of the base used for the deprotonation of excess of fluorene **2**-H: ● with potassium tert-butoxide, ■ with 1,1,3,3-tetramethylguanidine.

The reactions of the carbanions **1-3** with the benzhydrylium ions **4f-j** were too fast to be followed by a stopped-flow method and were studied using the laser-flash photolysis technique. The product of the recombination reaction was used as the precursor of the carbocation (the nucleophile thus playing also the role of the photo-leaving group, Scheme 3.2). As these experiments were performed in DMSO, which has a significant absorbance at the usual excitation wavelength of 266 nm, a laser flash photolysis setup with a near-parallel geometry (~ 15°) between pump and probe pulses was employed to study the kinetics of these reactions.[8] Kinetic experiments with variable concentrations of the fluorenyl anions were hampered by the fact that these ions also absorb at the excitation wavelength. Therefore, in each laser-flash experiment, the ratio between precursor and nucleophile concentrations (and thus their relative absorbances) was kept constant in order to ensure sufficient excitation of the precursor molecules.

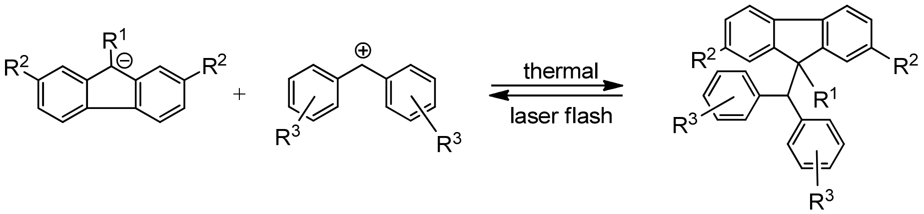

Scheme 3.2. The reaction of fluorenyl anions with benzhydrylium ions and the decomposition of the product under laser irradiation.

The solutions of the precursors of the carbocations were freshly prepared prior to use by combining solutions of **1-3** and benzhydrylium tetrafluoroborates **4f-j** in DMSO. The carbanions were generated by *in situ* deprotonation of corresponding C-H acids (**1-3**)-H with potassium tert-butoxide. To avoid side reactions of tert-butoxide with reference electrophiles, the fluorenes (**1-3**)-H were used in a slight excess over KO*t*Bu. As only a small fraction of the precursor molecules was cleaved by the laser pulse (~1%), a moderate excess of 1.5 equiv. of the nucleophile over the precursor was sufficient to ensure pseudo-first-order conditions for the kinetic experiment.

Evaluation of kinetic data

Reactions with benzhydrylium ions

All reactions of the carbanions **1-3** with the benzhydrylium ions **4(f-j)** proceeded with quantitative formation of the adducts, as indicated by immediate decolourization of the solutions of the electrophiles upon mixing with solutions of the carbanions in DMSO. After the photo-cleavage of the precursor, monoexponential decays were observed for the reactions of **1** with the cations **4(f-j)**. Plots of k_{obs} versus the nucleophile concentrations were linear, and the second-order rate constants k (M^{-1} s^{-1}) were obtained from the slopes of these plots, according to Equation 2.

$$k_{\text{obs}} = k\,[\text{Nu}] + k_0 \qquad (2)$$

A typical decay of the absorbance of the electrophile after the photo-cleavage of the precursor with a monoexponential fit and a plot of k_{obs} versus the nucleophile concentration are shown in Figure 3.2.

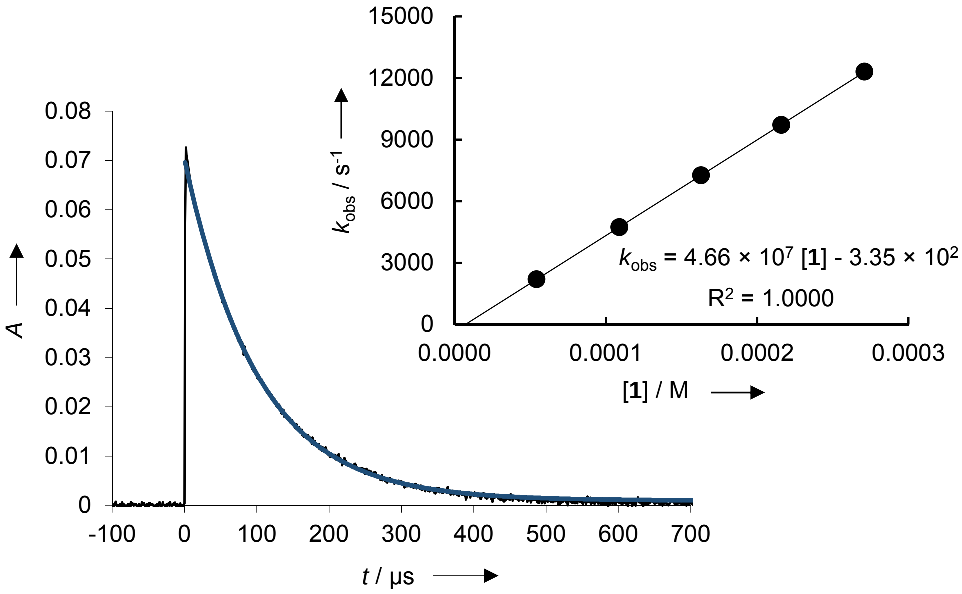

Figure 3.2. Plot of the absorbance (λ = 630 nm) versus *t* for the reaction **4f** with **1** in DMSO at room temperature, [**1**] = 2.16×10^{-4} M, laser-flash photolysis technique. The experimental curve is shown in black, the monoexponential fit in blue. Inset: Plot of the observed pseudo-first-order rate constants versus the concentrations of **1**.

However, more complicated time-dependent decays of the absorbance of the electrophiles were obtained in the reactions with the carbomethoxy-substituted anions **2** and **3** (an example is shown in Figure 3.3). These could not be fitted with a simple monoexponential function.

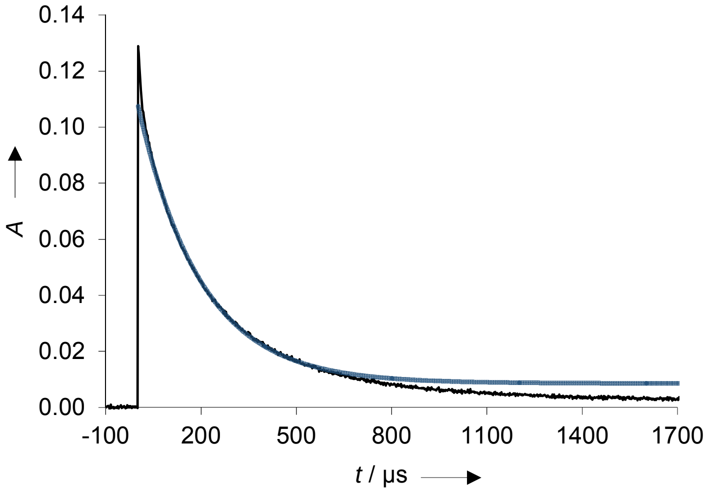

Figure 3.3. Plot of the absorbance (λ = 630 nm) versus *t* for the reaction **4f** with **2** in DMSO at room temperature, [**2**] = 2.16×10^{-4} M, laser-flash photolysis technique. The experimental curve is shown in black, the monoexponential fit in blue.

This may be due to a fast reversible attack of the cation by the oxygen site of the enolate, which is accompanied by a slower irreversible attack by the carbon site (Scheme 3.3). As we do not have any evidence for this mechanism, we only evaluated kinetics of the reactions of the cyano-substituted derivative **1** with benzhydrylium ions.

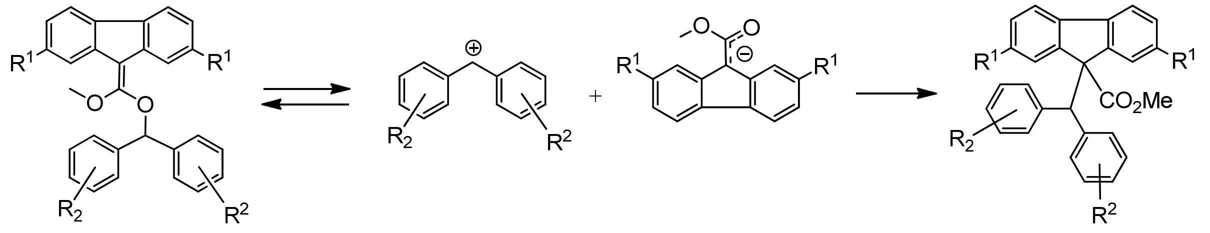

Scheme 3.3. Mechanism of the reactions of 9-carbomethoxyfluorenyl anions with benzhydryl cations.

Reactions with quinone methides

For all studied reactions of **1-3** with quinone methides in the presence of an excess of the corresponding conjugated acids (**1-3**)-H, the pseudo-first-order rate constants k_{obs} (s^{-1}) could be obtained by least-squares fitting of the monoexponential function $A = A_0\ e^{-k_{obs}t} + C$ to the time-dependent decays of the absorbances of the electrophiles. When the kinetics were followed at wavelengths between 350 and 450 nm, the presence of an excess of the fluorenyl anions caused final non-zero absorbances C, which were proportional to the remaining carbanion concentrations.

The kinetics of the reactions of quinone methides with carbanions **1-3** in presence of the corresponding C-H acids **1-3**-H showed three different reactivity patterns, which will be discussed in details in the following paragraphs.

In the first case (case A), the observed rate constants were linearly dependent on the concentration of the nucleophile and independent of the concentration of the corresponding C-H acid (Figure 3.4).

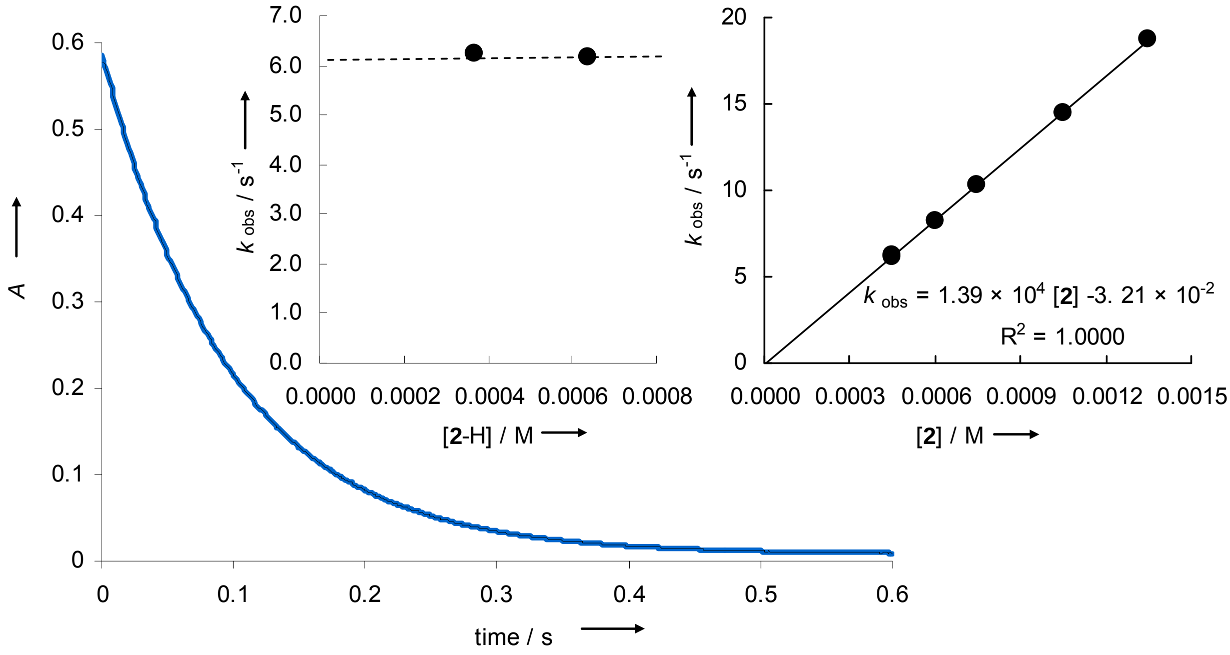

Figure 3.4. Case A: Kinetics of the reaction of **2** with **4d** in DMSO at 20°C, **2**-H deprotonated with TMG.

Plot of the absorbance (λ = 533 nm) versus t, [**2**] = 7.49×10^{-4} M, [**2**-H] = 6.09×10^{-4} M (in black) with a monoexponential fit (in blue). Insets: Plots of k_{obs} versus [**2**-H], [**2**] = 4.49×10^{-4} M (on the left) and of k_{obs} versus [**2**], [**2**-H] varies from 3.66×10^{-4} to 1.10×10^{-3} M (on the right).

In the second case (case B), the observed rate constants were found to depend on the concentration of the corresponding C-H acids. When the concentration of the fluorenyl anions was kept constant, k_{obs} increased with the concentration of the C-H acid when it was small, but reached a plateau at some point; further increase of the C-H acid concentration did not influence the rate constant anymore. When the experiments were performed with different concentrations of the anion and high concentrations of the C-H acid (where the plateau is definitely reached), k_{obs} were found to be linearly dependent on the nucleophile concentration (Figure 3.5).

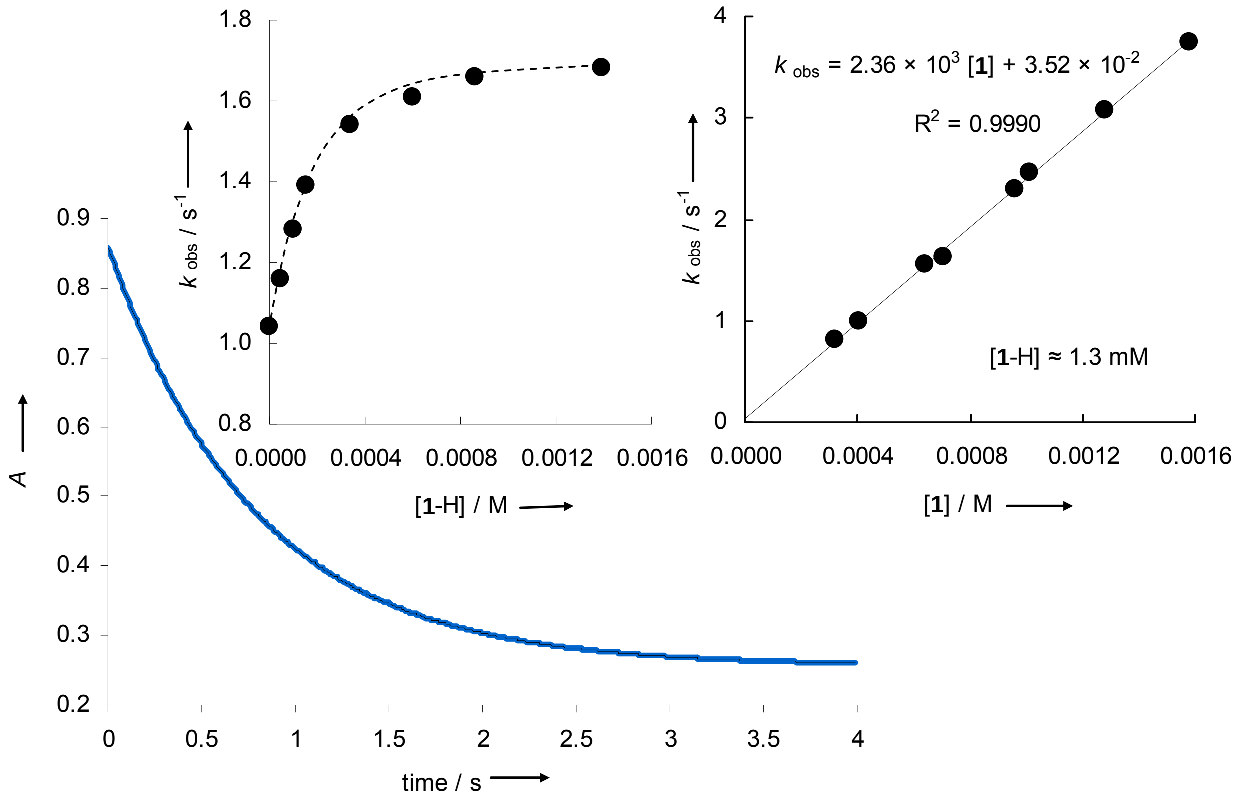

Figure 3.5. Case B: kinetics of the reaction of **1** with **4c** in presence of **1**-H in DMSO at 20°C, **1**-H deprotonated with benzoate.

Plot of the absorbance (λ = 355 nm) of **4c** versus t, [**1**] = 7.13×10^{-4} M, [**1**-H] = 1.02×10^{-4} M (in black) with a monoexponential fit (in blue). Insets: Plots of k_{obs} versus [**1**-H], [**1**] = 7.13×10^{-4} M (on the left) and of k_{obs} versus [**1**], [**1**-H] = $(1.23 - 1.37) \times 10^{-3}$M (on the right).

In the third case (case C), the reaction got faster as more C-H acid was present in the solution. In contrast to case B, the plots of the k_{obs} versus the C-H acid concentration at a fixed nucleophile concentration were linear and did not come to a plateau even at relatively high concentrations of the C-H acid (Figure 3.6). Therefore, plots of k_{obs} versus the concentration of the carbanion did not make sense in this case.

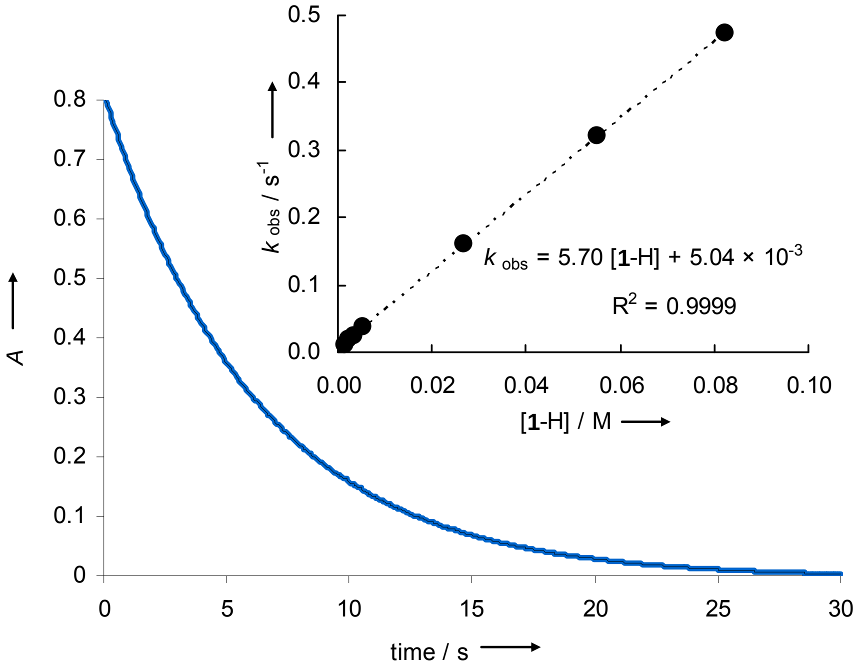

Figure 3.6. Case C: Kinetics of the reaction of **1** with **4a** in presence of **1**-H in DMSO at 20°C, **1**-H deprotonated with benzoate.

Plot of the absorbance (λ = 521 nm) versus *t*, [**1**] = 6.44×10^{-4} M, [**1**-H] = 2.69×10^{-4} M (in black) with a monoexponential fit (in blue). Inset: Plot of k_{obs} versus [**1**-H], [**1**] = $6.4 - 6.5 \times 10^{-4}$ M (is almost constant).

Cases A and B can be explained by the mechanism represented in Scheme 3.4.

In case A, bimolecular nucleophilic attack of the fluorenyl anion (**Nu**) at the quinone methide is rate-determining. The equilibrium constant k_1/k_{-1} is large, and the subsequent protonation of the intermediate **I** does not influence k_{obs} in this case. Therefore, no rate acceleration was observed in presence of the C-H acid, and the second-order rate constants k_1 could be obtained from the slopes of the plots of k_{obs} versus nucleophile concentration [**Nu**], according to Equation 2. This type of behaviour was observed in the reactions of the fluorenyl anions **1** and **2** with the most reactive quinone methides **4d** and **4e** as well as for the reaction of **2** with **4c**.

Kinetic experiments for the reactions of the fluorenyl anions **1** and **2** with **4d** were also performed using KO*t*Bu as deprotonation agent, and the resulting second-order rate constants k_1 were found to be independent on the nature of the base used for the deprotonation of the fluorene (for details, see the Experimental part).

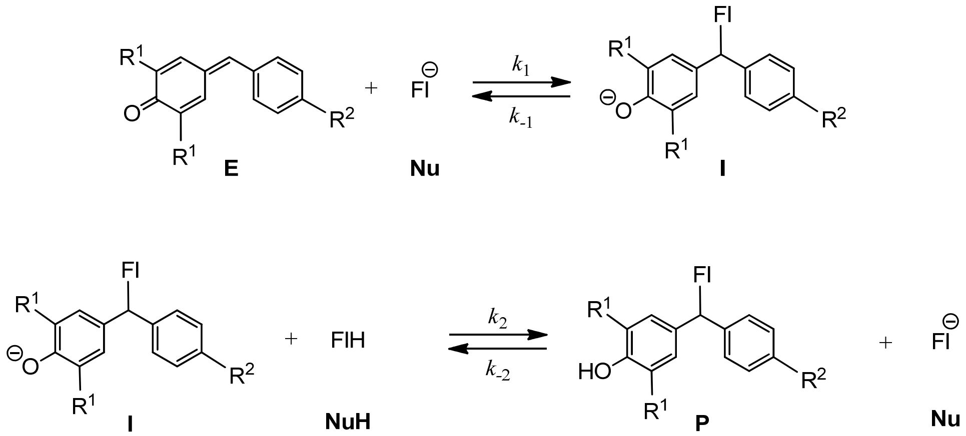

Scheme 3.4. Suggested mechanism of the reactions of quinone methides with fluorenyl anions (**Nu**) in presence of the conjugated C-H acid (**NuH**).

In case B, the equilibrium constant k_1/k_{-1} is small, and the attack of the nucleophile at the quinone methide is followed by a relatively slow proton transfer step, in which the C-H acid **NuH** and another acid, **BH** (conjugated to the deprotonating base) can act as general acid catalysts. Similar behaviour (nucleophilic attack followed by a rate-determining proton transfer step) was previously observed for the reactions of secondary amines and hydrazines with quinone methides,[9] as well as with thiocarbonates,[10] thionobenzoates,[11] and activated esters of indole-3-acetic acid.[12] When the concentration of the acid becomes sufficiently large, protonation of the intermediate **I** will be fast and the nucleophilic attack becomes rate-determining, resulting in a plateau in the plot of k_{obs} versus the C-H acid concentration. The second-order rate constants k_1 for the initial step of these reactions were obtained from the slopes of the linear plots of k_{obs} measured at high concentrations of the C-H acid versus [**Nu**], according to Equation 2. This reactivity pattern was observed in the reactions of the fluorenyl anions **1** and **2** with quinone methide **4c** as well as for the reactions of **2** with **4a-b** and of **3** with **4e**.

In case C, the linearity of the plot of k_{obs} versus the concentration of the C-H acid could be explained in different ways. One possible explanation would be such a small equilibrium constant k_1/k_{-1} that the plateau observed in case B cannot be reached, as $k_2[\mathbf{NuH}] << k_{-1}$ even at very high acid concentrations. If this was true, the expression for k_{obs} could be described by Eq. 3

$$k_{obs} = \frac{k_1}{k_{-1}} k_2 [\mathbf{NuH}] \qquad (3)$$

and the plots of k_{obs} versus [**NuH**] would indeed be linear. This quasi-equilibrium situation is sometimes observed for case B reactions at very low C-H acid concentrations (e.g., see the left inset of Figure 3.5). However, with this assumption it is difficult to explain why the reaction of **3**/**3**-H with **4c** represents case B while the reaction of **3** with the more electrophilic quinone methide **4d** follows the reactivity pattern of case C. As the Lewis acidities of the reference electrophiles are known to correlate roughly with their electrophilicity parameters in a wide range of *E* values,[13] it is hard to imagine that the equilibrium constant k_1/k_{-1} could be smaller in case of the reaction of **3** with **4d** than with less electrophilic **4c**. One would also expect a faster protonation step in case of **4d** at least for steric reasons.

Another, probably the strongest argument against the quasi-equilibrium assumption for case C is direct comparison of the measured rate constants k_{obs} for different reactions (Table 3.2).

If one compares k_{obs} for the reactions of **3** with **4a** and **4c**, one can see that at very similar concentrations of the nucleophile and the C-H acid, **4a** reacts faster than **4c**, although **4c** is two orders of magnitude more electrophilic than **4a**. At the same time, comparison of the data for the reaction of **3** with **4c** and **4e** (both represent case B) shows that the order of reactivity expected from the electrophilicity parameters for the quinone methides proves to be correct: the **4e** (E = -12.18) reacts about two orders of magnitude faster than **4c** (E = -14.50). This break in the reactivity trend can hardly be explained if one does not consider the change of the mechanism by which the reaction operates in case C.

Comparison of k_{obs} observed for the reactions of **4a** with **2** and **3** is also illustrative. At higher concentrations of both the nucleophile and the C-H acid, the more basic fluorenyl anion **2** reacts with **4a** much more slowly than **3**. However, the relative reactivites of **2** and **3** towards **4e** (represent cases A and B correspondingly) are in line with the basicities of the carbanions.

In general, one can see that reactions representing case C are faster than one would expect from the reactivity trends denoted in cases A and B. This acceleration of the reactions in Case C may be due to protonation of the quinone methide by the C-H acids **1**-H and **3**-H (Scheme 3.5).

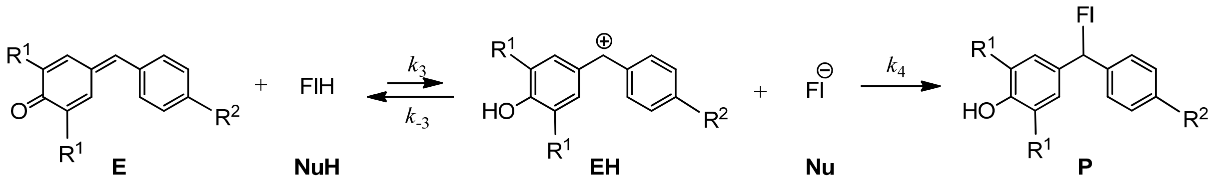

3.5. Protonation of a quinone methide by a fluorene with subsequent recombination of the charged species.

Table 3.2. Comparison of the measured rate constants k_{obs} for different reactions.

	E	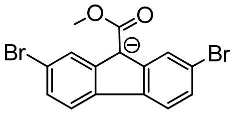 **3**	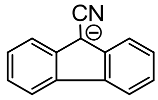 **1**	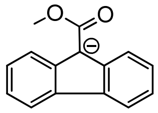 **2**
pK_{aH}		6.3	8.3	10.35
jul(tBu)$_2$QM (**4a**)	-17.90	**Case C** [**Nu**] = 7.67×10^{-4} M [**NuH**]=1.01×10^{-3} M $k_{obs} = 3.90 \times 10^{-1}$ s^{-1}	**Case C**	**Case B** [**Nu**] = 8.87×10^{-4} M [**NuH**]=6.72×10^{-3} M $k_{obs} = 7.12 \times 10^{-3}$ s^{-1}
dma(tBu)$_2$QM **(4b)**	-17.29	**Case C**	**Case C**	**Case B**
mF$_2$(tBu)$_2$QM **(4c)**	-14.50	**Case B** [**Nu**] = 7.15×10^{-4} M [**NuH**]=1.12×10^{-3} M $k_{obs} = 3.41 \times 10^{-2}$ s^{-1}	**Case B**	**Case A**
dma(Ph)$_2$QM **(4d)**	-13.39	**Case C** [**Nu**] = 7.61×10^{-4} M [**NuH**]=1.19×10^{-2} M k_{obs} = 30 s^{-1}	**Case A**	**Case A** [**Nu**] = 1.05×10^{-3} M k_{obs} = 14.5 s^{-1}
ani(Ph)$_2$QM **(4e)**	-12.18	**Case B** [**Nu**] = 5.39×10^{-4} M [**NuH**]= 4.47×10^{-4} M k_{obs} = 2.35 s^{-1}	**Case A**	**Case A** [**Nu**] = 4.55×10^{-4} M k_{obs} = 81.5 s^{-1}

The reaction of a fluorenyl anion (**Nu**) with the protonated electrophile (**EH**) occurs much faster than with the neutral quinone methide. As [**EH**] is proportional to [**NuH**], according to Eq. 4, the overall rate of the reaction increases significantly with increase of [**NuH**] (the C-H acid concentration), and the plot of k_{obs} versus [**NuH**] does not come to a plateau.

$$K = \frac{k_3}{k_{-3}} = \frac{[\mathbf{EH}][\mathbf{Nu}]}{[\mathbf{E}][\mathbf{NuH}]} \qquad (4)$$

This type of behaviour was only observed with amino-substituted quinone methides, where higher equilibrium constants k_3/k_{-3} are expected than in case of fluoro-substituted **4c** or methoxy-substituted **4e**.[14] The pK_{aH} values for fluorenyl anions **1-3** are also in agreement with the proposed mechanism. None of the reactions of fluorene **2**/**2**-H (**2**-H is the weakest of the studied acids) follows the pattern of case C, not even with amino-substituted quinone methides. At the same time, all three combinations of **3**/**3**-H with amine-substituted quinone methides belong to case C, due to the high acidity of **3**-H.

In case C, direct determination of the second-order rate constant for the reaction of the unprotonated quinone methide with fluorenyl anion was not possible.

Indirect evaluation of the kinetic data for the reactions of quinone methides with fluorenyl anions in cases B and C

Case B. In reactions of **1** (benzoate as base) with **4c**, **2** with **4b** (KO*t*Bu as base) and **3** with **4c** (benzoate as base) we did not reach a sufficiently high concentration of the C-H acid to observe the plateau where k_{obs} was constant at a fixed concentration of the carbanion. These experiments were evaluated indirectly in analogy to the method previously employed for the reactions of secondary amines and hydrazines with quinone methides.[9] However, we had to consider the fact that two different acids **NuH** and **BH** were present in the solution because of *in situ* deprotonation of the fluorene by **B** prior to the measurements (Scheme 3.6).

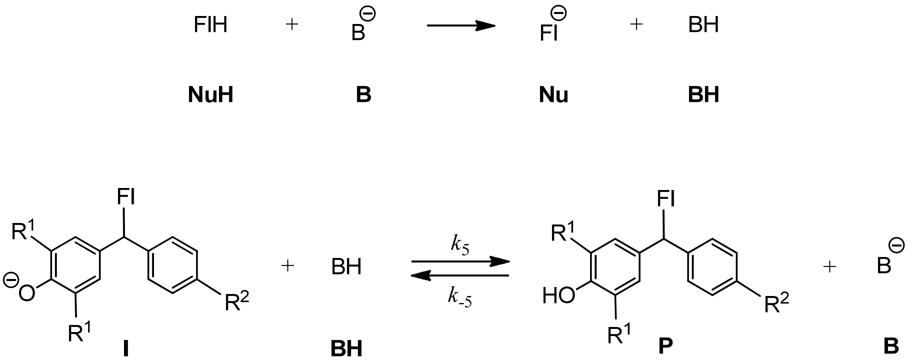

Scheme 3.6. Protonation of the intermediate **I** by the acid **BH**.

By following the absorbance of the fluorenyl anions in the UV-vis spectra before starting the kinetic experiment, we made sure that the deprotonation of the C-H acid by the base occurs very fast and quantitatively. Therefore, the following simple relationships are justfied:

For $[\mathbf{B}]_0 > [\mathbf{NuH}]_0 \Rightarrow [\mathbf{NuH}] \approx 0$, $[\mathbf{Nu}] = [\mathbf{BH}] = [\mathbf{NuH}]_0$ and $[\mathbf{B}] = [\mathbf{B}]_0 - [\mathbf{NuH}]_0$; (5)

For $[\mathbf{NuH}]_0 > [\mathbf{B}]_0 \Rightarrow [\mathbf{B}] \approx 0$, $[\mathbf{Nu}] = [\mathbf{BH}] = [\mathbf{B}]_0$ and $[\mathbf{NuH}] = [\mathbf{NuH}]_0 - [\mathbf{B}]_0$. (6)

We have to consider that both acids **NuH** and **BH** are able to protonate the intermediate **I** (Schemes 3.4 and 3.6). If the steady state for the intermediate [**I**] and a high equilibrium constant k_2/k_{-2} are assumed,[15] dependence of k_{obs} on the concentrations of both acids can be expressed with Eq. 7:[16]

$$k_{\text{obs}} = k_1[\mathbf{Nu}]\cdot\left(\frac{k_2[\mathbf{NuH}]+k_5[\mathbf{BH}]}{k_{-1}+k_2[\mathbf{NuH}]+k_5[\mathbf{BH}]}\right) \qquad (7)$$

We qualitatively compared k_2 and k_5 for **BH** = $PhCO_2H$ and **NuH** = **3**-H in the reaction with **4c**, by performing an experiment with an additional amount of benzoic acid. The result is depicted in Figure 3.7. When the reaction was performed with a small concentration of the C-H acid, addition of much larger amounts of benzoic acid had little influence on the observed rate constant k_{obs} (Figure 3.7b). When the reaction is performed without any excess of the C-H acid, it occurs quite slowly and the kinetic curves cannot be accurately fitted with a monoexponential function. This suggests that the C-H acid **3**-H is much more efficient in catalyzing the reaction of **3** with **4c** than benzoic acid. For an explanation of this specific behaviour of the fluorenes in the reactions with quinone methides, more detailed mechanistic studies are necessary.

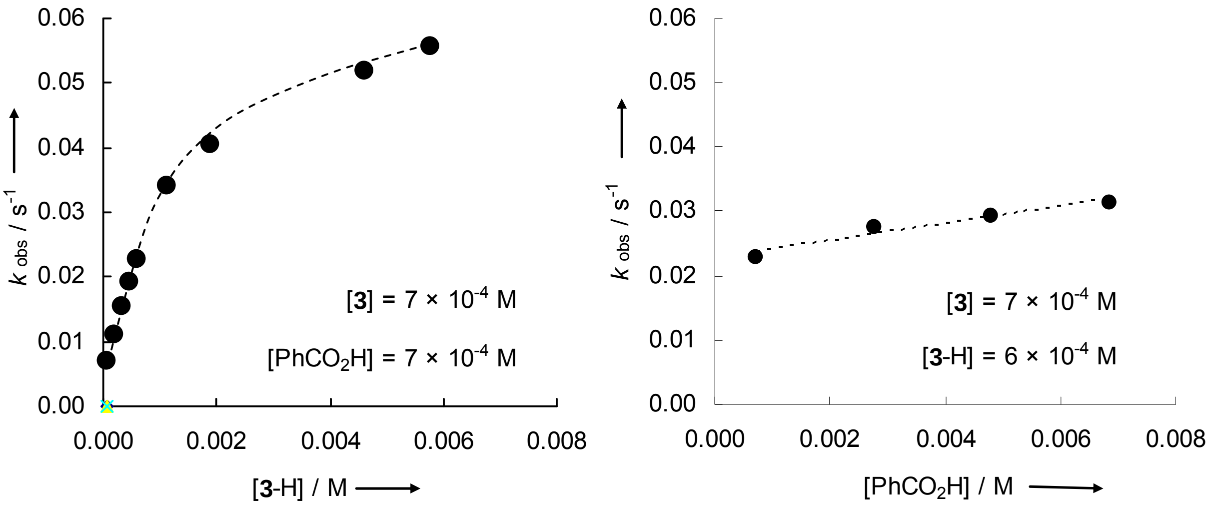

Figure 3.7. Kinetics of the reaction of **3** with **4c** in presence of **3**-H and benzoic acid. Plots of k_{obs} versus [**3**-H], [**3**] = [PhCO$_2$H] = 7.13 × 10^{-4} M (on the left) and of k_{obs} versus [PhCO$_2$H], [**3**] = 7.15 × 10^{-4} M, [**3**-H] = 5.96 × 10^{-4} (on the right).

The experiment unambiguously shows that $k_2 >> k_5$, and k_2[**NuH**] >> k_5[**BH**]. Consequently, Eq. 7 for k_{obs} can be reduced to Eq. 8, which suggests the linearity of the plot of [**Nu**]/k_{obs} versus 1/[**NuH**] when transformed into Eq. 9,

$$k_{\mathrm{obs}} = k_1[\mathbf{Nu}]\cdot\left(\frac{k_2[\mathbf{NuH}]}{k_{-1}+k_2[\mathbf{NuH}]}\right) \qquad (8)$$

$$\frac{[\mathbf{Nu}]}{k_{\mathrm{obs}}} = \frac{1}{k_1}+\frac{k_{-1}}{k_1 k_2[\mathbf{NuH}]} \qquad (9)$$

Indeed, in most cases, the plots of [**Nu**]/k_{obs} versus 1/[**NuH**] were linear in a wide range of the C-H acid concentrations. The k_1 values obtained from the intercepts of these plots are in a very good agreement with those directly determined from the slopes of the plots of k_{obs} (measured at high C-H acid concentrations) versus [**Nu**]. An example illustrating this way of evaluation is given in Figure 3.8. The rate constant for the reaction of **1** with **4c** obtained in this way is 2.40 × 10^3 M^{-1}s^{-1}, while direct evaluation (Figure 3.5) gives k_1 = 2.36 × 10^3 M^{-1}s^{-1}.

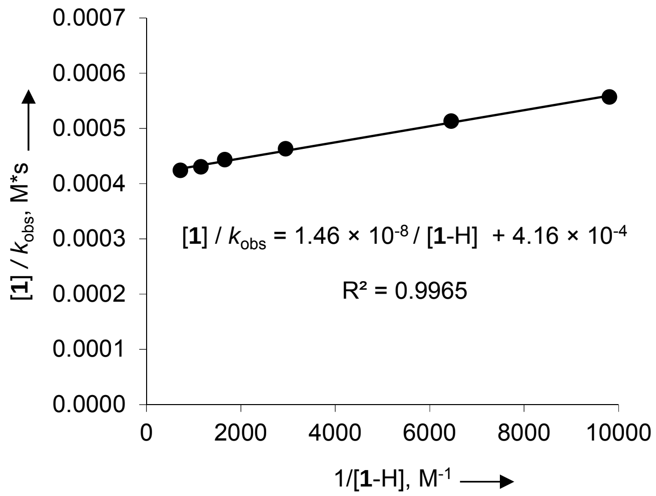

Figure 3.8. Plot of [**Nu**]/k_{obs} versus 1/[**NuH**] for the reaction of **1** with **4c** in presence of excess of **1**-H, deprotonation of **1**-H performed with nBu$_4$N$^+$PhCO$_2^-$, [**1**] = 7.13 × 10^{-4} M.

For the reactions of **2,** generated from **2**-H and TMG, with **4b**, k_{obs} decreased with increasing concentration of the C-H acid **2**-H and came to a plateau at [**2**-H] > 0.003M (Figure 3.9a). Plot of k_{obs} versus [**2**] was linear, when k_{obs} were measured at high concentrations of **2**-H (on the plateau), and the slope of this plot gave the second-order rate constant k_1, according to Eq. 2 (Figure 3.9b). Similar behaviour was observed in the reaction of **2** with **4a**, when **2** was generated from **2**-H with TMG.

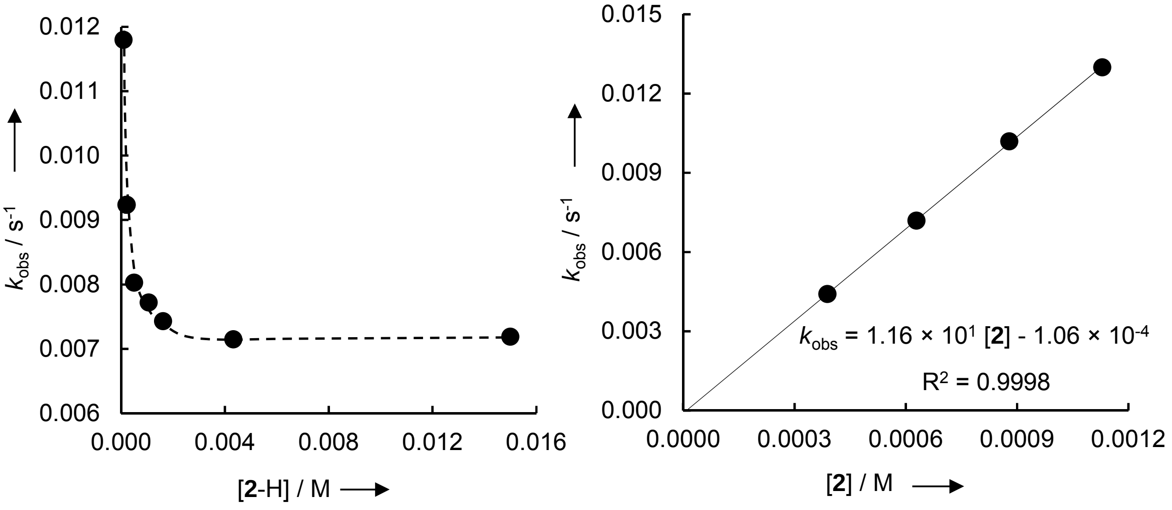

Figure 3.9. Plots of k_{obs} versus [**2**-H] for the reaction of **2** with **4b** in presence of **2**-H, deprotonation of **2**-H performed with TMG, [**2**] = 6.20 – 6.48 × 10^{-4} M (on the left) and of k_{obs} versus [**Nu**], [**2**-H] = 5.47 × 10^{-3} – 1.50 × 10^{-2}M (on the right).

However, when **2**-H was deprotonated with KO*t*Bu and the reaction of **2** with **4b** was performed, a "normal" increase of k_{obs} (like in Figure 3.7) was observed with increasing [**2**-H]. The second-order rate constant $k_1 = 1.16 \times 10^1$ M^{-1}s^{-1}, derived indirectly by the steady-state approximation method described above (for details, see Table 3.S16 in the experimental section), is in an excellent agreement with the value obtained directly in the experiment with TMG.

In case C, a quantitative analysis of the observed changes of the absorbances of the electrophile is quite complicated, because several processes have to be taken into account to mathematically model the system.

As none of the reactions of **2**/**2**-H with quinone methides **4a-e** followed pattern of case C, one can exclude protonation of these quinone methides by acids weaker than **2**-H, which means that none of the acids formed as a result of deprotonation of the fluorenes can protonate these quinone methides to any significant extent.

Thus, the concentration of the quinone methide should follow the rate law formulated in Equation 10.

$$\frac{\mathrm{d}[\mathbf{E}]}{\mathrm{d}t} = -k_1[\mathbf{E}][\mathbf{Nu}] + k_{-1}[\mathbf{I}] - k_3[\mathbf{E}][\mathbf{NuH}] + k_{-3}[\mathbf{EH}][\mathbf{Nu}] \tag{10}$$

Experimentally obtained time-dependent absorbances of **E** do not provide enough information for unambiguous determination of the second-order rate constants k_1. It is obvious that one should avoid using the amino-substituted quinone methides for the determination of the nucleophilic reactivities of weakly basic carbanions, when kinetic experiments have to be performed in presence of the corresponding strong C-H acids for thermodynamic reasons.

3.2.3. Determination of the Nucleophilicity Parameters for 9-Substituted Fluorenyl Anion

The second-order rate constants for the reactions of **1-3** with reference electrophiles **4** in DMSO are listed in Table 3.3. The logarithms of these rate constants were plotted versus the previously described electrophilicity parameters of the reference systems (Figure 3.10) and the nucleophilicity and sensitivity parameters N and s_N for carbanions **1-3** were calculated from the rate constants of the reactions with quinone methides on the basis of Equation 1.

Table 3.3. Second-order rate constants (k_1, DMSO 20°C) for the reactions of benzhydrylium tetrafluoroborates and quinone methides **4** with fluorenyl anions **1-3** and resulting N and s_N parameters.

Nucleophile	N	s_N	Reference electrophile	k_2 / $M^{-1}s^{-1}$
9-Cyanofluorenyl anion (**1**)	19.44	0.66	mF$_2$(tBu)$_2$QM (**4c**)	2.36×10^3
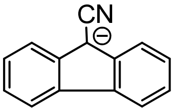			dma(Ph)$_2$QM (**4d**)	7.22×10^3
			ani(Ph)$_2$QM (**4e**)	7.75×10^4
			(lil)$_2$CH$^+$(**4f**)	4.66×10^7
			(jul)$_2$CH$^+$ (**4g**)	9.07×10^7
			(ind)$_2$CH$^+$ (**4h**)	1.59×10^8
			(thq)$_2$CH$^+$ (**4i**)	3.08×10^8
			(dma)$_2$CH$^+$ (**4j**)	5.51×10^8
9-Carbomethoxyfluorenyl anion (**2**)	18.84	0.79	jul(tBu)$_2$QM (**4a**)	7.48
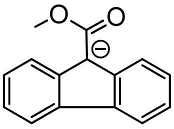			dma(tBu)$_2$QM (**4b**)	1.16×10^1
			mF$_2$(tBu)$_2$QM (**4c**)	6.41×10^3
			dma(Ph)$_2$QM (**4d**)	1.38×10^4
			ani(Ph)$_2$QM (**4e**)	1.82×10^5
2,7-Dibromo-9-carbomethoxyfluorenyl anion (**3**)	17.34	0.71	mF$_2$(tBu)$_2$QM (**4c**)	9.93×10^1
			ani(Ph)$_2$QM (**4e**)	4.42×10^3
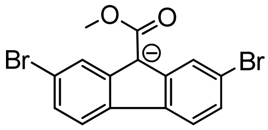				

The rate constants for the reactions of **1** with benzhydrylium ions were not used for the determination of N and s_N parameters for two reasons: The first one is that the rate constants for the reactions even with moderately reactive benzhydrylium ions are already close to the diffusion limit and give less information about the nucleophilic reactivity of **1** than the rate constants for the slower reactions with quinone methides. The second reason is that, unlike in reactions with many other carbanions, benzhydrylium ions and quinone methides do not follow the same correlation. Combining both series would result in a large scatter of the data points and a higher slope than the slopes of separate correlations. This would also be misleading when **1** is compared to **2** and **3**, as the rate constants for their reactions with benzhydrylium ions are not available.

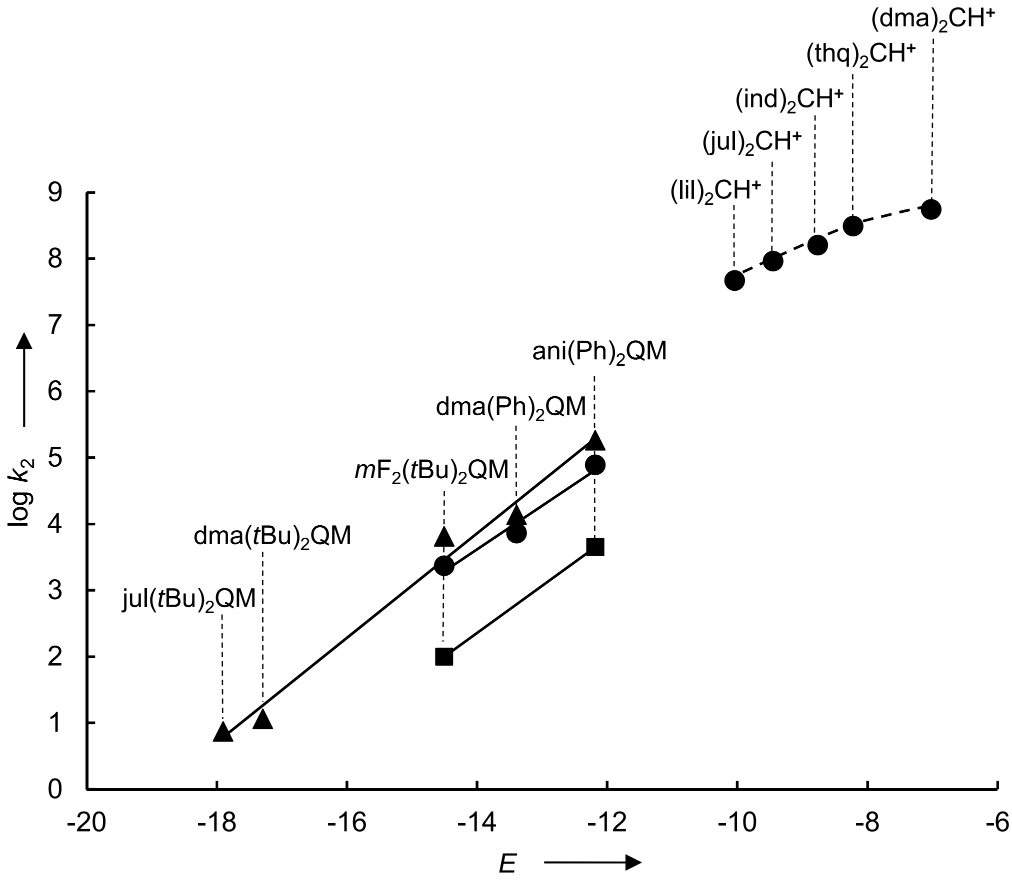

Figure 3.10. Correlation of the logarithms of the second-order rate constants for the reactions of **1-3** and **4a-j** with previously reported E parameters for the electrophiles (DMSO, 20°C). Data points: ● for **1,** ▲ for **2** and ■ for **3**.

Only few rate constants were available for the determination of the nucleophilicity parameters for **1** and **3**, because most of their reactions with amino-substituted quinone methides are complicated by protonation of the electrophile by the corresponding conjugated C-H acid. Despite this fact, the nucleophilicity and sensitivity parameters listed in Table 3.3 give a good idea of the reactivities of **1-3** in DMSO and allow us to compare them with those of other carbanions which are already included in our reactivity database.

It is noteworthy that, although they are relatively weak bases, carbanions **1-3** are very nucleophilic.

Figure 3.11 shows a moderate correlation of the log k_2 for the reactions of different carbanions with the quinone methide **4c** (calculated from their N and s_N values using Equation 23). The points for the carbanions **1-3** are located about two logarithmic units above the correlation line in Fig. 10, i. e., **1-3** are more nucleophilic than one would expect from their pK_{aH} values, indicating significantly lower intrinsic barriers of their reactions with our reference electrophiles compared to other carbanions.

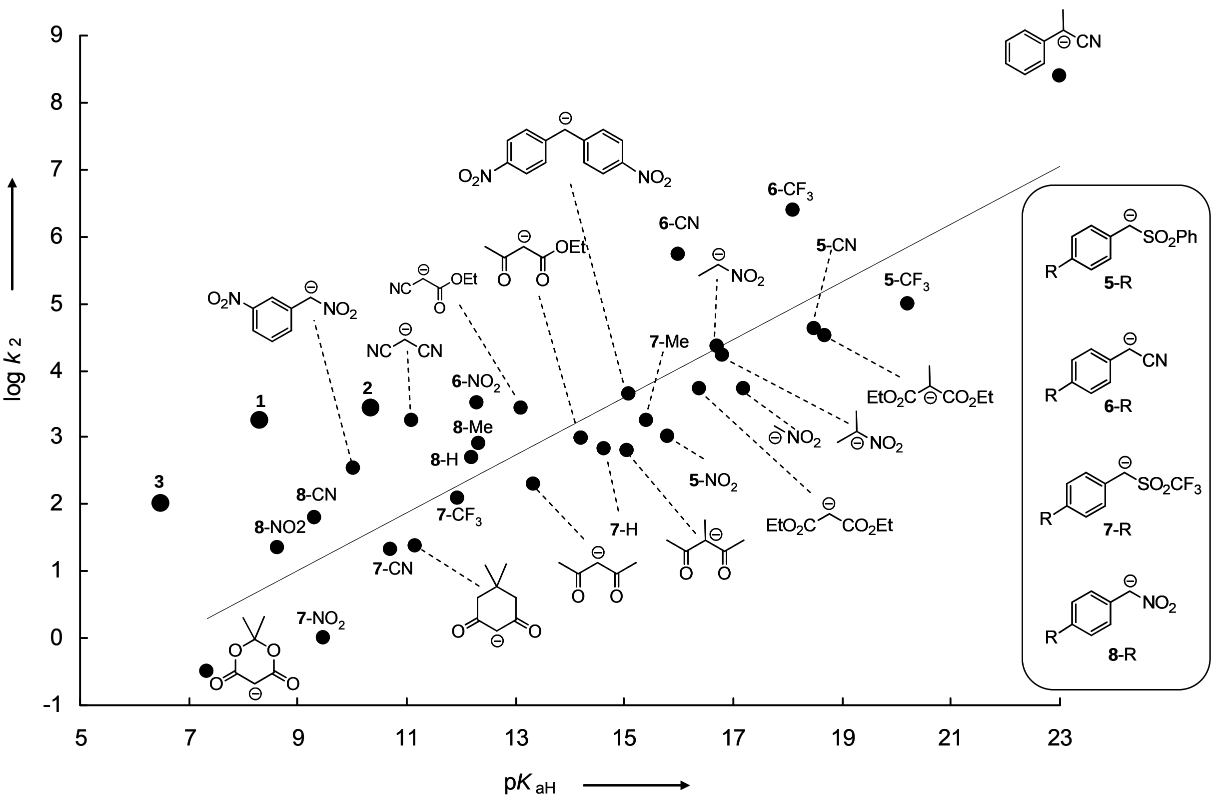

Figure 3.11. Correlation of the calculated second-order rate constants k_2 for the reactions of carbanions with quinone methide **4c** versus their pK_{aH} values in DMSO at 20°C (for nucleophilicity and sensitivity parameters for the carbanions, see ref.5h, pK_{aH} values are compiled in ref.17). Carbanions **1-3** are not considered for the calculation of the trend line.

3.2.4. Intrinsic Reactivities Towards C_{sp2} and C_{sp3} Electrophilic Centers

It was already mentioned that the major goal of this thesis is the investigation of the relationship between the reactivities towards C_{sp2} and C_{sp3} electrophilic centers. Despite the fact that there are only few carbanions for which the reactivities towards both reference benzhydrylium ions (or quinone methides) and S_N2 substrates have been measured, we can analyze the trends in intrinsic barriers which control the reactivities of **1-3** in different types of reactions and then compare them.

In both correlations of log k_2 vs pK_{aH} for the addition of anions **1-3** to quinone methides **4c** and **4e**, 9-cyanofluorenyl anion points deviate upwards from the line for methoxycarbonyl fluorenyl anions (Figure 3.12), indicative of the lower intrinsic barriers for the reactions of **1**.

Deprotonation by amines in DMSO-water mixtures was also found to be intrinsically more favourable for **1**-H than for **2**-H,[18] which is in agreement with other reports on the lower intrinsic barriers for the reactions of cyano-substituted anions.[17,19]

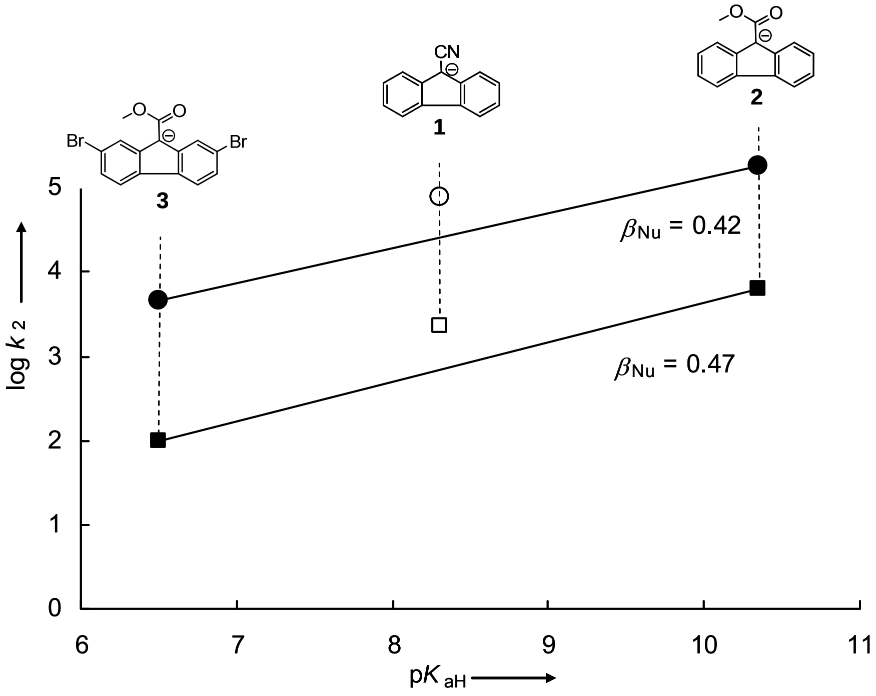

Figure 3.12. Plots of the second-order rate constants for the reactions of **1-3** and **4c,e** with previously reported pK_{aH} values for **1-3**.

Data points: ● (○) for the reactions with **4e** and ■ (□) for the reactions with **4c**.

The major factors that are believed to contribute to the difference in the intrinsic barriers for the deprotonation of **1**-H and **2**-H are: 1) the late development of the resonance stabilization for **2** along the reaction coordinate and 2) the stronger polar effect of the CN group, which stabilizes the negative charge in the transition state better than in the ground state, because of the late delocalization of the negative charge into the fluorenyl moiety.[18] These factors may also play a role in the addition reactions of carbanions **1-3** to quinone methides.

However, Bordwell and Hughes studied the reactivites of 9-substituted fluorenyl anions towards benzyl chloride in DMSO, and found that the point for 9-cyanofluorenyl anion exactly matched the plot of log k_2 versus pK_{aH} for a family of 9-carbomethoxy-subsituted fluorenyl anions (Figure 3.13).[1a] This indicates no particular difference in intrinsic barriers for the S_N2 reactions of these anions with benzyl chloride. Thus, the reactivities of 9-substituted fluorenyl anions towards Csp^3- and Csp^2-electrophilic centers appear to be controlled by different factors.

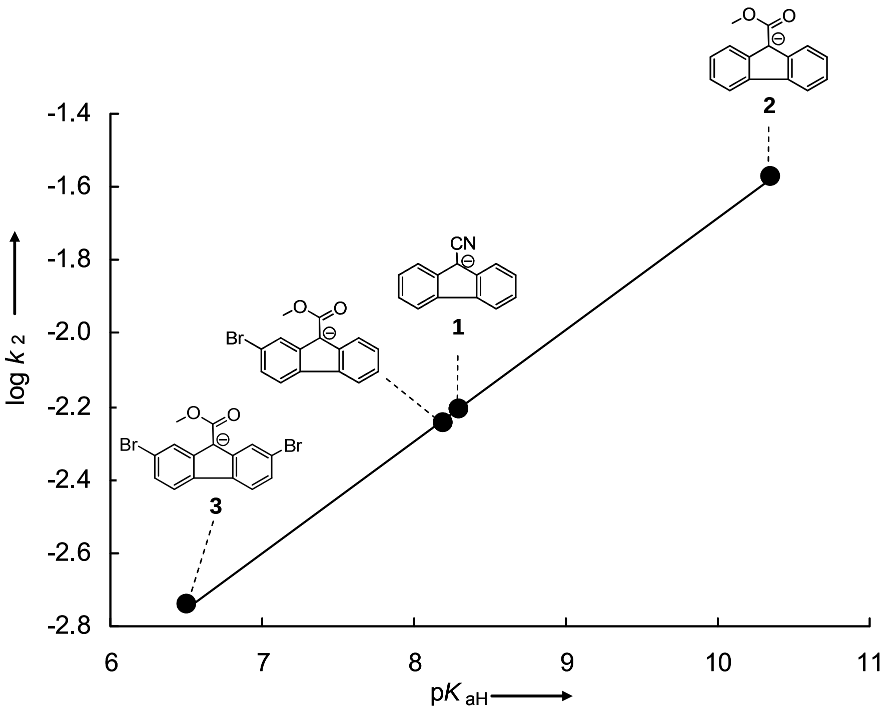

Figure 3.13. Plots of the second-order rate constants for the reactions of 9-substituted fluorenyl anions with benzyl chloride in DMSO at 25°C versus their pK_{aH} values. The data are taken from ref. 1a.

3.2.5. Comparison of the Reactivities of 9-Substituted Fluorenyl Anions and Amines towards Benzyl Chloride

In the previous chapter, we discussed the correlations of the reactivities of neutral nitrogen nucleophiles towards S_N2 substrates with those towards the lil$_2$CH$^+$ cation (**4f**), to compare the reactivities towards Csp^3- and Csp^2-electrophilic centers.

We cannot include the anions **2** and **3** into these correlations, as the rate constants for their reactions with lil$_2$CH$^+$ (**4f**) are neither experimentally accessible and nor predictable using N and s_N parameters derived from the rate constants for their reactions with quinone methides. Only for **1** are the rate constants for the reactions with benzhydrylium ions available. In order to include anions **1-3** into a correlation of the reactivities towards Csp^3- versus those towards Csp^2 center, we have plotted the logarithms of the rate constants for the reactions of several amines and anions **1-3** with benzyl chloride versus their reactivities towards ani(Ph)$_2$QM (**4e**) in DMSO, calculated from the s_N and N parameters (Figure 3.14).

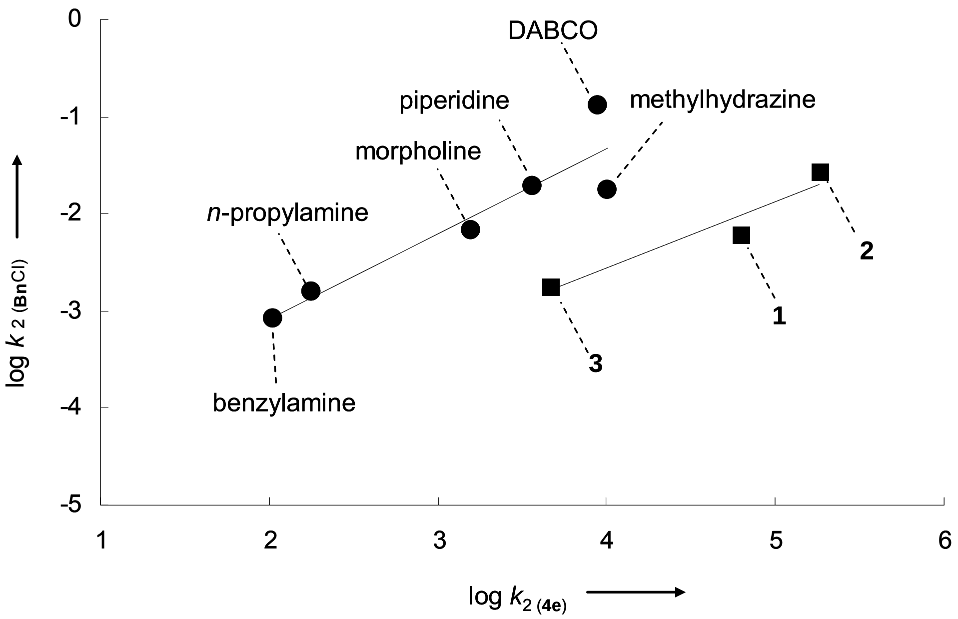

Figure 3.14. Correlation of log k_2 for the reactions of various amines (at 20° in DMSO) and anions **1-3** (at 25°C in DMSO, from ref. 1a) with benzyl chloride versus log k_2 for their reactions with ani(Ph)$_2$QM (**4e**) in DMSO.

Obviously, the carbanions **1-3** and neutral N-nucleophiles make two separate correlation lines, and the line for carbanions **1-3** is about one unit of the logarithmic scale lower than that for amines. This downward shift is comparable in size with the deviations of tertiary amines and triarylphosphanes from the correlation of log k_2 for the reactions of amines and phosphanes with 4-cyanobenzyl bromide versus log k_2 for their reactions with lil$_2$CH$^+$ (**4f**) (chapter 2, Figure 2.S5.6.2). As **1-3** are tertiary carbanions, this downward shift may be due to steric reasons.

3.3. Conclusion

The majority of the reactions of 9-substituted fluorenyl anions **1-3** with quinone methides are highly reversible and take place only in presence of the corresponding C-H acids. Under these conditions, the reactions of amino-substituted quinone methides with carbanions having pK_{aH} ≤ 9 in DMSO are most probably complicated by partial protonation of the quinone methide. It is therefore inexpedient to use these quinone methides as reference electrophiles for the determination of the nucleophilicity parameters of such carbanions in the future.

The rate constants for the reactions of carbanion **1-3** with quinone methides in DMSO follow the linear free energy relationship **1**, which allows determination of their N and s_N parameters. Kinetics of the reactions of **1** with several benzhydrylium ions, studied using laser-flash photolysis technique, show that the rate constants for these reactions are much higher (by ca. 3 orders of magnitude) than one can expect from the rate constants for the reactions with quinone methides.

Strong positive deviations of the rate constants for the reactions of carbanions **1-3** from the Brønsted plots indicate lower intrinsic barriers compared to other families of carbanions studied in our group.

The plot of the reactivities of the anions **1-3** and several amines towards benzyl chloride versus their reactivities towards ani(Ph)$_2$QM (**4e**) in DMSO gives two separate lines, the line for anions **1-3** is lower than that for amines by ca. 1 order of magnitude, probably for steric reasons.

3.S. Experimental Section

3.S.1. General

Materials. The benzhydrylium tetrafluoroborates[5c] **4f-j** and quinone methides[5b,20] **4a-e** were synthesized as described in the literature.
DMSO (99.7%, etra dry) was purchased and used without further purification.

Preparation of the stock solutions. Stock solutions for all measurements were prepared in volumetric flasks. After the compound (fluorene, base or electrophile) was introduced into the tared empty flask and weighed in the glove box, the flask was closed with a rubber septum, taken out of the glove box and filled with dry solvent to 5 or 10 mL. The pressure in the flask was always balanced with a balloon filled with dry nitrogen.
As all quinone methides tend to dissolve in pure DMSO very slowly, a few drops of dry dichloromethane were added before DMSO to facilitate homogenization of the solution. The solutions of fluorenes (**1-3**)-H were prepared in dichloromethane. The solutions of KO*t*Bu, TMG and *n*-$Bu_4N^+PhCO_2^-$, benzoic acid and benzhydrylium ions were prepared in DMSO. The solution of KO*t*Bu was used within 20 min. after preparation, after that a new solution was prepared when necessary.

Kinetic measurements. The kinetics of the reactions of **1-3** with the benzhydrylium ions and quinone methides **4** were followed by UV-vis spectroscopy.
J&M technique was used for slow reactions ($\tau 1/2$ > 10 s). All kinetic experiments were carried out in Schlenk glassware, which was degassed repeatedly by evacuating to less than 10 mbar and purging with dry nitrogen. After the empty reservoir was tared, ca. 20 mL DMSO was introduced via syringe and the reservoir was weighed again to determine the exact amount of liquid introduced.
After the UV-vis spectrum of the pure solvent was registered, the calculated amounts of the stock solutions were added via Hamilton syringes. The base was introduced first, followed by the fluorene. The solution of the fluorenyl anion was equilibrated at 20 ± 0.1 °C for ca. 1 min, then the quinone methide was added.
The temperature of the solutions during the kinetic studies was maintained at 20 ± 0.1 °C with a bath circulating thermostate. The spectra were collected at different times by using a diode array spectrophotometer that was connected to a quartz immersion probe (5 mm light path) by

fiber optic cables with standard SMA connectors. The decrease of the absorbance at the chosen wavelength (normally, the λ_{max} of the quinone methide) was cut out of full spectrum and evaluated.

Stopped-flow spectrophotometer systems were used for the investigation of faster reactions (10 ms < $\tau 1/2$ < 10 s). The solutions of the electrophiles for the stopped-flow experiments were prepared by dilution of the stock solutions with DMSO to make the concentration of the quinone methide ca. 0.01-0.02 mM (the exact concentrations in each case are given in the tables below). The solutions of the nucleophiles were freshly prepared prior to measurements as follows. Each volumetric flask (10 mL) was filled with argon in the glove box and closed with a rubber septum, then removed from the glove box and supplied with a balloon filled with dry nitrogen to balance the pressure in the flask. Few milliliters of dry DMSO was introduced into the flask via syringe. Then calculated amount of the base stock solution was added followed by the fluorene solution. In the end, the solution of the carbanion was diluted with dry DMSO to 10 mL and used for the measurement immediately.

The kinetic runs were initiated by mixing equal volumes of the solutions of the quinone methide and the carbanion. The decrease of the absorbance at the chosen wavelength (normally, the λ_{max} of the quinone methide) was registered. For each concentration, 3 to 10 single runs were averaged. The temperature of the solutions during the kinetic studies was maintained at 20 ± 0.1 °C.

In both J&M and stopped-flow experiments, the carbanions **1−3** were used in large excess (>8 equiv) relative to the quinone methides **4a-e** to ensure first-order conditions with $k_{obs} = k_2[Nu]_0 + k_0$. From the time-dependent decays of the absorbances at λ_{max} of **4a-e**, the first-order rate constants k_{obs} (s^{-1}) were obtained by least-squares fitting to the monoexponential curve $A = A_0\ e^{-k_{obs}t} + C$. The slopes of plots of k_{obs} versus the concentrations of the nucleophiles yielded the second-order rate constants k_2 ($M^{-1}\ s^{-1}$).

Reactions of **1** with **4f-j** (with $\tau 1/2$ < 10 ms) were analyzed by laser-flash photolytic generation of the cations from the corresponding adducts in the presence of a small (1.8-3.0 equiv.) excess carbanion. Solutions for the experiments were prepared as follows. To a 25 mL volumetric flask, filled with dry nitrogen and covered with a rubber septum with a ballon, ca. 10 mL of dry DMSO was introduced. Then the stock solution of KO*t*Bu was added followed by the fluorene solution (in a slight excess over KO*t*Bu, < 5%). After ca. 1 min., stock solution of the benzhydrylium ion was added and the blue colour of the electrophile disappeared immediately. Carbanion was present in a moderate excess over the benzhydrylium ion (for the exact ratio in each case, see the tables below). The solution was diluted with dry DMSO to 25 mL and used for the experiment immediately.

The carbocation precursors were irradiated with a 7 ns pulse from a quadrupled Nd:YAG laser (266 nm, 40−60 mJ/pulse), and a xenon lamp was used as probe light for UV-vis detection. The system was equipped with a fluorescence flow cell and a synchronized pump system, which allows complete exchange of the sample volume between subsequent laser pulses. For each concentration, ≥ 50 individual measurements were averaged.

3.S.2. Rate constants for the reactions of 9-Cyanofluorenyl anion (1) in DMSO

Table 3.S1. Rate constants for the reaction of 9-cyanofluorenyl anion (**1**) with jul(*t*Bu)$_2$QM (**4a**) at 20˚C in DMSO (0 – 1.2 % CH_2Cl_2), J&M and stopped-flow techniques. Deprotonation with tetrabutylammonium benzoate. Case C.

No	$[E]_0$ / M	$[Nu]_0$ / M[a]	$[NuH]_0$ / M[b]	$[Nu]_0$ / $[E]_0$	k_{obs} / s^{-1}
1	3.52×10^{-5}	6.47×10^{-4}	1.41×10^{-3}	18	1.20×10^{-2}
2	3.52×10^{-5}	6.48×10^{-4}	2.45×10^{-3}	18	1.86×10^{-2}
3	3.52×10^{-5}	6.47×10^{-4}	3.48×10^{-3}	18	2.48×10^{-2}
4	3.52×10^{-5}	6.46×10^{-4}	5.53×10^{-3}	18	3.66×10^{-2}
5	1.80×10^{-5}	6.44×10^{-4}	2.69×10^{-2}	36	1.61×10^{-1}
6	1.80×10^{-5}	6.44×10^{-4}	5.50×10^{-2}	36	3.20×10^{-1}
7	1.80×10^{-5}	6.44×10^{-4}	8.22×10^{-2}	36	4.72×10^{-1}

In this and all posterior tables, if not mentioned otherwise: (a) $[Nu]_0$ is considered to be equal to the calculated concentration of the deprotonating agent, (b) $[NuH]_0$ is the calculated concentration of the fluorene after the deprotonation.

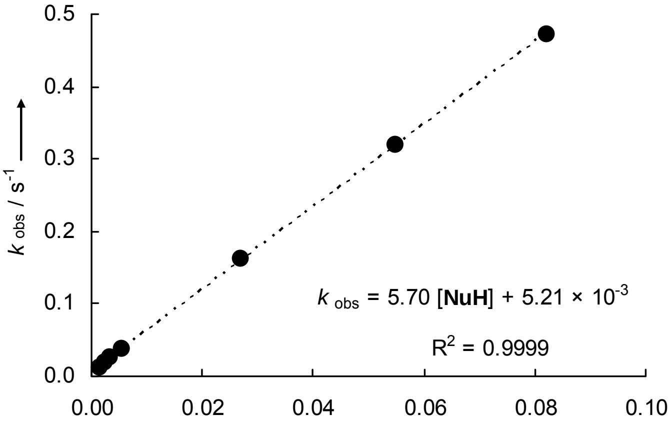

Table 3.S2. Rate constants for the reaction of 9-cyanofluorenyl anion (**1**) with dma(*t*Bu)$_2$QM (**4b**) at 20°C in DMSO (0 – 4.0 % CH_2Cl_2), J&M and stopped-flow techniques. Deprotonation with tetrabutylammonium benzoate. Case C.

No	$[E]_0$ / M	$[Nu]_0$ / M	$[NuH]_0$ / M	$[Nu]_0$ / $[E]_0$	k_{obs} / s^{-1}
1	3.24×10^{-5}	6.25×10^{-4}	3.08×10^{-3}	19	6.23×10^{-3}
2	3.26×10^{-5}	6.28×10^{-4}	6.81×10^{-3}	19	8.25×10^{-3}
3	3.25×10^{-5}	6.27×10^{-4}	1.17×10^{-2}	19	1.08×10^{-2}
4	1.30×10^{-5}	6.24×10^{-4}	2.56×10^{-2}	48	1.89×10^{-2}
5	1.30×10^{-5}	6.24×10^{-4}	1.29×10^{-1}	48	7.41×10^{-2}

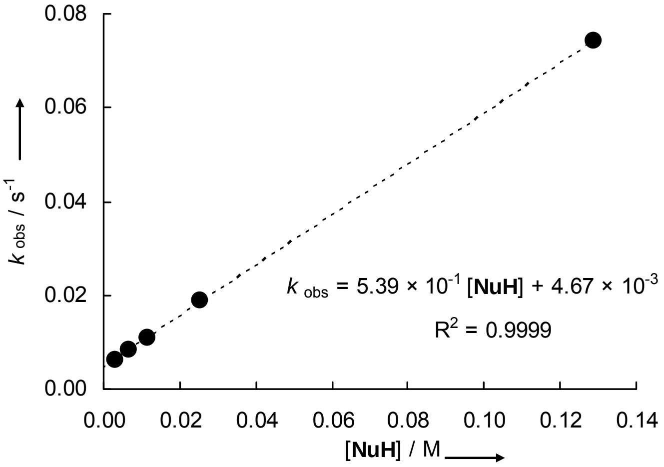

Table 3.S3. Rate constants for the reaction of 9-cyanofluorenyl anion (**1**) with F_2(*t*Bu)$_2$QM (**4c**) at 20°C in DMSO (3.0 – 4.0 % CH_2Cl_2), stopped-flow technique. Deprotonation with tetrabutylammonium benzoate. Case B. Indirect evaluation.

No	$[E]_0$ / M	$[Nu]_0$ / M	$[NuH]_0$ / M	$[Nu]_0$ / $[E]_0$	k_{obs} / s^{-1}	$[NuH]^{-1}$ / M^{-1}	[Nu] k_{obs}^{-1}/ M s
1	2.18×10^{-5}	7.10×10^{-4}	0	33	1.04	6.83×10^{-4}	-
2	2.18×10^{-5}	7.13×10^{-4}	4.98×10^{-5}	33	1.16	6.15×10^{-4}	-
3	2.18×10^{-5}	7.13×10^{-4}	1.02×10^{-4}	33	1.28	5.57×10^{-4}	9.80×10^{3}
4	2.18×10^{-5}	7.13×10^{-4}	1.55×10^{-4}	33	1.39	5.13×10^{-4}	6.45×10^{3}
5	2.18×10^{-5}	7.13×10^{-4}	3.39×10^{-4}	33	1.54	4.63×10^{-4}	2.95×10^{3}
6	2.18×10^{-5}	7.13×10^{-4}	6.02×10^{-4}	33	1.61	4.43×10^{-4}	1.66×10^{3}
7	2.18×10^{-5}	7.13×10^{-4}	8.65×10^{-4}	33	1.66	4.30×10^{-4}	1.16×10^{2}
8	2.18×10^{-5}	7.13×10^{-4}	1.39×10^{-3}	33	1.68	4.24×10^{-4}	7.19×10^{2}
$k_2 = 2.40 \times 10^{3}$ $M^{-1}s^{-1}$							

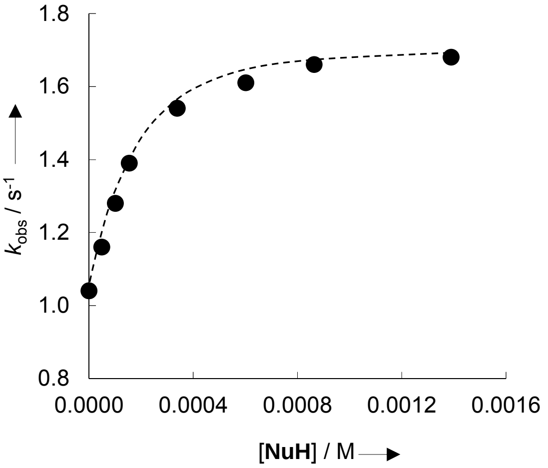

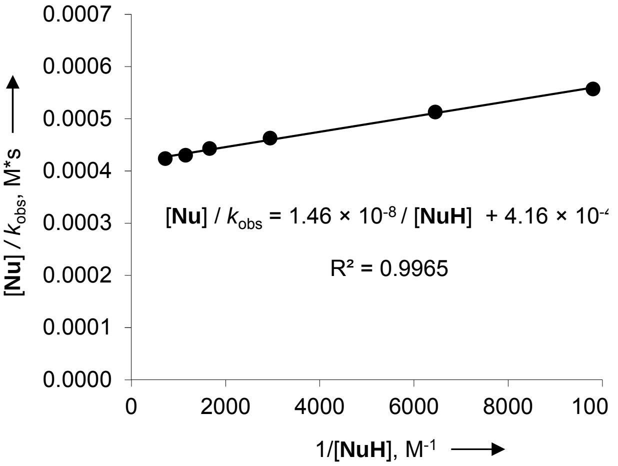

Table 3.S4a. Rate constants for the reaction of 9-cyanofluorenyl anion (**1**) with $F_2(t\mathrm{Bu})_2$QM (**4c**) at 20°C in DMSO (3.0 – 4.0 % CH_2Cl_2), stopped-flow technique. Deprotonation with tetrabutylammonium benzoate. Case B. Experiment with high amounts of benzoic acid, [NuH] = 0.

No	$[E]_0$ / M	$[Nu]_0$ / M	$[PhCO_2H]_0$ / M	$[Nu]_0$ / $[E]_0$	k_{obs} / s^{-1}
1	2.18×10^{-5}	7.10×10^{-4}	7.10×10^{-4}	33	1.04
2	2.18×10^{-5}	7.10×10^{-4}	1.94×10^{-3}	33	1.21
3	2.18×10^{-5}	7.10×10^{-4}	3.58×10^{-3}	33	1.37

Table 3.S4b. Rate constants for the reaction of 9-cyanofluorenyl anion (**1**) with $F_2(t\mathrm{Bu})_2$QM (**4c**) at 20°C in DMSO, stopped-flow technique. Deprotonation with tetrabutylammonium benzoate. Case B. Direct evaluation.

No	$[E]_0$ / M	$[Nu]_0$ / M	$[NuH]_0$ / M	$[Nu]_0$ / $[E]_0$	k_{obs} / s^{-1}
1	2.42×10^{-5}	3.21×10^{-4}	1.32×10^{-3}	13	8.09×10^{-1}
2	2.54×10^{-5}	4.03×10^{-4}	1.23×10^{-3}	16	9.97×10^{-1}
3	2.42×10^{-5}	6.42×10^{-4}	1.33×10^{-3}	27	1.55
4	2.54×10^{-5}	7.05×10^{-4}	1.25×10^{-3}	28	1.63
5	2.42×10^{-5}	9.63×10^{-4}	1.34×10^{-3}	40	2.30
6	2.54×10^{-5}	1.01×10^{-3}	1.28×10^{-3}	40	2.46
7	2.42×10^{-5}	1.28×10^{-3}	1.34×10^{-3}	53	3.07
8	2.42×10^{-5}	1.58×10^{-3}	1.37×10^{-3}	65	3.75
		$k_2 = 2.36 \times 10^3$ M^{-1}s^{-1}			

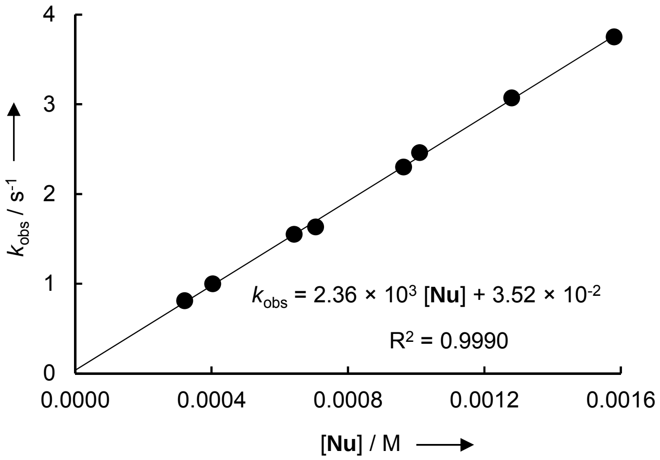

Table 3.S5. Rate constants for the reaction of 9-cyanofluorenyl anion (**1**) with dma(Ph)$_2$QM (**4d**) at 20˚C in DMSO, stopped-flow technique. Deprotonation with tetrabutylammonium benzoate. Case A.

No	$[E]_0$ / M	$[Nu]_0$ / M	$[NuH]_0$ / M	$[Nu]_0$ / $[E]_0$	k_{obs} / s^{-1}
1	1.27×10^{-5}	2.99×10^{-4}	1.14×10^{-3}	24	2.40
2	1.27×10^{-5}	5.90×10^{-4}	1.14×10^{-3}	46	4.49
3	1.27×10^{-5}	8.82×10^{-4}	1.13×10^{-3}	69	6.58
4	1.27×10^{-5}	1.17×10^{-3}	1.13×10^{-3}	92	8.65
5	1.27×10^{-5}	1.47×10^{-3}	1.12×10^{-3}	116	1.09×10^{1}
$k_2 = 7.24 \times 10^3$ M^{-1}s^{-1}					

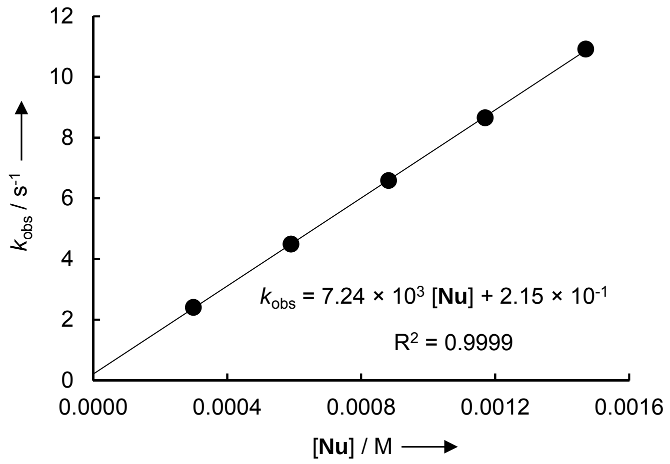

Table 3.S6. Rate constants for the reaction of 9-cyanofluorenyl anion (**1**) with dma(Ph)$_2$QM (**4d**) at 20˚C in DMSO, stopped-flow technique. Deprotonation with KO*t*Bu. Case A.

No	$[E]_0$ / M	$[Nu]_0$ / M	$[NuH]_0$ / M	$[Nu]_0$ / $[E]_0$	k_{obs} /s^{-1}
1	2.00×10^{-5}	6.59×10^{-4}	2.03×10^{-5}	33	4.49
2	2.00×10^{-5}	8.24×10^{-4}	2.54×10^{-5}	41	5.67
3	2.00×10^{-5}	9.89×10^{-4}	3.05×10^{-5}	49	6.90
4	2.00×10^{-5}	1.15×10^{-3}	3.56×10^{-5}	58	8.20
5	2.00×10^{-5}	1.32×10^{-3}	4.07×10^{-5}	66	9.15
$k_2 = 7.19 \times 10^3$ M^{-1}s^{-1}					

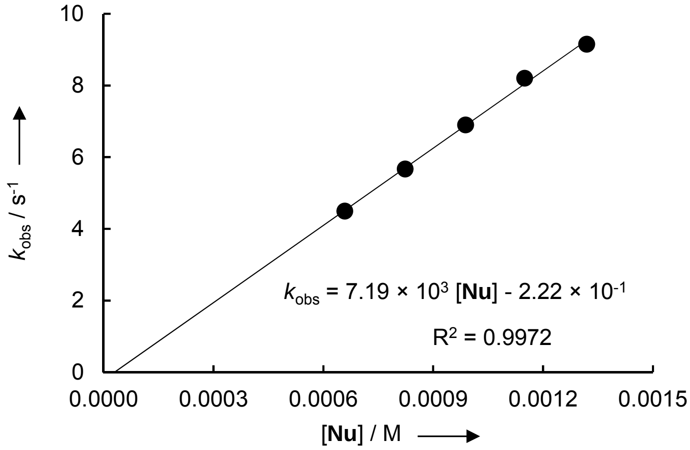

Table 3.S7. Rate constants for the reaction of 9-cyanofluorenyl anion (**1**) with ani(Ph)$_2$QM (**4e**) at 20˚C in DMSO, stopped-flow technique. Deprotonation with benzoate. Case A. Direct evaluation.

No	$[E]_0$ / M	$[Nu]_0$ / M	$[NuH]_0$ / M	$[Nu]_0$ / $[E]_0$	k_{obs} /s^{-1}
1	5.40×10^{-6}	9.13×10^{-5}	7.40×10^{-4}	17	7.16
2	5.40×10^{-6}	1.83×10^{-4}	6.49×10^{-4}	34	1.40×10^1
3	5.40×10^{-6}	2.28×10^{-4}	6.03×10^{-4}	42	1.77×10^1
4	5.40×10^{-6}	2.74×10^{-4}	5.58×10^{-4}	51	2.13×10^1
5	5.40×10^{-6}	3.20×10^{-4}	5.12×10^{-4}	59	2.48×10^1
$k_2 = 7.75 \times 10^4$ M^{-1}s^{-1}					

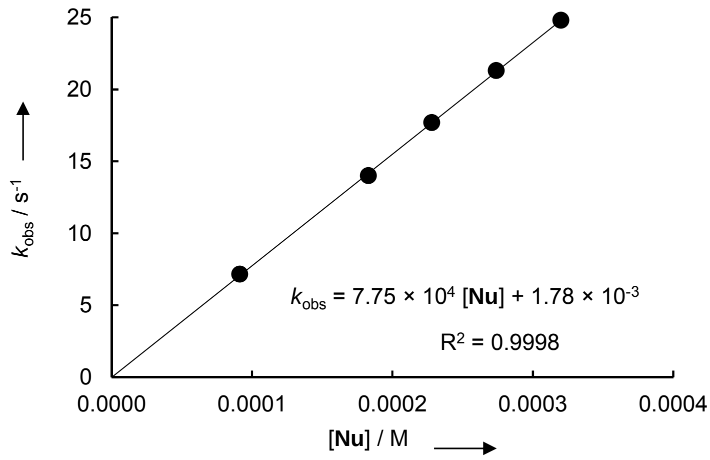

Table 3.S8. Rate constants for the reaction of 9-cyanofluorenyl anion (**1**) with $(lil)_2CH^+$(**4f**) at 20˚C in DMSO, laser-flash photolysis technique. Deprotonation with KO*t*Bu.

No	$[Pr]_0$ / M	$[Nu]_0$ / M	$[Nu]_{eff}$ / M	$[NuH]_0$ / M	$[Nu]_{eff}/[Pr]_0$	k_{obs}/s^{-1}
1	2.07×10^{-5}	7.49×10^{-5}	5.42×10^{-5}	1.97×10^{-5}	2.6	2.20×10^{3}
2	4.13×10^{-5}	1.50×10^{-4}	1.09×10^{-4}	3.94×10^{-5}	2.6	4.73×10^{3}
3	6.20×10^{-5}	2.25×10^{-4}	1.63×10^{-4}	5.91×10^{-5}	2.6	7.26×10^{3}
4	8.26×10^{-5}	2.99×10^{-4}	2.16×10^{-4}	7.87×10^{-5}	2.6	9.71×10^{3}
5	1.03×10^{-4}	3.74×10^{-4}	2.71×10^{-4}	9.84×10^{-5}	2.6	1.23×10^{4}
$k_2 = 4.66 \times 10^7$ M^{-1}s^{-1}						

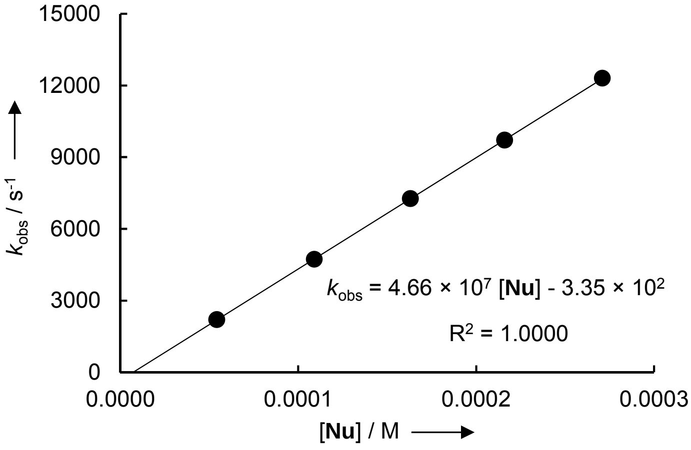

Table 3.S9. Rate constants for the reaction of 9-cyanofluorenyl anion (**1**) with $(\mathrm{jul})_2\mathrm{CH}^+$(**4g**) at 20°C in DMSO, laser-flash photolysis technique. Deprotonation with KO*t*Bu.

No	$[\mathrm{Pr}]_0$ / M	$[\mathrm{Nu}]_0$ / M	$[\mathrm{Nu}]_{\mathrm{eff}}$ / M	$[\mathrm{NuH}]_0$ / M	$[\mathrm{Nu}]_{\mathrm{eff}}/[\mathrm{Pr}]_0$	$k_{\mathrm{obs}}/\mathrm{s}^{-1}$
1	1.94×10^{-5}	7.77×10^{-5}	5.83×10^{-5}	1.68×10^{-5}	3.0	3.85×10^{3}
2	3.87×10^{-5}	1.55×10^{-4}	1.16×10^{-4}	3.37×10^{-5}	3.0	8.69×10^{3}
3	5.81×10^{-5}	2.33×10^{-4}	1.75×10^{-4}	5.05×10^{-5}	3.0	1.44×10^{4}
4	7.74×10^{-5}	3.11×10^{-4}	2.34×10^{-4}	6.73×10^{-5}	3.0	1.95×10^{4}
5	9.68×10^{-5}	3.89×10^{-4}	2.92×10^{-4}	8.42×10^{-5}	3.0	2.50×10^{4}
$k_2 = 9.07 \times 10^{7}\ \mathrm{M}^{-1}\mathrm{s}^{-1}$						

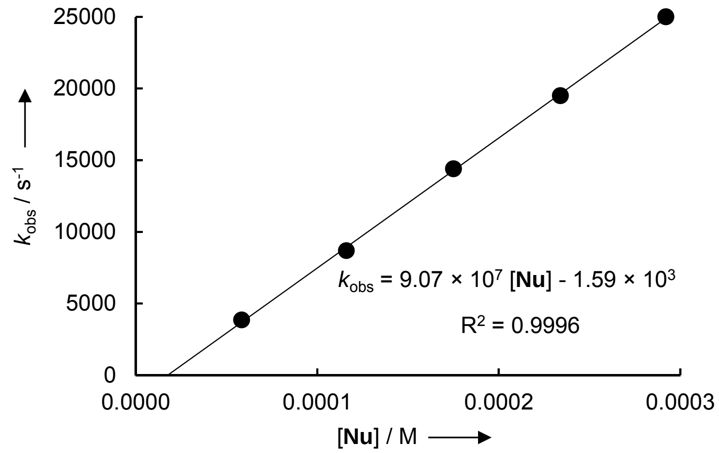

Table 3.S10. Rate constants for the reaction of 9-cyanofluorenyl anion (**1**) with $(\mathrm{ind})_2\mathrm{CH}^+$(**4h**) at 20°C in DMSO, laser-flash photolysis technique. Deprotonation with KO*t*Bu.

No	$[\mathrm{Pr}]_0$ / M	$[\mathrm{Nu}]_0$ / M	$[\mathrm{Nu}]_{\mathrm{eff}}$ / M	$[\mathrm{NuH}]_0$ / M	$[\mathrm{Nu}]_{\mathrm{eff}}/[\mathrm{Pr}]_0$	$k_{\mathrm{obs}}/\mathrm{s}^{-1}$
1	2.21×10^{-5}	7.77×10^{-5}	5.56×10^{-5}	1.68×10^{-5}	2.5	5.70×10^{3}
2	4.42×10^{-5}	1.55×10^{-4}	1.11×10^{-4}	3.37×10^{-5}	2.5	1.38×10^{4}
3	6.62×10^{-5}	2.33×10^{-4}	1.67×10^{-4}	5.05×10^{-5}	2.5	2.28×10^{4}
4	8.83×10^{-5}	3.11×10^{-4}	2.23×10^{-4}	6.73×10^{-5}	2.5	3.22×10^{4}
$k_2 = 1.59 \times 10^{8}\ \mathrm{M}^{-1}\mathrm{s}^{-1}$						

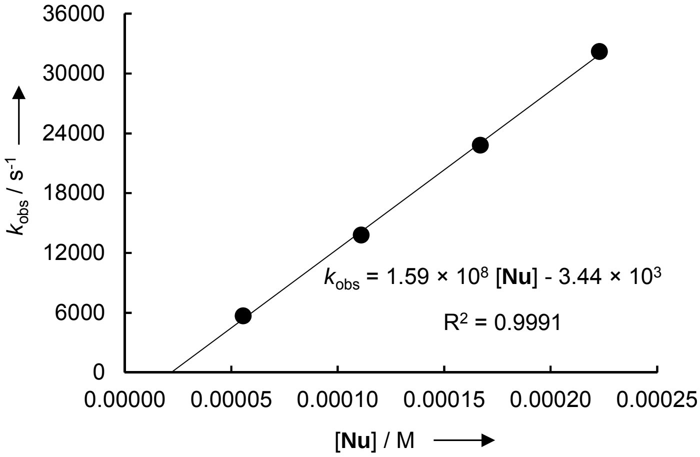

Table 3.S11. Rate constants for the reaction of 9-cyanofluorenyl anion (**1**) with $(thq)_2CH^+$(**4i**) at 20°C in DMSO, laser-flash photolysis technique. Deprotonation with KO*t*Bu.

No	$[Pr]_0$ / M	$[Nu]_0$ / M	$[Nu]_{eff}$ / M	$[NuH]_0$ / M	$[Nu]_{eff}/[Pr]_0$	k_{obs}/s^{-1}
1	2.50×10^{-5}	7.02×10^{-5}	4.52×10^{-5}	1.55×10^{-5}	1.8	1.09×10^{4}
2	5.00×10^{-5}	1.40×10^{-4}	9.00×10^{-5}	3.11×10^{-5}	1.8	2.41×10^{4}
3	7.50×10^{-5}	2.11×10^{-4}	1.36×10^{-4}	4.66×10^{-5}	1.8	3.88×10^{4}
4	9.99×10^{-5}	2.81×10^{-4}	1.81×10^{-4}	6.21×10^{-5}	1.8	5.30×10^{4}
5	1.25×10^{-4}	3.51×10^{-4}	2.26×10^{-4}	7.77×10^{-5}	1.8	6.61×10^{4}
$k_2 = 3.08 \times 10^{8}$ $M^{-1}s^{-1}$						

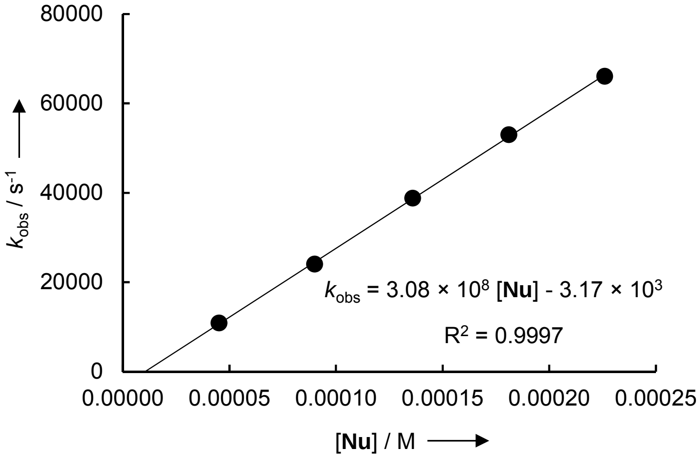

Table 3.S12. Rate constants for the reaction of 9-cyanofluorenyl anion (**1**) with $(dma)_2CH^+$(**4j**) at 20°C in DMSO, laser-flash photolysis technique. Deprotonation with KO*t*Bu.

No	$[Pr]_0$ / M	$[Nu]_0$ / M	$[Nu]_{eff}$ / M	$[NuH]_0$ / M	$[Nu]_{eff}/[Pr]_0$	k_{obs}/s^{-1}
1	2.01×10^{-5}	7.02×10^{-5}	5.01×10^{-5}	1.55×10^{-5}	2.5	2.09×10^{4}
2	4.02×10^{-5}	1.40×10^{-4}	9.98×10^{-5}	3.11×10^{-5}	2.5	4.81×10^{4}
3	6.03×10^{-5}	2.11×10^{-4}	1.51×10^{-4}	4.66×10^{-5}	2.5	7.82×10^{4}
4	8.04×10^{-5}	2.81×10^{-4}	2.01×10^{-4}	6.21×10^{-5}	2.5	1.06×10^{5}
5	1.01×10^{-4}	3.51×10^{-4}	2.50×10^{-4}	7.77×10^{-5}	2.5	1.30×10^{5}

$k_2 = 5.51 \times 10^8\ M^{-1}s^{-1}$

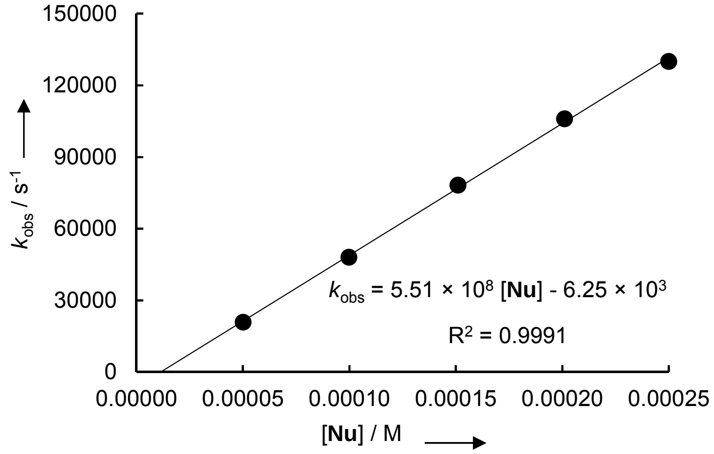

Determination of the nucleophilicity parameters N and s_N for 9-cyanofluorenyl anion (1) in DMSO.

Table 3.S13. Second-order rate constants (DMSO, 20°C) for the reactions of the electrophiles **4** with the fluorenyl anion **1**.

Electrophile	E	k_2 / $M^{-1}s^{-1}$	log k_2
$m\text{F}_2(t\text{Bu})_2\text{QM}$	-14.50	2.36×10^3	3.37
dma$(\text{Ph})_2\text{QM}$	-13.39	7.22×10^3	3.86
ani$(\text{Ph})_2\text{QM}$	-12.18	7.75×10^4	4.89
$(\text{lil})_2\text{CH}^+$	-10.04	4.66×10^7	7.67
$(\text{jul})_2\text{CH}^+$	-9.45	9.07×10^7	7.96
$(\text{ind})_2\text{CH}^+$	-8.76	1.59×10^8	8.2
$(\text{thq})_2\text{CH}^+$	-8.22	3.08×10^8	8.49
$(\text{dma})_2\text{CH}^+$	-7.02	5.51×10^8	8.74
$N = 19.44$, $s = 0.66$			

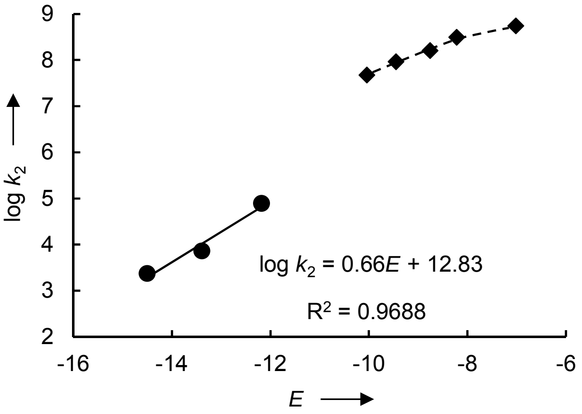

3.S.3. Rate constants for the reactions of 9-carbomethoxyfluorenyl anion (2) in DMSO

Table 3.S14. Rate constants for the reaction of 9-carbomethoxyfluorenyl anion (**2**) with jul$(t\text{Bu})_2\text{QM}$ (**4a**) at 20˚C in DMSO (0.2 – 1.6 % CH_2Cl_2), J&M technique. Deprotonation with TMG. Case B. Direct evaluation.

No	$[E]_0$ / M	$[Nu]_0$ / M	$[NuH]_0$ / M	$[Nu]_0$ / $[E]_0$	k_{obs} / s^{-1}
1	4.12×10^{-5}	6.37×10^{-4}	3.22×10^{-4}	15	6.75×10^{-3}
2	4.22×10^{-5}	6.51×10^{-4}	1.31×10^{-3}	15	5.63×10^{-3}
3	4.17×10^{-5}	6.44×10^{-4}	2.27×10^{-3}	15	5.39×10^{-3}
4	4.06×10^{-5}	6.27×10^{-4}	6.93×10^{-3}	15	5.32×10^{-3}
5	4.06×10^{-5}	8.77×10^{-4}	6.72×10^{-3}	22	7.12×10^{-3}
6	4.05×10^{-5}	1.13×10^{-3}	6.45×10^{-3}	28	9.00×10^{-3}
7	4.12×10^{-5}	1.40×10^{-3}	6.31×10^{-3}	34	1.11×10^{-2}
$k_2 = 7.48\ M^{-1}s^{-1}$					

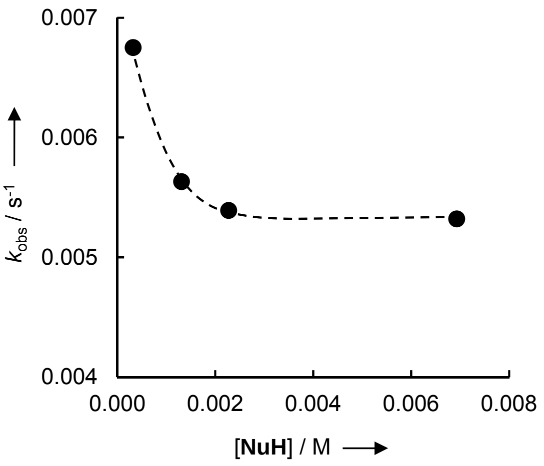

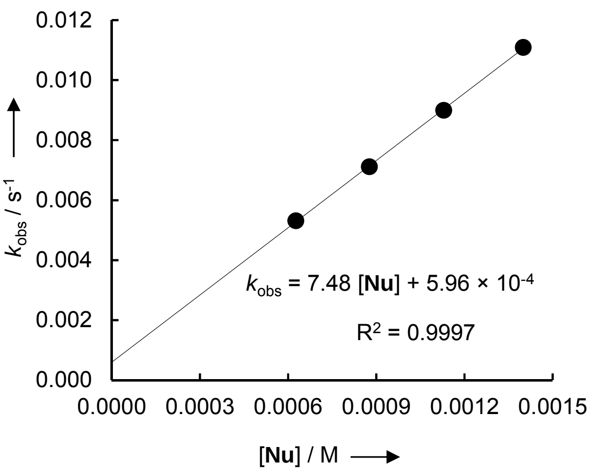

Table 3.S15. Rate constants for the reaction of 9-carbomethoxyfluorenyl anion (**2**) with dma(*t*Bu)$_2$QM (**4b**) at 20°C in DMSO (0.5 – 3.5 % CH_2Cl_2), J&M technique. Deprotonation with TMG. Case B. Direct evaluation.

No	$[E]_0$ / M	$[Nu]_0$ / M	$[NuH]_0$ / M	$[Nu]_0$ / $[E]_0$	k_{obs} / s^{-1}
1	5.27×10^{-5}	6.48×10^{-4}	9.80×10^{-5}	12	1.18×10^{-2}
2	5.18×10^{-5}	6.37×10^{-4}	2.09×10^{-4}	12	9.24×10^{-3}
3	5.25×10^{-5}	6.45×10^{-4}	2.12×10^{-4}	12	9.24×10^{-3}
4	5.23×10^{-5}	6.42×10^{-4}	4.95×10^{-4}	12	8.03×10^{-3}
5	5.21×10^{-5}	6.41×10^{-4}	1.06×10^{-3}	12	7.72×10^{-3}
6	5.19×10^{-5}	6.38×10^{-4}	1.62×10^{-3}	12	7.43×10^{-3}
7	5.04×10^{-5}	6.20×10^{-4}	4.32×10^{-3}	12	7.15×10^{-3}
8	5.12×10^{-5}	6.29×10^{-4}	1.50×10^{-2}	12	7.19×10^{-3}
9	3.37×10^{-5}	3.89×10^{-4}	5.47×10^{-3}	12	4.41×10^{-3}
10	3.26×10^{-5}	8.79×10^{-4}	5.74×10^{-3}	27	1.02×10^{-2}
11	3.27×10^{-5}	1.13×10^{-3}	6.45×10^{-3}	35	1.30×10^{-2}
$k_2 = 1.16 \times 10^{1}$ M^{-1}s^{-1}					

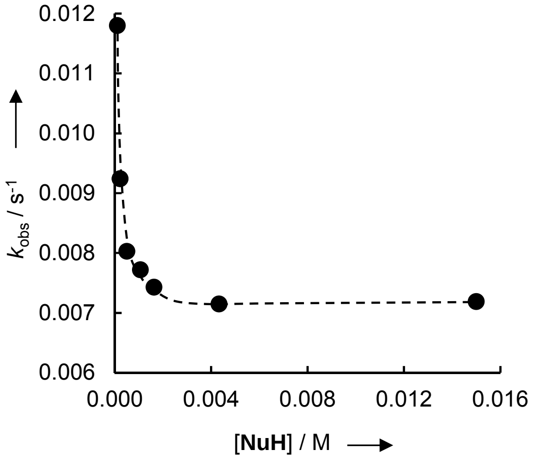

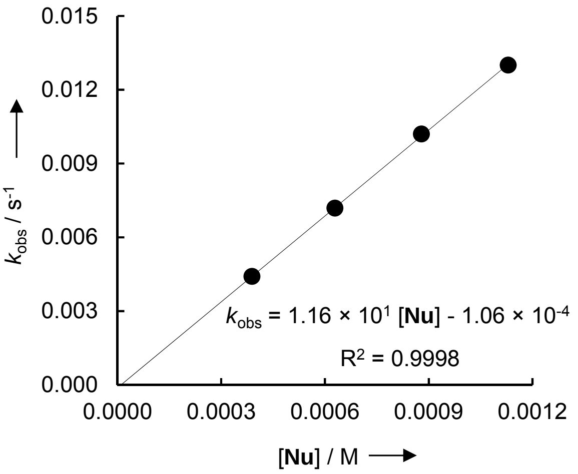

Table 3.S16. Rate constants for the reaction of 9-carbomethoxyfluorenyl anion (**2**) with dma(*t*Bu)$_2$QM (**4b**) at 20°C in DMSO (0.5 – 3.9 % CH$_2$Cl$_2$), J&M technique. Deprotonation with KO*t*Bu. Case B. Indirect evaluation.

No	[E]$_0$ / M	[Nu]$_0$ / M	[NuH]$_0$ / M	[Nu]$_0$ / [E]$_0$	k_{obs} / s^{-1}	[NuH]$^{-1}$ / M^{-1}	[Nu] k_{obs}^{-1}/ M s
1	5.28 × 10^{-5}	6.43 × 10^{-4}	1.04 × 10^{-4}	12	not first-order	-	9.62 × 10^{3}
2	5.22 × 10^{-5}	6.44 × 10^{-4}	1.63 × 10^{-3}	12	not first-order	-	6.14 × 10^{2}
3	5.06 × 10^{-5}	6.24 × 10^{-4}	4.88 × 10^{-3}	12	4.05 × 10^{-3}	1.54 × 10^{-1}	2.05 × 10^{2}
4	5.19 × 10^{-5}	6.41 × 10^{-4}	7.27 × 10^{-3}	12	4.87 × 10^{-3}	1.32 × 10^{-1}	1.38 × 10^{2}
5	5.13 × 10^{-5}	6.34 × 10^{-4}	1.50 × 10^{-2}	12	5.89 × 10^{-3}	1.08 × 10^{-1}	6.66 × 10^{1}
k_2 = 1.16 × 10^{1} M^{-1}s^{-1}							

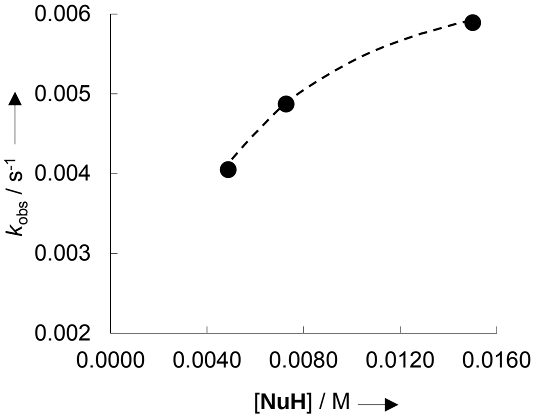

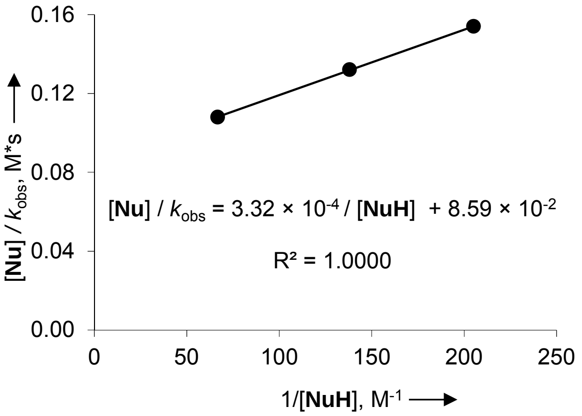

Table 3.S17. Rate constants for the reaction of 9-carbomethoxyfluorenyl anion (**2)** with $F_2(tBu)_2QM$ (**4c**) at 20°C in DMSO (0.5 – 3.5 % CH_2Cl_2), stopped-flow technique. Deprotonation with TMG. Case A. Direct evaluation.

No	$[E]_0$ / M	$[Nu]_0$ / M	$[NuH]_0$ / M	$[Nu]_0$ / $[E]_0$	k_{obs} / s^{-1}
1	2.18×10^{-5}	2.55×10^{-4}	7.57×10^{-4}	12	1.48
2	2.18×10^{-5}	3.82×10^{-4}	6.30×10^{-4}	18	2.15
3	2.18×10^{-5}	5.10×10^{-4}	5.02×10^{-4}	23	2.93
4	2.18×10^{-5}	6.37×10^{-4}	7.12×10^{-4}	29	3.92
5	2.18×10^{-5}	7.13×10^{-4}	7.35×10^{-5}	33	4.38
6	2.18×10^{-5}	7.13×10^{-4}	1.18×10^{-4}	33	4.46
7	2.18×10^{-5}	7.13×10^{-4}	1.63×10^{-4}	33	4.36
8	2.18×10^{-5}	7.13×10^{-4}	2.08×10^{-4}	33	4.37
9	2.18×10^{-5}	7.13×10^{-4}	2.98×10^{-4}	33	4.40
10	2.18×10^{-5}	8.92×10^{-4}	4.57×10^{-4}	41	5.46

$k_2 = 6.41 \times 10^3\ M^{-1}s^{-1}$

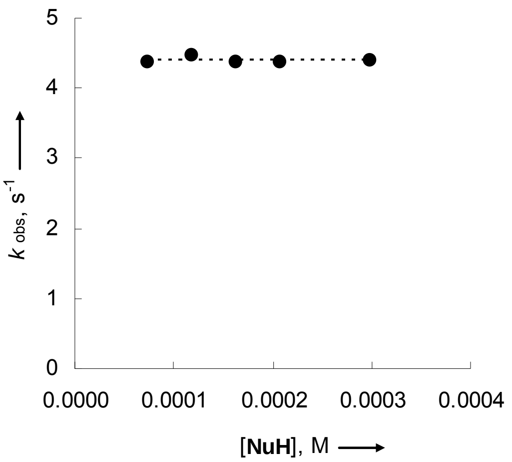

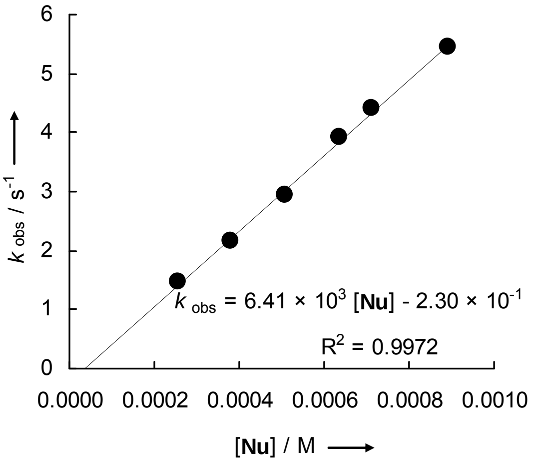

Table 3.S18. Rate constants for the reaction of 9-carbomethoxyfluorenyl anion (**2**) with dma(Ph)$_2$QM (**4d**) at 20°C in DMSO, stopped-flow technique. Deprotonation with TMG. Case A.

No	$[E]_0$ / M	$[Nu]_0$ / M	$[NuH]_0$ / M	$[Nu]_0$ / $[E]_0$	k_{obs} /s^{-1}
1	1.91×10^{-5}	4.49×10^{-4}	3.66×10^{-4}	24	6.24
2	1.91×10^{-5}	4.49×10^{-4}	6.37×10^{-4}	24	6.18
3	1.91×10^{-5}	5.99×10^{-4}	4.87×10^{-4}	31	8.26
4	1.91×10^{-5}	7.49×10^{-4}	6.09×10^{-4}	39	1.03×10^{1}
5	1.91×10^{-5}	1.05×10^{-3}	8.53×10^{-4}	55	1.45×10^{1}
$k_2 = 1.39 \times 10^4$ M^{-1}s^{-1}					

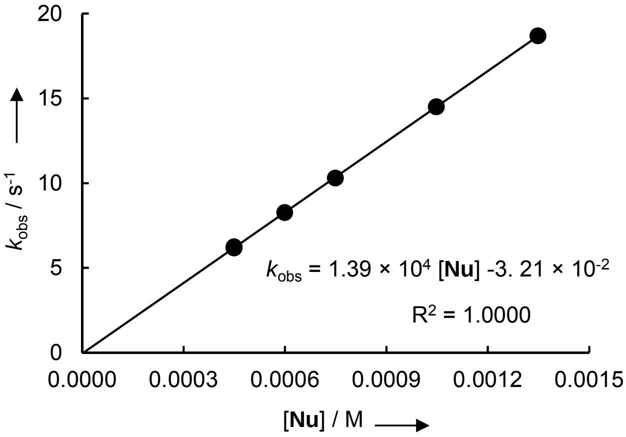

Table 3.S19. Rate constants for the reaction of 9-carbomethoxyfluorenyl anion (**2**) with dma(Ph)$_2$QM (**4d**) at 20°C in DMSO, stopped-flow technique. Deprotonation with ca. 1.05 eq. KO*t*Bu. Case A.

No	$[E]_0$ / M	$[Nu]_0$ / M^a	$[NuH]_0$ / M	$[Nu]_0$ / $[E]_0$	k_{obs} /s^{-1}
1	1.93×10^{-5}	3.43×10^{-4}	0	18	4.15
2	1.93×10^{-5}	5.14×10^{-4}	0	27	6.53
3	1.93×10^{-5}	6.86×10^{-4}	0	36	8.84
4	1.93×10^{-5}	8.57×10^{-4}	0	44	1.11×10^{1}
5	1.93×10^{-5}	1.03×10^{-3}	0	53	1.36×10^{1}
$k_2 = 1.37 \times 10^4$ M^{-1}s^{-1}					

[a] In this table, $[Nu]_0$ is equal to the calculated concentration of the fluorene **2**-H used for generation of **2**, as the base is used in a slight excess.

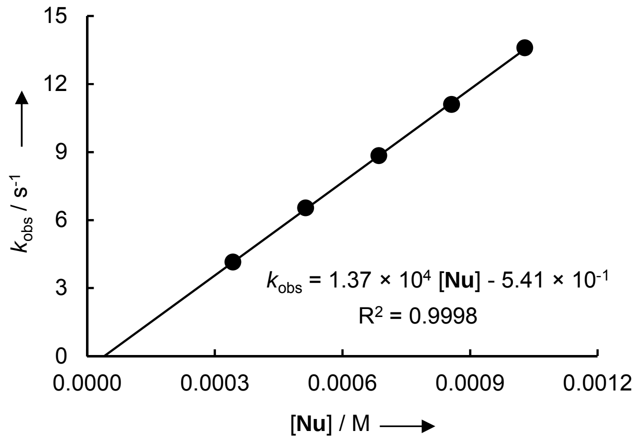

Table 3.S20. Rate constants for the reaction of 9-carbomethoxyfluorenyl anion (**2**) with ani(Ph)$_2$QM (**4e**) at 20°C in DMSO, stopped-flow technique. Deprotonation with TMG. Case A.

No	$[E]_0$ / M	$[Nu]_0$ / M	$[NuH]_0$ / M	$[Nu]_0$ / $[E]_0$	k_{obs} /s^{-1}
1	5.71×10^{-6}	9.09×10^{-5}	2.50×10^{-4}	16	1.49×10^{1}
2	7.13×10^{-6}	2.27×10^{-4}	6.81×10^{-4}	32	3.86×10^{1}
3	7.13×10^{-6}	3.64×10^{-4}	5.45×10^{-4}	51	6.30×10^{1}
4	7.13×10^{-6}	4.55×10^{-4}	6.81×10^{-4}	64	8.15×10^{1}
$k_2 = 1.82 \times 10^5$ M^{-1}s^{-1}					

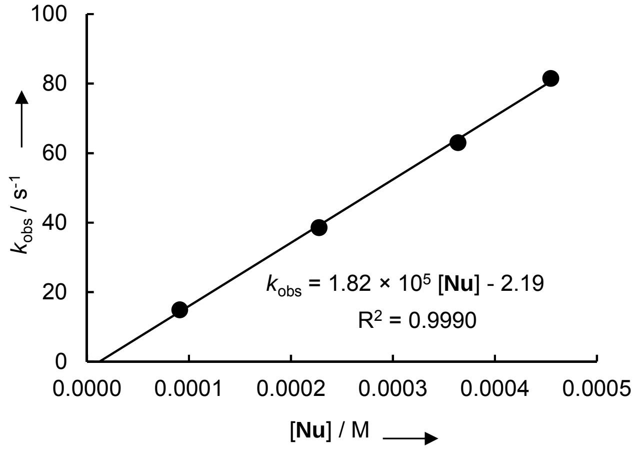

Determination of the nucleophilicity parameters *N* and s_N for 9-carbomethoxyfluorenyl anion (**2**) in DMSO.

Table 3.S21. Second-order rate constants (DMSO, 20°C) for the reactions of the quinone methides **4** with the fluorenyl anion **2**.

Electrophile	*E*	k_2 / $M^{-1}s^{-1}$	log k_2
jul(*t*Bu)$_2$QM	-17.90	7.48	0.87
dma(*t*Bu)$_2$QM	-17.29	1.16×10^1	1.06
*m*F$_2$(*t*Bu)$_2$QM	-14.50	6.41×10^3	3.81
dma(Ph)$_2$QM	-13.39	1.38×10^4	4.14
ani(Ph)$_2$QM	-12.18	1.82×10^5	5.26
$N = 18.84$, $s = 0.79$			

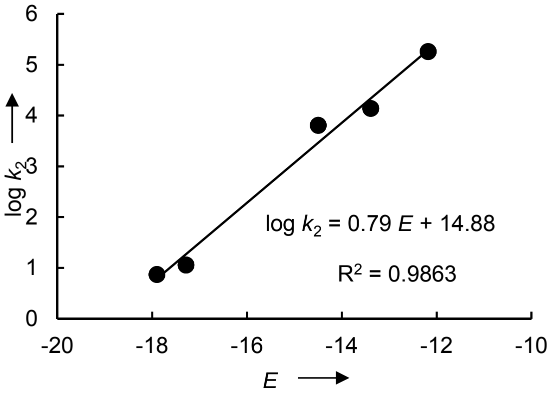

3.S.4. Rate constants for the reactions of 2,7-dibromo-9-carbomethoxyfluorenyl anion (3) in DMSO

Table 3.S22. Rate constants for the reaction of 2,7-dibromo-9-carbomethoxyfluorenyl anion (**3**) with jul(*t*Bu)$_2$QM (**4a**) at 20˚C in DMSO, stopped-flow technique. Deprotonation with tetrabutylammonium benzoate. Case C.

No	$[E]_0$ / M	$[Nu]_0$ / M	$[NuH]_0$ / M	$[Nu]_0$ / $[E]_0$	k_{obs} / s^{-1}
1	2.10×10^{-5}	7.67×10^{-4}	2.21×10^{-4}	37	8.64×10^{-2}
2	2.10×10^{-5}	7.67×10^{-4}	4.18×10^{-4}	37	1.60×10^{-1}
3	2.10×10^{-5}	7.67×10^{-4}	6.16×10^{-4}	37	2.36×10^{-1}
4	2.10×10^{-5}	7.67×10^{-4}	8.14×10^{-4}	37	3.10×10^{-1}
5	2.10×10^{-5}	7.67×10^{-4}	1.01×10^{-3}	37	3.90×10^{-1}
6	2.05×10^{-5}	2.20×10^{-4}	1.23×10^{-3}	11	7.78×10^{-1}
7	2.05×10^{-5}	4.40×10^{-4}	1.01×10^{-3}	21	4.20×10^{-1}
8	2.05×10^{-5}	6.60×10^{-4}	7.86×10^{-4}	32	2.48×10^{-1}
9	2.05×10^{-5}	8.80×10^{-4}	5.66×10^{-4}	43	1.42×10^{-1}
10	2.05×10^{-5}	1.10×10^{-3}	3.46×10^{-4}	54	6.84×10^{-2}

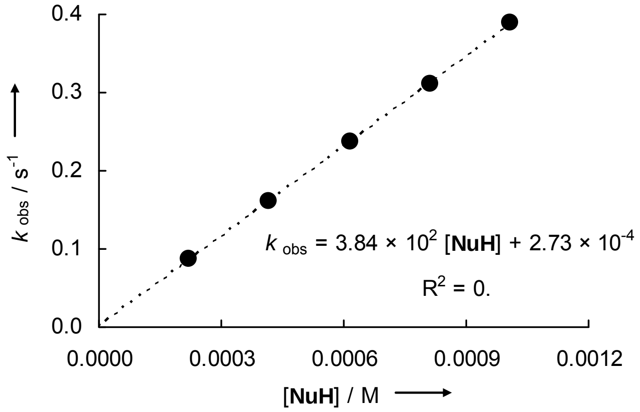

Table 3.S23. Rate constants for the reaction of 2,7-dibromo-9-carbomethoxyfluorenyl anion (**3**) with $F_2(t\mathrm{Bu})_2$QM (**4c**) at 20°C in DMSO (2.5 – 5% CH_2Cl_2), stopped-flow technique. Deprotonation with tetrabutylammonium benzoate. Case B. Indirect evaluation.

No	$[E]_0$ / M	$[Nu]_0$ / M	$[NuH]_0$ / M	$[Nu]_0$ / $[E]_0$	k_{obs} / s^{-1}	$[NuH]^{-1}$ / M^{-1}	[Nu] k_{obs}^{-1}/ M s
1	2.18×10^{-5}	7.15×10^{-4}	7.01×10^{-5}	33	7.10×10^{-3}	-	-
2	2.18×10^{-5}	7.15×10^{-4}	2.01×10^{-4}	33	1.10×10^{-2}	-	-
3	2.18×10^{-5}	7.15×10^{-4}	3.32×10^{-4}	33	1.54×10^{-2}	3.01×10^{3}	4.64×10^{-2}
4	2.18×10^{-5}	7.15×10^{-4}	4.63×10^{-4}	33	1.93×10^{-2}	2.16×10^{3}	3.70×10^{-2}
5	2.18×10^{-5}	7.15×10^{-4}	5.94×10^{-4}	33	2.28×10^{-2}	1.68×10^{3}	3.14×10^{-2}
6	2.18×10^{-5}	7.15×10^{-4}	1.12×10^{-3}	33	3.41×10^{-2}	8.95×10^{2}	2.10×10^{-2}
7	2.18×10^{-5}	7.15×10^{-4}	1.90×10^{-3}	33	4.06×10^{-2}	5.26×10^{2}	1.76×10^{-2}
8	2.18×10^{-5}	7.15×10^{-4}	4.61×10^{-3}	33	5.18×10^{-2}	2.17×10^{2}	1.38×10^{-2}
9	2.18×10^{-5}	7.13×10^{-4}	5.78×10^{-3}	33	5.55×10^{-2}	1.73×10^{2}	1.28×10^{-2}

$k_2 = 9.01 \times 10^1$ M^{-1}s^{-1}

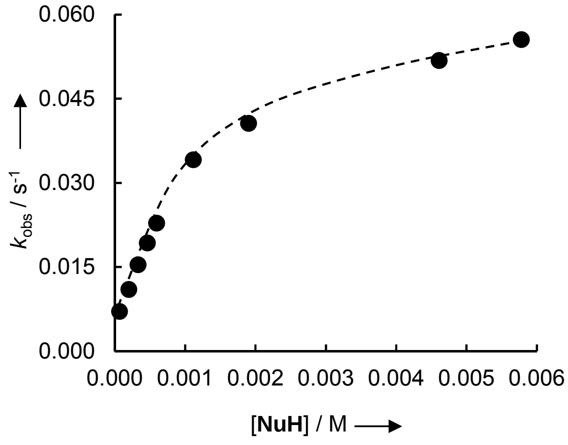

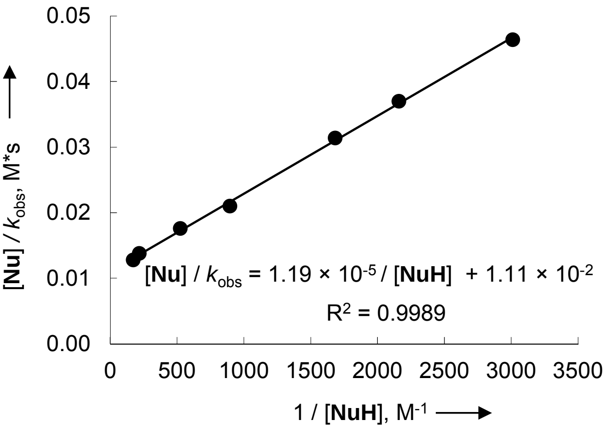

Table 3.S24. Rate constants for the reaction of 2,7-dibromo-9-carbomethoxyfluorenyl anion (**3**) with $F_2(tBu)_2QM$ (**4c**) at 20˚C in DMSO (2.5 % CH_2Cl_2), stopped-flow technique. Deprotonation with tetrabutylammonium benzoate. Case B. Experiment with different amounts of benzoic acid.

No	$[E]_0$ / M	$[Nu]_0$ / M	$[NuH]_0$ / M	$[PhCO_2H]_0$ / M	$[Nu]_0$ / $[E]_0$	k_{obs} / s^{-1}
1	2.18×10^{-5}	7.15×10^{-4}	5.94×10^{-4}	7.15×10^{-4}	33	2.28×10^{-2}
2	2.18×10^{-5}	7.13×10^{-4}	5.96×10^{-4}	2.76×10^{-3}	33	2.74×10^{-2}
3	2.18×10^{-5}	7.13×10^{-4}	5.96×10^{-4}	4.81×10^{-3}	33	2.93×10^{-2}
4	2.18×10^{-5}	7.13×10^{-4}	5.96×10^{-4}	6.86×10^{-3}	33	3.13×10^{-2}

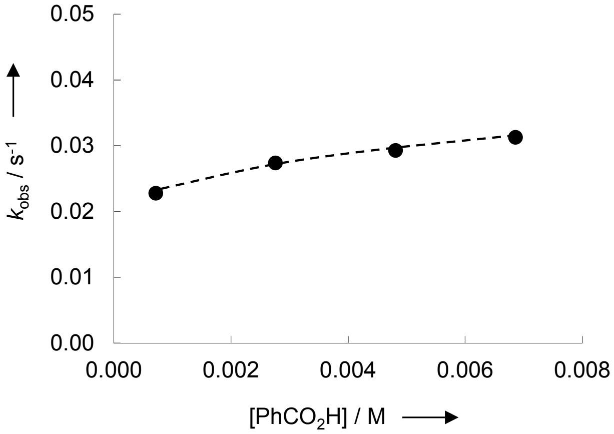

Table 3.S25. Rate constants for the reaction of 2,7-dibromo-9-carbomethoxyfluorenyl anion (**3**) with $F_2(tBu)_2QM$ (**4c**) at 20˚C in DMSO (1.3 – 5% CH_2Cl_2), stopped-flow technique. Deprotonation with TMG. Case B. Direct evaluation.

No	$[E]_0$ / M	$[Nu]_0$ / M	$[NuH]_0$ / M	$[Nu]_0$ / $[E]_0$	k_{obs} / s^{-1}
1	2.00×10^{-5}	3.59×10^{-4}	1.06×10^{-3}	18	3.10×10^{-2}
2	2.00×10^{-5}	5.39×10^{-4}	8.78×10^{-4}	27	4.88×10^{-2}
3	2.00×10^{-5}	7.18×10^{-4}	1.55×10^{-3}	36	6.70×10^{-2}
4	2.00×10^{-5}	7.18×10^{-4}	2.68×10^{-3}	36	6.75×10^{-2}
5	2.00×10^{-5}	7.18×10^{-4}	1.32×10^{-4}	36	6.80×10^{-2}
6	2.00×10^{-5}	7.18×10^{-4}	6.99×10^{-4}	36	6.54×10^{-2}
7	2.00×10^{-5}	8.98×10^{-4}	5.19×10^{-4}	45	8.49×10^{-2}
$k_2 = 9.93 \times 10^{1}\ M^{-1}s^{-1}$					

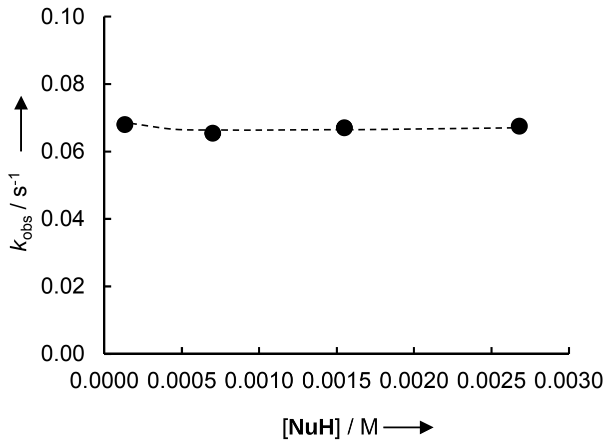

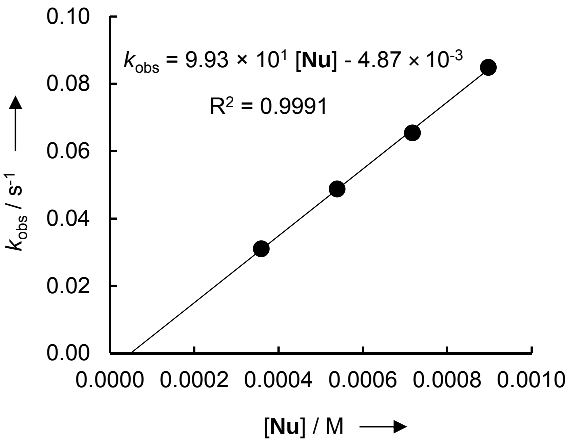

Table 3.S26. Rate constants for the reaction of 2,7-dibromo-9-carbomethoxyfluorenyl anion (**3**) with dma(Ph)$_2$QM (**4d**) at 20˚C in DMSO, stopped-flow technique. Deprotonation with KO*t*Bu. Case C.

No	[E]$_0$ / M	[Nu]$_0$ / M	[NuH]$_0$ / M	[Nu]$_0$ / [E]$_0$	k_{obs} / s^{-1}
1	2.17×10^{-5}	7.50×10^{-4}	2.46×10^{-4}	35	9.61×10^{-1}
2	2.17×10^{-5}	7.50×10^{-4}	5.78×10^{-4}	35	1.79
3	2.17×10^{-5}	7.50×10^{-4}	9.11×10^{-4}	35	2.44
4	2.17×10^{-5}	7.50×10^{-4}	1.24×10^{-3}	35	3.23
5	2.17×10^{-5}	7.50×10^{-4}	1.57×10^{-3}	35	4.03

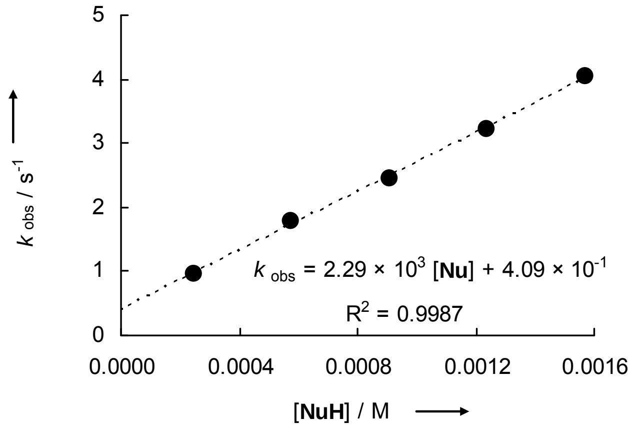

Table 3.S27. Rate constants for the reaction of 2,7-dibromo-9-carbomethoxyfluorenyl anion (**3**) with dma(Ph)$_2$QM (**4d**) at 20°C in DMSO, stopped-flow technique. Deprotonation with tetrabutylammonium benzoate. Case C.

No	$[E]_0$ / M	$[Nu]_0$ / M	$[NuH]_0$ / M	$[Nu]_0$ / $[E]_0$	k_{obs} / s^{-1}
1	2.17×10^{-5}	7.67×10^{-4}	2.25×10^{-4}	35	6.53×10^{-1}
2	2.17×10^{-5}	7.67×10^{-4}	4.23×10^{-4}	35	1.08
3	2.17×10^{-5}	7.67×10^{-4}	6.21×10^{-4}	35	1.50
4	2.17×10^{-5}	7.67×10^{-4}	8.20×10^{-4}	35	1.86
5	2.17×10^{-5}	7.67×10^{-4}	1.02×10^{-3}	35	2.29
6	2.17×10^{-5}	7.67×10^{-4}	1.22×10^{-3}	35	2.71
7	2.17×10^{-5}	7.67×10^{-4}	2.03×10^{-3}	35	4.78
8	2.17×10^{-5}	7.67×10^{-4}	4.83×10^{-3}	35	1.17×10^{1}

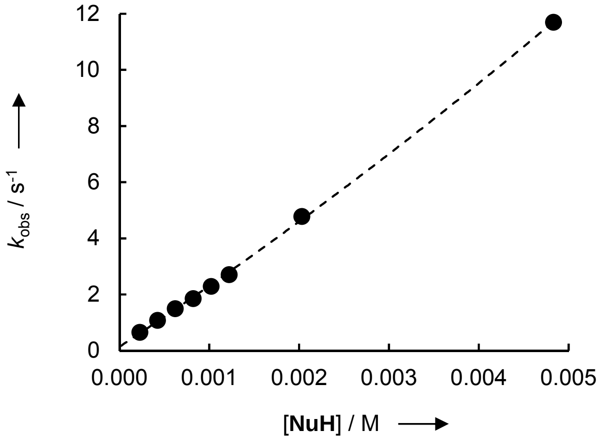

Table 3.S28. Rate constants for the reaction of 2,7-dibromo-9-carbomethoxyfluorenyl anion (**3**) with dma(Ph)$_2$QM (**4d**) at 20°C in DMSO (3.75 % CH_2Cl_2), stopped-flow technique. Deprotonation with TMG. Case C.

No	$[E]_0$ / M	$[Nu]_0$ / M	$[NuH]_0$ / M	$[Nu]_0$ / $[E]_0$	k_{obs} / s^{-1}
1	5.72×10^{-6}	7.61×10^{-4}	3.60×10^{-4}	133	1.35
2	5.72×10^{-6}	7.61×10^{-4}	3.45×10^{-3}	133	8.04
3	5.72×10^{-6}	7.61×10^{-4}	6.01×10^{-3}	133	1.35×10^{1}
4	5.72×10^{-6}	7.61×10^{-4}	9.50×10^{-3}	133	2.29×10^{1}
5	5.72×10^{-6}	7.61×10^{-4}	1.19×10^{-2}	133	3.00×10^{1}

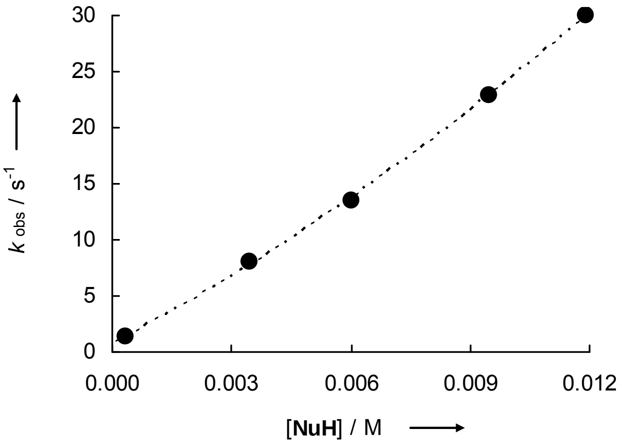

Table 3.S29. Rate constants for the reaction of 2,7-dibromo-9-carbomethoxyfluorenyl anion (**3**) with ani(Ph)$_2$QM (**4e**) at 20°C in DMSO (0.5 – 2.5 % CH_2Cl_2), stopped-flow technique. Deprotonation with TMG. Case B.

No	$[E]_0$ / M	$[Nu]_0$ / M	$[NuH]_0$ / M	$[Nu]_0$ / $[E]_0$	k_{obs} / s^{-1}
1	8.78×10^{-6}	1.80×10^{-4}	1.76×10^{-5}	21	7.52×10^{-1}
2	8.78×10^{-6}	1.80×10^{-4}	1.16×10^{-4}	21	7.75×10^{-1}
3	8.78×10^{-6}	1.80×10^{-4}	2.15×10^{-4}	21	7.97×10^{-1}
4	8.78×10^{-6}	1.80×10^{-4}	8.06×10^{-4}	21	7.66×10^{-1}
5	8.78×10^{-6}	2.69×10^{-4}	7.16×10^{-4}	31	1.20
6	8.78×10^{-6}	3.59×10^{-4}	6.26×10^{-4}	41	1.56
7	8.78×10^{-6}	4.49×10^{-4}	5.37×10^{-4}	51	2.00
8	8.78×10^{-6}	5.39×10^{-4}	4.47×10^{-4}	61	2.35
$k_2 = 4.42 \times 10^3$ M^{-1}s^{-1}					

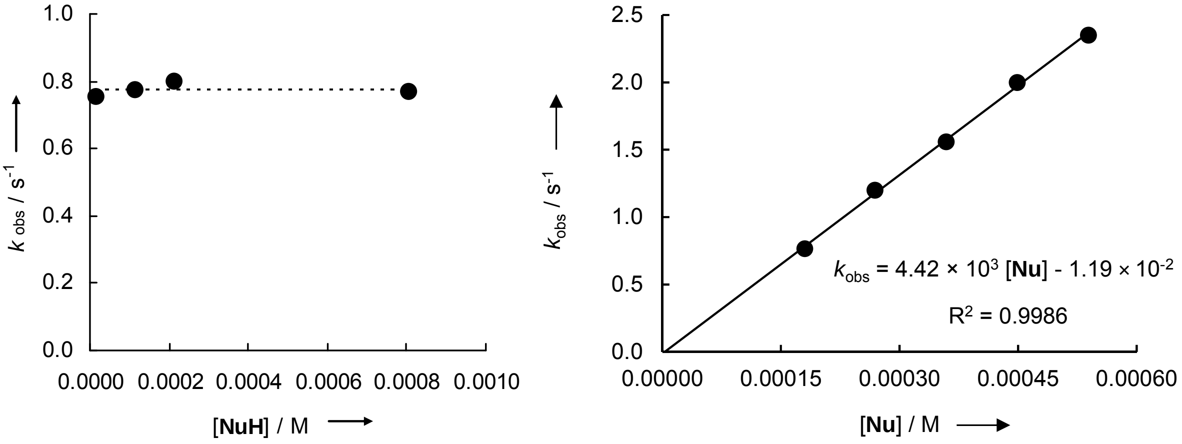

* As this experiment had to be carried out at very low carbanion concentrations for technical reasons, some scatter in the plot of k_{obs} versus [NuH] is to be seen. This is caused by oxidation of a small amount of the anion in DMSO solution. The ration of k_{obs}/A_{fin} was found to be the same at various concentrations of the C-H acid.

Determination of the nucleophilicity parameters *N* and s_N for 2,7-dibromo-9-carbomethoxyfluorenyl anion (**2**) in DMSO.

Table 3.S29. Second-order rate constants (DMSO, 20°C) for the reactions of the quinone methides **4** with the fluorenyl anion **3**.

Electrophile	*E*	k_2 / $M^{-1}s^{-1}$	log k_2
mF$_2$(tBu)$_2$QM	-14.50	9.93×10^1	2.00
ani(Ph)$_2$QM	-12.18	4.42×10^3	3.65
$N = 17.34$, $s = 0.71$			

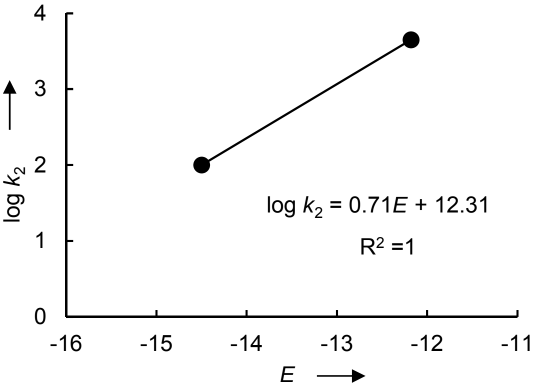

3.4. References

(1) a) F. G. Bordwell, D. L. Hughes, *J. Org. Chem.* **1980**, *45*, 3314-3320. b) F. G. Bordwell, D. L. Hughes, *J. Org. Chem.* **1980**, *45*, 3320-3325. c) F. G. Bordwell, S. R. Mrozack, *J. Org. Chem.* **1982**, *47*, 3802-3803.

(2) F. G. Bordwell, A. H. Clemens, J.-P. Cheng, *J. Am. Chem. Soc.* **1987**, *109,* 1773-1782.

(3) F. G. Bordwell, D. L. Hughes, *J. Am. Chem. Soc.* **1986**, *108,* 5991-5997.

(4) F. G. Bordwell, A. H. Clemens, *J. Org. Chem.* **1981**, *46*, 1035-1037.

(5) a) H. Mayr, M. Patz, *Angew. Chem.* **1994**, *106*, 990; *Angew. Chem. Int. Ed. Engl.* **1994**, *33*, 938–957; b) H. Mayr, T. Bug, M. F. Gotta, N. Hering, B. Irrgang, B. Janker, B. Kempf, R. Loos, A. R. Ofial, G. Remennikov, H. Schimmel, *J. Am. Chem. Soc.* **2001**, *123*, 9500–9512; c) R. Lucius, R. Loos, H. Mayr, *Angew. Chem.* **2002**, *114*, 97-102; *Angew. Chem. Int. Ed.* **2002**, *41*, 91–95; d) H. Mayr, B. Kempf, A. R. Ofial, *Acc. Chem. Res.* **2003**, *36*, 66–77; e) H. Mayr, A. R. Ofial, *Pure Appl. Chem.* **2005**, *77*, 1807–1821; f) H. Mayr, *Angew. Chem.* **2011**, *123*, 3692; *Angew. Chem. Int. Ed.* **2011**, *50*, 3612–3618; g) J. Ammer, C. Nolte, H. Mayr, *J. Am. Chem. Soc.* **2012**, *134*, 13902–13911; h) for a comprehensive listing of nucleophilicity parameters *N* and electrophilicity parameters *E*, see http://www.cup.uni-muenchen.de/oc/mayr/DBintro.html.

(6) a) For converting fluorene to 9-carbomethoxy- or 9-formylfluorene, see W. S. Matthews, J. E. Bares, J. E. Bartmess, F. G. Bordwell, F. J. Cornforth, G. E. Drucker, Z. Margolin, R. J. McCallum, G. J. McCollum, N. R. Vanier, *J. Am. Chem. Soc.* **1975**, *97*, 7006-7014. b)The crude aldehyde was converted to the nitrile by method described by W. Wislicenus, K. Russ, *Ber.*, **1910**, 2719; c) For bromination of **2**-H, the procedure was used described by T. Holbro, E. Tagmann, *Helv, Chim, Acta*, **1950**, *33*, 2178-2185.

(7) D. Richter, N. Hampel, T. Singer, A. R. Ofial, H. Mayr, *Eur. J. Org. Chem.* **2009**, 3203-3211.

(8) For a more detailed description of the setup, see chapter 1 of this thesis.

(9) a) T. Kanzian, T. A. Nigst, A. Maier, S. Pichl, H. Mayr, *Eur. J. Org. Chem.* **2009**, 6379-6385; b) T. A. Nigst, A. Antipova, H. Mayr, *J. Org. Chem.* **2012**, *77*, 8142-8155.

(10) a) I.-H. Um, S. Yoon, H.-R. Park, H.-J. Han, *Org. Biomol. Chem.* **2008**, *6*, 1618–1624; b) E. A. Castro, *Pure Appl. Chem.* **2009**, *81*, 685–696.

(11) I.-H. Um, J.-A. Seok, H.-T. Kim, S.-K. Bae, *J. Org. Chem.* **2003**, *68*, 7742–7746.

(12) M. J. Pfeiffer, S. B. Hanna, *J. Org. Chem.* **1993**, *58*, 735–740.

(13) H. Mayr, J. Ammer, M. Baidya, B. Maji, T. A. Nigst, A. R. Ofial, T. Singer, *J. Am. Chem. Soc.* **2015**, *137*, 2580-2599.

(14) This prediction is based on Hammett parameters for the substituents on the quinone methide: σ^+ for jul and NMe$_2$ are -2.03 and -1.70, correspondingly, while for OMe $\sigma^+ = -0.78$; σ_m for *t*Bu, Ph and F are -0.10, 0.06 and 0.34, correspondingly. The parameters are taken from C. Hansch, A. Leo, R. W. Taft, *Chem. Rev.* **1991**, *91*, 165-195; σ^+ for jul was determined in H. Mayr, T. Bug, M. F. Gotta, N. Hering, B. Irrgang, B. Janker, B. Kempf, R. Loos, A. R. Ofial, G. Remennikov, H. Schimmel, *J. Am. Chem. Soc.* **2001**, *123*, 9500-9512.

(15) pK_{aH} value for intermediates **I** are not available. However, pK_a values of about 18 for other 2,6-di-*tert*-butylphenoles (C. D. Ritchie , S. Lu, *J. Am. Chem. Soc.*, **1990**, *112* , 7748–7756) suggest that in our case the ratio k_2/k_{-2} should be sufficient to ensure irreversible deprotonation of **I** under reaction conditions.

(16) It was derived in the way similar to the one used for determination of the rate constants for the reactions of methylhydrazine with tert-butyl substituted quinone methides in the first chapter of this dissertation.

(17) O. Kaumanns, R. Appel, T. Lemek, F. Seeliger, H.Mayr, *J. Org. Chem.* **2009**, *74*, 75–81, supporting information.

(18) C. F. Bernasconi, F. Terrier, *J. Am. Chem. Soc.* **1987**, *109*, 7115-7121.

(19) (a) C. F.Bernasconi,. *Acc. Chem. Res.* **1987**, 20, 301-308; (b) C. F. Bernasconi, P. J. Wenzel, *J. Org. Chem.* **2003**, *68*, 6870-6879.

(20) (a) R Lucius,.H. Mayr, *Angew. Chem.* **2000**, *112*, 2086−2089; *Angew. Chem., Int. Ed.* **2000**, *39*, 1995−1997; (b) S. Evans, P. Nesvadba, S. Allenbach,(Ciba-Geigy AG) Patent EP-B744392, 1996; *Chem. Abstr.* **1997**, *126*, 46968v.